CIVIL ENGINEERING STUDIES

STRUCTURAL RESEARCH SERIES NO. 190

PRIVATE COMMUNICATION
NOT FOR PUBLICATION

DYNAMIC RESPONSE OF THREE-SPAN CONTINUOUS HIGHWAY BRIDGES

By
TSENG HUANG
and
A. S. VELETSOS

Issued as a Part
of the
TENTH PROGRESS REPORT
of the
HIGHWAY BRIDGE IMPACT INVESTIGATION

UNIVERSITY OF ILLINOIS
URBANA, ILLINOIS
SEPTEMBER, 1960

DYNAMIC RESPONSE OF THREE-SPAN CONTINUOUS HIGHWAY BRIDGES

by

Tseng Huang

and

A. S. Veletsos

Issued as a Part of the Tenth Progress Report of the

HIGHWAY BRIDGE IMPACT INVESTIGATION

Conducted by
THE ENGINEERING EXPERIMENT STATION
UNIVERSITY OF ILLINOIS

In Cooperation With
THE DIVISION OF HIGHWAYS
STATE OF ILLINOIS

and

U. S. DEPARTMENT OF COMMERCE
BUREAU OF PUBLIC ROADS

University of Illinois
Urbana, Illinois
September, 1960

TABLE OF CONTENTS

TABLE OF CONTENTS (Continued)

LIST OF TABLES

LIST OF FIGURES

LIST OF FIGURES (Continued)

LIST OF FIGURES (Continued)

LIST OF FIGURES (Concluded)

I. INTRODUCTION

1. Object and Scope

The purpose of this investigation has been to develop a method for the computation of the dynamic response of continuous highway bridges under the action of moving vehicles, and to obtain information on the behavior of representative three-span continuous bridges. In this study, the bridge is idealized as a continuous beam and the vehicle is represented by a sprung load unit having either one, two or three axles.

Whereas the dynamic response of simple span bridges has been studied at some length[(1)*-(16)], there is relatively little information available concerning the behavior of continuous bridges. Some studies on the response of continuous beams to the action of a moving load have been made by Jacobsen, Ayre and their associates[(13), (17)-(21)]; however, the results are not directly applicable to the highway bridge problem. Additional studies have been conducted at the Massachusetts Institute of Technology under the direction of Professor J. M. Biggs. These included a theoretical investigation of the response of two-span highway bridges to the action of a single-axle vehicle loading[(22)], and laboratory tests on two-span and three-span continuous beam models[(22),(23)]. Field tests on actual continuous span bridges have been reported in several publications[(4),(14),(24)-(27)].

The present investigation included: (a) the development of a general method for analyzing the dynamic response of continuous bridges; (b) the development of a computer program for use on the ILLIAC, the high speed digital computer of the University of Illinois, so that numerical solutions

---

* Numbers in parentheses, unless otherwise identified, refer to items listed in the Bibliography.

can be obtained conveniently; (c) the use of the computer program in the solution of specific problems; and (d) a study, based on the numerical results obtained, of the effects of the various variables entering into the problem.

In the analysis, the continuous beam which has an infinite number of degrees of freedom is replaced by a discrete system having a finite number of degrees of freedom. This discretization is effected by concentrating the distributed mass of the beam into a series of point masses, but considering the flexibility of the beam to be distributed as in the actual system. A vehicle of the tractor-trailer type is represented by a three-axle load unit consisting of two interconnected rigid masses. Each axle is represented by two springs in series and a frictional mechanism which simulates the effect of friction in the suspension spring of the vehicle. The use of this mechanism represents an important aspect of the present work. The equations governing the motion of the bridge-vehicle system are formulated in general terms. They can be applied to continuous bridges of any number of spans as well as to simple span bridges or cantilever bridges.

The ILLIAC program has been developed for three-span bridges having a uniform cross section and equal side spans and for a load unit having a maximum of three axles. The effects of damping in the bridge and of friction in the suspension system of the vehicle have been considered. The program can handle various combinations of the parameters defining the system, such as the stiffness and weight characteristics of the different parts of the load unit and the bridge. In addition, by an appropriate choice of the parameters, it can handle problems involving three single-axle loads or a single-axle load followed or preceded by a two-axle loading. The surface of the bridge is considered to be horizontal and smooth. However, with the aid of an additional subroutine, it will also be possible to consider the effects of surface unevenness, such as grade, dead load deflection, or roadway irregularities. The information output includes the interacting forces between the vehicle and the bridge, four reactions, moments over the interior supports, and moments and deflections at the middle of the center span and at a selected point in each side span.

Numerical solutions have been obtained for approximately 50 different cases. The object of this phase of the investigation has been to isolate the various variables entering into the problem and to study their effect in a systematic manner. Primary emphasis has been placed on a study of the dynamic effects produced by smoothly moving loads. The variables investigated include the speed of the vehicle, the weight of the vehicle relative to the weight of the bridge, the ratio of the natural frequencies of the vehicle and the bridge, and the number of axle loads. The effects of initial oscillation of the vehicle, of friction in the suspension system of the vehicle, and of bridge damping are also considered.

Because of the very large number of variables involved and the considerable machine time required for a solution, it is impractical to obtain solutions for all possible combinations of the variables. Accordingly, the principal effort was devoted to a study of the fundamental characteristics of the response of continuous bridges. Based on the results of this study, certain concepts have been formulated which may be used to predict the maximum dynamic effects in continuous bridges from the results of a relatively small number of judiciously selected solutions.

The method of analysis is presented in Chapter II. In Chapter III the details of application of the method are described for the case of a three span continuous bridge. The ILLIAC program is described in Chapter IV. In Chapter V the numerical solutions are presented and the effects of the various variables are discussed. A summary of the most important results is given in Chapter VI.

2. Notation

The symbols used in this report are defined in the text where they are first introduced. For convenience, the important ones are summarized here in alphabetical order.

a = ratio of the side span to the center span

a_1 = ratio of the horizontal distance between the center of gravity of the tractor and its rear axle to the axle spacing of the tractor

$a_2 = 1-a_1$

a_3 = ratio of the horizontal distance between the center of gravity of the trailer and its rear axle to the horizontal distance between that axle and the "fifth wheel pivot"

$a_4 = 1-a_3$

a_5 = ratio of the "fifth wheel" offset to the axle spacing of the tractor

c = coefficient of viscous damping for beam

c_{cr} = critical value of c corresponding to the fundamental mode of vibration

D_1 = deflection at a prescribed point on the left hand span of the beam

D_4 = deflection at a prescribed point on the right hand span of the beam

D_c = deflection at the center of the center span

d_{Pi} = deviation of bridge profile at the point of application of P_i, measured from a horizontal line passing through the left hand abutment

E = modulus of elasticity of the bridge material

F_i = frictional force in the suspension spring for the i^{th} axle

F_i' = maximum value of F_i

f_b = fundamental natural frequency of the bridge

$f_{t,i}$ = pseudo-frequency of the i^{th} axle if only the tire spring acts

$f_{ts,i}$ = pseudo-frequency of the i^{th} axle if both the tire and the suspension springs act in series

g = gravitational acceleration

h = length of a panel in the center span

h_r = length of the r^{th} panel

I = moment of inertia of the bridge cross-section

i_1, i_2 = dynamic indexes of the tractor and trailer, respectively

J_r^j = moment-deflection coefficient, defined in Art. 7

k_i = spring constant for the i^{th} axle; refer to Arts. 5.5 and 9.2

k_r' = modified carry-over factor defined in Art. 7

$k_{t,i}$ = effective stiffness of tires for the i^{th} axle

$k_{ts,i}$ = effective stiffness for the i^{th} axle when the suspension spring and tire spring act in series

L = length of the center span

ℓ_1, ℓ_2 = axle spacings, as shown in Fig. 3a

M_1, M_4 = moments at the sections where D_1 and D_4 are evaluated

M_2, M_3 = moments over the first and second interior support, respectively

M_c = moment at the center of the center span

m = number of panels in the center span

m_r = mass concentration at the r^{th} node

n = number of panels in either side span

P_i = interacting force between the i^{th} axle and the bridge or approach

$P_{i,s}$ = value of P_i at the end of the s^{th} time interval

$P_{st,i}$ = static reaction for the i^{th} axle

Q_r^i = reaction-load coefficient, defined in Art. 5.3

R_1, R_2, R_3, R_4 = reaction at the first abutment, first pier, second pier and second abutment, respectively

R_r^j = reaction-deflection coefficient, defined in Art. 5.3

s_1, s_2 = ℓ_1/L and ℓ_2/L, respectively

T_b = fundamental period of vibration of the bridge

T_2, T_3 = second and third natural periods of vibration of the bridge model

t = time, measured from the instant the first axle moves onto the bridge

u_i = shortening of the suspension-tire system of the i^{th} axle

V = speed of the vehicle

W = weight of the entire vehicle

W_b = weight of the center span of the bridge

W_1, W_2 = "sprung" weight of the tractor or trailer, respectively

w_1, w_2, w_3 = "unsprung" weights, as shown in Fig. 3a

X_{aa} = weighted average of the amplitudes of the waves in a dynamic increment curve

x = distance between the first abutment and the first axle

y_r = displacement of r^{th} node, measured from the position of static equilibrium of the bridge when the load is off the bridge

$y_{r,s}$ = value of y_r at t_s

y_{Pi} = deflection of the bridge under the i^{th} axle, measured from the static equilibrium position of the bridge under the action of its own weight

$y_{Pi,s}$ = value of y_{Pi} at t_s

z_i = generalized coordinate for the i^{th} axle, defined in Art. 5.2

$z_{i,s}$ = value of z_i at t_s

$\alpha = \dfrac{VT_b}{2L}$, a speed parameter

θ_r = angle coefficient for the r^{th} node, defined in Art. 7

λ_n = dimensionless coefficient in the expression for ω_n

$\mu_i = F_i'/P_{st,i}$

$\xi = x/(1+2a)L$, a measurement of time or of the position of the first axle on the bridge

ρ = mass per unit length of the bridge

σ_{std} = standard deviation

$\omega_n = \frac{\lambda_n^2}{L^2}\sqrt{\frac{EI}{\rho}}$, n^{th} natural circular frequency of the bridge

3. Acknowledgment

This study was made as part of the Illinois Cooperative Highway Research Program Project IHR-9, "Impact on Highway Bridges". The investigation was conducted in the Department of Civil Engineering of the University of Illinois in cooperation with the Division of Highways, State of Illinois, and the Bureau of Public Roads, U. S. Department of Commerce.

At the University of Illinois, the project was under the administrative supervision of W. L. Everitt, Dean of the College of Engineering, Ross J. Martin, Director of the Engineering Experiment Station, N. M. Newmark, Head of the Department of Civil Engineering, and Ellis Danner, Director of the Illinois Cooperative Highway Research Program and Professor of Highway Engineering.

At the Division of Highways of the State of Illinois, the project was under the administrative direction of R. R. Bartelsmeyer, Chief Highway Engineer, Theodore F. Morf, Engineer of Research and Planning, and W. E. Chastain, Sr., Engineer of Physical Research.

Guidance to the project staff has been provided by an Advisory Committee composed of the following:

Representing the Illinois Division of Highways:

W. E. Baumann, Bureau of Design

W. E. Chastain, Sr., Engineer of Physical Research

W. N. Sommer, Bureau of Design

Representing the Bureau of Public Roads:

Harold Allen, Chief, Division of Physical Research

E. L. Erickson, Chief, Bridge Division

Representing the University of Illinois

S. J. Fenves, Instructor in Civil Engineering

J. E. Stallmeyer, Professor of Civil Engineering

Valuable advice has also been contributed by Fred Kellam, Regional Bridge Engineer, Bureau of Public Roads, and G. S. Vincent, Chief, Bridge Research Branch, Division of Physical Research, Bureau of Public Roads, who participated in the meetings of the Advisory Committee.

The investigation was under the general direction of C. P. Siess, Professor of Civil Engineering, who acted as Project Supervisor and as ex-officio chairman of the Project Advisory Committee. The immediate supervision of the program was the responsibility of A. S. Veletsos, Professor of Civil Engineering.

This report was prepared as a doctoral dissertation under the direction of Professor Veletsos.

II. METHOD OF ANALYSIS

4. Idealization of Bridge and Vehicle

4.1 Idealization of Bridge. It is assumed that during vibration the deflection configuration of the bridge in the transverse direction remains the same at all times. Accordingly, the bridge may be represented by a beam. In the analysis of the beam, the actual distributed mass is lumped into a series of point masses, spaced at equal intervals within each span. However, the flexibility of the beam is considered to be distributed. Thus the actual system which has an infinite number of degrees of freedom is replaced by a system for which the number of degrees of freedom is equal to the number of mass concentrations used. Figure 1 shows the replacement system for a simple-span bridge and a three-span continuous bridge.

Damping in the bridge is assumed to be viscous. In the actual system the damping resistance is distributed along the length of the bridge. In the replacement system this resistance is assumed to be concentrated at the points of mass concentration, as shown by the dashpots in Fig. 1.

4.2 Idealization of Vehicle. Since the bridge has been idealized as a beam, the width of the vehicle and consequently, the rolling effect cannot be considered in the analysis. Even when treated as a plane system, a vehicle is a very complex mechanical system. However, insofar as its effect on a bridge is concerned it may be represented by one or two rigid bodies supported on a series of springs and dashpots.

Figure 2 shows diagrammatically the detailed features of what is believed to be a complete representation of a tractor-trailer combination. All shaded areas in this figure are considered to be rigid bodies. The quantity W_1 represents the weight of the tractor mounted on its suspension system. The quantity i_1 is the dynamic index[28] of the tractor. This is a measure of the rotary moment of inertia of the weight W_1, and it is defined as the ratio of the radius of gyration squared to the product of the horizontal distances between the two supports and the center of gravity of the weight. The dashpots at the center of gravity of W_1 represent damping resistances against vertical motion and rotary motion. The rigid bar represents the chassis of the tractor and its weight is designated as w_4. The point masses, with weights w_1 and w_2, represent the mass of the axles, springs, and tires for the two axles. The quantities W_2, i_2, and w_3 refer to the trailer and have the same meaning as that of the corresponding quantities for the tractor. For convenience in presentation, the weights W_1 and W_2 are referred to as "sprung" weights and the remaining weights are referred to as "unsprung" weights.

The dynamic characteristics of the tires for each axle of the vehicle are represented by a spring and a dashpot. The suspension system for each axle is represented by a massless spring, a dashpot, and a frictional device. The dashpot accounts for the effects of shock absorbers or air suspension, and the frictional device accounts for any frictional force that may develop in the suspension system, particularly in the leaf springs. The value of the frictional force developed at any time is designated by F and the limiting or maximum possible value is designated by F'. As long as $-F' < F < F'$ for a particular axle, the suspension spring for that axle is inactive (i.e. only the tire spring deflects), and the effective stiffness of that axle is equal to the stiffness of the tires. On the other hand, if $F = \pm F'$, both springs are active and the effective stiffness is that of the two springs acting in series. The characteristics of the suspension-tire system for a simplified case will be explained further in Art. 6.2.

In the present analysis the above system is further simplified by (a) neglecting all sources of viscous damping and (b) replacing the "unsprung" weights by concentrated "sprung" weights as shown in Fig. 3a. In this replacement the weight of the chassis, designated as w_4 in Fig. 2, is incorporated into the weights w_1 and w_2. This replacement is justified by the fact that the "unsprung" weights are quite small in comparison to the "sprung" weights. For a representative tractor the ratio of the total "unsprung" weights to the "sprung" weight is about 1/7, and for a trailer it is for all practical purposes negligible. In addition to the three-axle load unit, in Fig. 3 are shown specialized models for a two-axle and a single-axle load unit.

With its velocity specified, the three-axle load unit shown in Fig. 3a has three degrees of freedom. The parameters which define its characteristics are:

(a) the weight distribution parameters which include the weights W_1, W_2, w_1, w_2 and w_3, and the dynamic indices i_1 and i_2;

(b) the geometrical parameters which include the axle spacings ℓ_1 and ℓ_2, and the ratios a_1 through a_5, as defined in Fig. 3a;

(c) the stiffness parameters for the tires and the suspension springs; for the i^{th} axle $(i=1,2,3)$, the stiffness of the tires is denoted by $k_{t,i}$ and the stiffness of the tires and the suspension springs when acting in series is denoted by $k_{ts,i}$;

(d) the friction parameters, for the suspension systems of the vehicle. For the i^{th} axle this is the limiting frictional force F_i'.

5. Method of Analysis

5.1 Assumptions. The analysis is based on the ordinary beam theory, which neglects the effects of shearing deformation and axial forces. In addition, since the mass is treated as a series of point masses, the effect of rotary moment of inertia does not enter in the solution. The vehicle is assumed to remain in contact with the bridge at all times, and its angular displacements are considered to be small. It is further assumed that no longitudinal force can develop at the junction of the tractor and trailer. This junction is known as the "fifth wheel pivot". Finally, all springs of the vehicle are considered to be elastic.

5.2 Coordinates. The motion of the vehicle-bridge system is expressed in terms of the coordinates z_i and y_r shown in Fig. 4. The coordinate z_i denotes the vertical displacement, measured from a fixed horizontal plane, of the point of support of the vehicle mass for the i^{th} axle. The coordinate y_r denotes the deflection of the r^{th} node point of the beam. This deflection is measured from the static equilibrium position when the bridge is subject to its own weight alone. Both coordinates z and y are considered to be positive when downward.

5.3 Equations of Motion for Bridge Model. Let P_i be the interacting force between the bridge surface and the i^{th} axle of the vehicle. Then the equation of motion for the concentrated mass at the r^{th} node of the beam, m_r, may be expressed as follows:

$$m_r \ddot{y}_r + c m_r \dot{y}_r - \sum R_r^j y_j - \sum Q_r^i P_i = 0 \tag{1}$$

where y_r is the deflection of the r^{th} node, as previously defined, and a dot superscript denotes one differentiation with respect to time. The quantity R_r^j is defined as the reaction-deflection coefficient and represents the static reaction at the r^{th} node point induced by a unit deflection of the j^{th} node point, when all other nodes are supported against deflection. A reaction is considered as positive when directed upward. In an analogous manner, Q_r^i is defined as the reaction-load coefficient and represents the reaction at the r^{th} node point induced by a concentrated unit load at the point of application of P_i when all nodes are supported against deflection. Obviously, when the unit load is off the bridge, $Q_r^i = 0$.

In Eq. 1 the first term represents the inertia force for the r^{th} mass, the second term represents the concentrated damping force, and the last two terms represent the total resisting force provided by the beam. In particular, the third term denotes the resisting force produced by the displacements of the node points. The summation for this term is extended over all node points. The last term denotes the resisting force due to the interactive forces P_i when the nodes are held against deflection. The summation for this term is extended over all the axles considered. It should be noted that the interacting forces P_i are not known at this stage. The procedure used to evaluate these forces is described in Art. 5.5.

By application of Eq. 1 to each mass, one obtains as many equations as there are degrees of freedom for the bridge model. The quantities R depend only on the characteristics of the bridge model, whereas the quantities Q depend both on the characteristics of the bridge and the position of the load; hence the latter are time-dependent quantities. Both quantities can be evaluated in a number of different ways. The procedure used in this work will be described in Arts. 7 and 8.

Equation 1 is applicable to bridges having any boundary conditions and any number of spans, and is independent of whether the cross section of the bridge is uniform or not. It can, therefore, be applied to simple span, continuous or cantilever bridges. The reaction coefficients R and Q will, of course, be different in each case. It may be noted also that the speed of the vehicle may vary arbitrarily.

5.4 <u>Equations of Motion for a Vehicle</u>. Let $P_{st,i}$ be the reaction at the i^{th} axle when the vehicle is in a position of static equilibrium. With P_i denoting the dynamic reaction at any time t, the disturbing force for the i^{th} axle is $P_i - P_{st,i}$ and the equation of motion for a three-axle vehicle can be stated in the form:

$$\begin{bmatrix} a_{11} & a_{12} & a_{13} \\ a_{12} & a_{22} & a_{23} \\ a_{13} & a_{23} & a_{33} \end{bmatrix} \begin{bmatrix} \ddot{z}_1 \\ \ddot{z}_2 \\ \ddot{z}_3 \end{bmatrix} = -\frac{g}{W} \begin{bmatrix} P_1 - P_{st,1} \\ P_2 - P_{st,2} \\ P_3 - P_{st,3} \end{bmatrix} \tag{2}$$

where g is the gravitational acceleration, W is the total weight of the vehicle, and a_{11} through a_{33} are dimensionless coefficients given by the following expressions:

$$\left.\begin{aligned} a_{11} &= (a_1^2 + a_1 a_2 i_1)\frac{W_1}{W} + a_5\,(a_3^2 + a_3 a_4 i_2)\frac{W_2}{W} + \frac{w_1}{W} \\ a_{12} &= a_1 a_2\,(1-i_1)\frac{W_1}{W} + a_5\,(1-a_5)(a_3^2 + a_3 a_4 i_2)\frac{W_2}{W} \\ a_{13} &= a_3 a_4 a_5\,(1-i_2)\frac{W_2}{W} \\ a_{22} &= (a_2^2 + a_1 a_2 i_1)\frac{W_1}{W} + (1-a_5)^2\,(a_3^2 + a_3 a_4 i_2)\frac{W_2}{W} + \frac{w_2}{W} \\ a_{23} &= a_3 a_4\,(1-a_5)(1-i_2)\frac{W_2}{W} \\ a_{33} &= (a_4^2 + a_3 a_4 i_2)\frac{W_2}{W} + \frac{w_3}{W} \end{aligned}\right\} \tag{3}$$

The symbols in these expressions have already been defined. The details of derivation are presented in Appendix A. In the following the matrix of the coefficients <u>a</u> is denoted as matrix A.

Premultiplication of Eq. 2 by the inverse of matrix A yields,

$$\begin{bmatrix} \ddot{z}_1 \\ \ddot{z}_2 \\ \ddot{z}_3 \end{bmatrix} = \frac{g}{w} \begin{bmatrix} b_{11} & b_{12} & b_{13} \\ b_{12} & b_{22} & b_{23} \\ b_{13} & b_{23} & b_{33} \end{bmatrix} \begin{bmatrix} P_1 - P_{st,1} \\ P_2 - P_{st,2} \\ P_3 - P_{st,3} \end{bmatrix} \qquad (4)$$

Since the matrix A is symmetric, its inverse, matrix B, is also symmetric. For a case involving more than one vehicle, an equation of the above form must be written for each vehicle.

It can be shown that a sprung mass with a value of dynamic index i=1 is dynamically equivalent to two separate point masses attached directly to the supporting springs of the distributed mass. The weights of the two masses must be equal to the static reactions produced by the distributed mass. By making use of this fact, it is possible to consider certain special cases of a three-axle load unit. The following cases are of special interest.

(a) When $i_2 = 1$ and $a_3 = 0$, one obtains a single-axle load with a weight $W_2 + w_3$ preceded by a two-axle load unit. In this case, the coefficients a_{13} and a_{23} in Eq. 2 are equal to zero, and, consequently, in Eq. 4, $b_{13} = b_{23} = 0$. The two-axle load unit shown in Fig. 3b can be obtained from the above case by taking, in addition, $W_2 + w_3 = 0$. In this case, the coefficient $a_{33} = 0$, and the matrices A and B are of the second order.

(b) When $i_1 = 1$, $a_5 = 0$ and $a_1 = 1$, one has a single-axle load of weight $W_1 + w_1$ followed by a two-axle load. In this case, $a_{12} = a_{13} = b_{12} = b_{13} = 0$. The single-axle load unit shown in Fig. 3c can be obtained by taking, in addition, $W_2 = w_2 = w_3 = 0$. Then the matrices A and B reduce to a_{11} and b_{11}, respectively.

(c) By taking $i_1 = i_2 = 1$, $a_5 = 0$, and $a_1 = a_3 = 1$, one obtains three single axle load units of weights $W_1 + w_1$, $W_2 + w_2$ and w_3. In this case, A and B are diagonal matrices.

It should be noted that these specialized load units can be obtained also by a different combination of the parameters involved.

5.5 Evaluation of Interacting Forces. Equations 1 and 4 are coupled through the interacting forces P_i, which remain to be evaluated. Let time t be measured from the instant the first axle enters the bridge. Then the interacting force at time t is given by the equation

$$P_i = P_i\Big]_{t=o} + \int_o^t k_i \frac{du_i}{d\tau} d\tau \qquad (5)$$

where $P_i\Big]_{t=o}$ is the initial value of P_i, k_i is the instantaneous effective stiffness of the suspension-tire system for the i^{th} axle at any time τ, and u_i is the corresponding shortening of the suspension-tire system.

If at the instant it enters the bridge, the vehicle is at the position of static equilibrium, the initial force $P_i\Big]_{t=o} = P_{st,i}$. The instantaneous stiffness k_i depends on the magnitude of the frictional force F_i which, in turn, depends on the history of the shortening u_i. As previously noted, when the frictional force F_i for the i^{th} axle is less than its limiting value F_i', the quantity k_i is equal to the stiffness of the tires only, whereas when $F_i = F_i'$, k_i is equal to the combined stiffness of the suspension springs and the tires acting in series. The procedure used to evaluate k_i for a simplified case is described in detail in Art. 9.2.

The shortening u_i can be expressed in the form,

$$u_i = z_i + d_{Pi} - y_{Pi} + \text{constant} \qquad (6)$$

where z_i is the coordinate for the i^{th} axle, as previously defined. The quantity d_{Pi} represents the deviation of the bridge profile from a horizontal line passing through the first abutment for the point of application of P_i, as shown in Fig. 4, and it is positive when upward. This deviation may be due to dead load deflection, initial camber, grade, vertical curve or roadway unevenness. The quantity y_{Pi} represents the deflection of the bridge at the point where P_i acts. The deflection y_{Pi} is measured from the static equilibrium position of the beam, when acted upon by its own weight, and it is positive downward. This quantity is a function of the coordinates y_r (i.e. of the deflections of all node points) and of the magnitude and position of the interacting forces P_i. The constant term, while irrelevant in subsequent computation, is required in the above expression since z_i is measured from an arbitrary reference line.

5.6 Summary. Application of Eqs. 1 and 4 to each concentrated mass of the bridge model and to each axle of the vehicle yield a set of simultaneous, second order differential equations, equal in number to the number of degrees of freedom of the bridge-vehicle system. In these equations the independent variable is t and the dependent coordinates are y_r and z_i.

In the solution of equations of this type, it is usual to express all time-dependent quantities, other than the coordinates themselves, in terms of the coordinates and the independent variable. In the present case, the additional time-dependent variables in Eqs. 1 and 4 are the reaction-load coefficients, Q_r^i, and the interacting forces, P_i. With the vehicle speed specified, the quantities Q_r^i can be expressed explicitly in terms of the position of the load, which is a function of t, and the characteristics of the bridge model. However, the quantities P_i cannot be expressed explicitly, as can be appreciated by an examination of Eq. 5. It can be seen that the right side of this integral equation includes the quantities u_i and k_i, both of which are functions not only of the coordinates y_r and z_i and of other physically determinable quantities, but also of all interacting forces P_i. Furthermore, as explained in the preceding article, the value of the instantaneous stiffness k_i depends upon the past history of motion of the entire system.

These equations can be solved conveniently by a numerical method of integration in which the evaluation of the interacting forces P_i is a major intermediate step.

As the integration of the differential equations is carried out, the values of all the coordinates and of the interacting forces are determined. From these quantities the values of the corresponding deflections, moments and reactions at any desired section may then be evaluated by statics.

It is to be emphasized that the equations of motion presented in this chapter can be applied also to the cases for which the bridge material is non-linear or even plastic. For non-linear elastic material, the reaction-deflection coefficients R_r^j and the reaction-load coefficients Q_r^i in Eq. 1 depend on the value of the deflection at each node point and on the magnitudes and locations of the interacting forces P_i. For the plastic case, these two coefficients depend not only on the quantities mentioned above, but also on the deflection history of the node points.

III. APPLICATION OF METHOD TO ANALYSIS OF THREE-SPAN CONTINUOUS BRIDGES

This chapter is concerned with the detailed application of the method presented in the preceding chapter to the special case of a three-span continuous bridge traversed by a single vehicle.

6. System Considered

The system considered is shown in Fig. 5; its characteristics are as follows:

6.1 Bridge. The bridge model is a three-span continuous beam of equal side spans and uniform flexural rigidity, EI. The length of the center span is denoted by L and the length of a side span by aL. The center span is divided into m equal panels of length h, and each side span is divided into n equal panels of length $\frac{m}{n}$ ah. The nodes are numbered consecutively starting with zero at the left abutment and terminating with (2n+m) at the right abutment. The panel between nodes r and r-1 is designated as the r^{th} panel. As before, the mass is considered to be concentrated at the node points.

6.2 Vehicle. The vehicle is idealized by any one of the systems shown in Fig. 3. The following additional assumptions are made: (a) both the suspension springs and the tire springs are linearly elastic, (b) the maximum frictional force which can be mobilized in the suspension system of an axle is constant, and (c) the speed of the vehicle is constant.

Available test data on trucks [(28),(29)] show that the stiffness of the suspension springs is fairly constant but that the stiffness of the tires is dependent on the intensity of the applied load. These tests show further that the maximum frictional force which can be mobilized in the suspension of an axle is in general a complicated function of the load transmitted through the axle and depends on such factors as the condition and the age of the springs. However, when the variation in the magnitude of the interacting force is small, the assumption of linear elasticity for both springs and the assumption of constant maximum frictional forces are quite reasonable. These assumptions appear to be acceptable even for large variations of the interacting force. In selecting the stiffness of the suspension spring and of the tires of an axle, one should use the values corresponding to a load equal to the static reaction on that axle. Similarly, the value of the limiting frictional force for an axle should be determined for a mean load* equal to the static load on that axle.

The relationship between the interacting force, P, and the shortening, u, of the combined suspension-tire system is shown in Fig. 6. Included in this figure, is also a diagram showing the relationship between u and the frictional force, F. As an example, assume that a single-axle load unit is displaced from its position of equilibrium (i.e. when $P = P_{st}$), and that the initial value of the frictional force is equal to zero. As the displacement is increased, the frictional force first increases at the same rate as the interacting force. Accordingly, the initial paths of the P-u and F-u diagrams are parallel. The suspension spring remains inactive and the stiffness of the system, represented by the slope of line oa, is equal to the stiffness of the tires, k_t. As the displacement is increased further, the frictional force will eventually attain its limiting value F'. From that point on the frictional force will remain constant and the suspension spring will come into play. Accordingly, the slope of the P-u curve becomes equal to the stiffness, k_{ts}, of the suspension and tire springs acting in series. If at some instant, say the instant represented by point b on the diagrams, the displacement is

---

* On a load-displacement diagram, the mean load is represented by a curve midway between the loading and unloading curves.

decreased, the tire spring will rebound and the suspension spring will remain idle. The frictional force will then decrease at the same rate as the interacting force, and the unloading paths on the P-u and F-u diagrams will be parallel to the initial paths. If the displacement is decreased further, at an instant represented by points c on the diagrams the frictional force will become equal to $-F'$. Then both springs will act in series. A possible path beyond this instant is represented by the lines cd-de-ef-fg.

It is clear that the values of P and F depend not only on the value of u, but also on the past history of u. To determine whether the effective stiffness of the suspension-tire system is equal to k_{ts} or k_t, it is only necessary to know whether the locus of F-u follows a horizontal or an inclined line.

7. Characteristic Coefficients of Bridge Model

The reaction-deflection coefficients, R_r^j in Eq. 1 are constants for a given bridge model. These coefficients may be evaluated in a number of different ways. The method used in this study is based on the modified moment distribution procedure introduced by T. Y. Lin[30].

The essential feature of Lin's procedure is that an unbalanced moment at a joint is balanced and carried over to the other joints just once to obtain the final moments. The procedure makes use of the concept of the effective stiffness and effective carry-over factors which are defined as follows: Consider a bar ab resting on non-deflecting supports and elastically restrained against rotation at end b by a coil spring having a stiffness $\overline{R}$. The moment at end a necessary to produce a unit rotation at that end is defined as the effective stiffness of that end of the bar. Denoted by K_a', this stiffness is given by the equation,

$$K'_a = \left[1 - \frac{k_{a,b}\, k_{b,a}\, K_b}{K_b + \bar{R}}\right] K_a \tag{7}$$

where K_a and K_b are the Hardy Cross stiffnesses of the bar for the ends a and b respectively. Similarly $k_{a,b}$ and $k_{b,a}$ are the Hardy Cross carry-over factors from ends a to b and from b to a, respectively. The ratio of the moment produced at end b to the applied moment at a is defined as the effective carry-over factor, $k'_{a,b}$, and is given by the equation;

$$k'_{a,b} = \frac{\bar{R}}{(1 - k_{a,b}\, k_{b,a})K_b + \bar{R}}\, k_{a,b} \tag{8}$$

For a prismatic bar, $K_a = K_b = K$, $k_{a,b} = k_{b,a} = -1/2$, and the above equations become

$$K' = \left[1 - \frac{1}{4}\frac{K}{K + \bar{R}}\right] K \tag{9}$$

and

$$k'_{a,b} = -\frac{\bar{R}}{\frac{3}{2} K + 2\bar{R}} \tag{10}$$

For a continuous beam the coil spring symbolizes the continuity of a particular span with the adjacent spans.

In the course of calculating the coefficients R^j_r by this procedure, one calculates also the moments at the nodes due to a unit displacement at the j^{th} node. These moments are termed as moment-deflection coefficients and are designated by J^j_r. In evaluating the coefficients R^j_r and J^j_r, the following quantities are used. In all cases, it is assumed that the bridge model is supported against deflection at the node points.

(a) Effective Stiffness Coefficients. Consider the portion of the bridge model between the left hand abutment and the r^{th} node as a beam continuous over non-deflective supports at the nodes. Then the effective stiffness of the beam at end r may be stated as the product of a dimensionless stiffness coefficient C_r and the quantity $4EI/h$, where h refers to the length of a panel in the center span of the bridge model. By application of Eq. 9 it can be shown that the coefficient C_r is given by the following recurrence formula:

$$C_r = \frac{h}{h_r}\left[1 - \frac{1}{4}\ \frac{\frac{h}{h_r}}{\frac{h}{h_r} + C_{r-1}}\right] \tag{11}$$

where h_r is the length of the r^{th} panel. For a panel on the center span, $h_r = h$; and for a panel on a side span, $h_r = \frac{m}{n}\,ah$.

It should be noted that, because of symmetry, the dimensionless coefficient for the stiffness at node r for the portion of the beam between the r^{th} node and the right hand support is equal to C_{2n+m-r}.

(b) Effective Distribution Factors. The effective distribution factor for the right hand side of the r^{th} node, designated as d_r, is given by the expression,

$$d_r = \frac{C_{2n+m-r}}{C_r + C_{2n+m-r}} \tag{12}$$

The distribution factor for the left hand side of the r^{th} node is $1 - d_r$.

(c) Effective Carry-Over Factors. The effective carry-over factor from node r to node r-1 is designated as $k'_{r,r-1}$. By application of Eq. 10, one finds that

$$k'_{r,r-1} = \frac{-\,C_{r-1}}{\frac{3}{2}\frac{h}{h_r} + 2C_{r-1}} \tag{13a}$$

Since the beam is symmetrical about the center line, it follows that

$$k'_{r,r+1} = k'_{2n+m-r,\,2n+m-r-1}\ . \tag{13b}$$

For the sake of brevity, in the following discussion the quantity $k'_{r,r-1}$ is designated as k'_r.

To determine the moment-deflection coefficients J^j_r and the reaction-deflection coefficients R^j_r, the j^{th} node of the model is first displaced by a unit amount, and by keeping all nodes fixed against rotation the fixed-end moments produced at the nodes $(j - 1)$, j and $(j + 1)$ are evaluated. The resulting unbalanced moments (if $h_j = h_{j+1}$, there is no unbalanced moment at the j^{th} node) are then distributed and carried over by use of the quantities given in Eqs. 12 and 13. The final moments at the nodes yield the coefficients J^j_r. The reaction-deflection coefficients R^j_r are next evaluated from the equation

$$R^j_r = \frac{J^j_{r-1} - J^j_r}{h_r} - \frac{J^j_r - J^j_{r+1}}{h_{r+1}} \tag{14}$$

The quantities C_r and d_r are used only to evaluate the coefficients R^j_r and J^j_r, whereas the carry-over factors k' and the quantities R^j_r and J^j_r are used repeatedly in later stages of the solution.

Another quantity needed in subsequent computation is the total angle change produced at the r^{th} node when the beam is cut at the r^{th} node and a unit bending moment is applied on the two sides of that node. As before, all nodes are assumed to be held against deflection. This angle change is denoted by θ_r and is given by the expression,

$$\theta_r = \left[\frac{1}{C_r} + \frac{1}{C_{2n+m-r}}\right] \frac{h}{4EI}$$

By use of Eq. 13, the above expression may be written as

$$\theta_r = \frac{h}{EI}\left[\frac{h_r}{h}\left(\frac{2}{3} + \frac{1}{3} k'_r\right) + \frac{h_{r-1}}{h}\left(\frac{2}{3} + \frac{1}{3} k'_{2n+m-r}\right)\right] \tag{15}$$

It should be emphasized that the quantities defined in this article depend only on the characteristics of the bridge model.

8. Basic Operations

Certain operations are used repeatedly in the numerical solution of the equations of motion and in the computation of deflections, bending moments and reactions. A systematic treatment of these operations is desirable. The operations involved are as follows:

Op. 1: Evaluate the moment and deflection at any point of a simply supported beam due to moments applied at the ends of the beam.

Op. 2: Evaluate the moment and deflection produced at any point of a simply supported beam due to a concentrated load on the beam. The governing expressions for Operations 1 and 2 are quite simple.

Op. 3: Evaluate the moment at the r^{th} node produced by the i^{th} axle load P_i, when all nodes are held against deflection. This moment is equal to the product of P_i and the moment-load coefficient M_r^i. By Maxwell's law of reciprocity, the latter quantity is numerically equal to the deflection at the i^{th} axle produced by a unit moment applied at the r^{th} node (with the continuity there cut) divided by the coefficient θ_r. The latter coefficient is given by Eq. 15. To evaluate this deflection at the i^{th} axle, the moments at the ends of the panel supporting the i^{th} axle are first calculated. These are determined by multiplying successively the effective carry-over factors for the panels between the r^{th} node and the nodes where the moments are computed. The deflection at the i^{th} axle is then computed by application of Op. 1.

Op. 4: Calculate the reaction at the r^{th} node produced by the i^{th} axle load P_i, when all nodes are held against deflection. This reaction is equal to the product of P_i and the reaction-load coefficient Q_r^i. The latter coefficient is also equal to the deflection at the point of application of P_i due to a unit displacement at the r^{th} node. To evaluate this deflection, first the moment-deflection coefficients, J, for the nodes on either side of the panel supporting the i^{th} axle are selected, and then the deflection produced by these moments are determined by application of Op. 1. If the axle is on a panel connected to the r^{th} node, this deflection represents only one component of the desired deflection. The additional component is obtained by considering the deflection corresponding to a rigid body rotation for that panel.

Op. 5: Evaluate the moment at the r^{th} node due to known deflections of all node points. This moment is equal to $\sum_j y_j J_r^j$.

Op. 6: Compute the reaction at the r^{th} node due to known deflections of all node points. This is equal to $\sum_j y_j R_r^j$.

The last two operations may involve small differences of large numbers; therefore, the individual products must be evaluated to a large number of significant figures.

9. <u>Numerical Integration Procedure</u>

9.1 <u>General</u>. The equations of motion of the system have been solved numerically by means of a step-by-step method of integration. The time required for the vehicle to cross the bridge has been divided into a number of short intervals and the equations of motion have been "satisfied" only at these discrete instants. Let it be assumed that the values of the acceleration, velocity and displacement of each coordinate of the system are known at a time t_s, and that it is desired to find the corresponding values at time t_{s+1}, which differs from t_s by a short interval Δt. The method used to accomplish this consists of the following basic steps. First, an assumption is made regarding the manner in which the acceleration of each coordinate varies within the time interval. Second, the velocity and displacement for each coordinate are determined in terms of known accelerations, velocities and displacements for the beginning of the interval and in terms of unknown accelerations for the end of the interval. Next, these unknown accelerations are evaluated by "satisfying" the equation of motion at the end of the time interval. The velocities and displacements for this time are finally determined from the expressions established in the second step.

In the present study, the following generalized equations due to N. M. Newmark[31] have been used.

$$\dot{x}_{k,s+1} = \dot{x}_{k,s} + \frac{1}{2} (\Delta t)(\ddot{x}_{k,s} + \ddot{x}_{k,s+1}) \tag{16}$$

$$x_{k,s+1} = x_{k,s} + (\Delta t)\dot{x}_{k,s} + (\frac{1}{2} - \beta)(\Delta t)^2 \ddot{x}_{k,s} + \beta(\Delta t)^2 \ddot{x}_{k,s+1} \tag{17}$$

where β is a dimensionless parameter specifying the variation of the acceleration within the time interval; the quantity x_k represents the displacement of a coordinate (either y_r or z_i); and $\dot{x}_k$ and $\ddot{x}_k$ represent, respectively, the corresponding velocity and acceleration. The subscripts s and s+1 following a comma identify quantities corresponding to t_s and t_{s+1}, respectively. For the numerical results presented in this report β was taken equal to 1/6; this value corresponds to a linear variation of acceleration.

The following iterative procedure was used to evaluate the accelerations, velocities and displacements of the coordinates at the end of a time interval.

1. Define the position of each axle on the bridge for time t_{s+1}.

2. Assume that the accelerations $\ddot{y}_{r,s+1}$ and $\ddot{z}_{i,s+1}$ for the end of the time interval are the same as those at the beginning of the interval, and from Eqs. 16 and 17 evaluate the velocities $\dot{y}_{r,s+1}$ and $\dot{z}_{i,s+1}$ and the displacements $y_{r,s+1}$ and $z_{i,s+1}$.

3. Evaluate improved accelerations for the y_r coordinates proceeding as follows:

(a) By application of Eq. 1 to the first node (r=1), obtain an improved value for $\ddot{y}_{1,s+1}$. The major operation in this step concerns the computation of the quantities $\sum_j R_1^j \, y_{j,s+1}$ and $\sum_i Q_1^i \, P_{i,s+1}$. The former quantity is obtained by Op. 6 and the latter by repeating Op. 4 as many times as there are axles. The values of P_i used in this computation are those applicable to the beginning of the time interval (i.e. $P_{i,s}$), and the values of $y_{j,s+1}$ are those evaluated in step 2.

(b) By application of Eqs. 16 and 17 calculate the values of $\dot{y}_{1,s+1}$ and $y_{1,s+1}$ corresponding to the accelerations determined in step 3(a).

(c) Repeat steps 3(a) and 3(b) for the remaining y_r coordinates ($r = 2, 3, \ldots$), considering one coordinate at a time. For each computation, use the latest available values of $y_{j,s+1}$ and $\dot{y}_{j,s+1}$.

4. Evaluate improved accelerations for the z_i coordinates as follows:

(a) Compute the interacting force $P_{1,s+1}$ at the end of the time interval. The various steps involved in this computation are described in detail in the following subarticle.

(b) From Eq. 4 evaluate $\ddot{z}_{1,s+1}$, using the latest available value of $P_{i,s+1}$. For the first axle, the value of $P_{1,s+1}$ used is that evaluated in step 4(a), and the values of $P_{2,s+1}$ and $P_{3,s+1}$ are those obtained from the preceding cycle.

(c) From the acceleration obtained in step 4(b), determined improved values of $\dot{z}_{1,s+1}$ and $z_{1,s+1}$ by use of Eqs. 16 and 17.

(d) Repeat steps 4(a), 4(b) and 4(c) for the remaining axles (if any), considering one axle at a time, always using the latest available values of $P_{i,s+1}$ and $z_{i,s+1}$.

5. For each coordinate, compare the newly derived value of acceleration with the previously available value. If the difference between the two values for any coordinate exceeds a prescribed tolerance, repeat steps 3 through 5, always using the latest available values of $P_{i,s+1}$ and $y_{j,s+1}$. When all differences are less than the prescribed tolerance, the integration for this

time interval is considered to be completed. One then proceeds to the next interval. If desired, the values of reactions, bending moment and deflection at any selected point may be evaluated before proceeding to the next interval. Steps 3 and 4 constitute one cycle of iteration. To illustrate the details of the procedure, a numerical example is presented in Appendix B for one step of integration.

9.2 Evaluation of P_i. In the computation of P_i it is assumed that the effective stiffness of the suspension-tire system remains constant within a time interval of integration. In other words, the suspension spring is assumed to engage or disengage at the end of a time interval. Under this assumption, Eq. 5 may be written in the form:

$$P_{i,s+1} = P_{i,s} + (\Delta u_i)k_i$$

or

$$P_{i,s+1} = P_{i,s} + (u_{i,s+1} - u_{i,s})k_i \tag{18}$$

where the subscripts s and s+1 denote, as before, quantities corresponding to time t_s and t_{s+1}, respectively. The quantities $u_{i,s+1}$ and k_i are determined as follows:

(a) Computation of $u_{i,s+1}$. The value of $u_{i,s+1}$ is determined by application of Eq. 6. The value of d_{Pi} in this equation is specified, and the value of the deflection z_i is furnished by step 2 or 4(c) of the iterative procedure described in Art. 9.1. The deflection under the load, y_{Pi}, is evaluated by superimposing the following three components: (i) deflection due to the moments acting at the two ends of the panel; (ii) deflection due to the force or forces P_i acting on the panel; and (iii) deflection due to a rigid body displacement of the panel.

The moments at the ends of the panel are obtained with the aids of Ops. 5 and 3. Then component (i) of the deflection is obtained by Op. 1.

The component (ii) is obtained by application of Op. 2 for each axle on the panel. The rigid body displacement is determined from the known deflections of the end points of the panel, and the component (iii) is evaluated by simple proportion.

Strictly speaking the deflection y_{Pi} must be evaluated for each cycle of iteration in the integration process, since the values of y and P involved in the computation vary from one cycle to the next. Inasmuch as this computation is rather time consuming, an approximation was used. This consists in evaluating the first two components of y_{Pi} only for the first iterative cycle of an integration step. The third component was evaluated for each cycle of iteration. The results obtained by this approximation were found to be in good agreement with the "exact" values. A comparison is provided in Table 1 for a case for which the difference between the two sets of solutions is likely to be large. The response of the system at a few selected sections was compared for a few selected instants.

(b) Determination of k_i. The effective stiffness of the suspension-tire system for an axle is determined by making use of the F-u diagram for that axle, as shown in Fig. 6. Let the frictional force corresponding to $u_{i,s}$ be denoted by $F_{i,s}$. In the F-u diagram, imagine a straight line which passes through the point ($u_{i,s}$, $F_{i,s}$) and is parallel to the initial line oa. Let $u^u_{i,s}$ be the abscissa of the point of intersection of this inclined line and a horizontal line corresponding to the positive value of F'. Similarly, let $u^\ell_{i,s}$ represent the point of intersection of this inclined line with a horizontal line corresponding to the negative value of F'. Then the value of k_i to be used in Eq. 18 is determined from the following criteria:

Case	Condition		Consequence
1	$\Delta u_i > o$	$u_{i,s} + \Delta u_i \leq u^u_{i,s}$	$k_i = k_{t,i}$
2		$u_{i,s} + \Delta u_i > u^u_{i,s}$	$k_i = k_{ts,i}$
3	$\Delta u_i < o$	$u_{i,s} + \Delta u_i > u^\ell_{i,s}$	$k_i = k_{t,i}$
4		$u_{i,s} + \Delta u_i \leq u^\ell_{i,s}$	$k_i = k_{ts,i}$

It follows that the selection of k_i depends only on the value of Δu, u^u and u^ℓ. The value of F need not be computed. For cases 1 and 3 the values of u^u and u^ℓ at time t_{s+1} are the same as those at time t_s, whereas for cases 2 and 4 they differ by the amount Δu.

9.3 Initial Conditions. In order to start the integration procedure, it is necessary to specify the initial values of the deflection and velocity of each node point, the velocity of each z-coordinate, the interacting force for each axle, and the frictional force for the suspension system of each axle. These values refer to the time the front axle enters the bridge.

9.4 Choice of Time Interval. In the application of the numerical procedure described in Art. 9.1, the time interval used should be small enough so that successive cycles of iteration converge and the solution is stable. The criteria for convergence and stability of this procedure have been established by N. M. Newmark(31). For $\beta = 1/6$, convergence and stability are insured if

$$\Delta t < 0.389T$$

where T is the shortest natural period of vibration of the system; in this case, the system is the beam-vehicle combination. Strictly speaking, this period depends both on the position of the vehicle on the span and also on whether the limiting frictional force of the suspension system of the vehicle has been overcome or not.

The total time between the instant the front axle enters the bridge and the instant the last axle leaves the bridge is $(1 + 2a + s_1 + s_2)\, L/V$. Let N be the number of steps used for a complete solution, then

$$N > \frac{(1 + 2a)L}{0.389\ VT} + \frac{(s_1 + s_2)L}{0.389\ VT} \tag{19}$$

The right side of this inequality represents the minimum number of steps required for a complete solution, on the assumption that Δt is constant and that the criteria for convergence and stability are independent of the position of the vehicle on the bridge and the condition of the vehicle. For the bridge model considered with a=0.8, n=3 and m=4, the shortest natural period $T = 0.208 T_b$, where T_b is the fundamental period of vibration of the bridge model. In this case, Eq. 19 reduces to

$$N > \frac{16.1}{\alpha} + \frac{s_1 + s_2}{0.1615\ \alpha} \tag{20}$$

where

$$\alpha = \frac{VT_b}{2L} \tag{21}$$

For a single-axle loading, the minimum value of N given by Eq. 20 is 215 when $\alpha = 0.075$, and 135 when $\alpha = 0.12$. For a multiple axle vehicle, the corresponding minimum values of N are of course larger.

In Table 2 solutions are presented for the maximum dynamic effects in a three-span continuous bridge model considering different values of N. The characteristics of the system are defined in the table heading. Solutions are given for a value of $\alpha = 0.075$, with three different values of N, and for a value of $\alpha = 0.15$ with two values of N. It can be seen that differences between corresponding solutions are generally small. For the numerical results presented in the remaining part of this report the value of α ranges between 0.12 and 0.18. For these solutions a constant value N = 600 was used.

10. Computation of Deflections, Moments and Reactions

10.1 Static Effects. The static effects are determined by application of the basic operations described in Art. 8. It is only necessary to consider $n = m = 1$ and $P = P_{st}$. In particular, the deflection and moment at a prescribed point of a span are determined in two steps. First, by considering the span to be simply supported the effects of the force or forces P_{st} acting on that span are determined. To these effects are added the effects produced by the moments at the ends of the span considered. The reaction at a support is obtained by application of Op. 4 for each axle on the bridge.

10.2 Dynamic Effects. At the end of an integration step, the deflections of the node points and the interacting forces are known. From this information the deflections of other points and the magnitude of moments and reactions can be evaluated as follows: The deflection of a point within a panel is determined by the addition of three deflection components in a manner similar to that described in Art. 9.2 in connection with the computation of y_{Pi}. Moments are evaluated in a similar way, with the exception that only the effects of the end moments and of the interacting forces need be considered. The reaction at a support is determined in two steps. First, the effect of the interacting forces is calculated by considering the beam to be held against deflections at all node points. To this is added the effect of the known deflections of the nodes. The first component is determined by Op. 4, and the second component by Op. 6.

11. Summary of Parameters

The parameters of the problem are expressed in dimensionless form and include the following:

Bridge Parameters

(1) The span ratio, a. This is the ratio of the side span to the center span.

(2) The damping factor, c/c_{cr}, where c is the damping force per unit mass per unit velocity, and c_{cr} is the critical damping coefficient corresponding to the fundamental mode of vibration of the bridge.

Vehicle Parameters

(3) The distance parameters, a_1, a_3 and a_5. As shown in Fig. 3a, these parameters define the locations of the centers of gravity of the tractor and trailer and the location of the "fifth wheel pivot".

(4) The weight distribution parameters, W_1/W, W_2/W, w_1/W, w_2/W and w_3/W. (See Fig. 3a).

(5) The dynamic indices i_1 and i_2 for the tractor and trailer, as defined in Art. 4.2.

(6) The coefficient of friction, μ, for the suspension system of each axle. For the i^{th} axle, $\mu_i = F_i'/P_{st,i}$.

Bridge-Vehicle Parameters

(7) The speed parameter α, defined by Eq. 21.

(8) The weight ratio W/W_b, where W is the total weight of the vehicle and W_b is the weight of the center span of the bridge.

(9) The frequency ratios f_t/f_b and f_{ts}/f_b for each axle. The quantity f_b is the fundamental natural frequency of the bridge, and f_t and f_{ts} are pseudo-frequencies which are measures of the stiffnesses of the tire and of the suspension springs for an axle. The quantity f_t represents the

frequency of a mass with a weight P_{st} vibrating on the tire spring, whereas f_{ts} represents the corresponding frequency of the same mass vibrating on the tire and suspension springs acting in series. For the i^{th} axle,

$$f_{t,i} = \frac{1}{2\pi}\sqrt{\frac{g}{P_{st,i}/k_{t,i}}} \tag{22a}$$

and

$$f_{ts,i} = \frac{1}{2\pi}\sqrt{\frac{g}{P_{st,i}/k_{ts,i}}} \tag{22b}$$

When the limiting frictional force F_i' is so large that the effective stiffness of the suspension-tire system for the i^{th} axle is always equal to $k_{t,i}$, or when F_i' is so small that the effective stiffness may be considered to be always equal to $k_{ts,i}$, then it is necessary to specify a single frequency. This frequency is denoted by f_{vi}.

(10) The profile variation parameter, $d_{Pi}k_{t,i}/P_{st,i}$. The numerator of this expression represents the change in the interacting force for the i^{th} axle when the tire spring is shortened by an amount equal to d_{Pi}.

(11) The axle spacing parameters, s_1 and s_2, defined by the equations

$$s_1 = \ell_1/L, \quad \text{and } s_2 = \ell_2/L$$

in which ℓ_1 and ℓ_2 are the axle spacings, as shown in Fig. 3a.

IV. COMPUTER PROGRAMS

12. General

The method described in the preceding chapter has been programmed for the ILLIAC, the digital computer of the University of Illinois. The programs that have been developed can be used to compute the dynamic response of uniform three-span continuous bridges with equal side spans when traversed by a single vehicle load having either one, two or three axles. It is also possible to consider three single-axle loads, or a two-axle load followed or preceded by a single-axle load. Two different programs have been prepared. The first provides results for the complete history of the response of the system, while the other can be used to determine only the amplification factors for deflections, moments and reactions. The term "amplification factor" defines the ratio of a maximum dynamic effect to the corresponding maximum static effect and is abbreviated as "A.F.".

The parameters which must be specified in using the programs include the dimensionless parameters summarized in Art. 11, the parameters n, m and N which define the number of panels in the bridge model, and the number of the time intervals of integration. In addition, for the "dynamic history program" certain parameters must be input to specify the end of the computation and the interval between print-outs.

If the maximum static effects are not available, they are computed within the machine. However, if they are known, they may be input at the beginning of the computation. At the start of the dynamic computation, that is, when the front axle of the vehicle enters the bridge, the program considers the system to be in the so-called "neutral condition". For this condition, the bridge is at rest $(y_r = \dot{y}_r = 0)$, the vehicle has no vertical motion

($\dot{z}_i = 0$, $P = P_{st}$), and the frictional force in the suspension system of the vehicle is equal to zero ($F_i = 0$). If the initial conditions are different, only those conditions which are different from the "neutral condition" must be specified.

For each program, the information output includes the reactions at the four supports, the moments over the interior piers, the moment and deflection at the center of the center span, and the moment at a selected point in each side span. The program for the history of the response yields, in addition, the interacting forces between the axles of the vehicle and the bridge, and the deflection at the points of the side spans where the moments are evaluated. With one exception, the magnitude of the dynamic deflection, moment, or reaction at a point is expressed in terms of the corresponding maximum static value. The exception concerns the deflection at the side span which is expressed in terms of the maximum static deflection at the center of the center span. The interacting force for an axle is expressed in terms of the static reaction for that axle.

In their present form, the programs utilize the entire Williams (fast) memory of the ILLIAC, which has a capacity of 1024 locations, and approximately 1200 locations of the magnetic drum (slow) memory. With certain modifications, the programs can be specialized to the case of simple span bridges, two-span continuous bridges or cantilever bridges.

13. Description of Programs

The computer program for the computation of either the complete history of the response or the maximum values of the response consists of three major parts. Each part consists of a block of instructions which are stored (recorded) on the magnetic drum memory of the computer. Because of the limited capacity of the Williams memory, at each stage of the computation only the "functioning" part of the program is retained in the fast memory. Furthermore, the program is arranged so that once the integration process is started no further reference is made to information retained in the magnetic drum memory.

A general flow diagram for the complete program is shown in Fig. 8. The function of each part and the sequence of operations involved are described in the following. The write-up of the complete program will be placed in the ILLIAC Library of the Department of Civil Engineering.

(a) Part I. The program starts with the reading in of the data (parameters) specifying the characteristics of the vehicle and bridge, excluding those parameters which specify the initial conditions of the system. Next the subroutine labeled (G1) is entered, and the time-independent characteristic coefficients for the bridge model are computed and stored in the Williams memory. These coefficients include the effective carry-over factors, k_r', the moment-deflection coefficients, J_r^j, the reaction-deflection coefficients, R_r^j, and the angle coefficients, θ_r. The coefficients required for the static computation are determined by taking $n = m = 1$. Following this, subroutine (G2) is entered to compute the values of P_{st} and the elements of the matrix B in Eq. 4. The values of P_{st} are determined in terms of the parameters specifying the geometry and weight distribution of the vehicle. The matrix B is determined by first forming matrix A in Eq. 2 and then inverting it. The inversion of matrix A is performed with the aid of subroutine (3SEB1). The last operation of this part of the program is to play back (transfer) the second part of the program from the drum memory to the Williams memory and then transfer control to the second part of the program.

Up to this point, the machine operation for both the "dynamic history program" and the "amplification factor program" are identical. However, in the latter program, there is an additional subroutine (OUTPT) for punching out the values of the amplification factors at the completion of the computation. A more detailed description of the function of this subroutine is given after the presentation of the third part of the program.

(b) Part II. This part is the same for both the "dynamic history program" and the "A.F. program", and performs four major tasks. The first is to determine the maximum static effects. This is carried out by routine (SS) and the results are punched out by use of subroutine (SMAX). Routine (SS) makes use of a number of subroutines, of which the most important are: (a) subroutine (STP), which defines the position of the axles on the bridge, (b) subroutines (SDC-M), (SDC-P), (SMCP) and (SQ) which perform, respectively, the basic operations 1, 2, 3 and 4 described in Art. 8, and (c) subroutines (SMC), (SMD) and (SRC) which compute, respectively, the moment over the interior supports, the moment and deflection at any selected point of the bridge, and the reaction at any support. The last three subroutines make use of the basic operation subroutines (SDC-M), (SDC-P), (SMCP) and (SQ).

In this part of the computation the characteristic coefficients corresponding to $n = m = 1$ are used. Effects are evaluated only for the positions of the vehicle considered in the integration of the equations of motion. The maximum static effects are considered to be the maxima of the computed effects. These may be slightly smaller than the actual maxima which may occur between two successive positions considered. If the maximum static effects are known, they may be fed into the machine at the beginning of the problem. Also, if these effects are already in the machine from a previous computation, the calculation of the maximum static effects may be bypassed by transferring control directly to the next operation.

The second function of this part of the program is to set the initial conditions of the problem at the so-called "neutral condition". This is done by subroutine (NIC). If the initial conditions are different from these, the appropriate parameters are read in at this stage.

The third function is to establish for each axle the values of u^u and u^ℓ which are consistent with the initial values of F_i. These values are required to determine the value of the effective stiffness of the suspension-tire system as discussed in Art. 9.2.

The final operation of this part of the program is to set the time counter that records the value of (s + 1) equal to zero and to play back the third part of the program from the drum memory. The setting of (s + 1) = 0 implies that the front axle of the vehicle is at the entrance of the bridge. Finally, control is transferred to the third part of the program.

(c) Third Part. The principal functions of the third part are to integrate Eqs. 1 and 4 numerically and to compute dynamic deflections, moments and reactions. The major operations involved are:

(i) To determine the position of the vehicle at the end of each time interval by use of subroutine (DTP).

(ii) To integrate the equations of motion for this time interval, and to store the values of P, u_o, u^u and u^ℓ at the end of this time interval. This operation is carried out by subroutine (DINTE) together with an auxiliary subroutine (DAUX).

(iii) To evaluate dynamic deflections, moments and reactions. In the "dynamic history program", a check is made to determine whether these quantities are desired at the end of the time interval considered. If these quantities are needed, they are computed and punched out. In the "A.F. program", these quantities are computed at the end of each time interval, they are compared with the maximum values of the corresponding quantities computed previously, and the new maxima are retained.

The foregoing steps are repeated until the last interval is reached. At the end of this interval, the first part of the program is played back to the Williams memory. In the "A.F. program" the amplification factors are then punched out with the aid of subroutine (OUTPT). This constitutes the last step in the solution of a problem.

In Fig. 9 is shown a general flow diagram of the integration routine. This is a modified version of routine SRLC 21 of the ILLIAC Library of the Structural Research group. It is used to evaluate the velocity and displacement for each coordinate in accordance with Eqs. 16 and 17. The accelerations $\ddot{y}_{r,s+1}$ and $\ddot{z}_{i,s+1}$ needed in the application of these equations are computed by the auxiliary subroutine (DAUX), the flow diagram of which is given in Fig. 10. This auxiliary subroutine, in turn, makes use of subroutines (DDRET) and (DMDIN). Flow diagrams for these subroutines are given in Figs. 11 and 12.

Subroutine (DDRET) is used to compute the quantity

$$\sum_j y_j R_r^j + \sum_i Q_r^i P_i$$

for a specified node point. For this computation this subroutine performs Op. 6 and enters subroutine (DQ) to perform Op. 4. The latter subroutine is entered as many times as the number of axles considered.

Subroutine (DMDIN) is used to compute the approximate value of y_{Pi} as discussed in Art. 9.2. As previously noted, this deflection is evaluated as the sum of three components. The first component is determined with the aid of subroutines (DMC) and (DDC-M). Subroutine (DMC) (refer to Fig. 13) is used to perform Ops. 3 and 5 and to compute the total moment at a specified node point. This subroutine is entered twice to compute the moments at the ends of the panel under consideration. Subroutine (DDC-M) is used to perform Op. 1. It is entered once. The second component of deflection is computed by subroutine (DDC-P) which performs Op. 2. Since the last two subroutines are straightforward, their flow diagrams are not included. The third component of deflection is evaluated by simple proportion.

Figure 14 shows a general flow diagram for the part of the program used to calculate deflections, moments and reactions at specified sections. In addition to subroutine (DDRET) which is used to obtain the reactions, this part of the program makes use of subroutine (DMD) which yields the deflection and moment at any specified point. This subroutine is similar to (DMDIN) and its flow diagram is also presented in Fig. 12.

14. Time Required for Solution of a Problem

The machine time required to obtain a solution depends on the particular problem considered. The following is an estimate of the time required for the solution of a problem by use of the "A.F. Program" or the "dynamic history program".

(a) Read in time for complete program: 3 minutes and 40 seconds.

(b) Time required for the first part of the program: 45 seconds.

(c) Time required for the second part of the program: It depends on whether the maximum static effects are to be computed or not. If the maximum static effects are not computed, the time required is approximately 20 seconds. The computation of the static effects for each position of the load requires 0.18 sec. for a single-axle loading, 0.25 sec. for a two-axle loading, and 0.33 sec. for a three-axle loading.

(d) Time required for the third part of the program: This time is the sum of the following: (i) time required for integration, (ii) time required to calculate dynamic effects, and (iii) time required to punch the desired information.

The time required for one step of integration depends on the number of concentrated masses considered in the beam model, the number of axles considered, and the number of axles actually present on the bridge. The same factors govern the time required for the computation of dynamic effects. This time may be estimated from the following relations.

Condition				Estimate of Time Required, in Seconds	
n	m	Number of Axles Considered	Number of Axles on Bridge	For One Step of Integration	For Computation of One Set of Dynamic Effects
2	3	1	1	0.11 + 0.19 I	0.55
		2	1	0.11 + 0.22 I	0.58
			2	0.29 + 0.27 I	0.79
		3	1	0.12 + 0.24 I	0.60
			2	0.30 + 0.30 I	0.81
			3	0.54 + 0.36 I	1.02
3	4	1	1	0.14 + 0.39 I	0.70
		2	1	0.14 + 0.41 I	0.72
			2	0.36 + 0.52 I	0.94
		3	1	0.15 + 0.46 I	0.74
			2	0.37 + 0.55 I	0.97
			3	0.68 + 0.63 I	1.19

In this table I denotes the number of cycles of iteration per step of integration. It should be noted that the value of I may be different for different steps of integration. From the results of a few numerical solutions, it has been found that, in general, the quantity I increases with increasing number of degrees of freedom. It is approximately between 2 and 3 for a single-axle loading, between 3 and 4 for a two-axle loading and 4 and 5 for a three-axle loading.

The time required for punching out one set of dynamic effects is approximately two seconds.

V. RESULTS OF INVESTIGATION

15. General

The numerical results presented herein are for continuous bridges with uniform cross section and equal side spans. The length of each side span is considered to be eight tenths of that of the center span, and the bridge surface is considered to be smooth and horizontal. The vehicle is represented by a load unit having either one, two, or three axles. Most of the solutions presented are for single-axle loading. Unless otherwise noted, it should be understood that a single-axle loading is considered. The major parameters investigated are the weight of the vehicle relative to the weight of the bridge, the relative frequencies of the two systems, and the speed of the vehicle. Although the majority of the solutions are for smoothly moving vehicles, some results are included for initially oscillating vehicles. Also included are solutions indicating the effect of the frictional force in the suspension system of the vehicle and the effects of damping in the bridge.

The range of parameters considered is such that the results are representative of the behavior of bridges of the SC-6-53 type as specified in the manual: "Standard Plans for Highway Bridge Superstructure", Bureau of Public Roads, Washington, D. C., 1957. These are three-span continuous bridges with steel girders and a concrete deck designed for H20-S16 loading. The span lengths are in the ratios of 4:5:4. The weights of the center span and the fundamental natural frequencies of vibration of the bridges are summarized in Table 3. These were determined as follows: The total weight of a bridge was taken equal to the sum of the dead load reactions tabulated in the manual, and the weight of the center span was determined on the assumption that the total weight is uniformly distributed along the bridge. In the computation of the natural frequencies, the mass per unit of length of the bridge and the cross sectional area were considered to be uniform. The flexural rigidity of the cross section was determined for full composite action between the beams and the slab, considering the entire width of the slab to be effective.

The three-axle load unit considered in this study corresponds to an H20-S16 truck loading and is referred to as a "typical" three-axle vehicle. The characteristics of this loading are summarized in the third column of Table 4. These are average characteristics and were obtained from information given in reference (28) and from manufacturers' data. Included in this table are the characteristics of a "typical" two-axle trailer which corresponds to the trailer unit of the three-axle vehicle, and also a single-axle loading. It should be noted that the weight of the latter loading is taken equal to the total weight of the two-axle loading. Similarly, the frequency and frictional parameters are considered to be the same for the two systems.

The quantities evaluated are summarized in Fig. 7. These include the deflections D_1 and D_4 at a distance 0.42 aL from the end supports, the corresponding bending moments, M_1 and M_4, the moments over the two interior supports, M_2 and M_3, the moment and deflection at the center of the center span, and the four reactions, R_1, R_2, R_3 and R_4. In addition, the interacting forces between the vehicle axles and the bridge were evaluated and studied. The sections of a distance 0.42aL from the end supports represent approximately the locations where the positive moment in the end spans is maximum.

16. Representative History Curves

The solution presented in this article is for a three-span undamped bridge, traversed by a smoothly moving single-axle loading. The spans are in the ratios of 4:5:4, the weight ratio $W/W_b = 0.175$, and the speed parameter

$\alpha = 0.15$. The frictional force in the suspension system of the load is considered to be so large that the suspension spring is not engaged and the load oscillates on the tire spring only.* The frequency ratio is taken as $f_v/f_b = 1$. These parameters are representative of those for a three-span I-beam bridge with 64'-80'-64' spans traversed by an H20-S16 truck loading moving at approximately 60 m.p.h. The solution was obtained by considering a total of seven mass concentrations for the beam model, as shown by the sketch in the upper part of Fig. 15. Included in this figure are also the first four natural modes of vibration of the beam model.

The results of the solution are presented in Figs. 16a through 16h in the form of history curves. A history curve is a plot of the variation of some effect (such as deflection, moment or reaction) as a function of time, or the position of the load on the bridge. The curve in Fig. 16a is for the interacting force and the curves in Figs. 16b through 16h are for deflection, bending moments, and reactions at a few selected sections, and for the corresponding dynamic increments. Designated as D.I., the dynamic increment for a particular effect is the difference between the dynamic value of that effect and the corresponding static value.

The abscissa ξ in the history curves represents the distance between the first support and the position of the load on the bridge in terms of the total length of the bridge. Since this distance is proportional to the product of time and the speed of the vehicle, the coordinate ξ represents also the time the load has been on the bridge as a fraction of the total time required for the load axle to cross the bridge. The ordinates of the history curves are expressed in terms of the maximum static value of the particular effect considered. The maximum static effects for this problem are given in the third column of Table 5. Included in this table are also the maximum static effects for the two-axle and three-axle loadings considered later.

In Fig. 16a it should be noted that the maximum variation in the value of the interacting force is 7.3 percent of the static value, P_{st}. It follows then that this solution is also applicable to those cases for which the coefficient of friction for the suspension spring, μ, is larger than 0.073. Inasmuch as for ordinary vehicles the value of μ is of the order of 0.12 to 0.28, the present solution is a realistic one, and it indicates that the suspension spring will not engage.

Concerning the curves presented in Figs. 16b through 16h, it is worth noting the following:

(1) Although the dynamic increment curves are not periodic, for each of these curves one can identify waves with certain distinct periods. In general, the periods of these waves correspond to the lowest three natural periods of vibration of the beam, indicating that the major contribution to the dynamic response arises from the participation of the first three natural modes.

(2) There is a striking similarity between the dynamic increment curves for D_c and M_c presented in Figs. 16b and 16d. Also the dynamic increment curve for moment over an interior support appears to be similar to that for reaction at the same support.

(3) Although the dynamic increment curves for deflection and moment shown in Figs. 16b and 16d are for all practical purposes equal, the amplification factors for moment and deflection, and the load positions for which these effects are maximum are different in the two cases. The maximum dynamic deflection is 10.2 percent larger than the maximum static deflection and it occurs when the load is slightly away from midspan. The maximum

dynamic moment is only 6.6 percent larger than the corresponding static moment and it occurs when the load is exactly at midspan. These differences are due to the fact that the shape of the static curves are different in the two cases.

17. Effect of Number of Mass Concentrations on Accuracy of Results

In order to investigate the accuracy of the solution obtained with seven mass concentrations, the problem considered in Art. 16 was also solved by using four mass concentrations ($n = 2$, $m = 3$). Both solutions were obtained for a time interval of integration of $T_o/600$, where T_o is the time required for the axle to cross the bridge, and results were evaluated and printed at intervals of $T_o/100$.

In Table 6 are listed the amplification factors for the two cases and the position of the axle producing the maximum effects. The tabulated values of the response are the largest among the printed values. It can be seen from this table that there are differences both in the values of the maximum effects and in the positions of the axle for which the maximum values are attained. The difference between corresponding amplification factors ranges from zero for D_1, to a maximum of 0.104 for M_4. It can be seen further that the magnitude of this difference increases as the value of ξ corresponding to the maximum effect increases.

The cause of this difference can be seen from Fig. 17 in which are plotted the history curves for M_4 for the two solutions and the corresponding dynamic increment curves. It can be seen that the dynamic increment curves are very similar, except for a phase shift which becomes progressively more pronounced as ξ increases. This phase shift is attributed to the fact that the natural periods of the two models are not the same. The lowest four natural periods are given in Table 7. Included in this table are also the corresponding periods for a beam with distributed mass. The latter values were computed by the method described in Ref. 32. It can be seen that whereas the fundamental periods for the two models are the same, the other periods differ slightly. If it is assumed that the period of the predominant waves in the dynamic increment curves in Fig. 17 is equal to the third natural period of the bridge, T_3, one finds that the phase difference between the two curves, $\Delta\xi$, is given by the expression

$$\Delta\xi = \frac{\Delta T_3}{T_3}\,\xi \tag{23}$$

where ΔT_3 is the difference in the values of the third natural period for the two models. For the case considered and $\xi = 1$, this equation gives

$$\Delta\xi = \frac{0.007}{0.269} = 0.03$$

which agrees with the phase shift shown in Fig. 17.

Since the shortest period of the predominant waves in the dynamic increment curves given in Figs. 16b through 16h appears to be equal to the third natural period of the beam, it is believed that the solution will be accurate if the lowest three natural periods of the analytical model used are in good agreement with those for the beam with distributed mass. Inasmuch as the natural periods of the model with $n = 3$ and $m = 4$ are close to those of the continuous beam, the results obtained from this model are believed to be sufficiently accurate. Because of limitations in the computer program, it was not possible to obtain solutions with a larger number of mass concentrations.

18. Effect of Speed

The system considered in Art. 16 was analyzed for values of the speed parameter, α, in the range between 0.12 and 0.18 at increment of 0.01. The values of the remaining parameters were considered to be the same as before.

The results of these analyses are presented in this article in the form of history curves and spectrum curves.

18.1 <u>History Curves</u>. To indicate the manner in which the response of the bridge is influenced by a small change in the value of the speed parameter, the history curves presented previously in Fig. 16d are compared in Fig. 18 with the corresponding curves obtained for a value of $\alpha = 0.16$ or 0.01 larger than for the previous case. This change in α corresponds to a change in vehicle speed of approximate 4 m.p.h. on the prototype bridge.

It can be seen from this comparison that the dynamic increment curves for the two cases are quite similar, except for a phase shift which appears to increase proportionally with ξ. The amplitudes of the waves in these curves appears to be somewhat larger for the larger value of α; however, the difference is of no practical consequence.

Considering that the time required for the vehicle to cross the bridge is inversely proportional to the speed parameter, α, and that the "periods" of the waves in the dynamic increment curves depend predominantly on the characteristics of the bridge, one finds that the effect of changing α by a small amount $\Delta\alpha$ is approximately the same as changing the scale of the ξ-axle by an amount $\Delta\alpha/\alpha$. In Fig. 18, if the dynamic increment curve for $\alpha = 0.15$ is conceived to be an elastic spring fixed at the left end, then the curve for $\alpha = 0.16$ may be obtained simply by displacing the right end of the spring to the right by an amount equal to

$$\frac{\Delta\alpha}{\alpha} = \frac{0.01}{0.15} = \frac{1}{15}$$

times the projected length of the spring. Having thus determined the dynamic increment curve for $\alpha = 0.16$, one may then obtain the curve for the dynamic bending moment by superposing the dynamic increment curve on the static moment curve. This technique, which obviously is applicable to any effect, may be used to study the influence of a small change in α, and is particularly useful in predicting approximately the value of α which will produce the maximum dynamic effect at a particular section.

In Fig. 19 are shown time histories of the dynamic increments for deflection at the center of the center span for values of α in the range between 0.12 and 0.18. These curves confirm the observations made previously. In particular, it can be seen that consecutive curves are generally quite similar and that an increase in α is equivalent to a "stretching" of the curve to the right. The waves which produce the maximum deflection at the center of the center span are shown shaded, and corresponding waves are identified by the same letter.

There is a marked increase in the amplitude of the waves in the dynamic increment curves as α increases from 0.12 to 0.18, the amplitudes for $\alpha = 0.18$ being roughly twice as large as those for $\alpha = 0.12$. The values of X_{aa} listed on the right hand margin represent the average values of the amplitudes of the waves for each curve. In evaluating these averages only waves with amplitudes in excess of 0.05 were considered. Associated with each value of X_{aa} is given the standard deviation, σ_{std}, of the amplitudes from the average value. This quantity is defined by the equation

$$\sigma_{std} = \sqrt{\frac{\Sigma(X_{aa} - X_a)^2}{N-1}} , \qquad (24)$$

where X_a represents the amplitudes of the individual waves considered and N the number of these waves; σ_{std} is a measure of the uniformity of the amplitudes. The smaller the value of σ_{std} the more homogeneous is the distribution of the amplitudes. It can be seen that X_{aa} increases from about 0.06 for $\alpha = 0.12$ to about 0.11 for $\alpha = 0.18$. The standard deviation is approximately 0.02.

18.2 <u>Spectrum Curves</u>. The amplification factors for deflection, moment and reaction for all the sections for which dynamic effects have been evaluated are plotted in Figs. 20a through 20k as a function of the speed parameter α. As previously noted, the term amplification factor is used to designate the ratio of the maximum dynamic effect at a section to the corresponding maximum static effect. The amplification factor curve for R_1 is omitted since for the smoothly moving, single-axle loading considered, it is equal to unity for all values of α. The numerical data used to plot these curves are also summarized in Table 8 together with the values of ξ for which the maximum effects occur and some additional information to be discussed later.

It can be seen from these curves that the amplification factors for the various effects are generally fairly small. The maximum amplification factor for deflections occurs at the side span and is equal to 1.17. The maximum amplification factor for positive moment is 1.15, and for negative moment over an interior support it is 1.22. It should be pointed out, however, that for a single-axle loading the maximum static moment over an interior support is comparatively small (see Table 5). The maximum amplification factor for reaction occurs over an interior pier and is 1.13.

The over-all characteristics of the curves in Figs. 20a through 20k are similar to those for simple span beams reported previously[(5),(10)]. The curves are undulatory in nature and the peak values of the undulations increase with increasing α. That the peak values should increase with increasing α follows from the fact that the amplitudes of the waves in the dynamic increment curves increase with increasing α. The nature of the undulations in these plots may be explained readily by examining these curves in the light of the corresponding dynamic increment curves. As an example consider the amplification factor for D_c (solid curve in Fig. 20b) and the corresponding dynamic increment curves presented in Fig. 19. Recalling the maximum static deflection at the center of the center span occurs when the load is at midspan, from the latter curves one finds that the wave which produces the maximum dynamic deflection at midspan is "wave a" when $\alpha = 0.12$ and 0.13, it is "wave b" when α is 0.14 through 0.17, and it is "wave c" when $\alpha = 0.18$. In the spectrum curve, the cusp at $\alpha = 0.138$ marks the transition between the condition for which "wave a" governs and the condition for which "wave b" governs. Similarly, the cusp at $\alpha = 0.171$ represents the transition between the cases for which "wave b" or wave c" governs. Between these cusps, the maximum amplification factor occurs at the value of α for which the peak of the wave which produces the maximum effect coincides with the maximum static effect. In the following discussion, the wave which for a particular case produces the maximum effect will be referred to as the "critical wave".

It is of interest to note that the length of the undulations in the spectrum curves are different for the different effects and sections considered. For example, the length of the undulation of the curve for D_c is smaller than that for D_1. A similar result is found on comparing the curves for M_1 and M_c. These differences arise from the fact that the positions of the "critical wave" in the dynamic increment curves for D_c and M_c are more sensitive to changes in the speed parameter α than for the curves of D_1 and M_1. If $\Delta\alpha$ represents the change in the speed parameter and $\Delta\xi$ represents the corresponding change in the position of the critical wave, then

$$\Delta\xi = \frac{\Delta\alpha}{\alpha}\,\xi_s \tag{25}$$

where ξ_s represents the position of the load for which the effect at the section considered is maximum. It follows that for a given value of α, the larger the value of ξ_s the more sensitive is the position of the critical wave to a given change in α and, consequently, the smaller is the length of the undulation in the corresponding spectrum curve.

19. Comparison of Effects at Neighboring Sections

In Fig. 21 the solid curves are the same as those presented in Fig. 16d. They represent the variation of the moment and the corresponding dynamic increment at the center of the center span for the system considered in Art. 16. The dotted curves show the variation of the corresponding quantities at a section for which $\xi = 0.485$. This section lies at a distance 0.05L to the left of the center of the center span and coincides with the position of the load for which the ordinate of the "critical wave" in the dynamic increment curve for M_c is maximum. The moment at this section is designated as M_n. Both moments and the corresponding dynamic increments are expressed in terms of the maximum static moment at the center of the center span. For clarity of presentation only that portion of the M_n curve close to midspan is shown.

It can be seen from this plot that the dynamic increment curves for the two sections are for all practical purposes identical. Furthermore, since the peak values of the two static curves are approximately the same, the maximum dynamic moment away from midspan is somewhat larger than that at midspan. To be specific, the amplification factor for M_c is 1.066 and the amplification factor for M_n is 1.093. It should be remembered that both amplification factors are expressed in terms of the maximum static moment at midspan.

The above comparison shows that the dynamic increment curve for a particular effect at a given section may be used to predict also the variation of that effect at a neighboring section. Furthermore, since the envelope of the maximum static effects in the vicinity of a section is generally fairly flat, the maximum amplification factor for that vicinity is approximately equal to one plus the amplitude of the "critical wave" for the particular section investigated. Obtained in this manner, the dashed-dotted line in Fig. 20b is believed to constitute a good approximation for the largest amplification factor close to midspan. It may be noted that this curve may be further approximated by a smooth curve which is tangent to the peaks of the actual spectrum curve for D_c (solid curve).

20. Effect of Weight Ratio

The bridge considered in Art. 16 was also analyzed for a value of $W/W_b = 0.3$ which represents a practical upper bound for present day vehicles and three-span I-beam bridges with center spans larger than about 50 ft. The speed parameter was varied between $\alpha = 0.12$ and 0.18. As before, the effect of bridge damping was neglected and the suspension spring of the vehicle was assumed to remain inactive. The frequency ratio f_v/f_b was taken equal to unity.

In Fig. 22 the time history of the deflection at the center of the center span and the history of the corresponding dynamic increment for $\alpha = 0.15$ are compared with the corresponding curves obtained previously for a weight ratio of 0.175. It can be seen that the over-all characteristics of the two sets of curves are similar and that the maximum values of the response do not differ appreciably. Similar results are obtained for the other effects.

The maximum values of the various effects that were evaluated and the corresponding values of ξ are listed in Table 8 together with the corresponding values for a weight ratio of 0.175. From an examination of these results it can be seen that the maximum effects are somewhat larger for the larger weight ratio. For convenience, the maximum amplification factors for the various effects are summarized in the following table. The values listed are the maxima for the complete range of speeds considered.

$\frac{W}{W_b}$	Largest Amplification Factor For					
	D_1 or D_4	D_c	M_1 or M_4	M_c	M_2 or M_3	Reactions
0.175	1.17	1.11	1.15	1.07	1.22	1.12
0.300	1.22	1.17	1.19	1.10	1.27	1.20

21. Effect of Frequency Ratio

The effect of this parameter was investigated by obtaining numerical solutions for values of f_v/f_b in the range between 0.5 and 1.5. The weight ratio and speed parameter used are: $W/W_b = 0.175$ and $\alpha = 0.18$. The remaining parameters are the same as for the problem discussed in Art. 16. The results are summarized in Figs. 23 to 25.

In Fig. 23 are shown the variations of the interacting force, P, for frequency ratios of 0.6, 1.0 and 1.5. It should be noted that in each case the dominant "period" of load variation is very close to the natural period of vibration of the axle. The maximum change in P is equal to 0.12 P_{st}. The amplification factor for the interacting force and the corresponding value of ξ are summaried in the following table.

f_v/f_b	0.5	0.6	0.7	0.8	0.9	1.0	1.25	1.5
A.F. for P	1.11	1.07	1.07	1.07	1.09	1.06	1.09	1.12
ξ	0.52	0.90	0.83	0.17	0.46	0.87	0.88	0.86

In Fig. 24 are shown dynamic increment curves for D_c for all the frequency ratios considered. It can be seen that for values of f_v/f_b less than 0.8, the curves do not exhibit high frequency oscillations and that the period of the predominant oscillations is close to the fundamental period of vibration of the bridge. The same is true of the curve corresponding to a value of $f_v/f_b = 1.5$. For intermediate cases, the contribution of higher modes becomes more pronounced. The high frequency oscillations present in the curves for values of f_v/f_b between 0.8 and 1.5 correspond to the higher natural modes of vibration of the bridge. It is important to note that the magnitude of the oscillations in these curves are about the same for all the cases. In particular, the oscillations for $f_v/f_b = 1.0$ are no larger than those for the other frequency ratios. The average value, X_{aa}, of the amplitude of the waves for each dynamic increment curve and the standard deviation, σ_{std}, are given on the right hand margin of Figs. 24a and 24b. It can be seen that the values of X_{aa} are fairly constant and close to 0.12. The values of σ_{std} are approximately equal to 0.04.

In Figs. 25a through 25k the amplification factors for the various effects are plotted as a function of the frequency ratio. The maximum values of these amplification factors are listed in the following table together with the corresponding values obtained for the set of the problems presented in Art. 18 for which $f_v/f_b = 1$ and the speed parameter α ranged between 0.12 and 0.18. It can be seen that the two sets of solutions are for all practical

Variable	Largest Amplification Factor For					
	D_1 or D_4	D_c	M_1 or M_4	M_c	M_2 or M_3	Reactions
f_v/f_b	1.18	1.15	1.15	1.14	1.26	1.15
α	1.17	1.13	1.15	1.08	1.22	1.13

purposes the same. The largest difference occurs in the case of M_c. In this connection it is worth noting from Fig. 20f that, for values of α between 0.18 and 0.20, the A.F. is likely to be as high as 1.14. It appears from these results that, whereas the amplification factor for a particular effect at a section of a bridge may be sensitive to a change in the frequency ratio, the maximum value of this amplification factor for a range of speeds may be considered to be independent of the frequency ratio. It is to be emphasized that this conclusion is applicable only to smoothly moving loads.

22. Effect of Initial Vehicle Oscillation and Interleaf Friction

The response of the three-span bridge considered before was also investigated under the passage of an initially oscillating single-axle loading. The initial oscillation was assumed to be such that at the instant the load enters the span, the bouncing velocity of the sprung mass is equal to zero and the interacting force, P, is equal to 0.70 P_{st}. The weight ratio and the speed parameter was taken as follows:

$$W/W_b = 0.175 \text{ and } \alpha = 0.15$$

Solutions were obtained for three different values of the coefficient of interleaf friction: $\mu = \infty$, $\mu = 0$ and $\mu = 0.15$.

As explained previously, for $\mu = \infty$ the suspension spring remains idle and the vehicle oscillates on its tires only. For $\mu = 0$, the suspension spring acts in series with the tire spring. The frequency ratios for the system were

$$f_t/f_b = 1.0 \text{ and } f_{ts}/f_b = 0.6$$

For the case of $\mu = 0.15$, the initial value of the frictional force in the suspension spring was assumed to be equal to zero.

Representative results for these solutions are given in Figs. 26 through 28. The solid curve and the dashed-dotted curve in Fig. 26 show the variation of the interacting force for $\mu = \infty$ ($f_v/f_b = 1$) and $\mu = 0$ ($f_v/f_b = 0.6$), respectively. In both cases the "period" of the load variation corresponds to the natural period of vibration of the load. It should be noted that, whereas for $f_v/f_b = 1$ the amplitude of the force varies continuously, for $f_v/f_b = 0.6$ it is approximately constant. It appears that when the frequency ratio f_v/f_b

is small compared to unity and the initial oscillation is of the order of magnitude considered in this example, the load unit may be approximated by a constant moving force equal to the weight of the vehicle combined with an alternating force. It is worth noting further that the amplitude of the variation in P when the load is close to midspan is about 0.26 P_{st} for both cases.

The dotted curve in Fig. 26 shows the time history of P for $\mu = 0.15$. In addition, the diagram on the right hand shows the variation of the frictional force in the suspension system as a function of the total shortening of the springs, u. Both quantities are expressed in dimensionless forms. Corresponding points on the two diagrams are identified by the same letter. For example, at the instant represented by point a the frictional resistance of the suspension spring becomes fully mobilized and the effective stiffness of the system changes from k_t to k_{ts}. From these diagrams it can be seen that the suspension spring is engaged only in the intervals ab, cd, fg and ij. Of course, the frequency of load variation in these intervals is f_{ts}. It is important to note that the history curve of P for $\mu = 0.15$ has no resemblance to the corresponding curve for $\mu = \infty$ or $\mu = 0$. The most important effect of the interleaf friction is the reduction in the amplitude of the load variation. This reduction is due to the fact that in the intervals ab, cd, fg and ij, energy is dissipated by the frictional force in the spring. For $\mu = 0.15$ the maximum amplitude of variation in P when the load is in the neighborhood of midspan is 0.15. This value should be compared with the value of 0.26 when $\mu = 0$ or $\mu = \infty$.

In Fig. 27 are shown time histories of the dynamic increment for deflection at the center of the center span for the three values of μ considered. The corresponding curves for moment are very similar, but are not presented here. It is of interest to note that for $f_v/f_b = 0.6$, the "periods" of the waves are between the natural period of the load and the fundamental period of vibration of the bridge. In fact, they appear to be closer to the period of the bridge. This result should be contrasted with the fact that the period of variation of the interacting force is close to the natural period of the load. The largest amplitude of the curves for $\mu = 0$ and $\mu = \infty$ is about 43 percent of the maximum static deflection. Obviously these effects are large. For $\mu = 0.15$, because of the energy dissipated in the suspension spring, this amplitude is reduced by over 40 percent or to a value of 23 percent of the maximum static deflection.

In Figs. 28a through 28d are shown history curves for D_c, M_2, M_c and R_2. The amplification factors for the various effects and the corresponding values of ξ are listed in the last three columns of Table 9. It may be observed that for this particular set of problems, the largest amplification factors are generally obtained for $\mu = 0$ and the smallest for $\mu = \infty$. However, it should not be inferred that the condition $\mu = 0$ is generally more severe than $\mu = \infty$ or that the amplification factor for $\mu = 0.15$ is, in general, larger than for $\mu = \infty$. This may be appreciated by considering, as an example, the curve given in Fig. 28a and the corresponding dynamic increment curve presented in Fig. 27. It can be seen that for $\mu = 0$ and for $\mu = 0.15$ the peak values of the dynamic increment curves are almost coincident with the peak value of the static curve, whereas for $\mu = \infty$ the peak static value combined with a relatively small ordinate of the dynamic increment curve. The principal effect of a small change in either the speed, frequency or initial condition of the vehicle is to displace the waves of these curves along the ξ-axis. Since the peak amplitudes of the waves for both $\mu = 0$ and $\mu = \infty$ are approximately the same and appreciably larger than those for $\mu = 0.15$, it is expected that, within a range of speeds, frequencies and initial conditions, the smallest effects will correspond to $\mu = 0.15$.

23. Effect of Bridge Damping

Although information on the damping characteristics of continuous bridges is scarce, the limited data available[14] suggest that a reasonable value for the damping factor c/c_{cr} is about 0.01. The problem considered in the preceding article was reanalyzed for $c/c_{cr} = 0.01$, using $\mu = \infty$. In Fig. 29 the time history of the interacting force is compared with that determined previously by neglecting the effect of bridge damping. In Figs. 30 and 31 are given the time histories of the deflection D_c and of the corresponding dynamic increment. The maximum values of the computed effects and the corresponding values of ξ are summarized in the first column of Table 9.

It can be seen from the curves presented in Figs. 29 through 31 that the principal effect of bridge damping is to reduce the amplitude of the oscillation in the response curves. As might be expected, the reduction in the amplitudes increases with increasing time, or increasing value of ξ. It follows that the effect of bridge damping on the amplification factors will be most pronounced in those cases for which the maximum effects occur at a large value of ξ. This fact may be seen by comparing the results presented in the first two columns of Table 9. In general, one finds that the reduction is small and, unless there is reason for considering larger values of c/c_{cr}, it appears that the effect of bridge damping may be neglected. Obviously, additional solutions are necessary to substantiate this conclusion.

24. Effect of Multiple-Axle Loadings

24.1 Solutions for a Two-Axle Loading. The solutions presented in this article are for a three-span bridge without damping traversed by a smoothly moving two-axle loading. As before, the weight ratio is taken equal to 0.175; however, in this case the total weight of the vehicle, W, is assumed to be equally supported by the two axles. The axle spacing, ℓ, and the dynamic index, i, are taken as follows:

$$\ell/L = 0.3, \text{ and } i = 1.$$

The speed parameter, α, was varied between 0.12 and 0.18.

In Figs. 32a through 32f are shown time histories of the interacting forces, P_1 and P_2, and of deflection, moments and reaction at selected sections and of the corresponding dynamic increments. These results are for $\alpha = 0.15$. Included in Figs. 32b and 32d are also portions of the history curves for values of $\alpha = 0.16$, 0.17 and 0.18. In these curves the abscissa ξ defines the position of the front axle. A value of $\xi = 1$ corresponds to the instant the front axle leaves the bridge.

In Fig. 32a it can be seen that the maximum variation in the interacting force is about 7.5 percent of the static value and occurs for the rear axle. This variation is about the same as for the single-axle solution presented in Art. 16. The characteristics of the dynamic increment curves in Figs. 32b through 32f are very similar to those presented in Figs. 16b through 16h for a single-axle loading, and the comments made previously are also applicable in this case.

In Fig. 33 are shown the dynamic increment curves for deflection at the center of the center span for values of α in the range between 0.12 and 0.18. Obviously, the observation made previously in connection with the curves presented in Fig. 19 applies also to those curves. It is particularly important to note that the values of X_{aa} and σ_{std} listed on the right hand margin are generally very similar to the corresponding values given in Fig. 19 for the single-axle loading. It appears that, within a range of speeds, the maximum effects for the two-axle loading and the single-axle loading will probably be the same.

For $\alpha = 0.15$, the time between the passage of the two axles over a point on the bridge is equal to the fundamental natural period of vibration of the unloaded bridge. This coincidence of the period of application of the axle loads with the natural period of the bridge has been considered to produce a condition of resonance which may lead to large dynamic effects[10]. It is noteworthy that the dynamic increment curves for this case ($\alpha = 0.15$) do not exhibit any unusually larger oscillations.

The maximum values of the various effects evaluated are plotted in Figs. 34a through 34ℓ in the form of amplification factors as a function of α. These values are also tabulated in Table 10 together with the corresponding values of ξ. The corresponding maximum static values are given in the second column of Table 5. The general features of these spectrum curves are the same as those for the single-axle loading presented in Fig. 20. However, the detailed characteristics differ primarily because of the fact that the static history curves for the two cases are different. For example, it may be noted that the curve for M_c in Fig. 32d is flatter than the corresponding curves for the single-axle loading presented in Fig. 16d. Referring to Fig. 32d, one finds that the ordinates of the static history curve for the two-axle loading are fairly constant in the neighborhood of midspan, whereas the corresponding curves for the single-axle loading shown in Fig. 16d exhibit a sharp cusp. It follows that in the former case the maximum dynamic value of M_c is less sensitive to a change in α. It may be recalled that a small increase in α is equivalent to a "stretching" of the dynamic increment curve.

For the range of α considered the largest amplification factors for the various effects are summarized in the following table for both the single-axle loading and for the two-axle loading.

Item	Largest A. F.	
	Single-axle	Two-axle
Side Span Deflections, D_1 and D_4	1.17	1.17
Center Span Deflection, D_c	1.13	1.17
Side Span Positive Moments, M_1 and M_4	1.15	1.15
Center Span Positive Moment, M_c	1.08	1.12
Negative Moments over interior supports, M_2 and M_3	1.22	1.11
Reactions at End Supports, R_1 and R_4	1.04	1.05
Reactions at Interior Supports, R_2 and R_3	1.13	1.11

It can be seen that the two sets of values are in general quite similar.

24.2 Solution for a Three-axle Loading. In Figs. 35a through 35f are given history curves for the response of the bridge considered in the preceding article when traversed by a smoothly moving three-axle tractor-trailer combination with a speed corresponding to a value of $\alpha = 0.15$. The parameters for the trailer are considered to be the same as those for the two-axle loading considered before. The weight of the front axle is considered to be 1/9 of the total weight of the vehicle. The values of the remaining parameters for the first axle are identified in the figures. In these figures, time is measured from the instant the front axle enters the bridge. Accordingly, ξ defines the position of the front axle.

It is of interest to compare the dynamic increment curves for this problem with the corresponding curves for the two-axle loading starting from the instant the first heavy axle (second axle for the three-axle load) moves onto the bridge. To effect this comparison, the curves for the three-axle loading must be shifted to the left by an amount equivalent to the axle spacing of the tractor; this corresponds to a value of $\xi = 0.0462$. One then finds that the two sets of curves are practically identical. The amplification factors for the various effects and the corresponding values of ξ are compared in Table 11. It can be seen that the two sets of results are for all practical purposes equal.

25. Correlation Between Dynamic Increments for Deflection and Moment

In discussing the effect of a single-axle loading in Art. 16, it was noted that the dynamic increment curve for moment at the center of the center span is similar to the corresponding curve for deflection. This similarity is true also for multiple-axle loadings. This is illustrated in Fig. 36 wherein the dynamic increment curves for midspan moment for three different loadings are compared with the corresponding curves for deflection. In the following paragraphs it is shown that under certain broad conditions the dynamic increments for deflection and moment at the same point are linearly correlated.

Let the deflection of the beam, y, be expressed by the equation,

$$y(x,t) = y_s(x,t) + \sum_{n=1}^{\infty} \varphi_n(x)\, q_n(t) \tag{26}$$

where y_s denotes the static deflection, φ_n^* is the n^{th} natural mode, and q_n is an arbitrary function of time. Since the position of the vehicle on the bridge is a function of time, the deflection y_s is also a time dependent quantity. For each span, the expression for the natural mode may be written in the form:

---

* Refer to Eq. 117 on p. 325 in Reference 33.

$$\varphi_n(x) = A_n \sin \lambda_n \frac{x}{L} + B_n \cos \lambda_n \frac{x}{L} + C_n \operatorname{Sinh} \lambda_n \frac{x}{L} + D_n \operatorname{Cosh} \lambda_n \frac{x}{L} \tag{27}$$

where A_n through D_n are constants of integration, generally different for each span, x is the distance from a support, λ_n is a dimensionless coefficient, related to the n^{th} natural circular frequency of vibration of the beam, ω_n, by the equation

$$\lambda_n^4 = \frac{\rho L^4}{EI} \omega_n^2 \quad .$$

Then the bending moment in each span, M, is given by the equation.

$$M = - EI\, y'' = - EI\, y_s'' - EI \sum_{n=1}^{\infty} \varphi_n''\, q_n ,$$

where a prime superscript denotes one differentiation with respect to x. Noting that the first term on the extreme right hand expression represents the static moment, M_s, and making use of Eq. 27, one obtains,

$$M = M_s + \lambda_1^2 \frac{EI}{L^2} \sum_{n=1}^{\infty} \left(\frac{\lambda_n}{\lambda_1} \right)^2 \left(\varphi_n - 2\, C_n \operatorname{Sinh} \lambda_n \frac{x}{L} - 2\, D_n \operatorname{Cosh} \lambda_n \frac{x}{L}\right) \tag{28}$$

Then the ratio of the dynamic increment for moment to the corresponding increment for deflection may be written as follows:

$$\frac{M - M_s}{y - y_s} = \lambda_1^2 \frac{EI}{L^2} (1 + \epsilon) \tag{29}$$

where

$$\epsilon = \frac{1}{\sum_{n=1}^{\infty} \varphi_n\, q_n} \sum_{n=1}^{\infty} \left[\left(\frac{\omega_n}{\omega_1} - 1\right)\varphi_n - 2\, \frac{\omega_n}{\omega_1} \left(C_n \operatorname{Sinh} \lambda_n \frac{x}{L} + D_n \operatorname{Cosh} \lambda_n \frac{x}{L}\right) \right] q_n \tag{30}$$

It is assumed that the denominator is different from zero.

Let $(D.I.)_M$ be the dynamic increment for moment for a specified section, expressed in terms of the maximum static moment at that section, $(M_s)_m$. Also let $(D.I.)_y$ be the corresponding increment for deflection in terms of the corresponding maximum static deflection, $(y_s)_m$. Then

$$\frac{(D.I.)_M}{(D.I.)_y} = \lambda_1^2 \frac{EI}{L^2} \frac{(y_s)_m}{(M_s)_m} (1 + \epsilon) \tag{31}$$

This expression is applicable to any point of the beam, and there is no restriction as to the type of the bridge or the number of axles involved.

Now, if the coefficients, C_1 and D_1 for the fundamental mode of vibration are small and, in addition, the functions q_n for $n > 1$ are negligible in comparison to the function q_1, then the quantity ϵ defined by Eq. 30 may be neglected. These conditions are satisfied for simple span bridges, since C_n and D_n are identically equal to zero and the contribution of the higher modes of vibration are known to be insignificant (i.e., q_n for $n > 1$ may be neglected). For this case, recalling that $\lambda = \pi$, one finds that Eq. 31 reduces to

$$\frac{(D.I.)_M}{(D.I.)_y} \approx \pi^2 \frac{EI}{L^2} \frac{(y_s)_m}{(M_s)_m} \tag{32}$$

As an example, consider a two-axle vehicle with the same weight on each axle and traversing a simple span bridge. For the center of the bridge, Eq. 32 gives

$$\frac{(D.I.)_M}{(D.I.)_y} \approx \frac{\pi^2}{24} (2 + 2s - s^2), \quad \text{for } s \leq \frac{1}{2} \tag{33}$$

where s is the ratio of the axle spacing to the span length. For a single axle loading, $s = 0$, and the above expression reduces to

$$\frac{(D.I.)_M}{(D.I.)_y} \approx \frac{\pi^2}{12} \tag{34}$$

The latter expression has been used previously by Biggs[16] to relate the maximum dynamic increment for moment and deflection at midspan for a bridge traversed by a single-axle loading.

For three-span continuous bridges, C_1 and D_1 are identically equal to zero only if the spans are equal. Furthermore, since q_2 may not be small in comparison to q_1, the quantity ϵ in Eq. (29) may not be negligible in comparison to unity. However, it is of some interest to correlate the computed dynamic increment for moment and deflection and to compare the results with those obtained from Eq. 29 assuming that $\epsilon = 0$.

The scatter diagram presented in Fig. 37 correlates the dynamic increments for moment and deflection at the center of the center span for the system considered in Art. 24.2. Each point in this diagram defines the values of the two increments for a particular time. It can be seen that the points fall on a straight line, indicating that the quantity ϵ in Eq. 29 may be considered as a constant. The equation of the line, determined by the method of least squares, is

$$(D.I.)_M = 1.04(D.I.)_y + 0.000 \tag{35}$$

and has a standard error of estimation* of 0.003.

For this problem, the maximum static effects at the center of the center span are

$$(y_s)_m = 0.00867\ WL^3/EI, \qquad (M_s)_m = 0.1072\ WL$$

and $\lambda^2 = 12.491$.

Then with $\epsilon = 0$, Eq. 29 leads to

$$(D.I.)_M = 1.01\ (D.I.)_y \tag{36}$$

---

* This means that 68% of values of $(D.I.)_M$ estimated by Eq. 35 are in error by less than 0.003.

The close agreement between Eqs. 35 and 36 suggests that the quantity ϵ may be considered to be negligible. However, further study of this point is necessary to substantiate this preliminary conclusion.

In Figs. 38 and 39 the dynamic increment curves for bending moment over the interior supports are compared with the increment curves for reaction at the corresponding supports. These results are for the problem considered in Arts. 16, 24.1 and 24.2 when $\alpha = 0.15$. It appears that the two sets of dynamic increments are also linearly correlated, except perhaps for the instant when the load is close to the support for which the dynamic increments are evaluated.

26. A Possible Basis for Design

While the information presented in the preceding articles is not directly applicable to design, it suggests means of arriving at a design procedure for dynamic effects in highway bridges. In this connection it should be kept in mind that the values of the majority of the parameters that influence the response of highway bridges cannot, in general, be controlled. A bridge in service is subjected to the passage of vehicles having different weights, frequencies and dimensions. Moreover, the speeds of the vehicles are neither constant nor uniform, and the initial conditions of the bridge and the vehicle and the conditions of the bridge surface are generally unknown. The fact must also be considered that the characteristics of known vehicles and known bridges cannot be calculated accurately. Under these conditions, it is meaningful to attempt to estimate only the values of the maximum effects produced under the most unfavorable but likely combinations of the parameters involved.

From the information presented in this report, it appears that a design procedure can be formulated most effectively on the basis of the dynamic increment curves rather than the spectrum curves. The reason for this is that the dynamic increment curves, as previously explained, provide more useful information than the spectrum curves and show more clearly the influence and relative importance of the various parameters involved.

Although the detailed characteristics of the dynamic increment curves are generally quite sensitive to changes in the various parameters entering into the problem, the over-all characteristics of these curves are affected only to a minor extent by changes in some of the parameters. It appears reasonable, therefore, to take as a basis for design some average property of the dynamic increment curves. For a given section of the bridge, the design value of the dynamic increment for moment or deflection, $(D.I.)_d$, may then be expressed in the form,

$$(D.I.)_d = X_{aa} + e\,\sigma_{std} \tag{37}$$

where $(D.I.)_d$ is equivalent to the impact factor, X_{aa} and σ_{std} are as previously defined, and e is a factor which, for a given set of dynamic increment curves, defines the percentage of the waves for which the amplitudes are smaller than the computed value of $(D.I.)_d$. The latter statement is based on the assumption that the amplitudes of waves are normally distributed. The values of these percentages for different values of e can be found in standard texts on statistics[34]. For e = 0, 1, 2 and 3, these percentages are 50, 84.1, 97.7 and 99.8, respectively.

In Eq. 37 the choice of the value of e should be governed by the shape of the curve for the static effect at the section considered. If the curve is flat in the neighborhood the maximum static effect, then the possibility of having a large dynamic effect at that section is great, provided of course that all other factors are the same. On the other hand, if the static curve exhibits a sharp cusp, there is a smaller possibility of having a large dynamic effect at that section. Therefore, the flatter the static curve is, the larger must be the value of e. For a flat curve, a value of e between 2.5 and 3 is recommended, while for curves which are steep in the region of the maximum effect a value of e from 1.5 to 2 appears to be reasonable.

Strictly speaking, the values of X_{aa} and σ_{std} are functions of all the parameters considered in the previous articles. However, because they are insensitive to changes in some of the parameters, these quantities can be determined from a relatively small number of solutions. For example, for smoothly moving loads it has been shown that the most significant variable is the speed parameter α and that both X_{aa} and σ_{std} increase with increasing α. On the other hand, the value of these quantities appear insensitive to changes in the frequency ratio, weight ratio, and the number of axles involved, provided these parameters are within the practical range. Under these conditions, it appears that for a given type of bridge the values of X_{aa} and σ_{std} in Eq. 37 may be determined from the dynamic increment curve for a solution determined as follows: The speed parameter must correspond to the maximum vehicle speed expected; the weight ratio must preferably correspond to the maximum design load, the frequency ratio may have any reasonable value, and the vehicle may be represented by a single-axle loading.

In this presentation the problem has been over-simplified by neglecting the effect of a possible initial oscillation of the vehicle. It has been shown both here and elsewhere[5],[6] that this effect may be quite important. Obviously then, the values of X_{aa} and σ_{std} will depend both on the magnitude of the initial oscillation and the value of the limiting frictional force in the suspension system of the vehicle. Additional studies are necessary to investigate the dependence of X_{aa} and σ_{std} on these quantities. Consideration should also be given to the influence of roadway unevenness. In this connection field measurements are needed to provide realistic values for the magnitudes of initial vehicle oscillations and the magnitude of roadway unevenness for different types of bridges.

27. Pedestrian's Reaction to Bridge Vibration

One aspect of the problem of bridge vibration relates to the reaction of pedestrians to the motion of the bridge. From the limited data that are available[(29),(35)] it appears that the reaction of a person to vibration depends primarily on the rate of change of acceleration, ordinarily referred to as the "jerk", instead of only on the magnitude of the deflection. In Refs. (28) and (29) limiting values are given for zones of human comfort and discomfort for vertical sinusoidal vibration. Values of "jerk" less than 700 in./sec.^{3} (or 1.8g/sec.) are considered to define a zone of comfort, values between 700 in./sec.^{3} and 2400 in./sec.^{3} (or 6.2 g/sec.) define a zone of discomfort, and values greater than 6.2 g/sec. define a zone of extreme discomfort. For the design of trucks, an upper value of 500 in./sec.^{3} (1.3g/sec.) has been recommended[(29)].

Figure 40 shows the variation of "jerk" at the center of the center span for the problem considered in Art. 24.2. The ordinate of the curve shows the "jerk" that would be experienced by a person standing at the center of the center span. The physical system considered is a standard 64'-80'-64' I-beam bridge[(36)] traversed by a "typical" H20-S16 tractor-trailer combination. The speed parameter corresponds to a speed of 61 m.p.h. This curve was evaluated by the method of finite difference from the history curve for D_c presented in Fig. 35b. It is of interest to note that the maximum value of "jerk" is less than the recommended limit of comfort. It is noted further that the predominant "period" of the oscillations in this curve is very close to the third natural period of the unloaded bridge.

VI. SUMMARY

A numerical method has been presented for the computation of the response of continuous bridges subjected to the action of moving vehicles. In this study the bridge has been idealized as a continuous beam with distributed flexibility and concentrated point masses, and the vehicle has been represented as a sprung load unit having one, two or three axles. An important feature of the vehicle model used is that it incorporates the effect of interleaf friction for the suspension system.

Computer programs have been prepared for use on the ILLIAC, the digital computer of the University of Illinois. These programs are for three-span continuous bridges of uniform cross section and equal side spans and for a single vehicle.

Numerical solutions have been obtained for a range of the parameters entering into the problem. For smoothly moving vehicles, the parameters studied include the speed parameter, α, the frequency ratio, f_v/f_b, the weight ratio, W/W_b, and the number of axles of the vehicle model. For a single-axle loading, one series of problems were studied for values of α between 0.12 and 0.18, with the frequency ratio taken equal to one and the weight ratio taken equal to 0.175 and 0.30. In a second series of problems, the frequency ratio was varied between 0.5 and 1.5, with the speed parameter and the weight ratio taken equal to 0.18 and 0.175, respectively. For a two-axle load unit, a set of problems were solved for values of α between 0.12 and 0.18, with the frequency ratio for each axle equal to one and $W/W_b = 0.175$. Only one solution was obtained for a three-axle loading. For a vehicle having an initial bouncing motion, the major factors investigated were the role of the interleaf friction and the effect of bridge damping.

The major conclusions drawn from these solutions are briefly as follows:

(1) For the solutions involving a smoothly moving vehicle, the maximum variation in the interacting force between the vehicle and the bridge is approximately 12 percent of the static reaction. For ordinary vehicles the coefficient of friction for the suspension system is generally greater than 12 percent. Accordingly, for the conditions considered the suspension springs do not engage and the vehicle vibrates only on its tire springs.

(2) If for any reason, such as a large initial vehicle oscillation or an irregularity in the roadway surface, the variation of the interacting force is large enough to engage the suspension springs, then it is important that the effect of the interleaf friction be considered in the solution. Unless this is done, the over-all characteristics of the computed response may be quite unrealistic.

(3) Both for smoothly moving loads and for initially oscillating loads the predominant period of variation of the interacting forces is close to the natural period (or periods) of vibration of the vehicle.

(4) From an examination of the dynamic increment curves for the various effects at different sections of the bridge, it follows that the major contribution to the dynamic response arises from the participation of the first three natural modes of vibration of the bridge.

(5) For smoothly moving loads, the amplification factors for the various effects are generally fairly small. For the complete range of parameters considered, the maximum amplification factors are 1.18 for deflection, 1.15 for positive moment, 1.26 for negative moment, and 1.15 for reaction.

(6) For smoothly moving loads, the most significant variable is the speed parameter α. In general the larger the α, the larger is the amplitudes of the waves in the dynamic increment curves, and, consequently, the greater

are likely to be the dynamic effects. Although the detailed characteristics of the dynamic increment curves and the spectrum curves may be sensitive to variations in the other parameters, the over-all characteristics of the curves are affected only to a minor extent by changes in the frequency ratio, weight ratio, and the number of axles, provided that these variations are kept within the practical range. Therefore, for design purposes the latter parameters may be considered to be secondary.

(7) For an initially oscillating vehicle, the magnitudes of the maximum effects in the bridge depend predominately on the amplitude of the initial oscillation and on the limiting value of the interleaf frictional force. The over-all effect of this frictional force is to dissipate energy and to reduce the magnitude of the dynamic effects.

(8) The effect of bridge damping appears to be negligible for values of $c/c_{cr} \leq 0.01$.

(9) There is a linear relationship between the dynamic increments for moment and deflection for a section of the bridge away from a support. Accordingly, if the history curve for deflection at a section is known, the corresponding curve for moment can be estimated. It appears, moreover, that the dynamic increment for moment over an interior support is linearly correlated with the corresponding increment for reaction at the same support.

BIBLIOGRAPHY

1. Hillerborg, A., "Dynamic Influences of Smoothly Running Loads on Simply Supported Girders," Institution of Structural Engineering and Bridge Building of the Royal Institute of Technology, Stockholm, Sweden, 1951.

2. Biggs, J. M., "Vibration Measurements on Simple-Span Bridges," Highway Research Board, Bulletin 124, 1956, pp. 1-15.

3. Scheffey, C. F., "Dynamic Load Analysis and Design of Highway Bridges," Highway Research Board, Bulletin 124, 1956, pp. 16-32.

4. Foster, G. M., and Oehler, L. T., "Vibration and Deflection of Rolled-Beam and Plate-Girder Bridges," Highway Research Board Bulletin 124, 1956, pp. 79-110.

5. Tung, T. P., Goodman, L. E., Chen, T. Y., and Newmark, N. M., "Highway Bridge Impact Problems," Highway Research Board, Bulletin 124, 1956, pp. 111-134.

6. Milley, W. H., "Experimental Studies of Dynamic Effects of Smoothly Rolling Loads on Simply-Supported Beams," M. S. Thesis, University of Illinois, 1952.

7. Boehning, R. H., "Single and Tandem Axle Dynamic Effects on a Highway Bridge Model," Civil Engineering Studies, Structural Research Series No. 57, University of Illinois, 1953.

8. Taylor, J. E., "Influence of Vehicle Suspensions on Highway Bridge Impact," M. S. Thesis, University of Illinois, 1953.

9. Eichmann, E. S., "Influence of Vehicle Suspensions on Highway Bridge Impact," Civil Engineering Studies, Structural Research Series No. 70, University of Illinois, 1954.

10. Wen, K. L., "Dynamic Behavior of Simple-Span Highway Bridges Traversed by Two-Axle Vehicles," Civil Engineering Studies, Structural Research Series No. 142, University of Illinois, 1957.

11. Toledo-Leyva, J., and Veletsos, A. S., "Effects of Roadway Unevenness on Dynamic Response of Simple Span Highway Bridges," Civil Engineering Studies, Structural Research Series No. 168, University of Illinois, 1958.

12. Prince-Alfaro, J., and Veletsos, A. S., "Dynamic Behavior of an I-Beam Bridge Model Under a Smoothly Rolling Load," Civil Engineering Studies, Structural Research Series No. 167, University of Illinois, 1958.

13. Ayre, R. S., and Jacobsen, L. S., "Transverse Vibration of a Two-Span Beam Under the Action of a Moving Alternating Force," Journal of Applied Mechanics, vol. 17, 1950, pp. 283-290.

14. Oehler, LeRoy T., "Vibration Susceptibilities of Various Highway Bridge Types," Michigan State Highway Department, Research Laboratory Testing and Research Division, Report No. 272, January 1957. See also, Proceedings, ASCE, Paper 1318, July 1957.

15. Looney, C. T. G., "High-Speed Computer Applied to Bridge Impact," Proceedings, ASCE, Paper 1759, September 1958.

16. Biggs, J. M., Suer, H. S., and Louw, J. M., "Vibration of Simple-Span Highway Bridges," Transactions, ASCE, Paper No. 2979, 1959, pp. 291-318.

17. Ayre, R. S., Ford, G., and Jacobsen, L. S., "Transverse Vibration of a Two-Span Beam under Action of a Moving Constant Force," Journal of Applied Mechanics, vol. 17, 1950, pp. 1-12.

18. Ayre, R. S., Jacobsen, L. S., and Hsu, C. S., "Transverse Vibration of One- and of Two-Span Beams under the Action of a Moving Mass Load," Proceeding of First U. S. National Congress on Applied Mechanics, 1951, pp. 81-90.

19. Jacobsen, L. S., and Ayre, R. S., "Transverse Vibration of One- and of Two-Span Beams under the Combined Action of a Moving Mass Load and a Moving Alternating Force," Stanford University, Structural Dynamics Tech. Rept. 10, 1950.

20. Jacobsen, L. S., and Ayre, R. S., "Transverse Vibration of One- and of Two-Span Beams under the Action of a Moving Combined Load Consisting of a Spring-Borne Mass and an Alternating Force," Stanford University, Structural Dynamics Tech. Rept. 12, 1951.

21. Jacobsen, L. S., and Ayre, R. S., "Transverse Vibration of Multi-Span Continuous Beams under the Action of a Moving Alternating Force," Stanford University, Structural Dynamics Tech. Rept. 15, 1951.

22. Louw, J. M., "Dynamic Response of Continuous Span Highway Bridges to Moving Vehicle Loads," Thesis for Doctor of Science Degree, Massachusetts Institute of Technology, 1958.

23. Chen, W. L., and Koetje, E. L., "Model Investigation of the Vibration of Continuous Three-Span Steel Bridges," M. S. Thesis, Massachusetts Institute of Technology, 1958.

24. Vandegrift, L. E., "Vibration Studies of Continuous Span Bridges," Bulletin 119, Engineering Experiment Station, Ohio State University, 1944.

25. Edgerton, R. C., and Beecroft, G. W., "Dynamic Studies of Two Continuous Plate-Girder Bridges," Highway Research Board, Bulletin 124, 1956, pp. 33-46.

26. Hayes, J. M., and Sbarounis, J. A., "Vibration Study of Three-Span Continuous I-Beam Bridge," Highway Research Board, Bulletin 124, 1956, pp. 47-78.

27. Edgerton, R. C., and Beecroft, G. W., "Dynamic Stresses in Continuous Plate Girder Bridges," Transactions, ASCE, vol. 123, 1958, pp. 266-292.

28. "Tractor-Trailer Ride," Technical Board of Society of Automotive Engineers, Inc., 485 Lexington Ave., New York 17, New York.

29. Janeway, R. N., "A Better Truck Ride for Driver and Cargo," A report given at the 1958 Annual Meeting of The Society of Automotive Engineers, Inc., 485 Lexington Ave., New York 17, New York.

30. Lin, T. Y., "A Direct Method of Moment Distribution," Transactions of ASCE, vol. 102, 1937, pp. 561-571.

31. Newmark, N. M., "A Method of Computation of Structural Dynamics," Journal of Engineering Mechanics Division, Proceedings, ASCE, July 1959, pp. 67-94.

32. Veletsos, A. S., Newmark, N. M., "Natural Frequencies of Continuous Flexural Members," Transactions, ASCE, vol. 122, 1957, pp. 249-278.

33. Timoshenko, S., "Vibration Problems in Engineering," 3rd edition, D. Van Nostrand Co., New York, 1955.

34. Waugh, A. E., "Statistical Tables and Problems," McGraw-Hill Co., New York, 1952.

35. Meister, F. J., "Die Empfindlichkeit des Menschen gegen Erschutterungen," Forschung auf dem Gebiete des Ingenieurwesens, vol. 6, 1935, Berlin, Germany.

36. "Standard Plans for Highway Bridge Superstructure," Bureau of Public Roads, Washington, D. C., 1957.

TABLE 1

COMPARISON OF RESULTS OBTAINED BY "EXACT" AND "APPROXIMATE" METHODS

$a = 0.8$, $n = 2$, $m = 3$, $c/c_{cr} = 0$, $N = 400$

Single-Axle Loading, $W/W_b = 0.175$, $f_v/f_b = 1$, $\alpha = 0.15$

Quantity	Value of Quantity							
	"Exact"	"Approx."	"Exact"	"Approx."	"Exact"	"Approx."	"Exact"	"Approx."
	for ξ = 0.25		for ξ = 0.50		for ξ = 0.75		for ξ = 1.00	
D_1	+0.417	+0.417	-0.429	-0.428	+0.109	+0.108	-0.049	-0.048
D_c	-0.216	-0.216	+1.125	+1.124	-0.191	-0.192	-0.020	-0.019
D_4	+0.102	+0.101	-0.477	-0.476	+0.412	+0.412	+0.078	+0.077
M_1	+0.229	+0.229	-0.222	-0.222	+0.076	+0.075	-0.045	-0.045
M_2	-0.628	-0.628	-1.066	-1.065	+0.069	+0.070	+0.080	+0.079
M_c	-0.105	-0.105	+1.090	+1.089	-0.086	-0.087	-0.013	-0.013
M_3	+0.118	+0.119	-1.013	-1.012	-0.664	-0.664	-0.058	-0.057
M_4	+0.066	+0.065	-0.264	-0.264	+0.229	+0.229	+0.065	+0.064
R_1	+0.113	+0.113	-0.110	-0.110	+0.037	+0.037	-0.022	-0.022
R_2	+0.986	+0.986	+0.697	+0.696	-0.011	-0.012	-0.057	-0.056
R_3	-0.049	-0.049	+0.658	+0.657	+1.013	+1.013	+0.043	+0.043
R_4	+0.032	+0.032	-0.131	-0.130	+0.113	+0.113	+1.016	+1.015

TABLE 2

COMPARISON OF RESULTS OBTAINED BY USE OF DIFFERENT TIME INTERVALS OF INTEGRATION

$a = 0.8$, $n = 3$, $m = 4$, $c/c_{cr} = 0$,
Single-Axle Loading, $W/W_b = 0.175$

Quantity	Maximum Value of Quantity				
	N = 400	N = 600	N = 800	N = 600	N = 800
	$\alpha = 0.075$			$\alpha = 0.15$	
D_1	1.026	1.026	1.026	1.088	1.088
D_c	1.040	1.035	1.033	1.102	1.101
D_4	1.017	1.025	1.026	1.052	1.051
M_1	0.999	0.999	0.999	1.062	1.062
M_2	1.051	1.051	1.049	1.127	1.124
M_c	1.005	1.009	1.007	1.066	1.068
M_3	1.041	1.045	1.049	1.168	1.160
M_4	1.011	1.019	1.019	0.966	0.971
R_1	1.000	1.000	1.000	1.000	1.000
R_2	1.018	1.027	1.029	1.028	1.031
R_3	1.030	1.034	1.030	1.026	1.034
R_4	0.975	0.981	0.977	0.954	0.958

TABLE 3

WEIGHTS AND NATURAL FREQUENCIES OF SC-6-53 BRIDGES

Spans in ft.	Wt. of Center Span in kips	Fundamental Natural Frequency f_b in c.p.s.
40-50-40	221	6.4
48-60-48	273	5.2
56-70-56	326	4.4
64-80-64	383	3.7
72-90-72	450	3.1
80-100-80	524	2.6

Note: $T_b = 1/f_b$, $T_2 = 0.654\ T_b$, $T_3 = 0.532\ T_b$

TABLE 4

DATA FOR "TYPICAL" VEHICLES

Quantity	Unit	Three-Axle Vehicle	Two-Axle Vehicle	Single-Axle Loading
W	kips	72	64	64
ℓ_1	ft.	12	14 ~ 35	--
ℓ_2	ft.	14 ~ 35	--	--
W_1/W		0.08	0.90	--
W_2/W		0.80	--	--
w_1/W		0.03	0.05	--
w_2/W		0.05	0.05	--
w_3/W		0.04	--	--
i_1		0.5 ~ 1.0	0.9 ~ 1.7	--
i_2		0.9 ~ 1.7	--	--
a_1		0.602	0.5	--
a_3		0.494	--	--
a_5		0.083	--	--
μ_1		0.05 ~ 0.10	0.12 ~ 0.28	0.12 ~ 0.28
μ_2		0.12 ~ 0.28	0.12 ~ 0.28	--
μ_3		0.12 ~ 0.28	--	--
$f_{t,1}$	c.p.s.	3.13 ~ 3.72	3.13 ~ 3.72	3.13 ~ 3.72
$f_{t,2}$	c.p.s.	3.13 ~ 3.72	3.13 ~ 3.72	--
$f_{t,3}$	c.p.s.	3.13 ~ 3.72	--	--
$f_{ts,1}$	c.p.s.	1.57 ~ 1.65	1.99 ~ 2.14	1.74 ~ 2.36
$f_{ts,2}$	c.p.s.	1.99 ~ 2.14	1.74 ~ 2.36	--
$f_{ts,3}$	c.p.s.	1.74 ~ 2.36	--	--
$P_{st,1}$	kips	8	32	64
$P_{st,2}$	kips	32	32	--
$P_{st,3}$	kips	32	--	--

TABLE 5

MAXIMUM STATIC EFFECTS FOR SINGLE-AXLE AND MULTIPLE-AXLE LOADINGS

Three Span Uniform Beam; $a = 0.8$

For Two-Axle Loading: $P_{st,1} = P_{st,2} = W/2$, $\ell/L = 0.3$

For Three-Axle Loading: $P_{st,1} = W/9$, $P_{st,2} = P_{st,3} = 4W/9$,

$\ell_1/L = 0.15$, $\ell_2/L = 0.3$

Quantity	Unit	Maximum Static Value		
		Single-Axle Loading	Two-Axle Loading	Three-Axle Loading
D_1	$\frac{WL^3}{EI}$	0.00772	0.00617	0.00581
D_c	"	0.01064	0.00903	0.00867
D_4	"	0.00772	0.00617	0.00583
M_1	WL	0.1660	0.1057	0.0945
M_2	"	0.0877	0.0776	0.0749
M_c	"	0.1685	0.1081	0.1072
M_3	"	0.0877	0.0776	0.0748
M_4	"	0.1660	0.1057	0.1040
R_1	W	1.0000	0.7686	0.7252
R_2	"	1.0001	0.9526	0.9404
R_3	"	1.0001	0.9526	0.9405
R_4	"	1.0000	0.7686	0.6834

TABLE 6

COMPARISON OF MAXIMUM EFFECTS OBTAINED BY USE OF DIFFERENT NUMBER OF MASS CONCENTRATIONS IN BRIDGE MODEL

$a = 0.8$, $c/c_{cr} = 0$, Single-Axle Loading
$W/W_b = 0.175$, $f_v/f_b = 1$, $\alpha = 0.15$

Quantity	Values of Amplification Factor and of Corresponding ξ			
	4 Masses (n=2 m=3)		7 Masses (n=3, m=4)	
	A.F.	ξ	A.F.	ξ
D_1	1.087	0.12	1.087	0.12
D_c	1.129	0.49	1.102	0.49
D_4	1.102	0.86	1.052	0.84
M_1	1.075	0.13	1.062	0.13
M_2	1.112	0.49	1.127	0.48
M_c	1.087	0.50	1.066	0.50
M_3	1.138	0.55	1.168	0.53
M_4	1.070	0.87	0.966	0.87
R_1	1.000	0	1.000	0
R_2	1.098	0.36	1.123	0.35
R_3	1.051	0.62	1.026	0.77
R_4	1.013	1.00	0.954	1.00

TABLE 7

NATURAL PERIODS OF VIBRATION OF BRIDGE MODELS AND OF CONTINUOUS BEAM

Three-Span Uniform Beam; $a = 0.8$

Order of Natural Period	Value of $\frac{T}{\sqrt{\rho L^4/EI}}$		
	Discrete System		Continuous System
	4 Masses (n=2, m=3)	7 Masses (n=3, m=4)	
1	0.503	0.503	0.503
2	0.336	0.330	0.329
3	0.276	0.269	0.268
4	0.140	0.133	0.131

TABLE 8 (Cont'd on next page)

MAXIMUM EFFECTS FOR SMOOTHLY MOVING, SINGLE-AXLE LOADING

$a = 0.8,\ c/c_{cr} = 0,\ f_v/f_b = 1$

α	W/W_b	P		D_1		D_c		D_4		M_1		M_2		M_c	
		A.F.	ξ	A.F.	ξ	A.F.	ξ	A.F.	ξ	A.F.	ξ	A.F.	ξ	A.F.	ξ
0.12	0.175	1.04	0.89	1.00	0.16	1.08	0.49	1.01	0.86	0.98	0.13	1.08	0.47	1.05	0.50
	0.300	1.06	0.20	1.00	0.14	1.08	0.51	1.01	0.85	1.00	0.13	1.07	0.47	1.05	0.50
0.13	0.175	1.06	0.76	1.00	0.11	1.06	0.52	1.05	0.88	0.99	0.13	1.07	0.42	0.99	0.50
	0.300	1.07	0.43	1.02	0.11	1.03	0.52	1.08	0.88	1.02	0.13	1.07	0.42	1.00	0.50
0.14	0.175	1.05	0.23	1.04	0.12	1.04	0.49	1.11	0.85	1.02	0.13	1.14	0.45	1.03	0.50
	0.300	1.08	0.46	1.07	0.11	1.11	0.49	1.11	0.84	1.04	0.13	1.13	0.45	1.07	0.50
0.15	0.175	1.06	0.87	1.09	0.12	1.10	0.49	1.05	0.84	1.06	0.13	1.13	0.48	1.07	0.50
	0.300	1.07	0.13	1.11	0.12	1.12	0.52	1.04	0.84	1.09	0.13	1.12	0.48	1.06	0.50
0.16	0.175	1.06	0.38	1.12	0.13	1.11	0.51	1.09	0.83	1.11	0.13	1.11	0.44	1.06	0.50
	0.300	1.11	0.85	1.15	0.12	1.06	0.51	1.13	0.88	1.14	0.13	1.16	0.44	1.05	0.50
0.17	0.175	1.06	0.40	1.15	0.13	1.04	0.54	1.14	0.87	1.13	0.13	1.13	0.47	0.92	0.50
	0.300	1.10	0.42	1.19	0.13	1.06	0.46	1.15	0.87	1.17	0.13	1.17	0.47	0.94	0.50
0.18	0.175	1.06	0.42	1.17	0.14	1.09	0.48	1.03	0.86	1.15	0.13	1.22	0.43	1.05	0.50
	0.300	1.12	0.44	1.22	0.14	1.17	0.49	1.06	0.85	1.19	0.13	1.19	0.49	1.10	0.50

TABLE 8 (Concluded)

α	W/W_b	M_3		M_4		R_1		R_2		R_3		R_4	
		A.F.	ξ	A.F.	ξ	A.F.	ξ	A.F.	ξ	A.F.	ξ	A.F.	ξ
0.12	0.175	1.02	0.53	1.00	0.87	1.00	0	1.10	0.28	1.06	0.72	0.98	1.00
	0.300	1.06	0.53	0.98	0.87	1.00	0	1.09	0.28	1.08	0.72	0.98	1.00
0.13	0.175	1.10	0.53	1.04	0.87	1.00	0	1.11	0.30	1.09	0.67	1.03	1.00
	0.300	1.08	0.56	1.06	0.87	1.00	0	1.11	0.30	1.09	0.67	1.02	1.00
0.14	0.175	1.10	0.56	0.99	0.87	1.00	0	1.12	0.33	1.07	0.72	0.97	1.00
	0.300	1.06	0.50	1.05	0.87	1.00	0	1.11	0.33	1.10	0.72	1.01	1.00
0.15	0.175	1.17	0.53	0.97	0.87	1.00	0	1.12	0.35	1.03	0.77	0.95	1.00
	0.300	1.22	0.53	0.96	0.87	1.00	0	1.13	0.35	1.09	0.77	0.89	1.00
0.16	0.175	1.17	0.57	0.98	0.87	1.00	0	1.10	0.37	1.06	0.70	0.91	1.00
	0.300	1.27	0.56	1.08	0.87	1.00	0	1.12	0.37	1.07	0.70	0.97	1.00
0.17	0.175	1.15	0.54	1.12	0.87	1.00	0	1.09	0.26	1.08	0.60	0.97	1.00
	0.300	1.18	0.60	1.14	0.87	1.00	0	1.10	0.26	1.15	0.60	0.93	1.00
0.18	0.175	1.14	0.57	1.03	0.87	1.00	0	1.11	0.28	1.09	0.63	0.96	1.00
	0.300	1.12	0.56	1.00	0.87	1.00	0	1.12	0.28	1.20	0.63	0.97	1.00

TABLE 9

MAXIMUM EFFECTS FOR INITIALLY OSCILLATING, SINGLE-AXLE LOADING

$a = 0.8, \quad W/W_b = 0.175$

$\alpha = 0.15, \quad P]_{t=o} = 0.7\ P_{st}$

Quantity	$\mu = \infty$, $f_v/f_b = 1$				$\mu = 0$, $f_v/f_b = 0.6$		$\mu = 0.15$, $f_t/f_b = 1$, $f_{st}/f_b = 0.6$	
	$c/c_{cr} = 0.01$		$c/c_{cr} = 0$		$c/c_{cr} = 0$		$c/c_{cr} = 0$	
	A.F.	ξ	A.F.	ξ	A.F.	ξ	A.F.	ξ
D_1	1.11	0.19	1.11	0.19	1.32	0.12	1.21	0.11
D_c	1.14	0.48	1.17	0.48	1.45	0.49	1.20	0.50
D_4	1.25	0.87	1.31	0.87	1.34	0.87	1.23	0.90
M_1	0.81	0.08	0.81	0.08	1.24	0.13	1.11	0.12
M_2	1.11	0.18	1.11	0.18	1.34	0.47	1.13	0.48
M_c	0.99	0.50	1.01	0.50	1.38	0.50	1.11	0.50
M_3	1.11	0.52	1.14	0.52	1.27	0.49	1.25	0.54
M_4	1.21	0.87	1.28	0.87	1.29	0.87	1.03	0.90
R_1	0.99	0.06	0.99	0.06	0.85	0.08	0.85	0.06
R_2	1.03	0.30	1.03	0.30	1.27	0.30	1.09	0.36
R_3	1.08	0.67	1.12	0.67	1.24	0.70	1.10	0.61
R_4	1.12	0.99	1.18	0.99	0.83	0.91	1.01	1.00

TABLE 10

MAXIMUM EFFECTS FOR SMOOTHLY MOVING, TWO-AXLE LOADING

$a = 0.8,\ c/c_{cr} = 0,\ W/W_b = 0.175,\ P_{st,1} = P_{st,2} = W/2,\ f_{v1}/f_b = f_{v2}/f_b = 1,\ \ell/L = 0.3$

α	P_1		P_2		D_1		D_c		D_4		M_1		M_2	
	A.F.	ξ	A.F.	ξ	A.F.	ξ	A.F.	ξ	A.F.	ξ	A.F.	ξ	A.F.	ξ
0.12	1.06	0.19	1.05	0.61	1.05	0.20	1.05	0.58	1.08	0.91	0.99	0.22	1.05	0.52
0.13	1.06	0.20	1.07	0.65	1.08	0.20	1.10	0.53	1.03	0.90	1.01	0.21	1.07	0.52
0.14	1.06	0.22	1.06	0.92	1.12	0.21	1.14	0.56	1.08	0.91	1.05	0.21	1.07	0.56
0.15	1.06	0.23	1.06	0.36	1.13	0.22	1.08	0.59	1.10	0.91	1.09	0.22	1.05	0.53
0.16	1.06	0.47	1.08	0.91	1.13	0.23	1.08	0.53	1.07	0.93	1.12	0.23	1.07	0.51
0.17	1.06	0.59	1.06	0.83	1.12	0.23	1.15	0.55	1.06	0.87	1.15	0.24	1.07	0.52
0.18	1.06	0.62	1.07	0.88	1.10	0.24	1.16	0.57	1.17	0.91	1.15	0.24	1.08	0.53

α	M_c		M_3		M_4		R_1		R_2		R_3		R_4	
	A.F.	ξ	A.F.	ξ	A.F.	ξ	A.F.	ξ	A.F.	ξ	A.F.	ξ	A.F.	ξ
0.12	1.08	0.50	1.08	0.61	1.01	0.91	0.95	0.12	1.07	0.39	1.07	0.73	1.01	1.00
0.13	1.08	0.52	1.03	0.58	1.01	0.87	0.96	0.12	1.03	0.31	1.06	0.78	1.01	1.00
0.14	1.08	0.56	1.09	0.56	1.02	0.90	0.98	0.12	1.07	0.33	1.04	0.72	0.98	1.00
0.15	1.11	0.60	1.11	0.59	1.06	0.89	0.99	0.12	1.10	0.35	1.08	0.77	1.04	1.00
0.16	1.11	0.51	1.04	0.56	1.00	0.89	0.99	0.12	1.10	0.37	1.02	0.81	0.95	1.00
0.17	1.10	0.54	1.03	0.59	1.14	0.87	0.99	0.12	1.06	0.39	1.03	0.71	1.06	1.00
0.18	1.10	0.57	1.09	0.57	1.08	0.90	0.98	0.12	1.00	0.41	1.06	0.75	0.97	1.00

TABLE 11

COMPARISON OF MAXIMUM EFFECTS OBTAINED FOR TWO-AXLE AND THREE-AXLE LOADINGS

$a = 0.8, \quad c/c_{cr} = 0, \ \alpha = 0.15$

For Two-Axle Loading: $W/W_b = 0.175$, $f_{v1}/f_b = f_{v2}/f_b = 1$, $\ell/L = 0.3$

For Three-Axle Loading: $W/W_b = 0.2$, $f_{v1}/f_b = f_{v2}/f_b = f_{v3}/f_b = 1$

$\ell_1/L = 0.15$, $\ell_2/L = 0.3$

Quantity	Two-Axle Loading		Three-Axle Loading	
	A.F.	ξ	A.F.	ξ
D_1	1.13	0.22	1.11	0.27
D_c	1.08	0.59	1.05	0.64
D_4	1.10	0.90	1.08	0.95
M_1	1.09	0.22	1.12	0.28
M_2	1.05	0.53	1.05	0.58
M_c	1.11	0.60	1.04	0.56
M_3	1.11	0.59	1.10	0.65
M_4	1.06	0.89	1.02	0.94
R_1	0.99	0.12	0.96	0.18
R_2	1.10	0.35	1.08	0.41
R_3	1.08	0.77	1.05	0.83
R_4	1.04	1.00	0.99	1.05

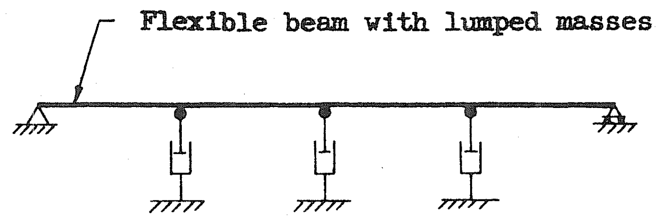

(a) Simply Supported Bridge

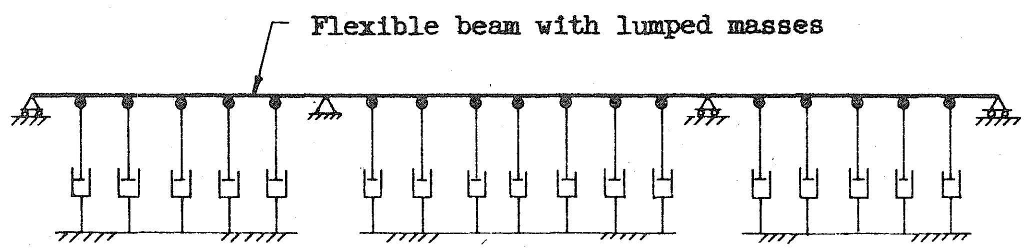

(b) Three Span Continuous Bridge

FIG. 1 BRIDGE MODELS

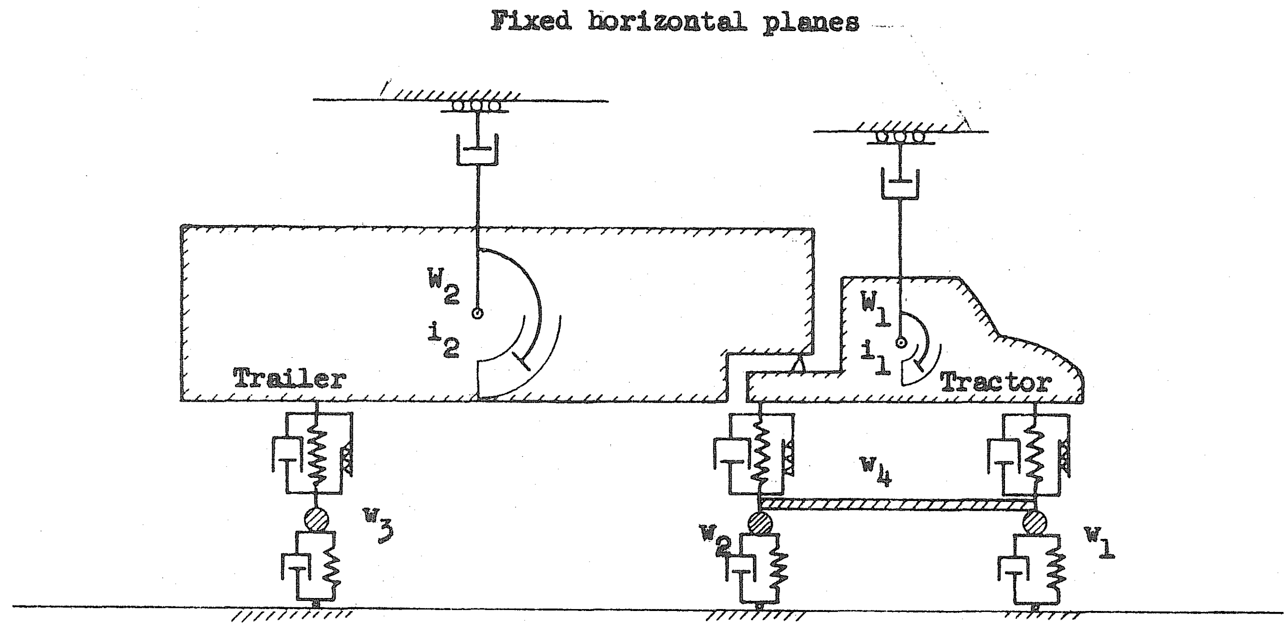

FIG. 2 REPRESENTATION OF A TRACTOR-TRAILER TYPE VEHICLE

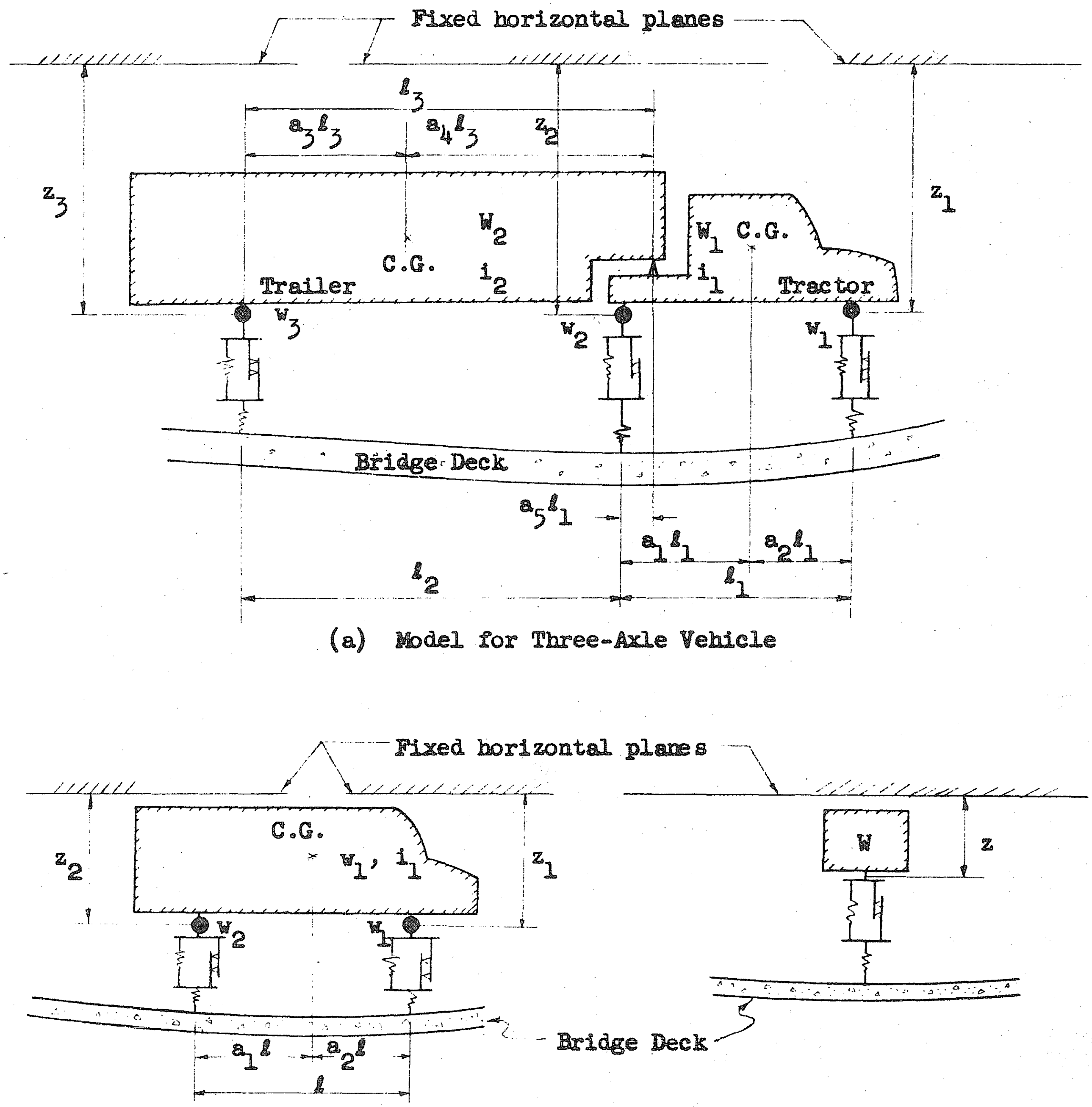

(a) Model for Three-Axle Vehicle

(b) Model for Two-Axle Vehicle

(c) Model for Single-Axle Load Unit

FIG. 3 VEHICLE MODELS

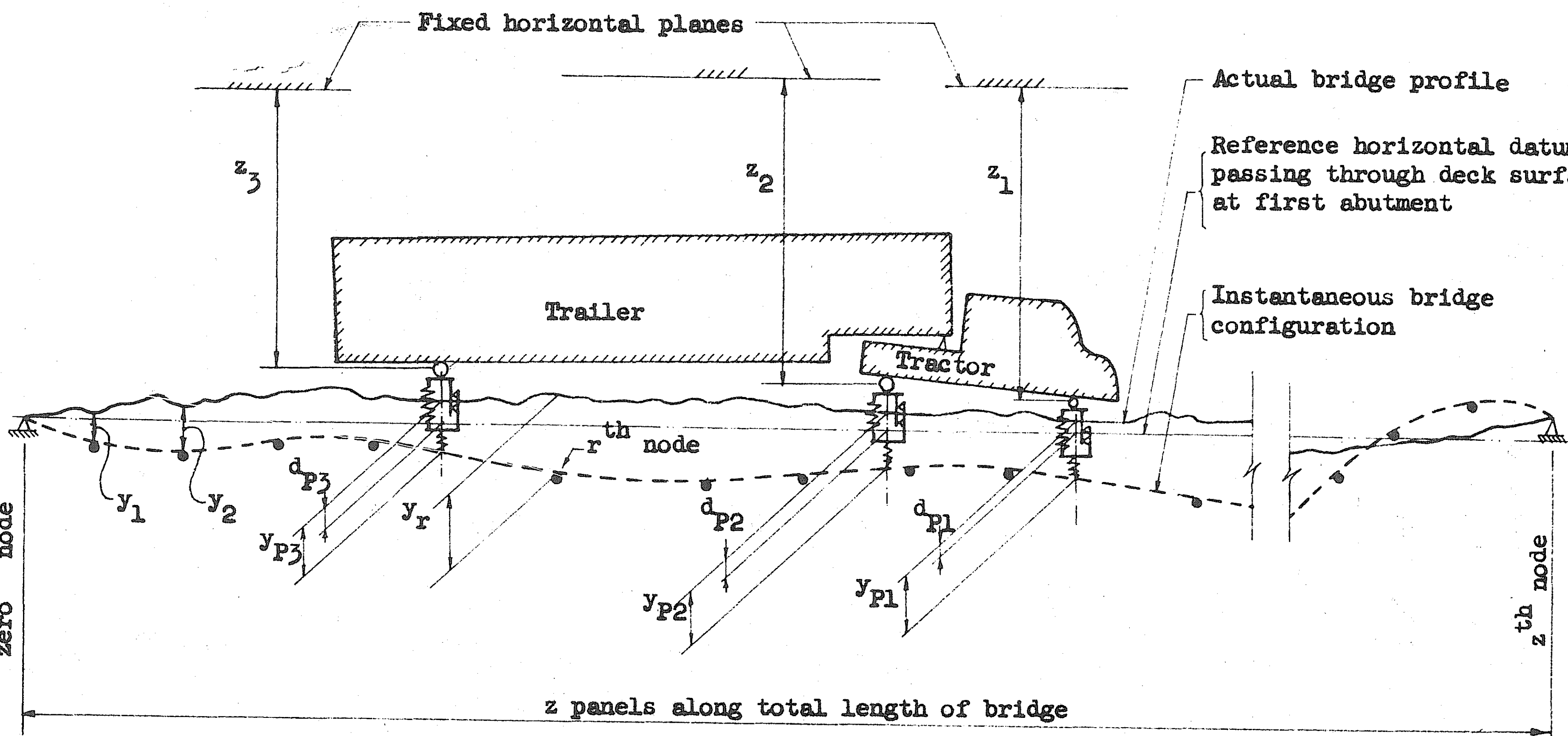

FIG. 4 COMBINATION OF BRIDGE AND VEHICLE MODELS -- ANY TYPE OF BRIDGE

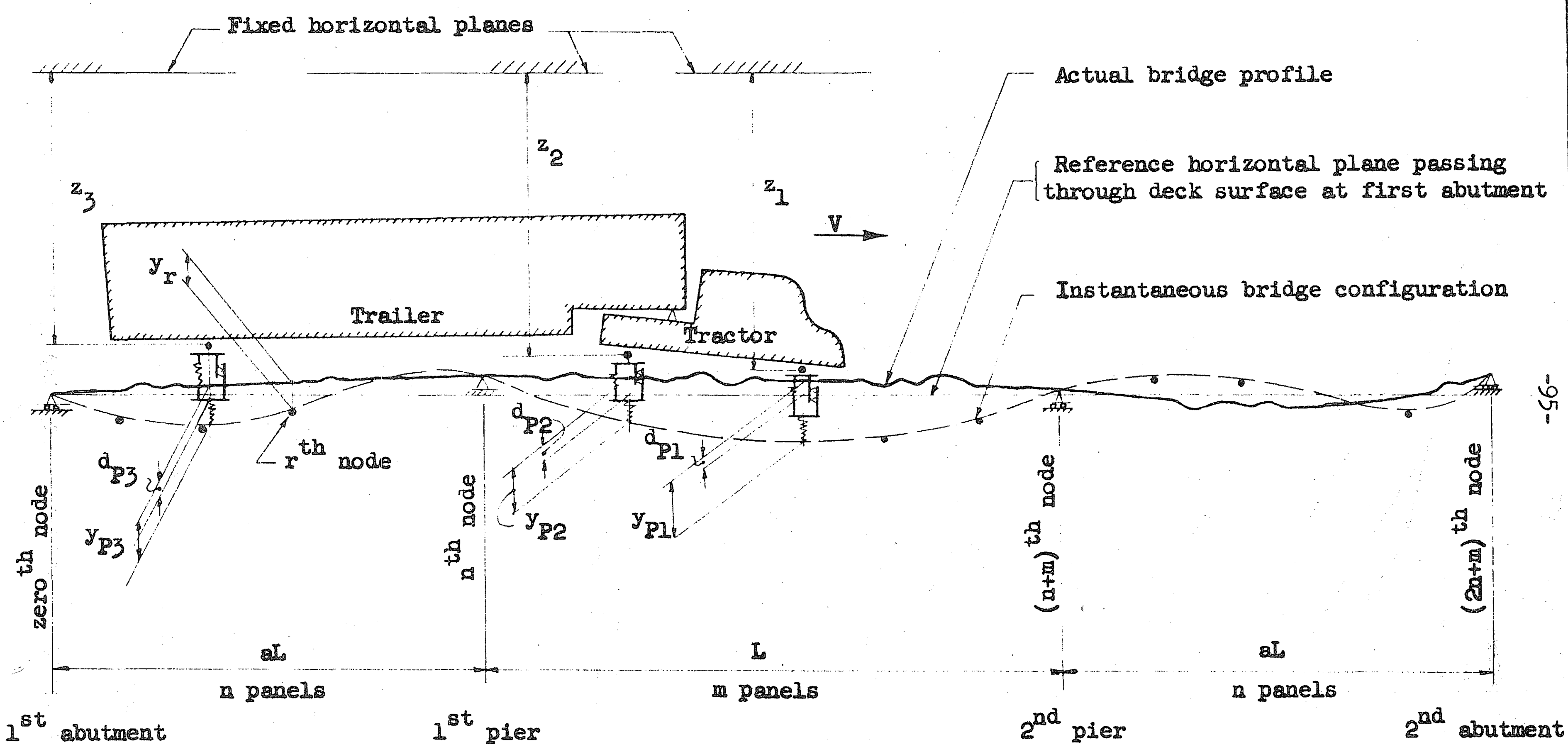

FIG. 5 COORDINATE SYSTEM FOR A THREE SPAN CONTINUOUS BRIDGE

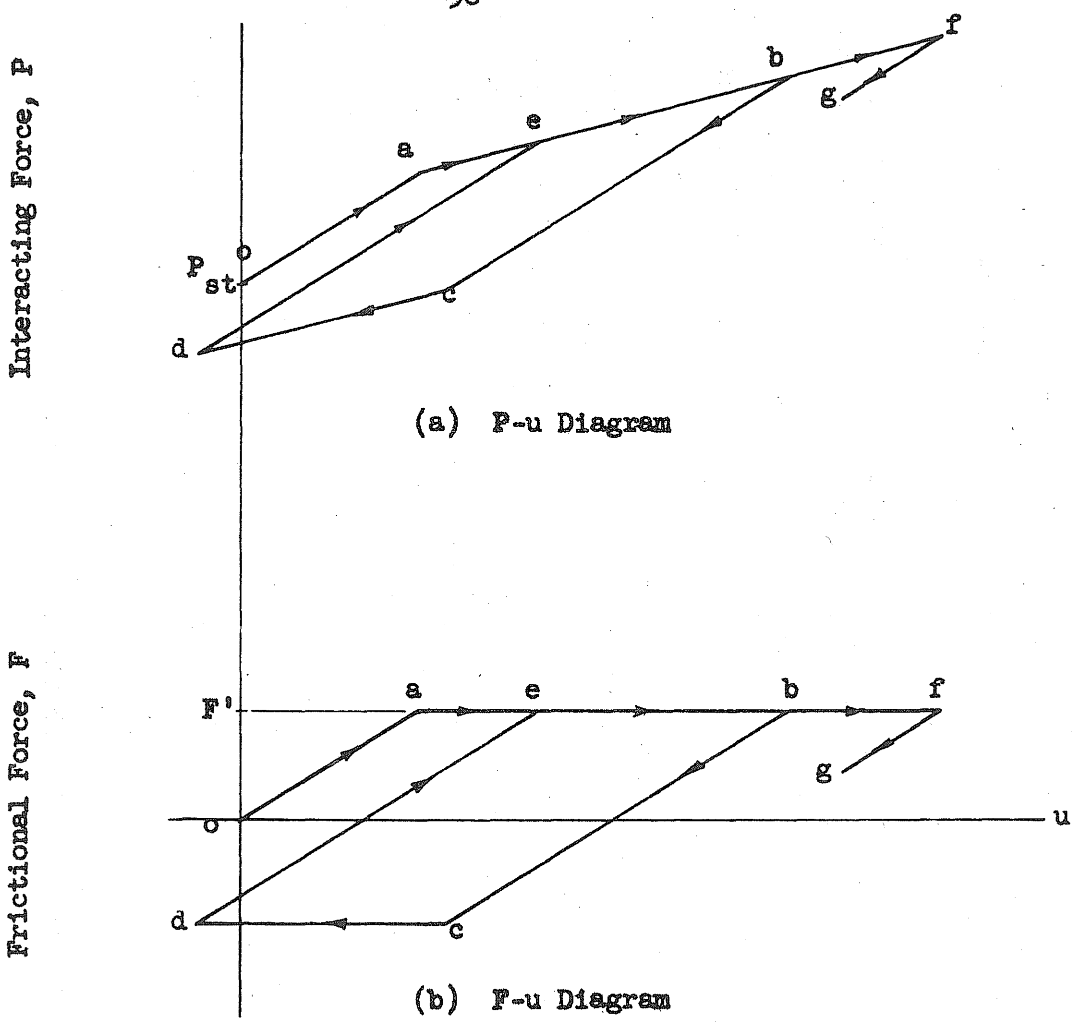

FIG. 6 INTERACTING FORCE, P, AND FRICTIONAL FORCE, F, VERSUS SHORTENING OF SUSPENSION-TIRE SYSTEM, u

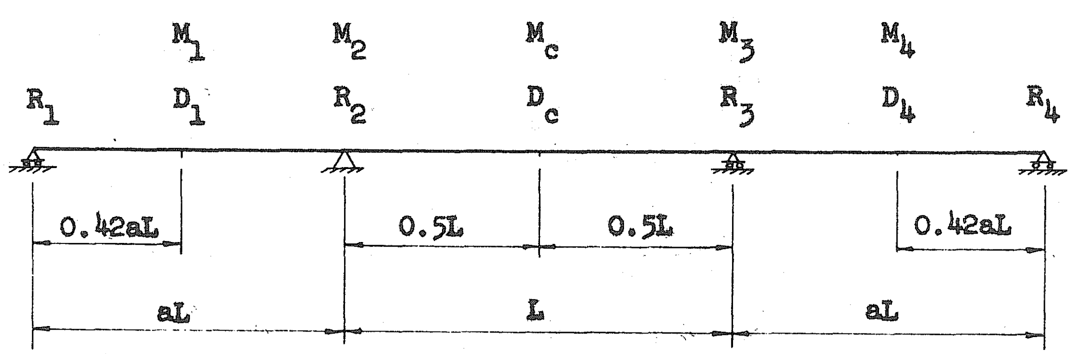

FIG. 7 LOCATIONS FOR WHICH DYNAMIC RESPONSE WAS CALCULATED

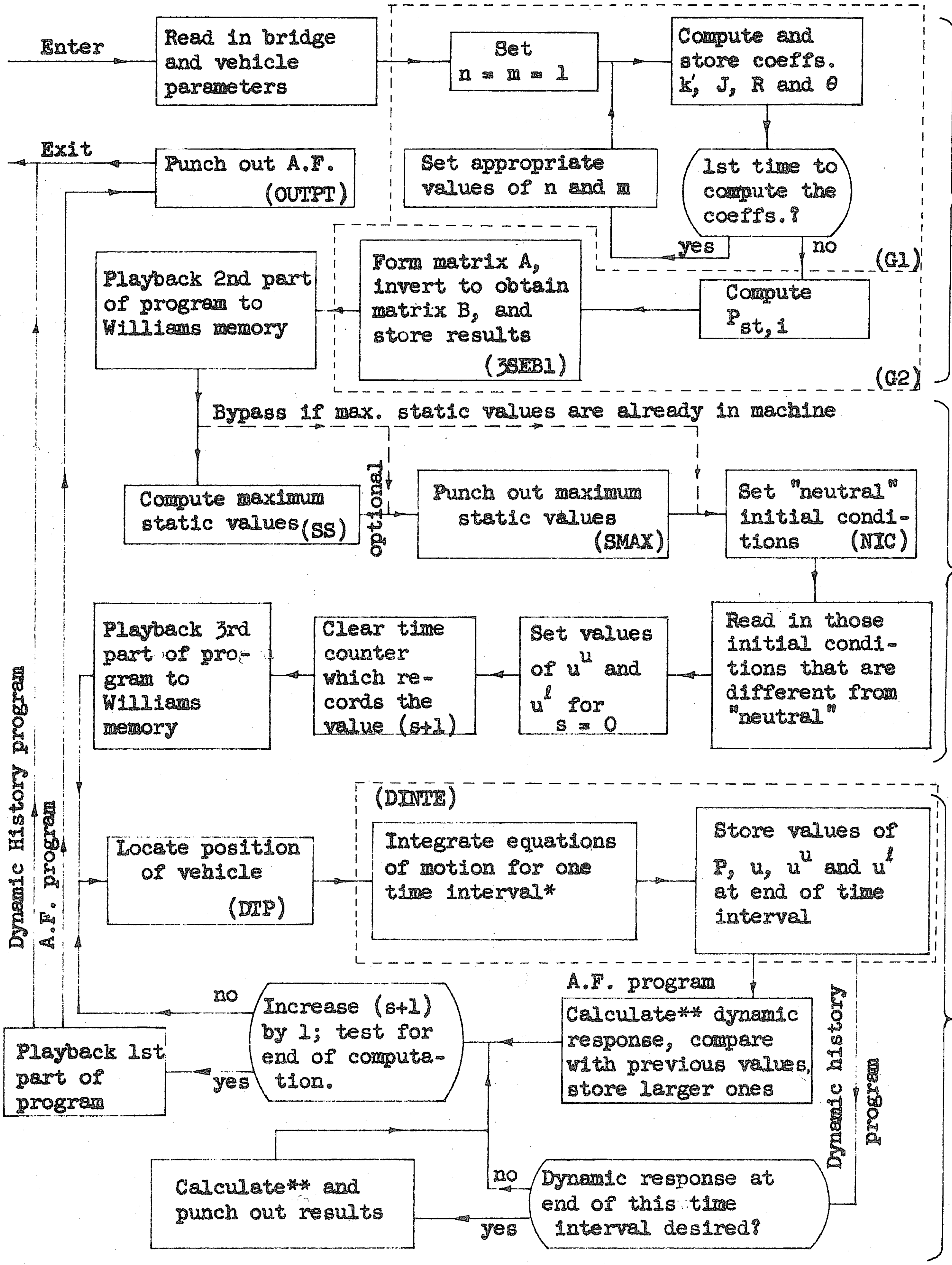

* Refer to Fig. 9
** Refer to Fig. 14

FIG. 8 GENERAL FLOW CHART FOR COMPLETE PROGRAM

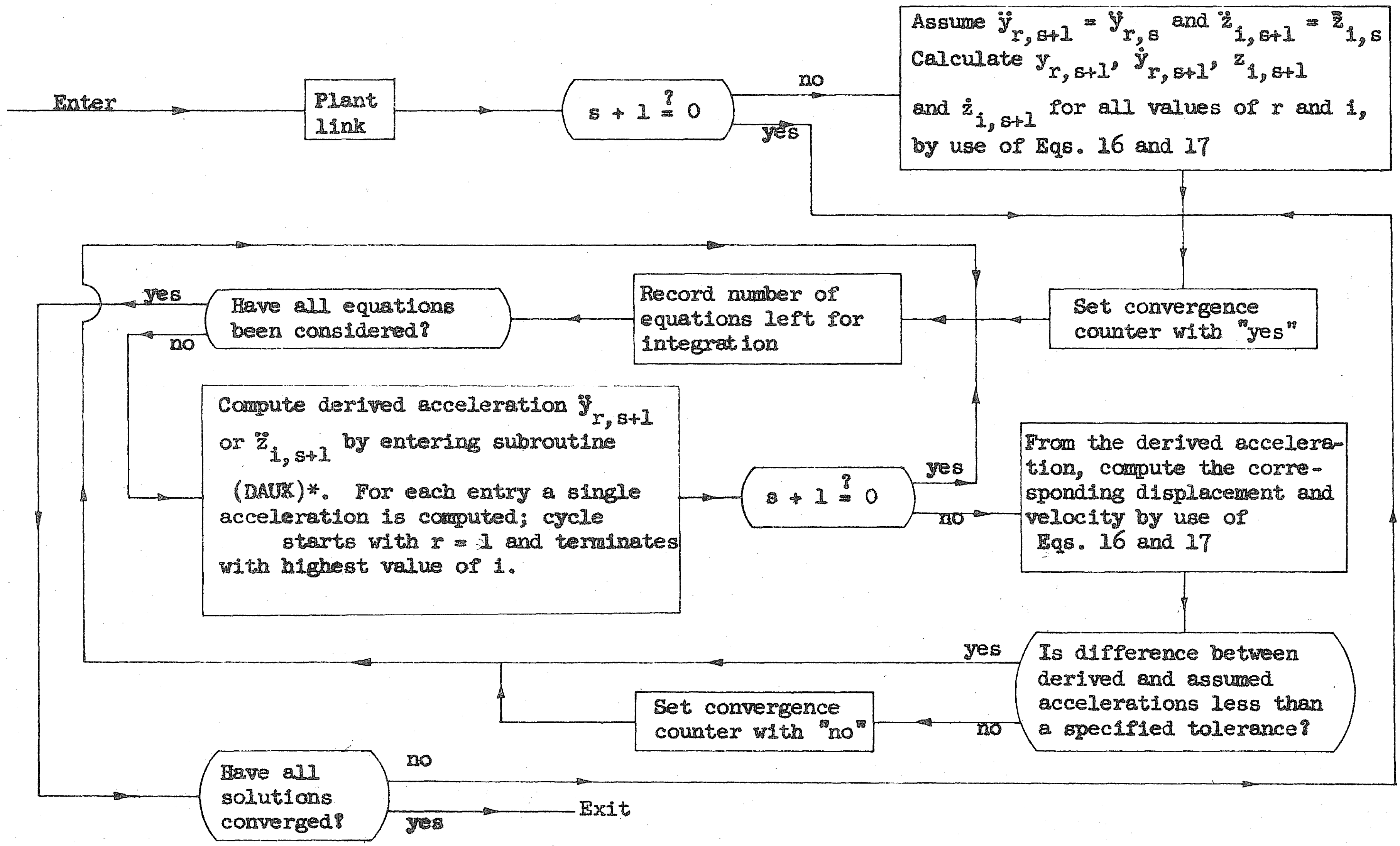

*Refer to Fig. 10

FIG. 9 GENERAL FLOW CHART FOR INTEGRATING EQUATIONS OF MOTION FOR A SINGLE TIME INTERVAL

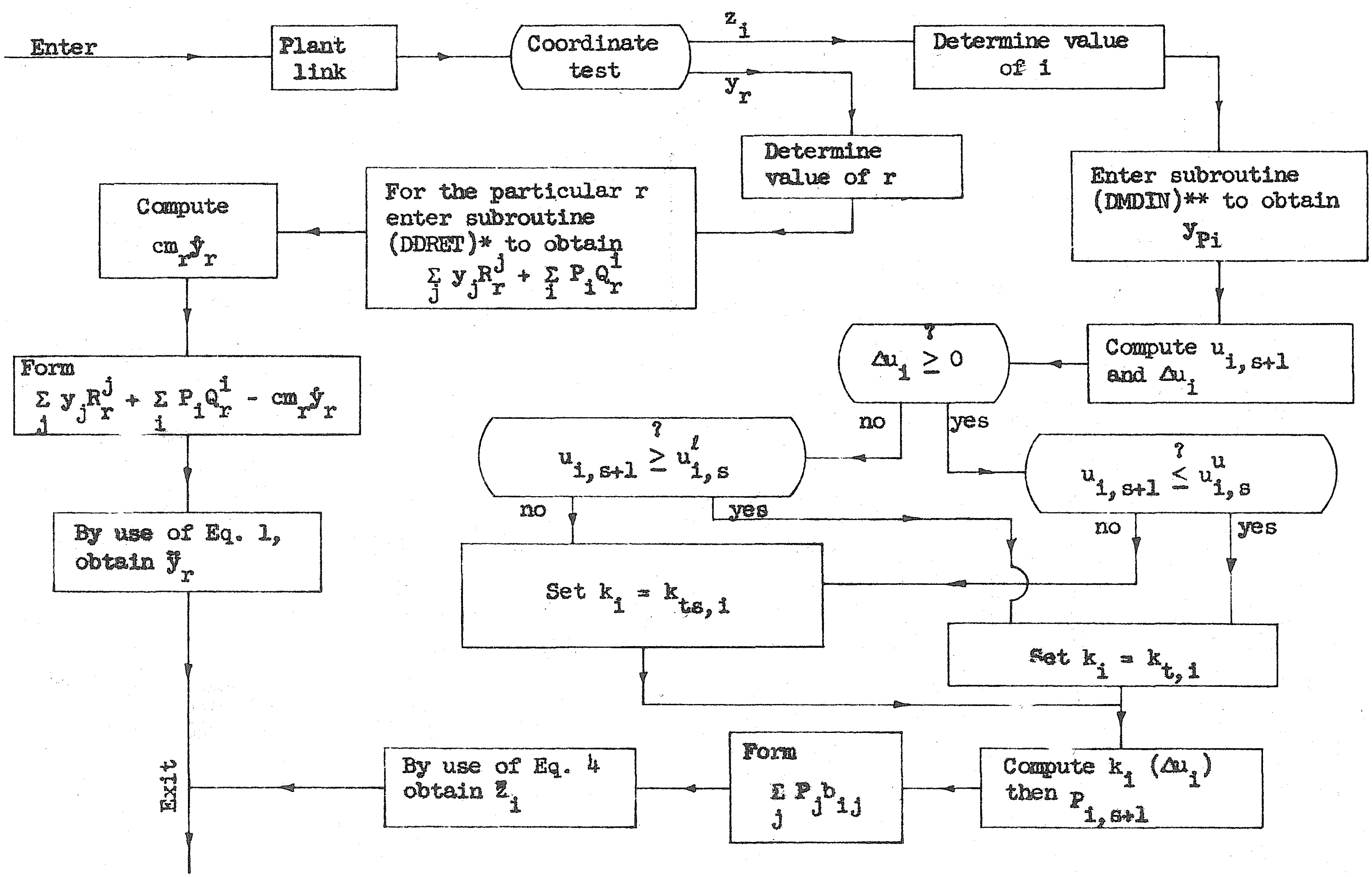

* Refer to Fig. 11
** Refer to Fig. 12

FIG. 10 GENERAL FLOW CHART FOR SUBROUTINE (DAUX) -- USED IN COMPUTATION OF DERIVED ACCELERATION

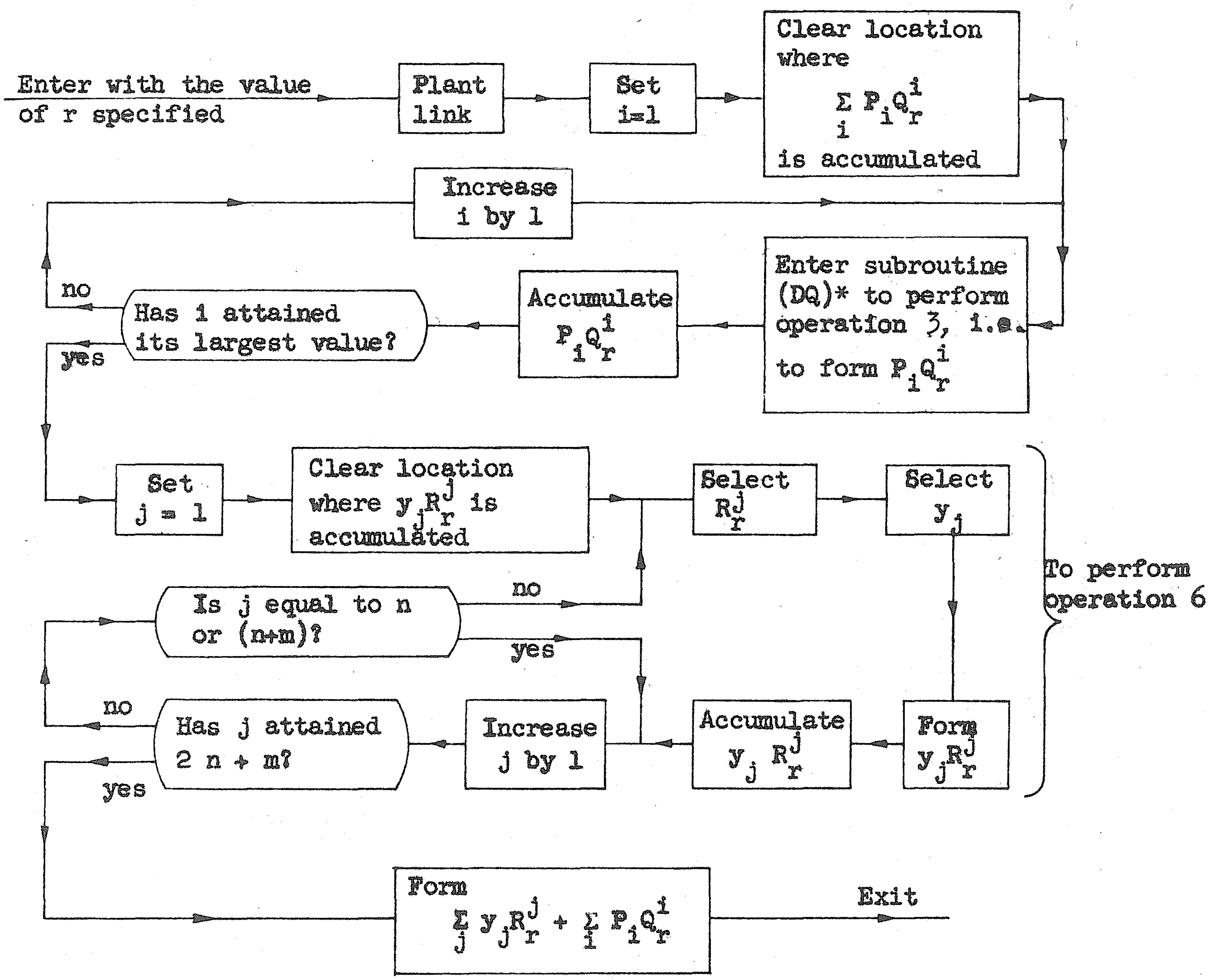

*In the process of computing the value of Q_r^i, the subroutine (DQ) utilizes the moment-deflection coefficients, J, and calls the subroutine (DDC-M) to perform operation 1.

FIG. 11 GENERAL FLOW CHART FOR SUBROUTINE (DDRET)-- FOR COMPUTATION OF "REACTION" AT THE r^{th} NODE POINT

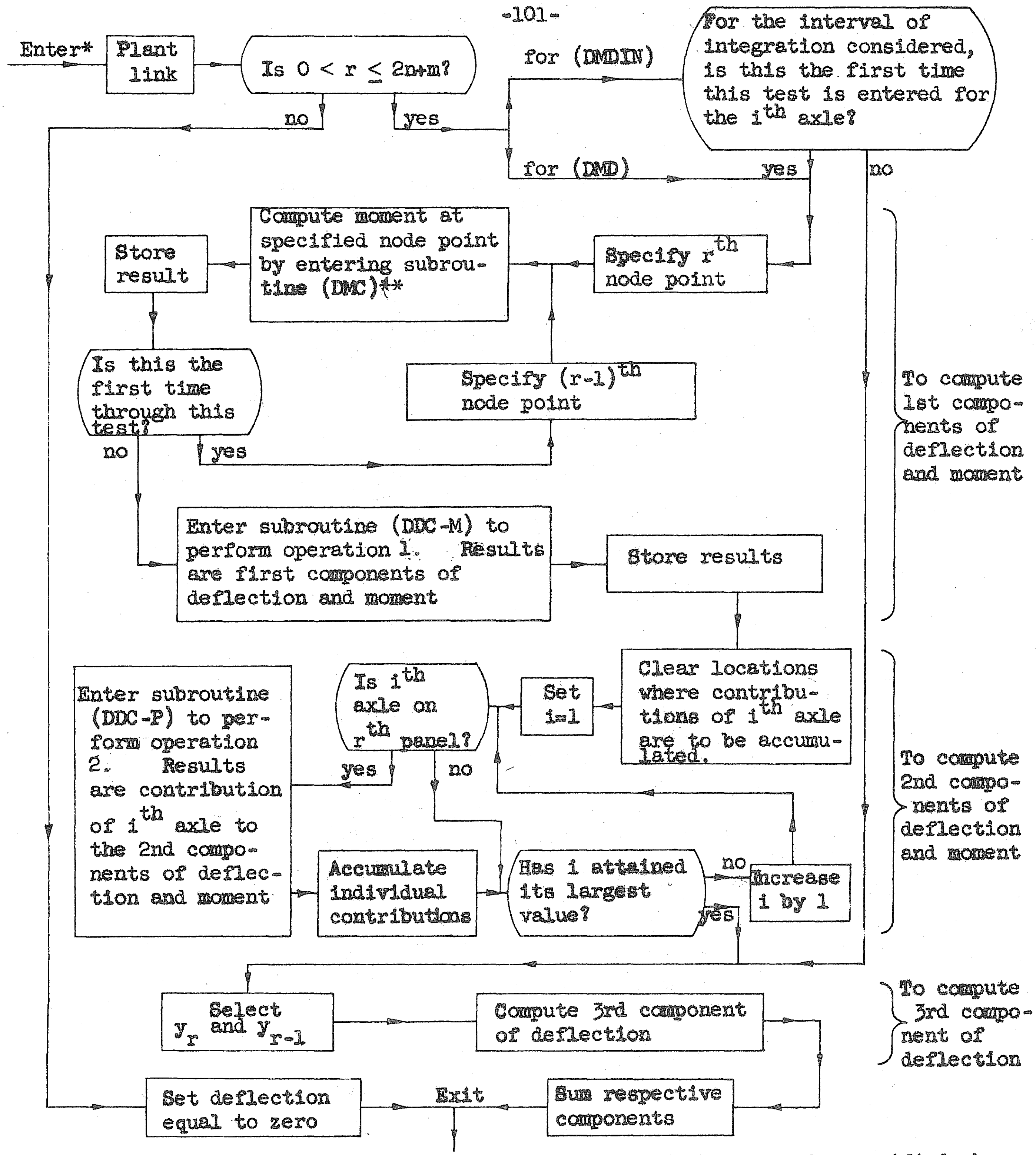

* Before entering this subroutine, the coordinate of the point is specified where the deflection and moment are to be evaluated. Let this point be on the r^{th} panel; a value of r less than one or greater than 2n+m denotes that the point under consideration is not on the bridge.

** See Fig. 13

FIG. 12 GENERAL FLOW CHART FOR SUBROUTINE (DMD) AND (DMDIN)
(For Function of These Subroutines, See Text)

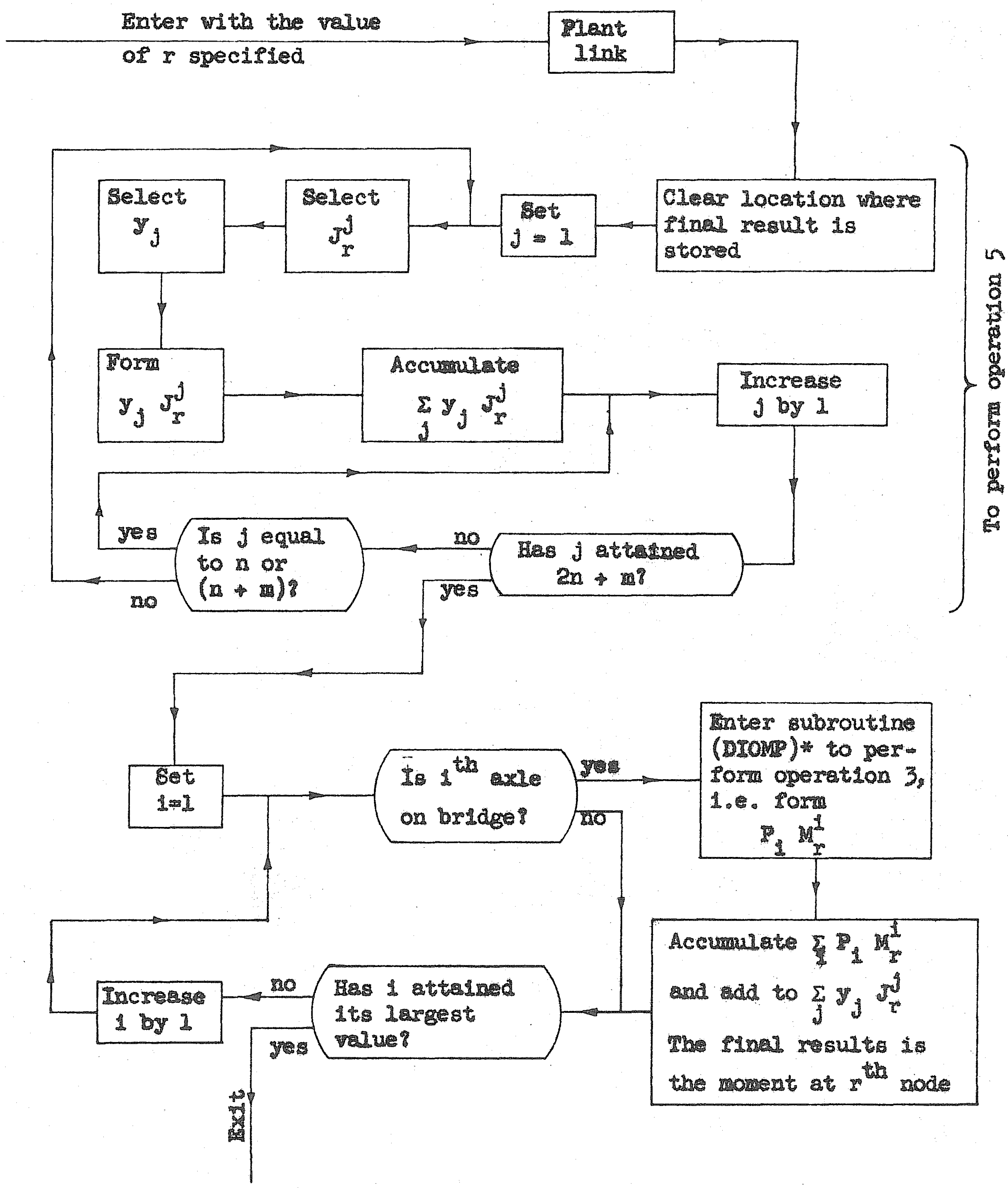

* In the process of computing the value of M_r^i, the subroutine (DIOMP) utilizes the effective carry-over factors, $^r k'$, and calls the subroutine (DDC-M) to perform operation 1, the deflection obtained divided by the angle coefficient θ_r is equal to M_r^i.

FIG. 13 GENERAL FLOW CHART FOR SUBROUTINE (DMC) -- COMPUTATION OF MOMENT AT r^{th} NODE POINT

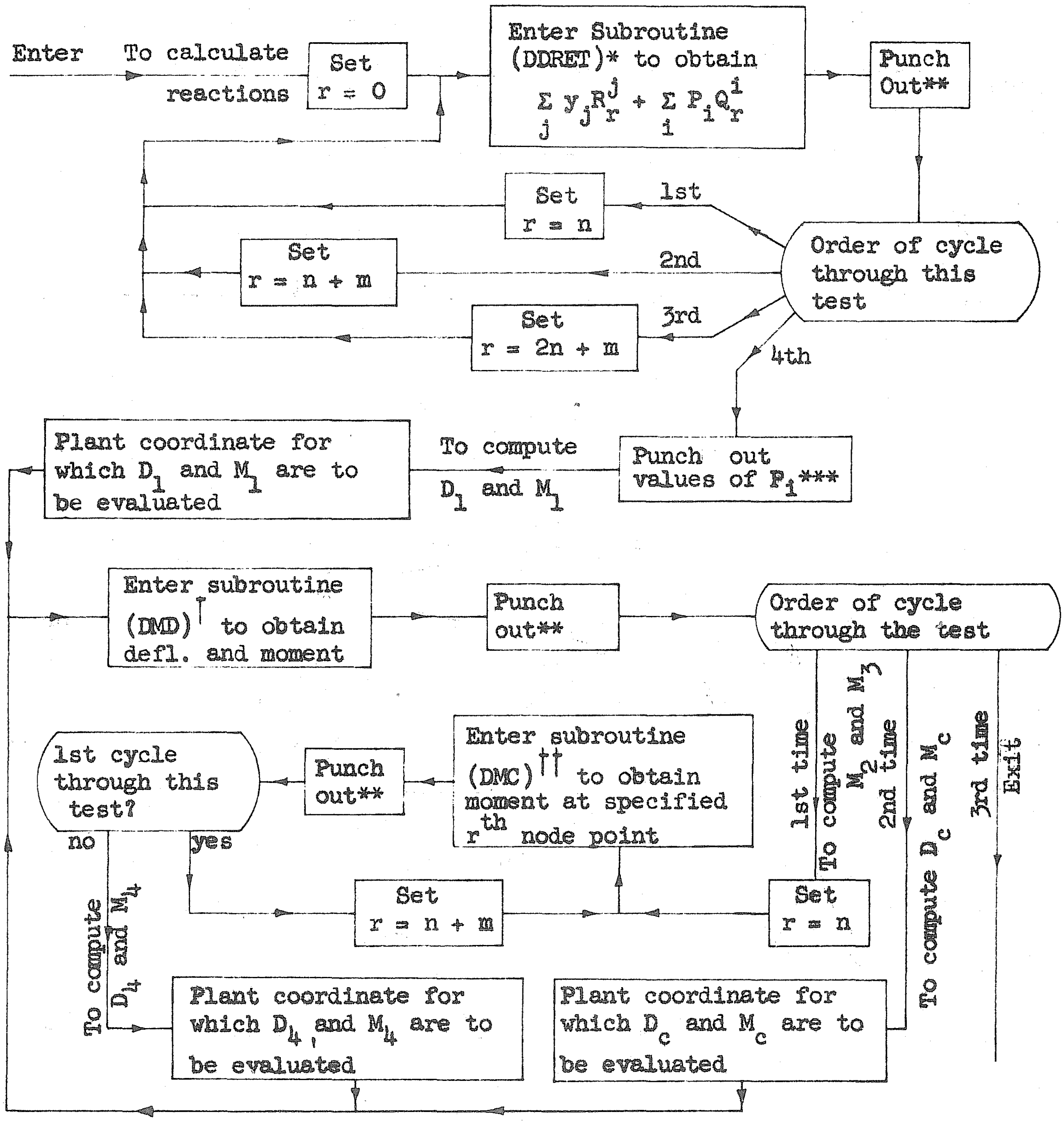

* Refer to Fig. 11

** In the dynamic history program, the information is punched out, in the A.F. program, the result is compared with the corresponding result already in the machine, and the larger value is stored.

*** In the A.F. program, this step is omitted.

† Refer to Fig. 12

†† Refer to Fig. 13

FIG. 14 GENERAL FLOW CHART FOR CALCULATING DYNAMIC RESPONSE

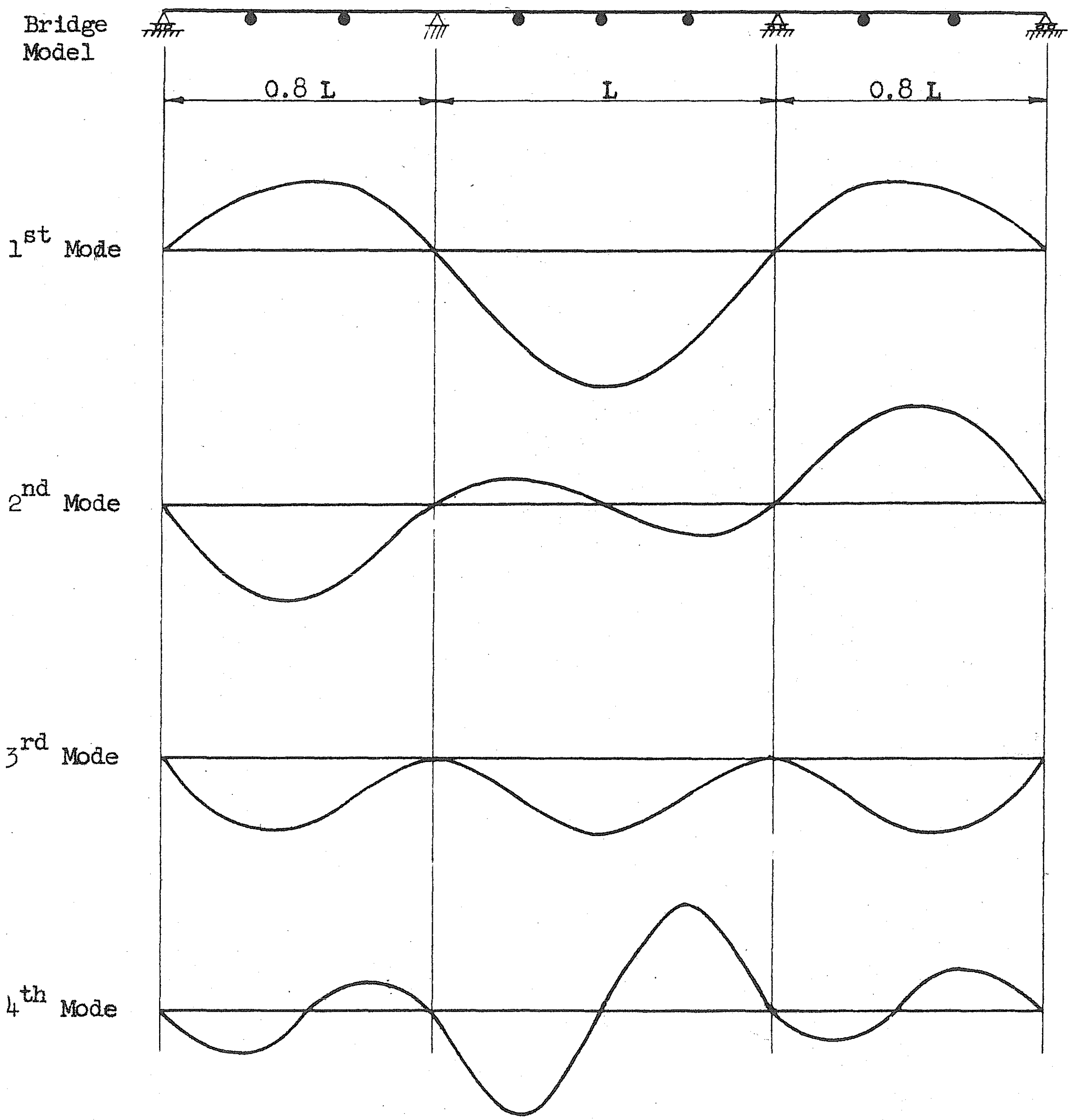

FIG.15 FIRST FOUR NATURAL MODES OF VIBRATION
OF A THREE-SPAN CONTINUOUS BEAM

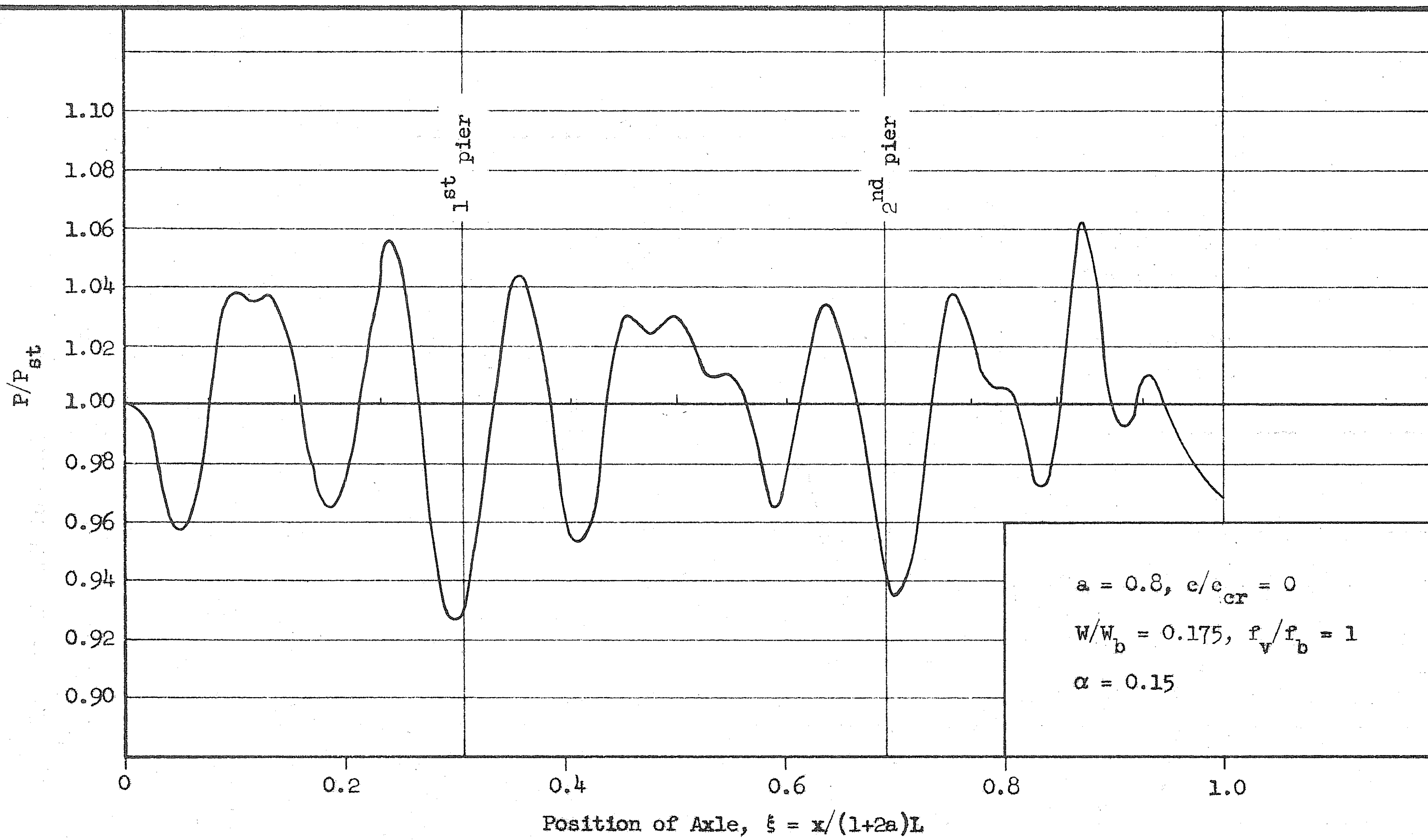

FIG. 16a HISTORY CURVE FOR INTERACTING FORCE, P -- SINGLE-AXLE LOADING

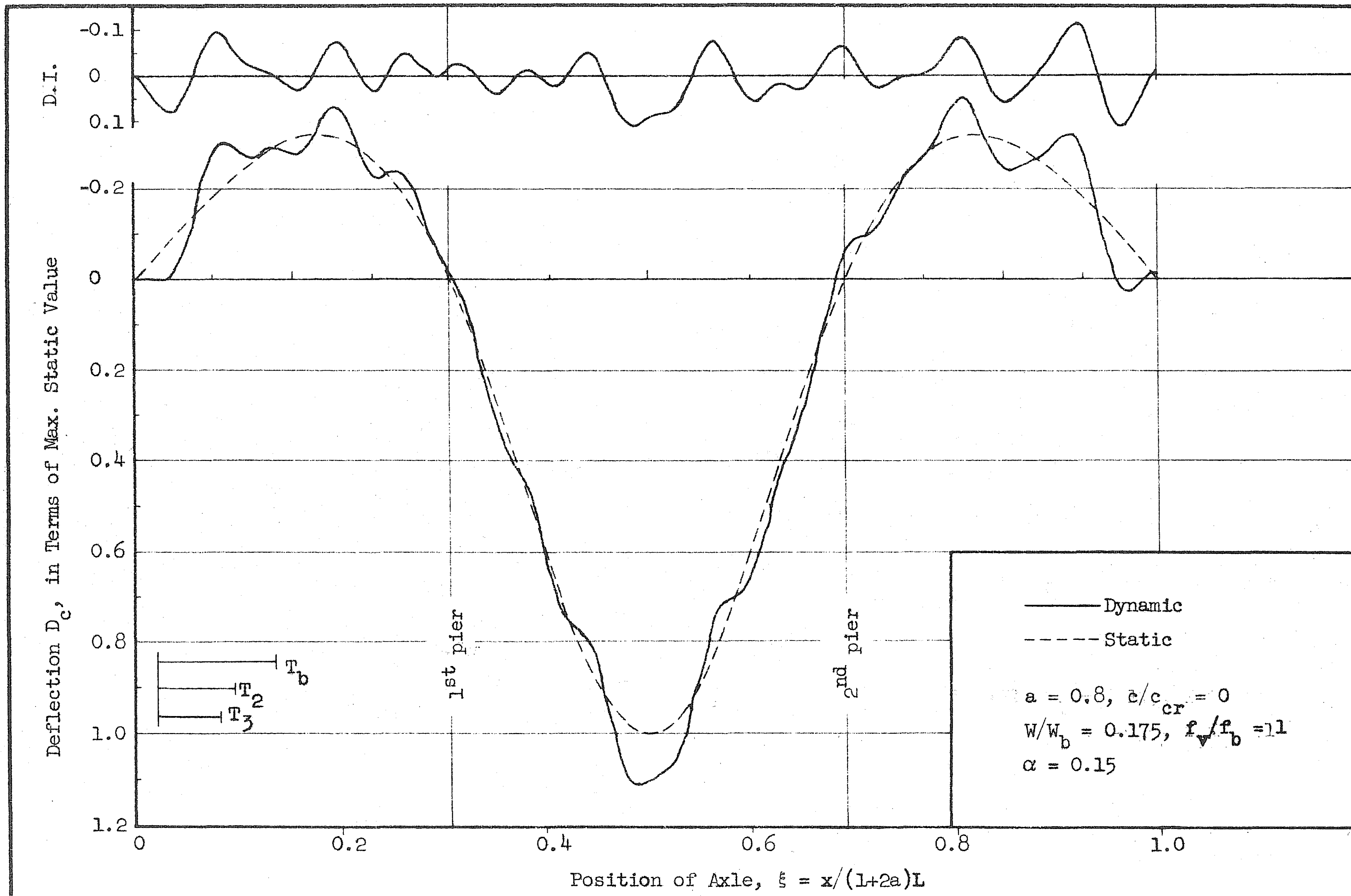

FIG. 16b HISTORY CURVES FOR D_c AND CORRESPONDING DYNAMIC INCREMENT -- SINGLE-AXLE LOADING

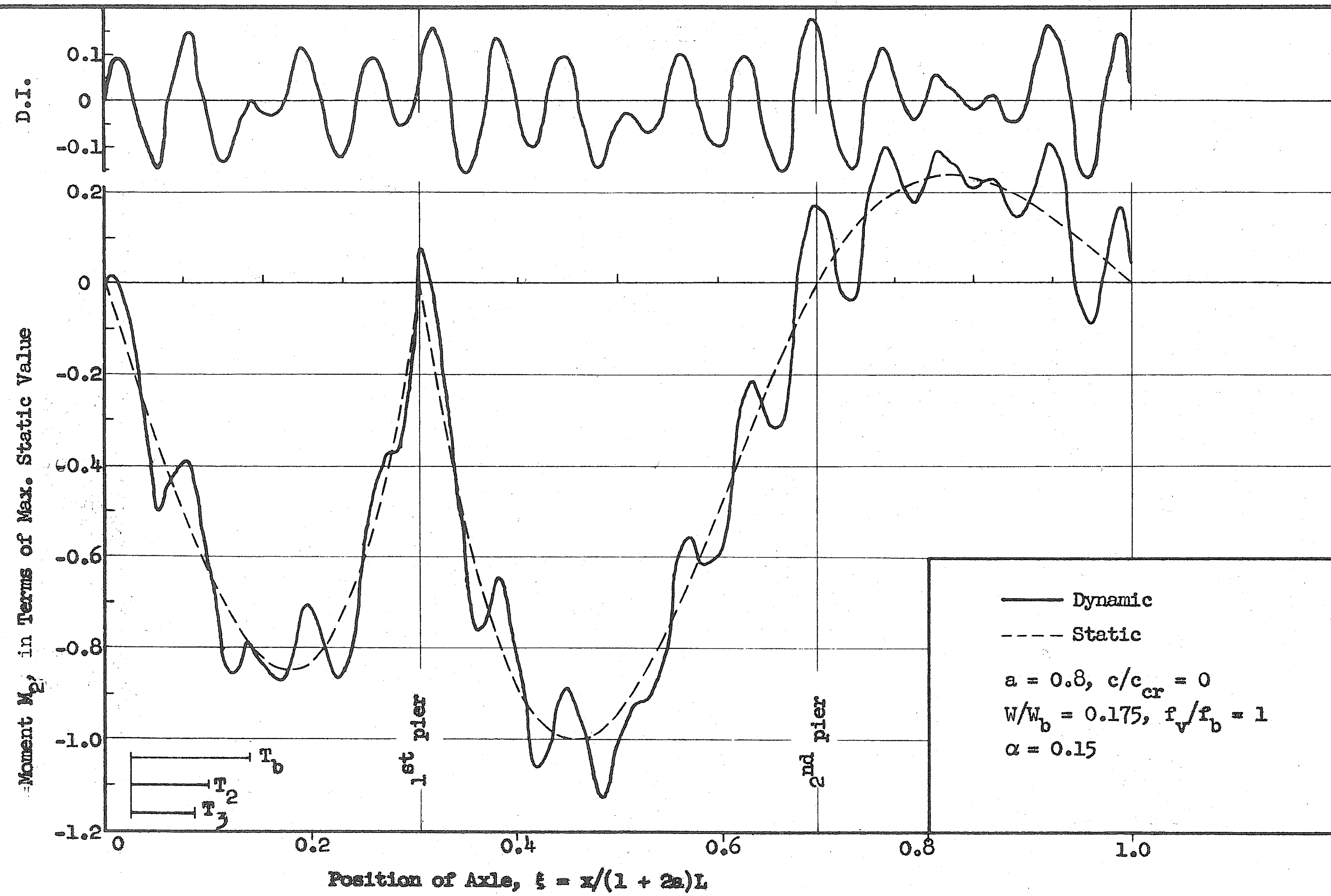

FIG. 16c HISTORY CURVES FOR M_2 AND CORRESPONDING DYNAMIC INCREMENT -- SINGLE AXLE-LOADING

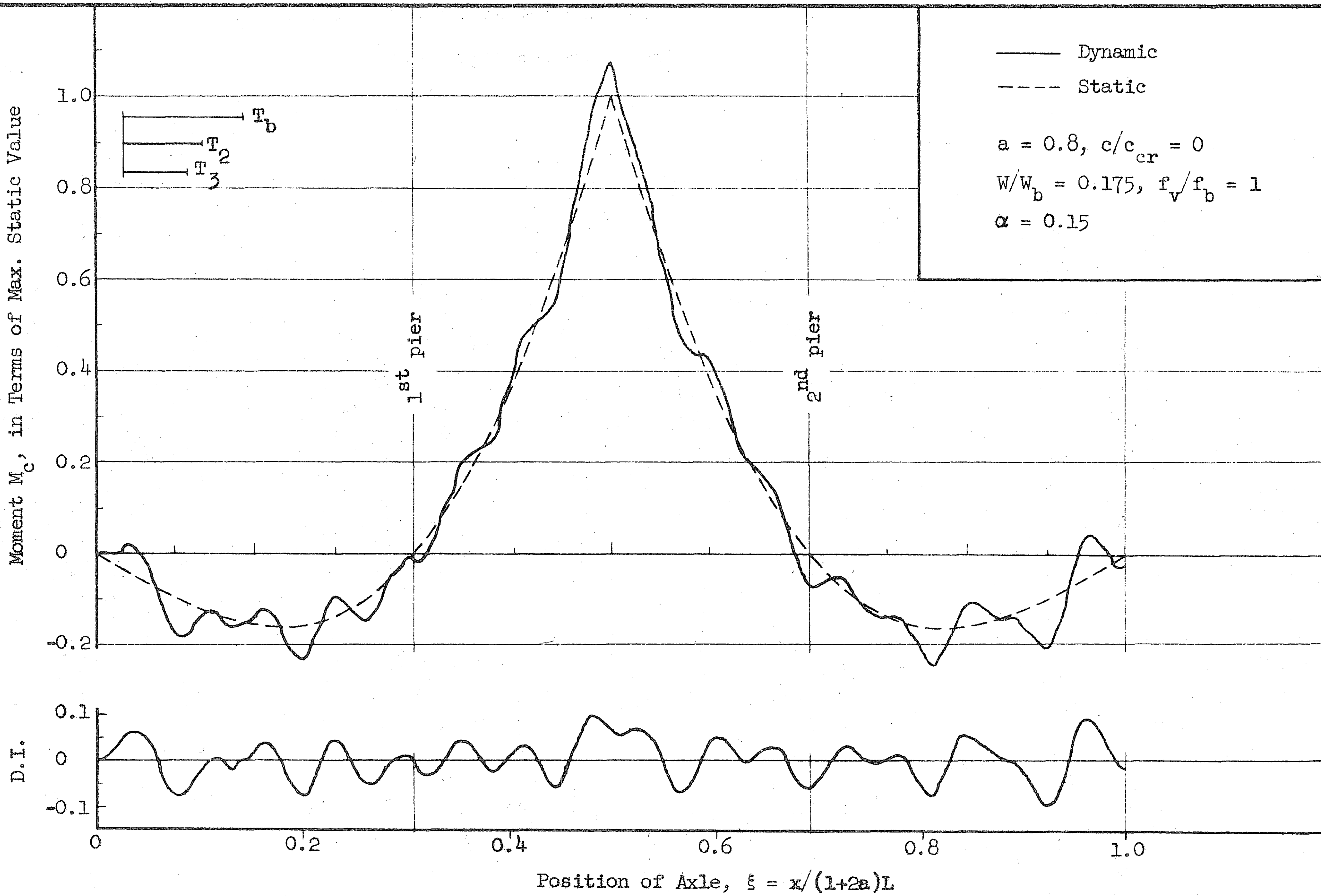

FIG. 16d HISTORY CURVES FOR M_c AND CORRESPONDING DYNAMIC INCREMENT -- SINGLE-AXLE LOADING

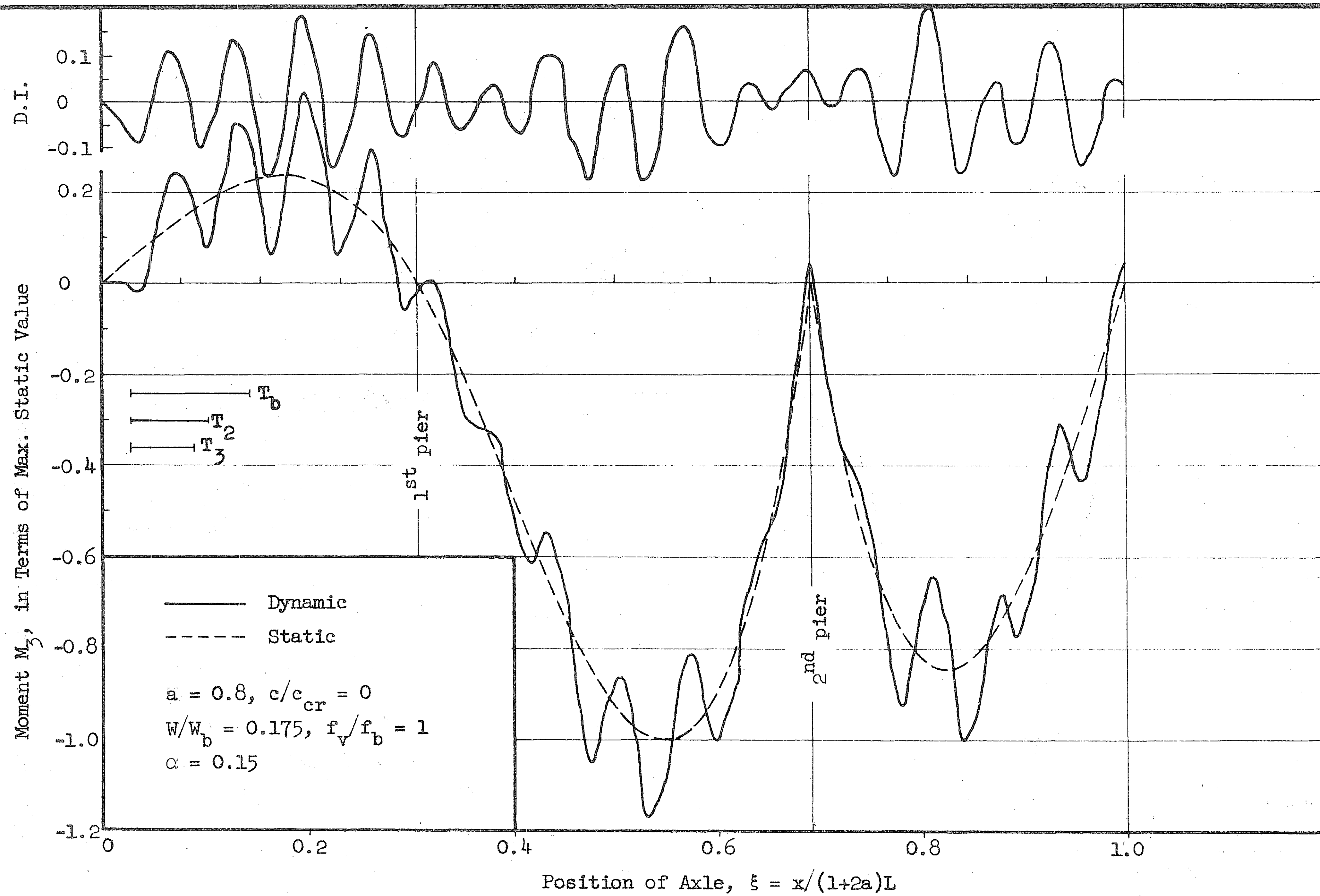

FIG. 16e HISTORY CURVES FOR M_3 AND CORRESPONDING DYNAMIC INCREMENT -- SINGLE-AXLE LOADING

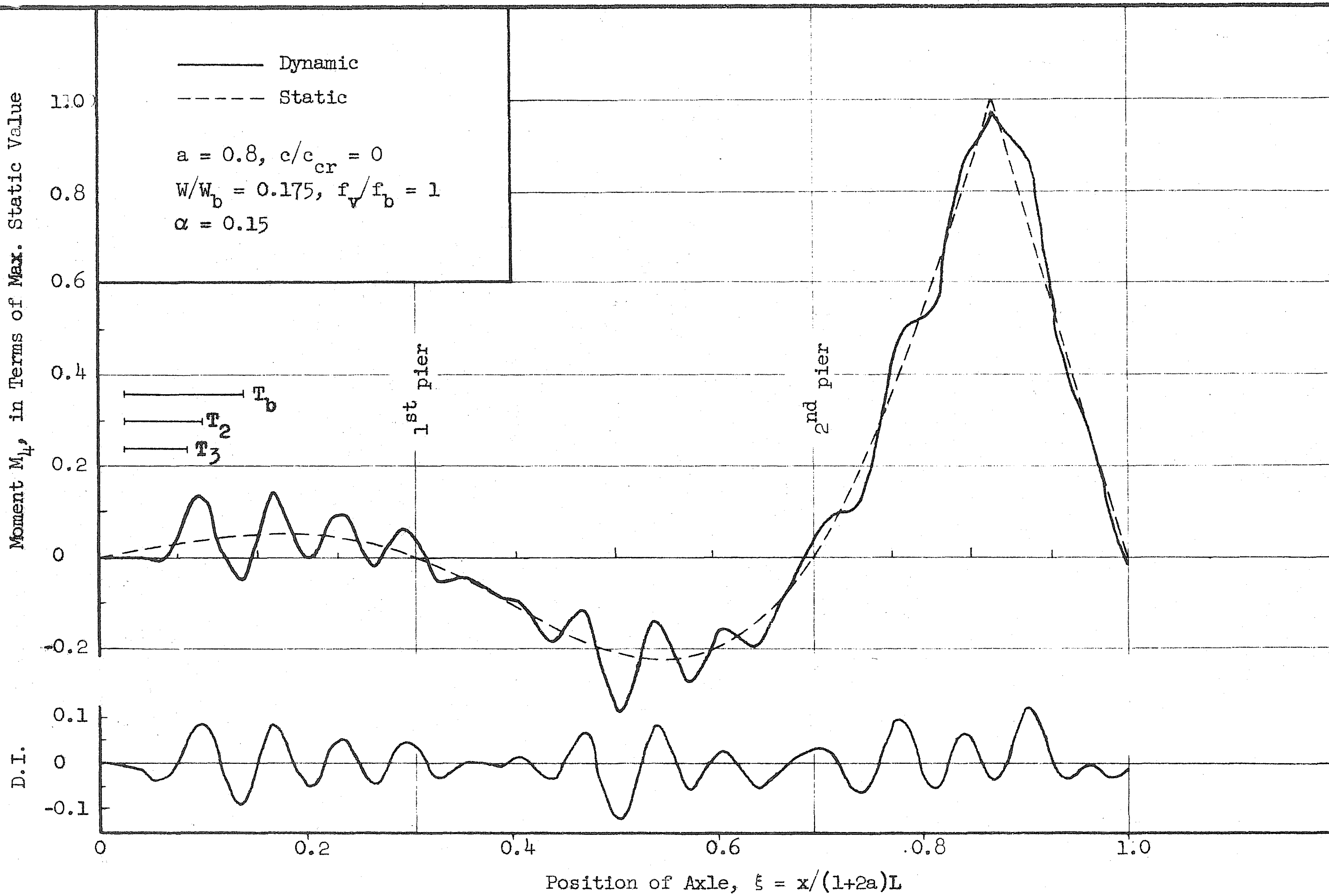

FIG. 16f HISTORY CURVES FOR M_4 AND CORRESPONDING DYNAMIC INCREMENT -- SINGLE-AXLE LOADING

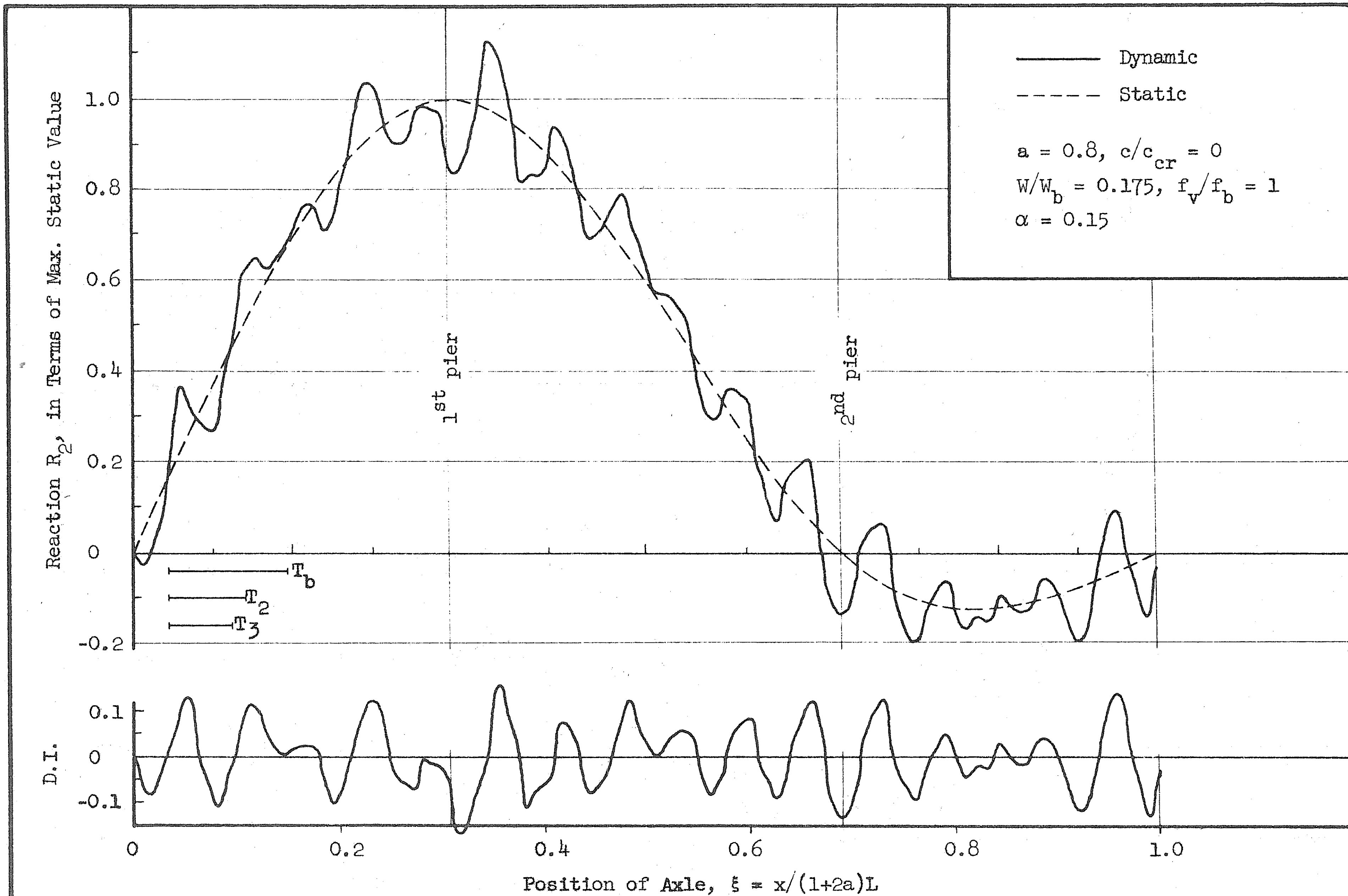

FIG. 16a HISTORY CURVES FOR R_2 AND CORRESPONDING DYNAMIC INCREMENT -- SINGLE-AXLE LOADING

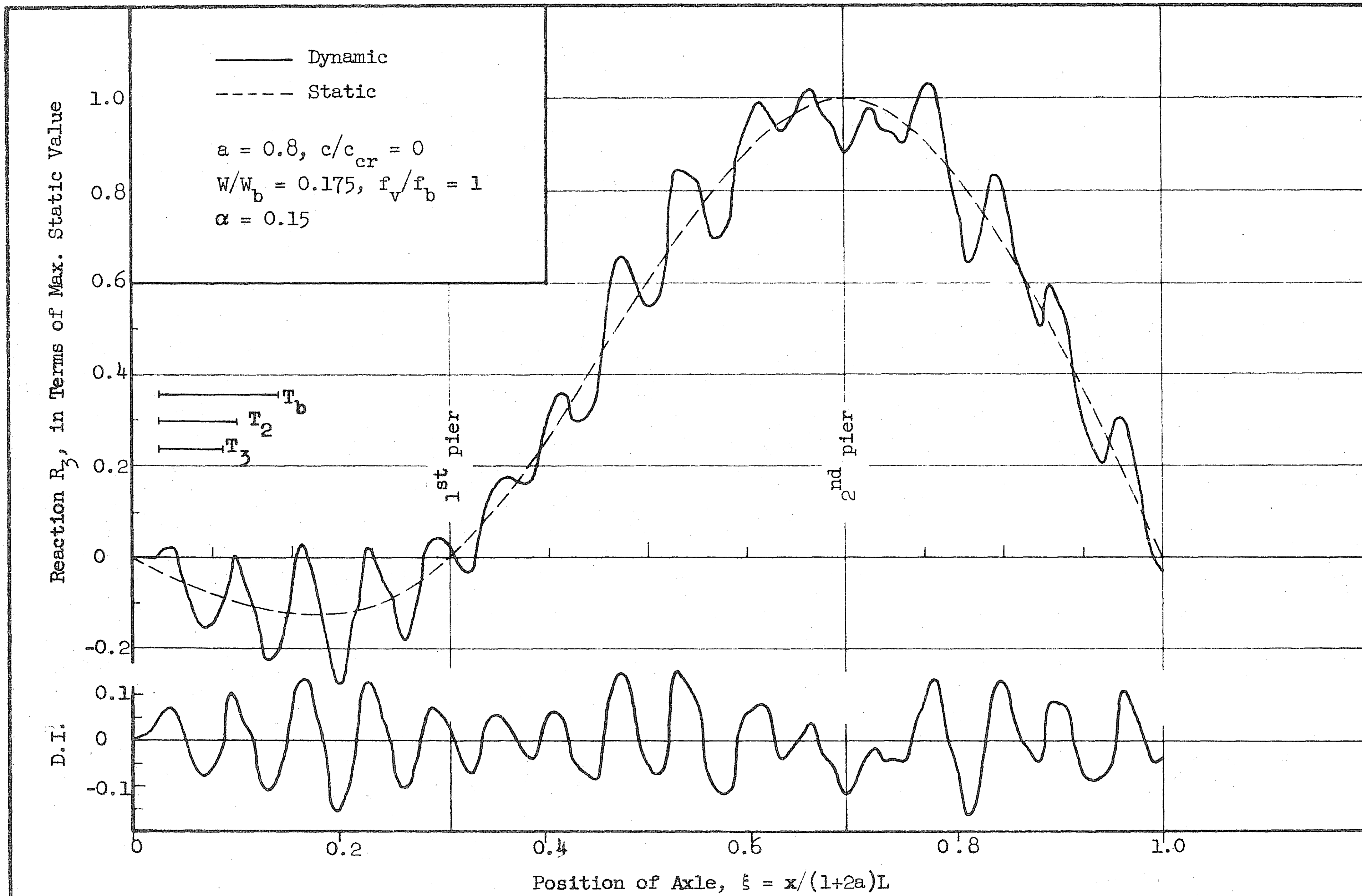

FIG. 16h HISTORY CURVES FOR R_3 AND CORRESPONDING DYNAMIC INCREMENT -- SINGLE-AXLE LOADING

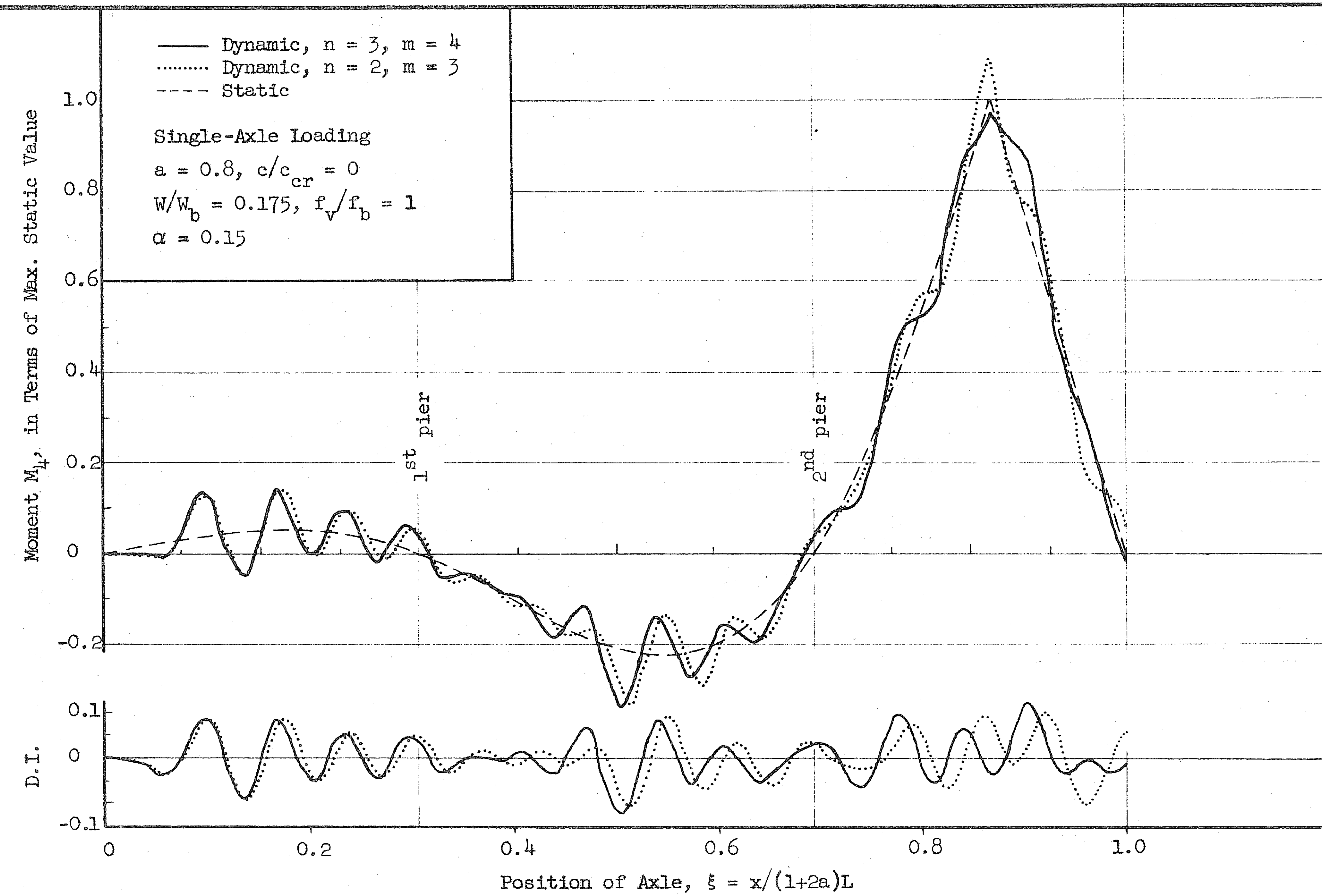

FIG. **17** EFFECT OF NUMBER OF MASSES CONSIDERED ON MOMENT M_4

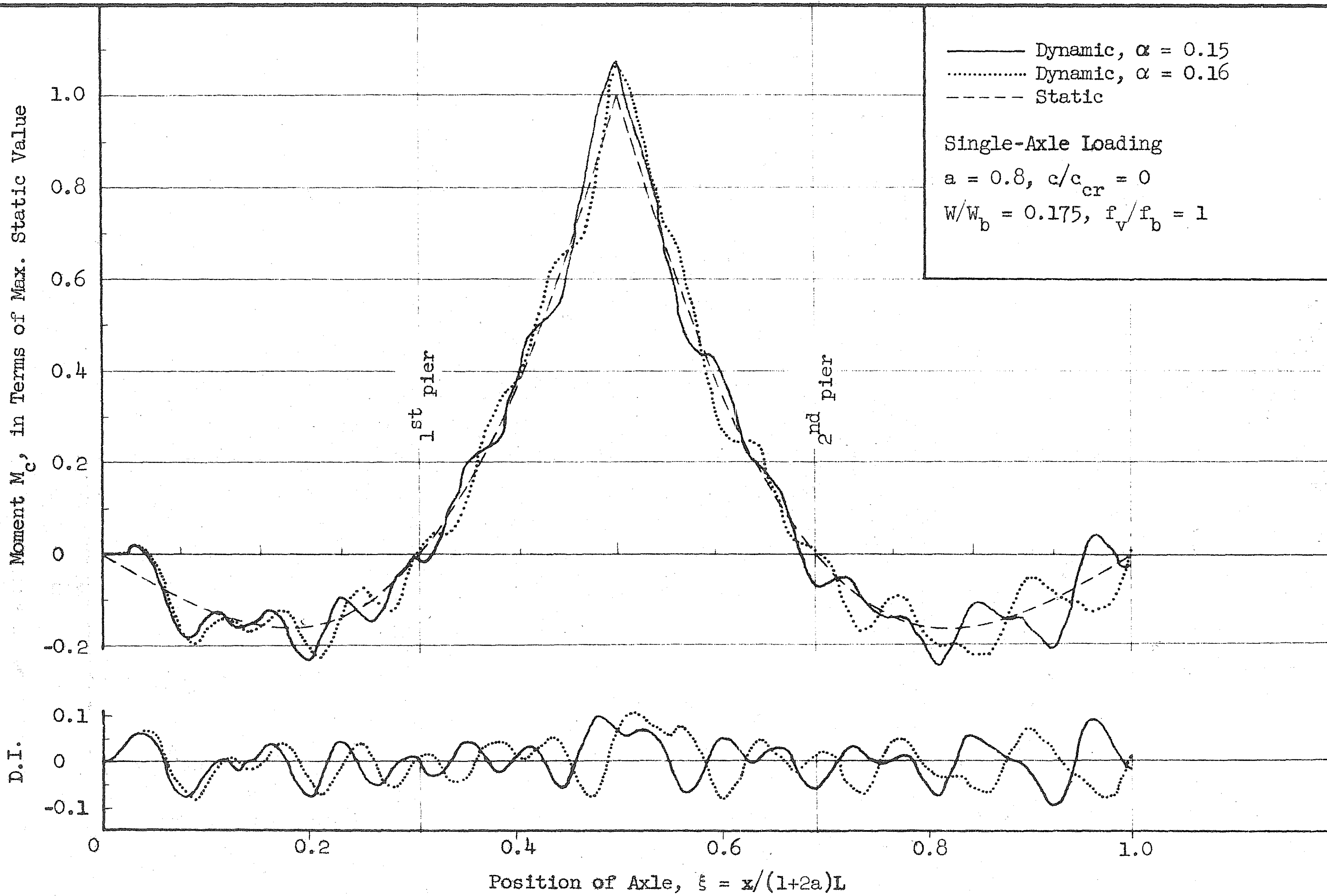

FIG. 18 EFFECT OF SPEED ON HISTORY OF RESPONSE -- CURVES FOR M_c

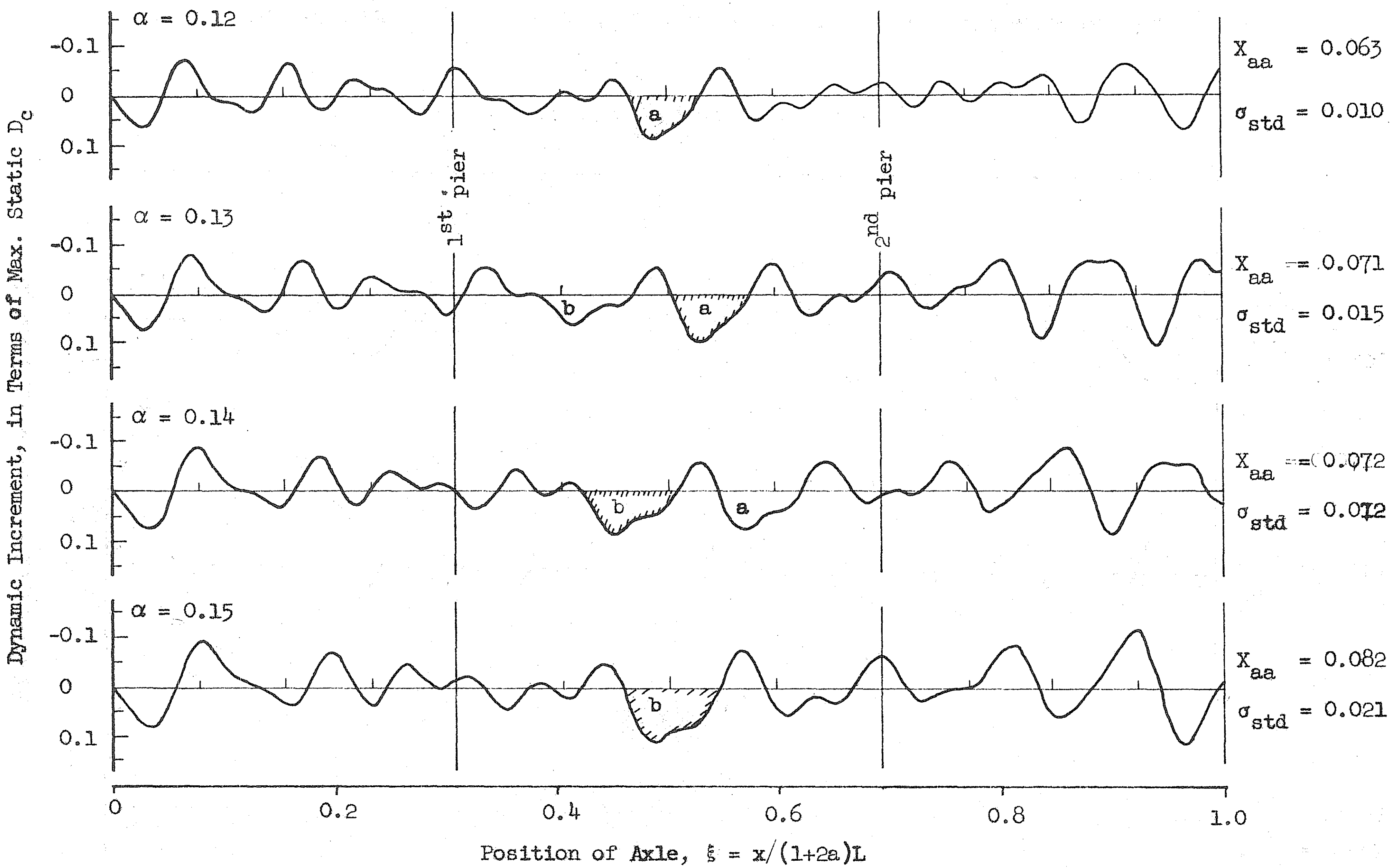

FIG. 19a EFFECT OF SPEED ON DYNAMIC INCREMENT FOR D_c -- SINGLE-AXLE LOADING

$a = 0.8$, $c/c_{cr} = 0$, $W/W_b = 0.175$, $f_v/f_b = 1$

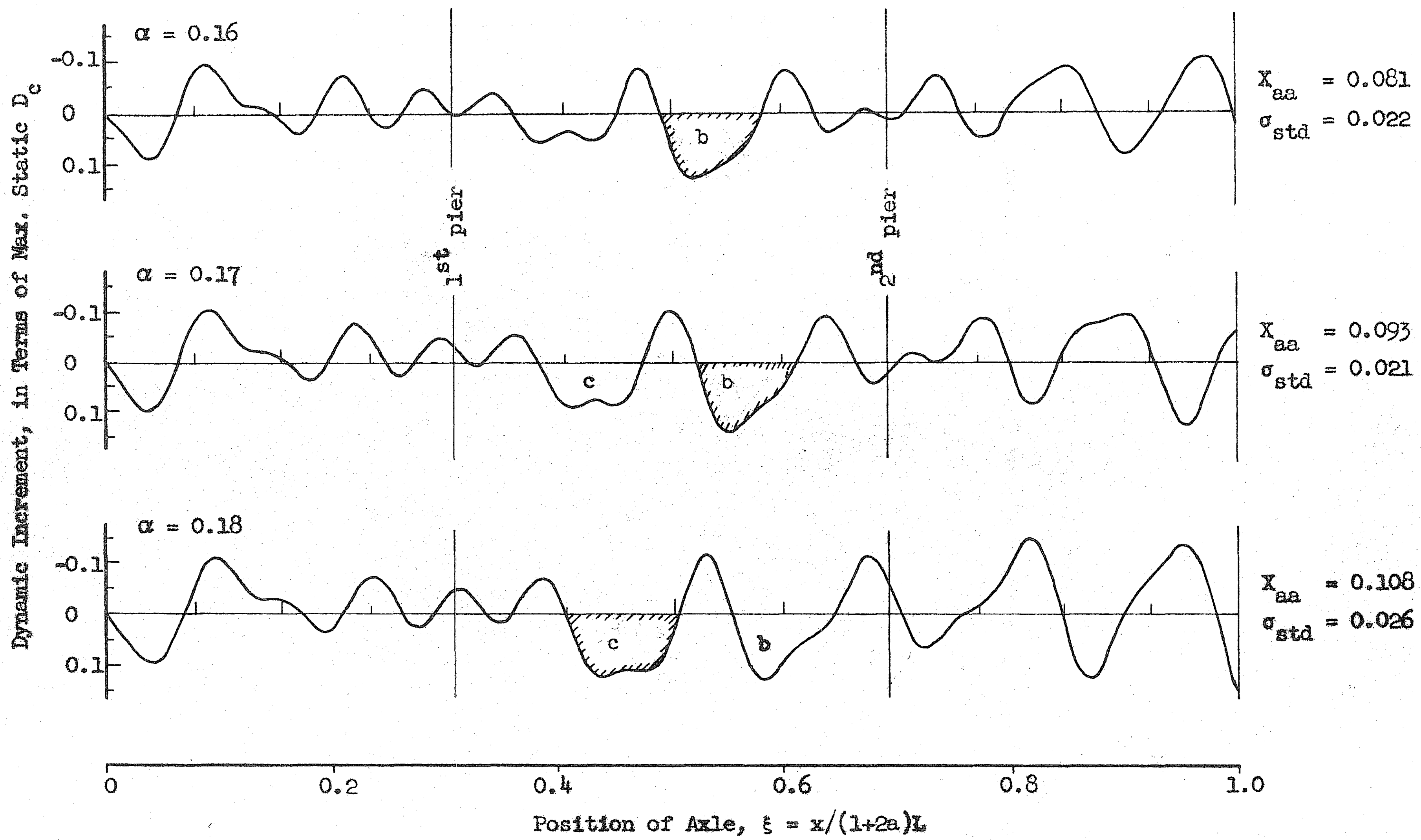

FIG. 19b EFFECT OF SPEED ON DYNAMIC INCREMENT FOR D_c -- SINGLE-AXLE LOADING

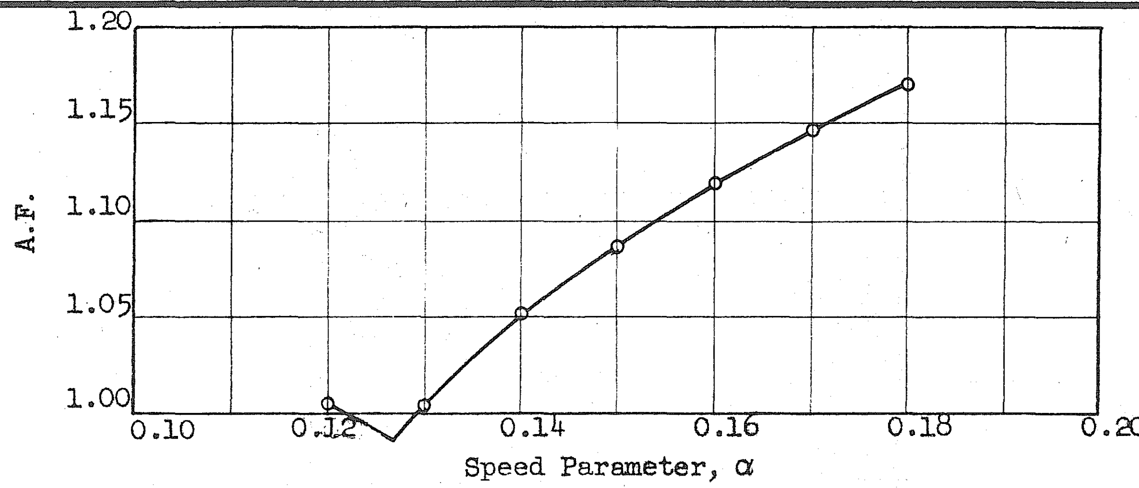

(a) Amplification Factor for D_1

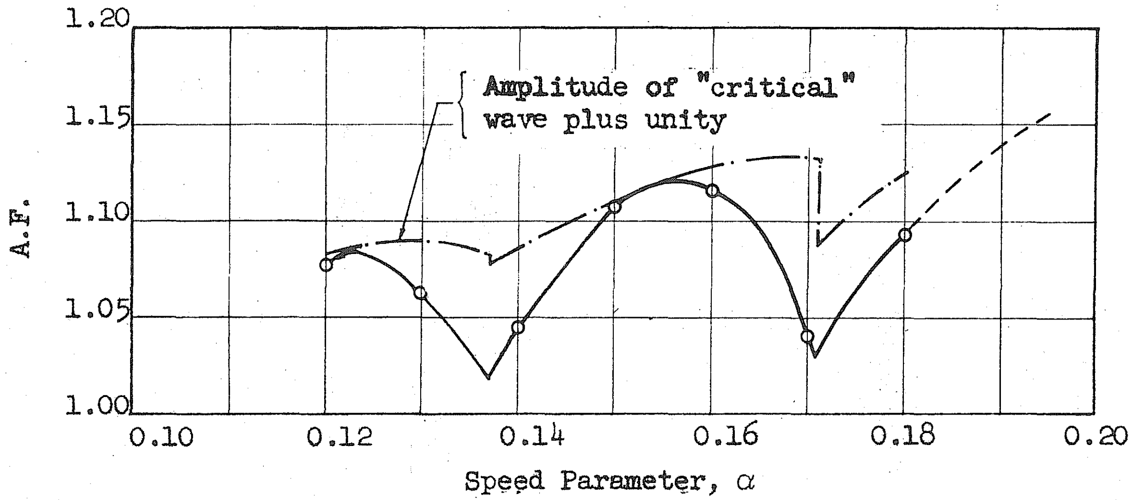

(b) Amplification Factor for D_c

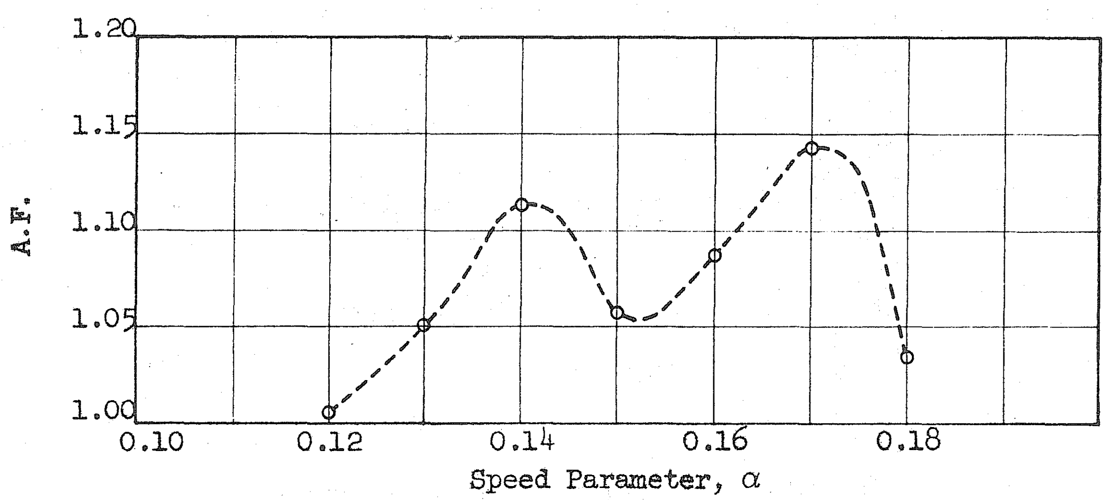

(c) Amplification Factor for D_4

FIG. 20 EFFECT OF SPEED ON AMPLIFICATION FACTORS -- SINGLE-AXLE LOADING

$a = 0.8$, $c/_{cr} = 0$, $W/W_b = 0.175$, $f_v/f_b = 1$

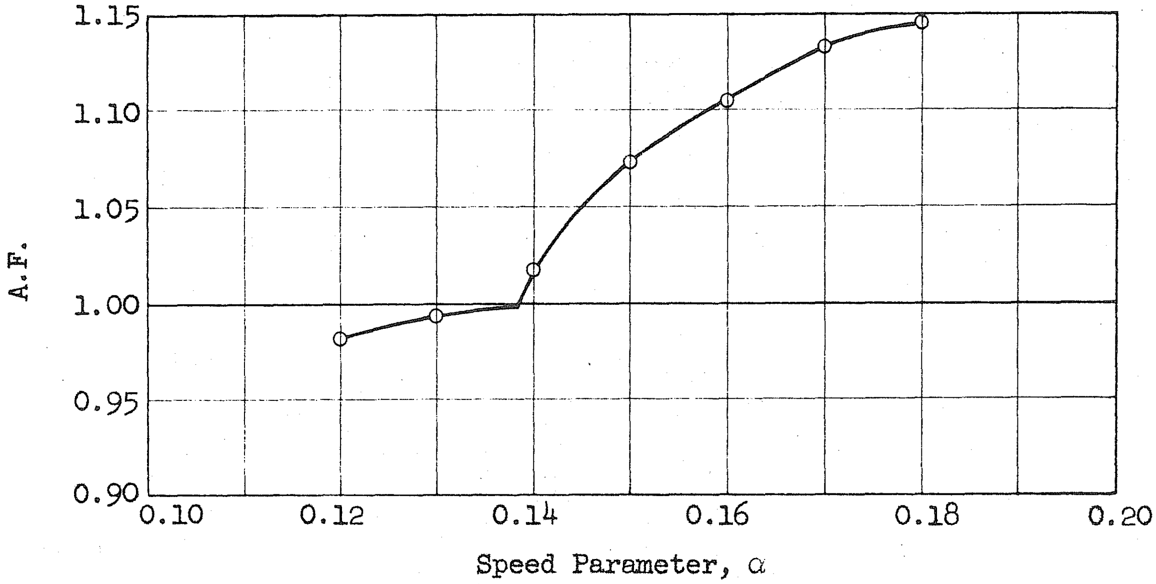

(d) Amplification Factor for M_1

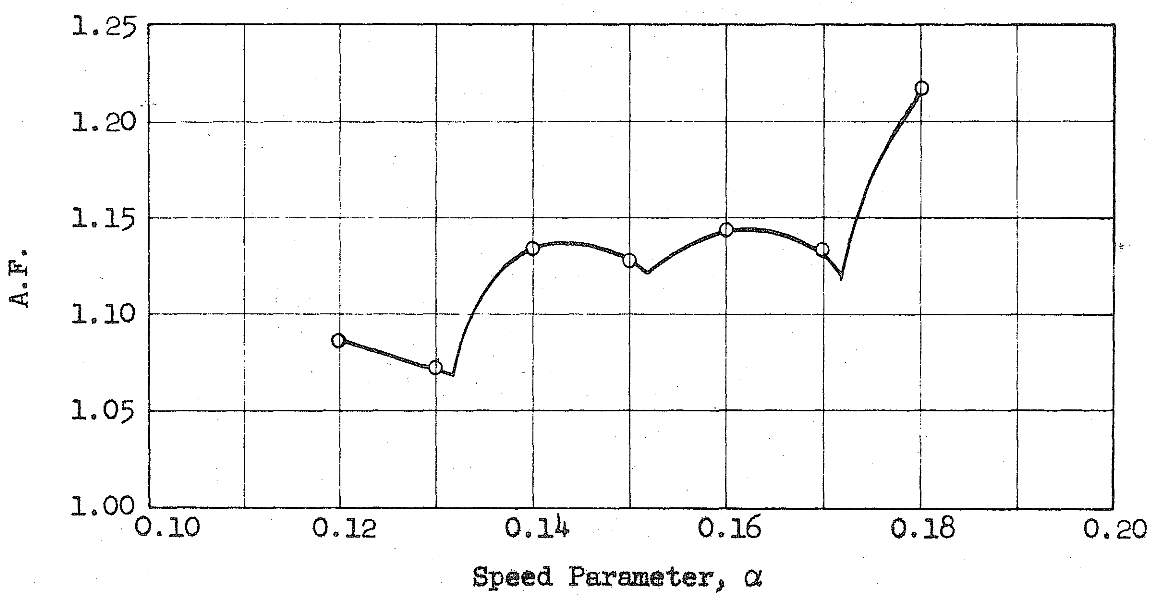

(e) Amplification Factor for M_2

FIG. 20 (Cont'd) EFFECT OF SPEED ON AMPLIFICATION FACTORS -- SINGLE-AXLE LOADING

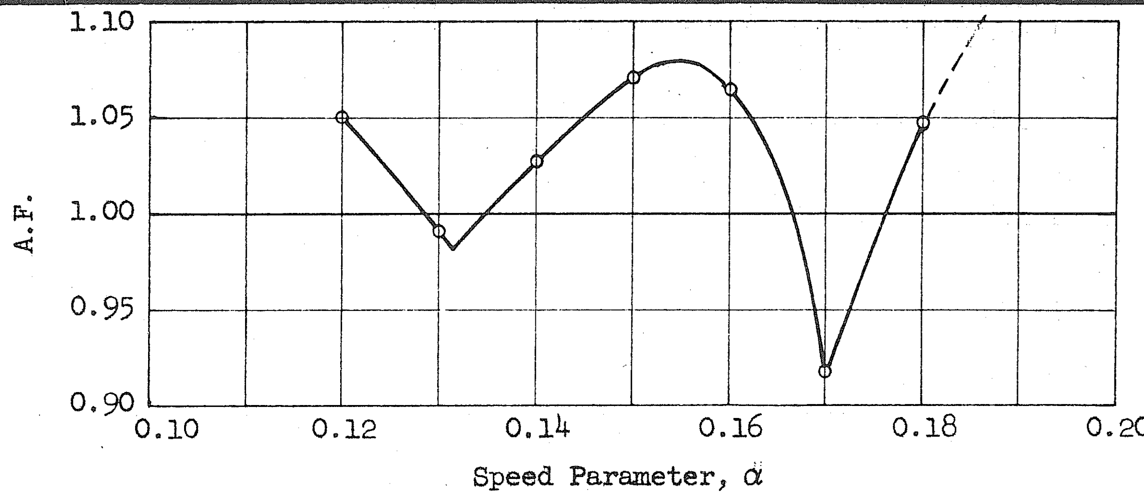

(f) Amplification Factor for M_c

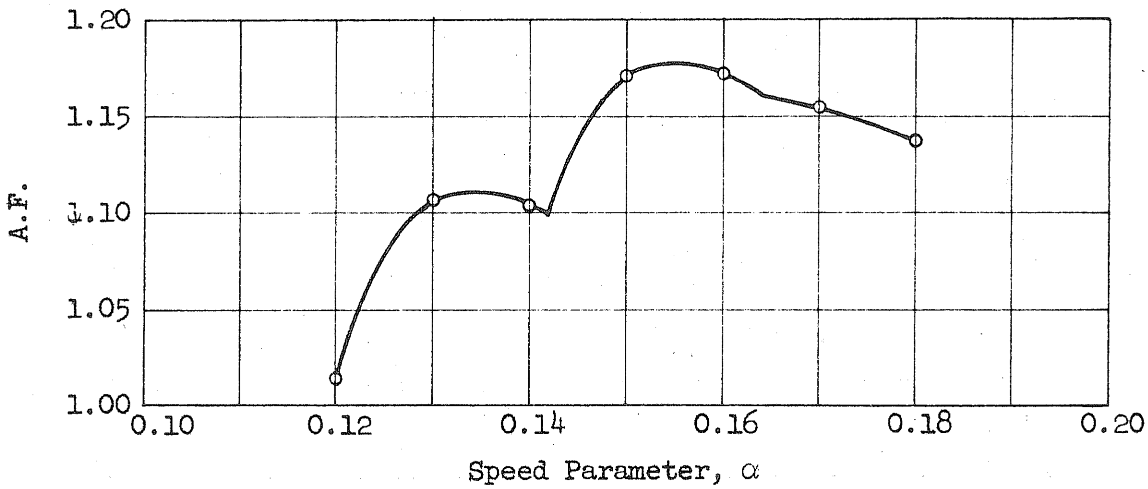

(g) Amplification Factor for M_3

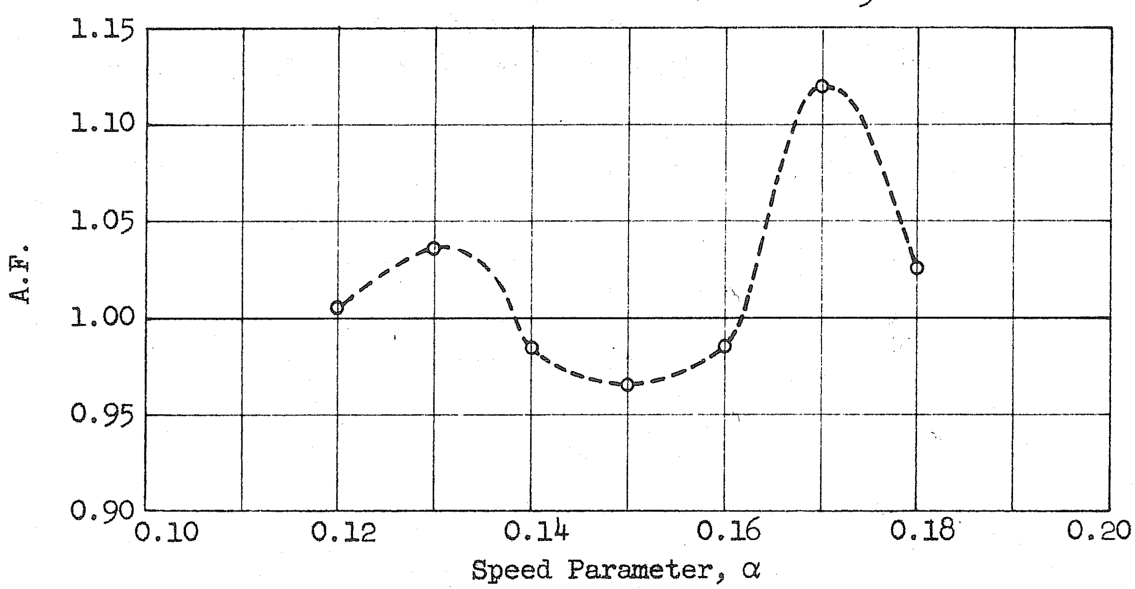

(h) Amplification Factor for M_4

FIG. 20 (Cont'd) EFFECT OF SPEED ON AMPLIFICATION FACTORS -- SINGLE-AXLE LOADING

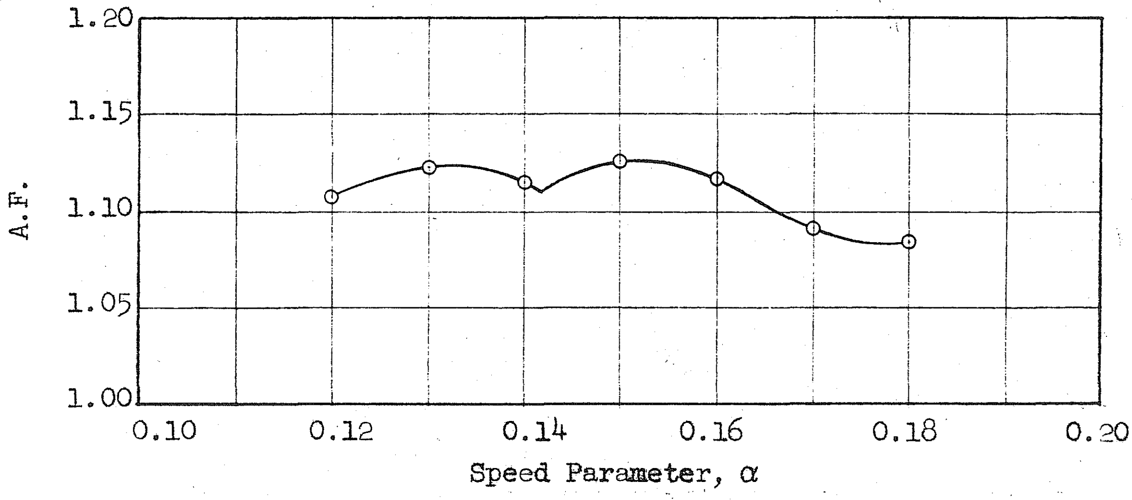

(i) Amplification Factor for R_2

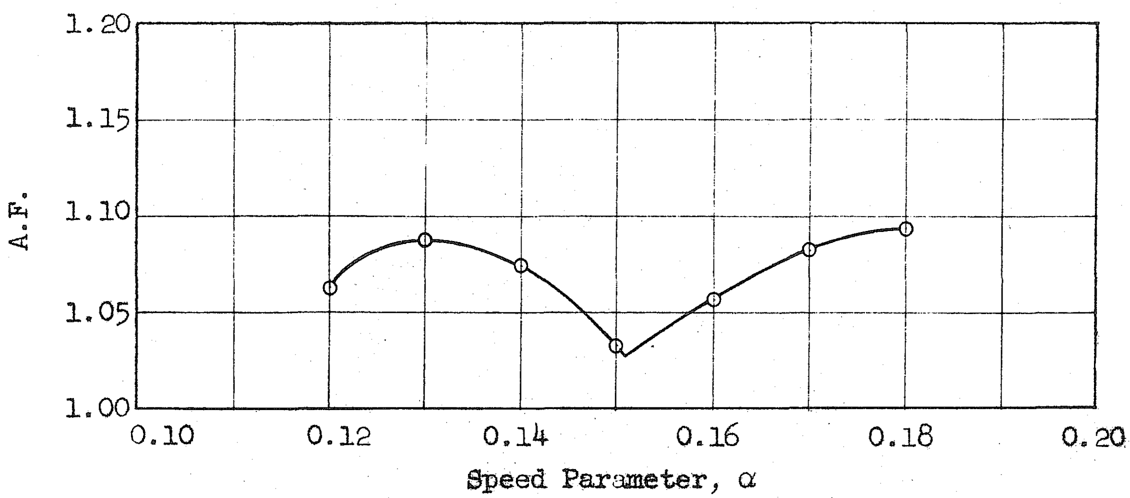

(j) Amplification Factor for R_3

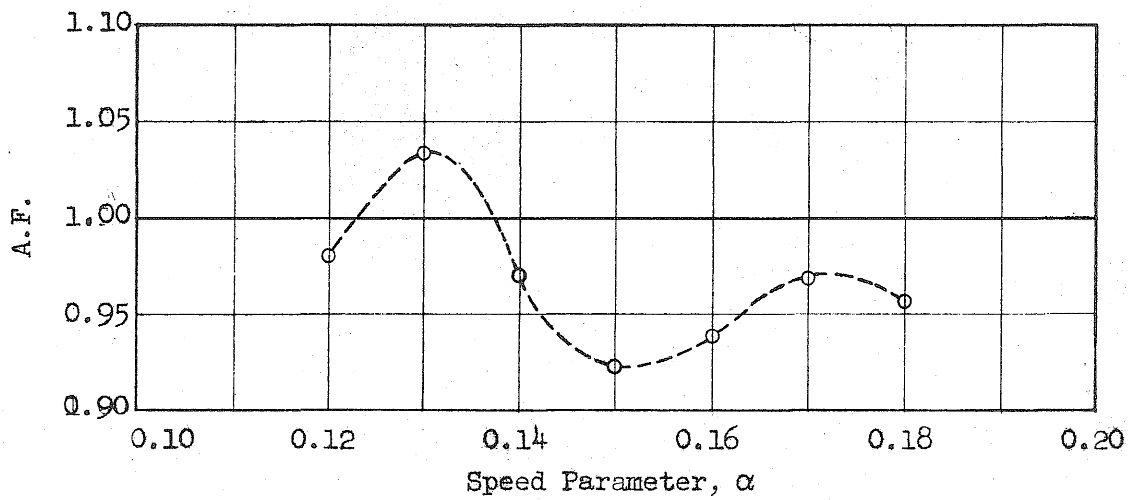

(k) Amplification Factor for R_4

FIG. 20 (Cont'd) EFFECT OF SPEED ON AMPLIFICATION FACTORS -- SINGLE-AXLE LOADING

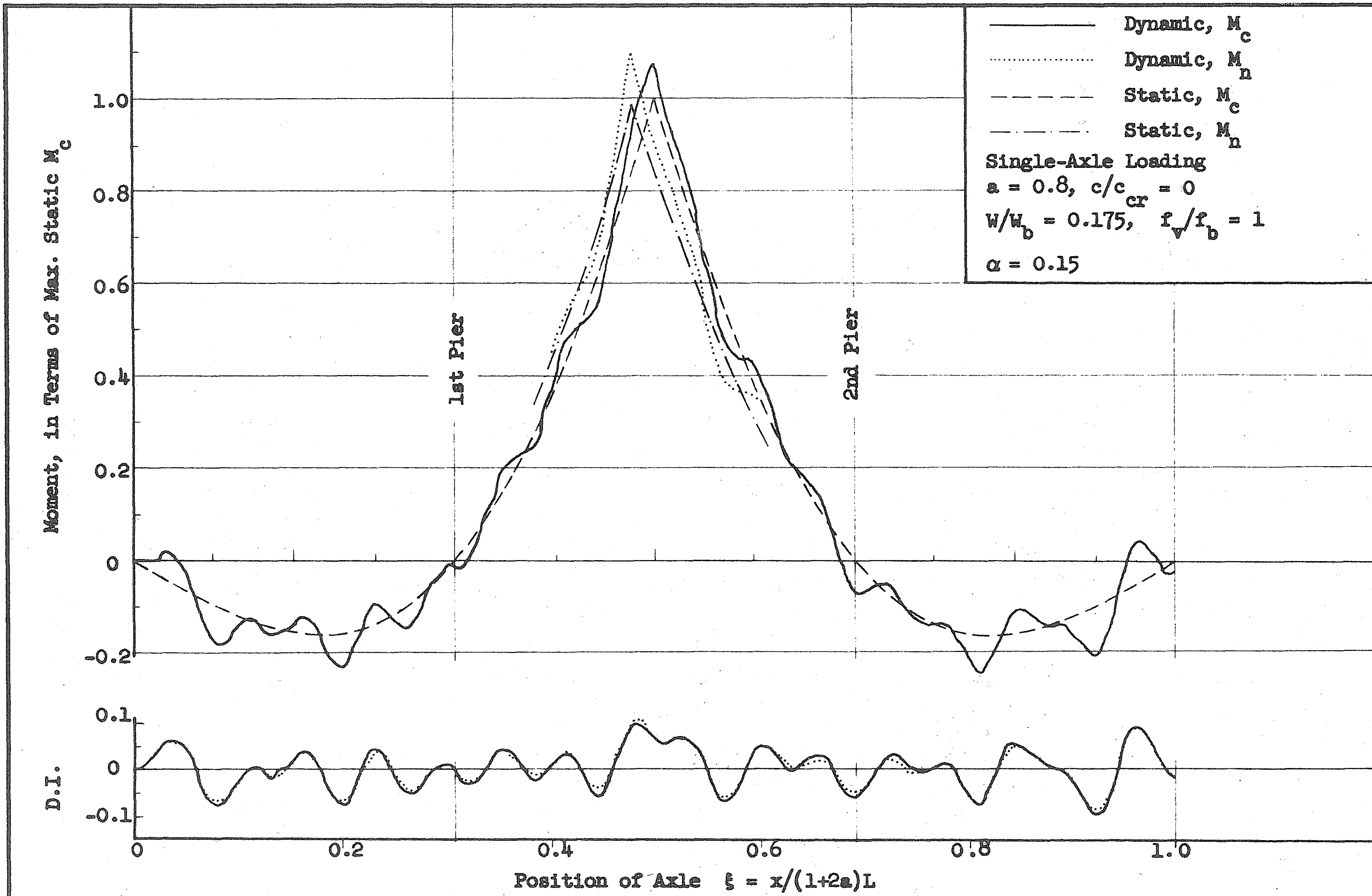

FIG. 21 COMPARISON OF DYNAMIC RESPONSES AT TWO NEIGHBORING SECTIONS -- CURVES FOR M_c AND M_n

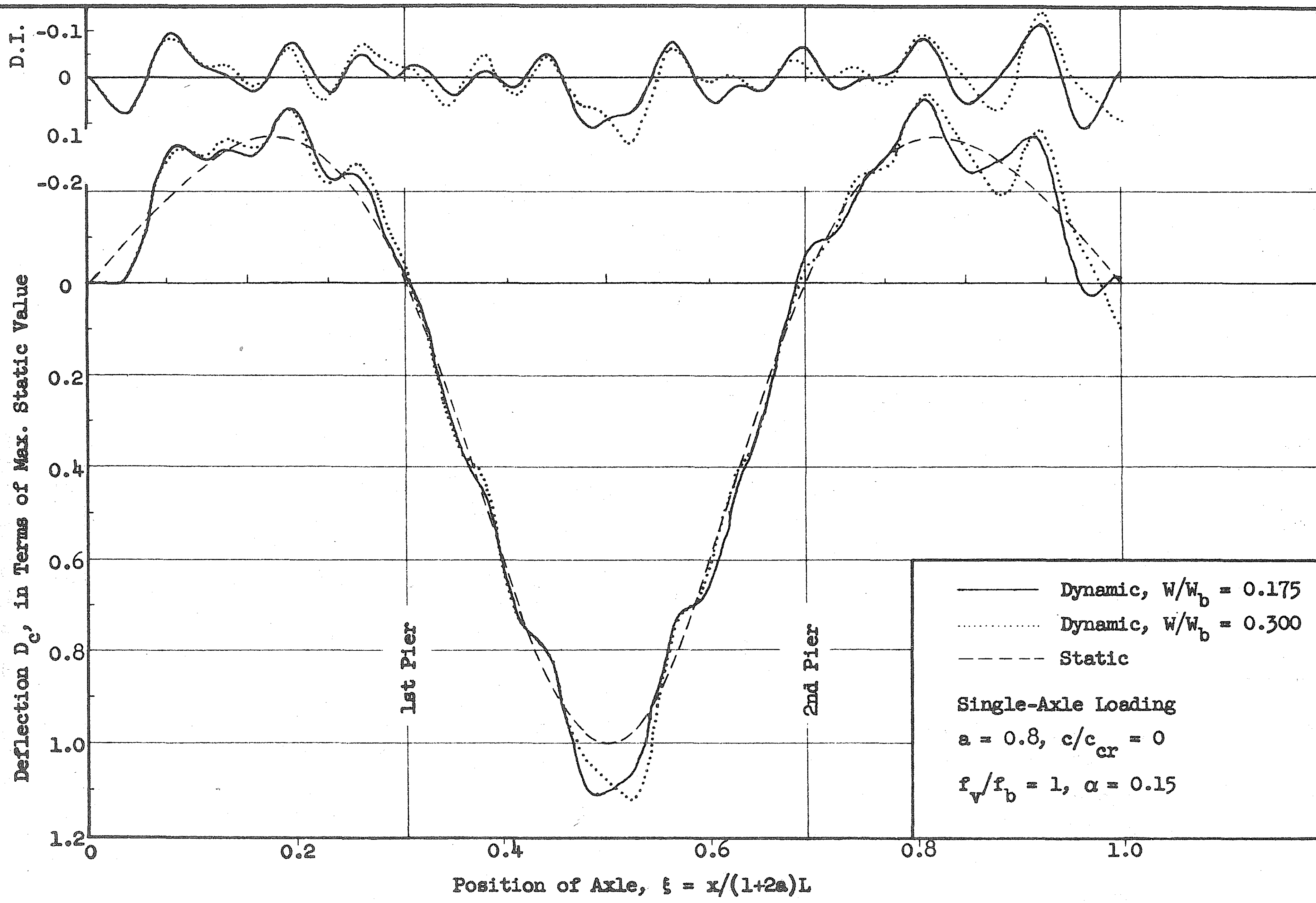

FIG. 22 EFFECT OF WEIGHT RATIO ON HISTORY OF RESPONSE -- CURVES FOR D_c

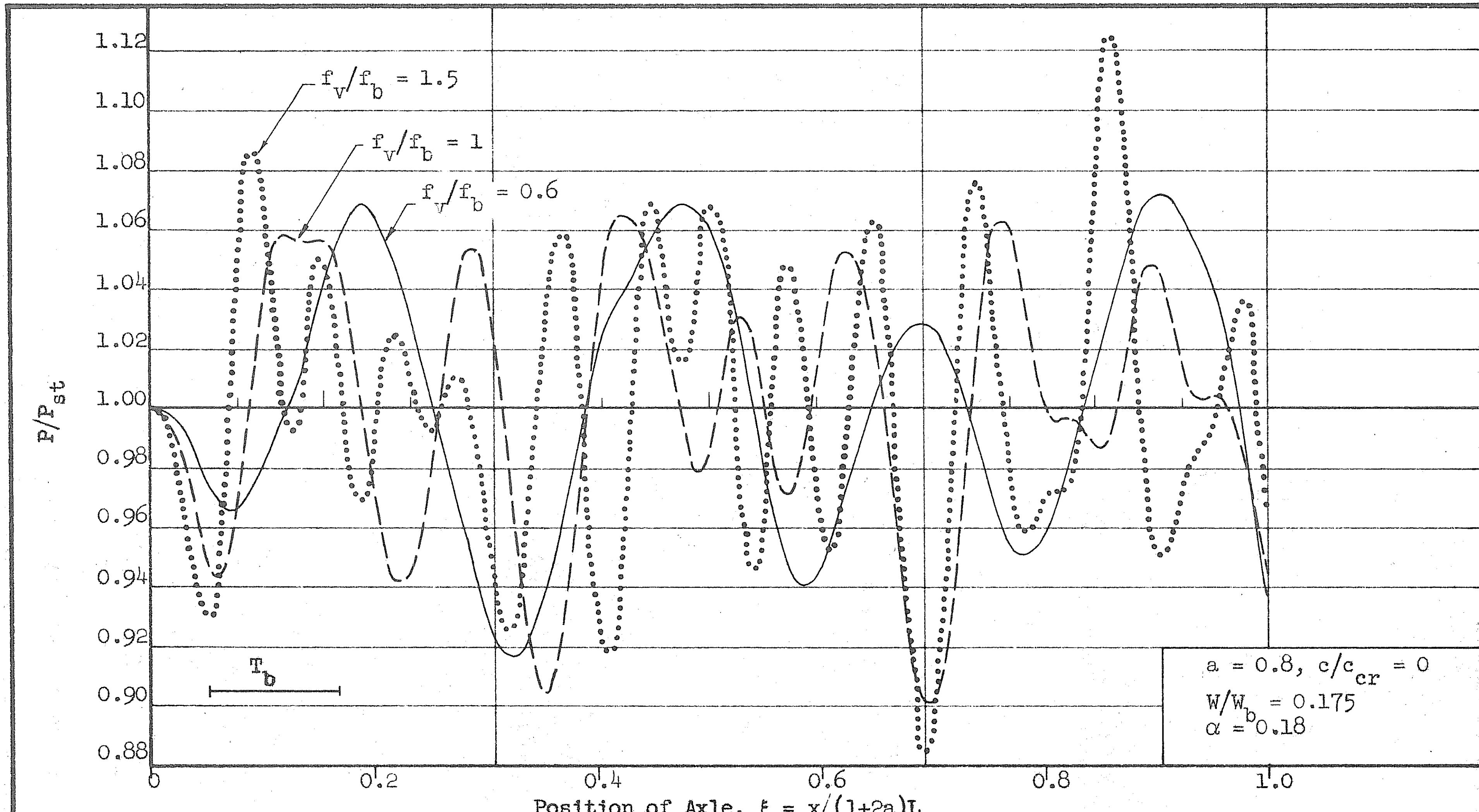

FIG. 23 EFFECT OF FREQUENCY RATIO ON INTERACTING FORCE, P -- SINGLE-AXLE LOADING

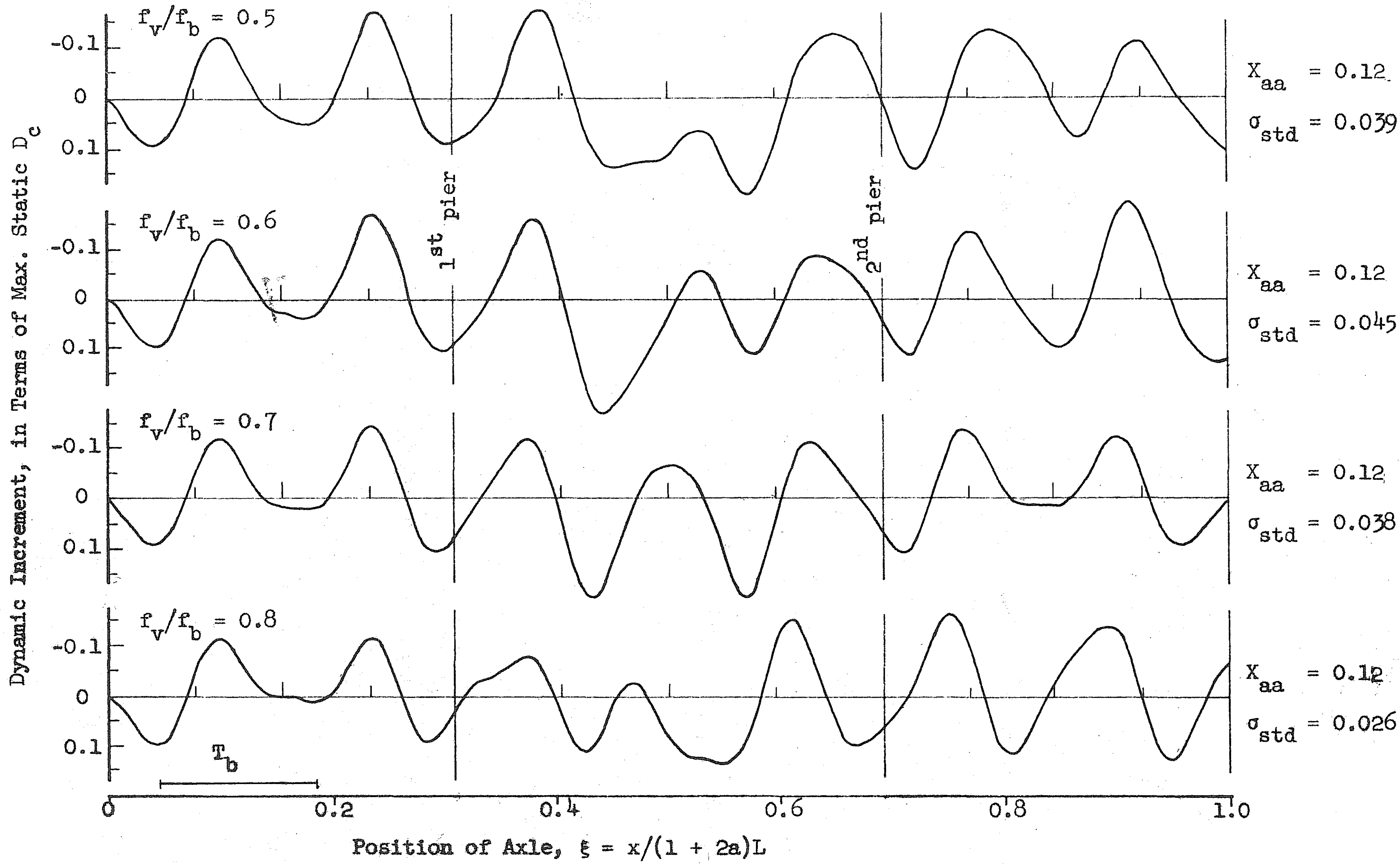

FIG. 24a EFFECT OF FREQUENCY RATIO ON DYNAMIC INCREMENT FOR D_c -- SINGLE-AXLE LOADING

$a = 0.8$, $c/c_{cr} = 0$, $W/W_b = 0.175$, $\alpha = 0.18$

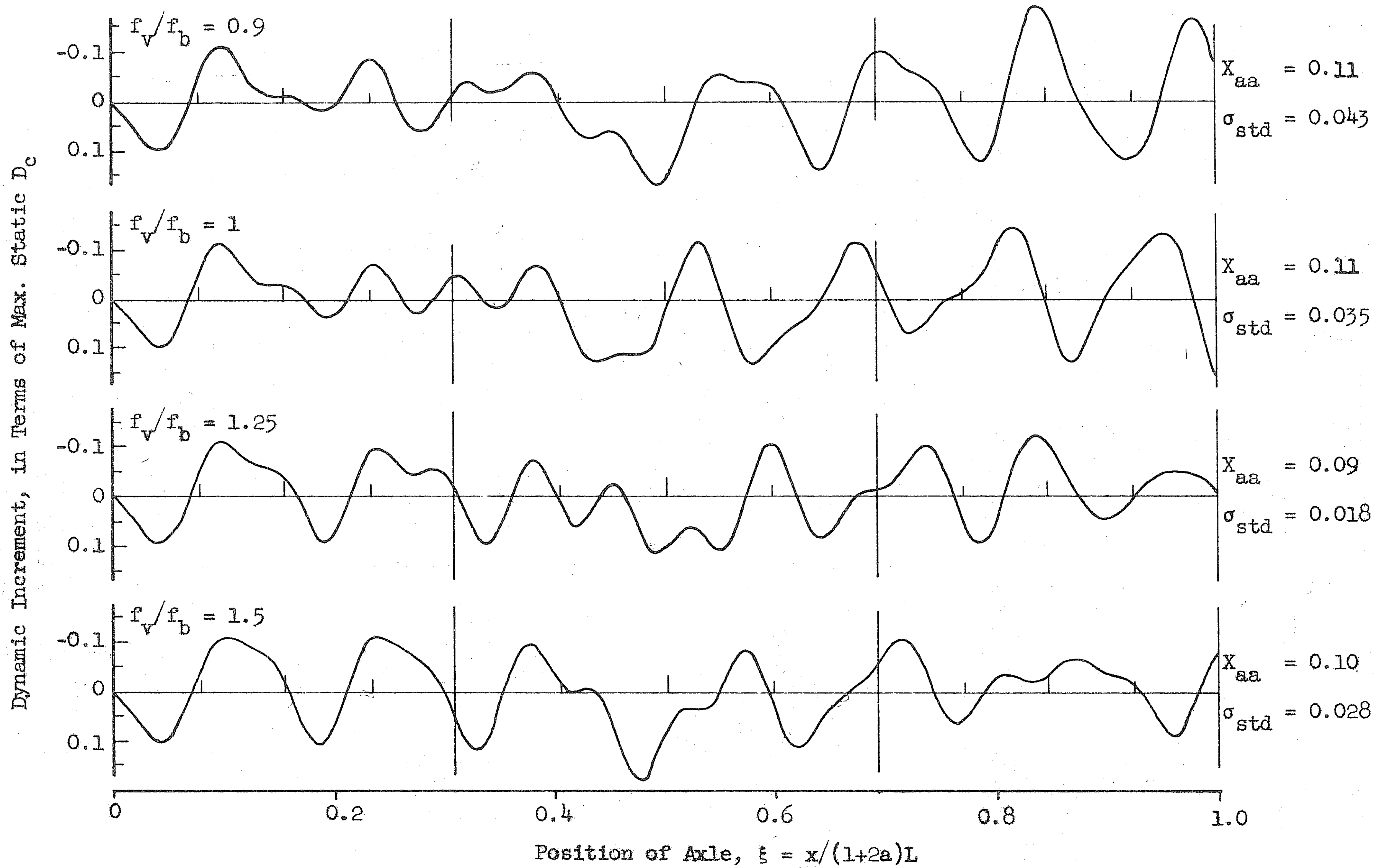

FIG. 24b EFFECT OF FREQUENCY RATIO ON DYNAMIC INCREMENT FOR D_c -- SINGLE-AXLE LOADING

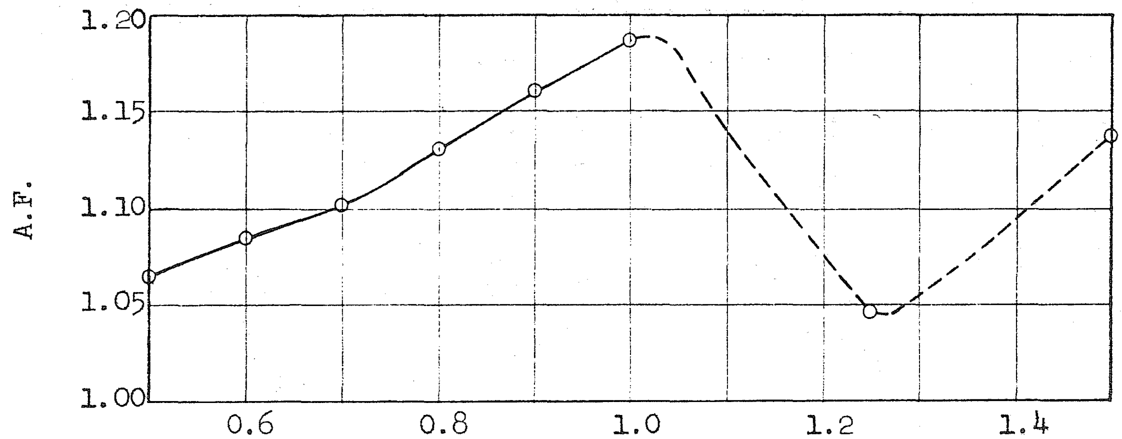

Frequency Ratio, f_v/f_b

(a) Amplification Factor for D_1

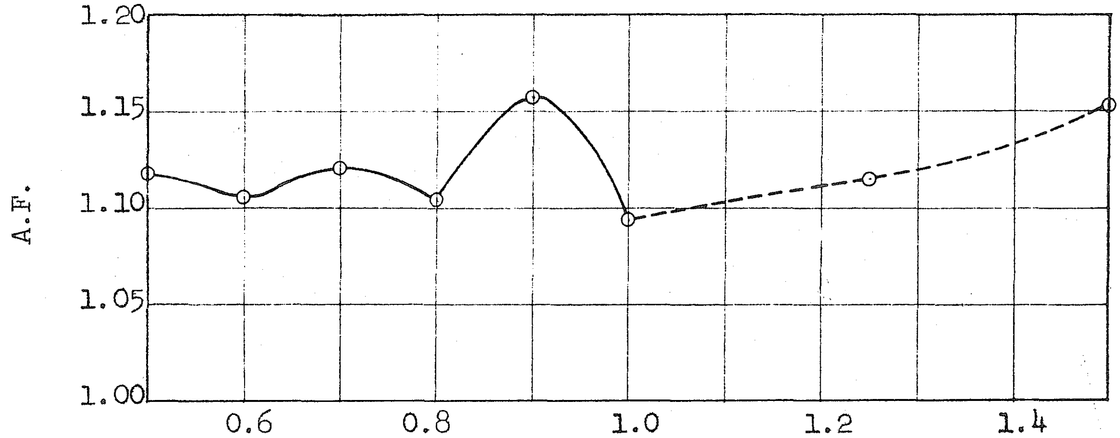

Frequency Ratio, f_v/f_b

(b) Amplification Factor for D_c

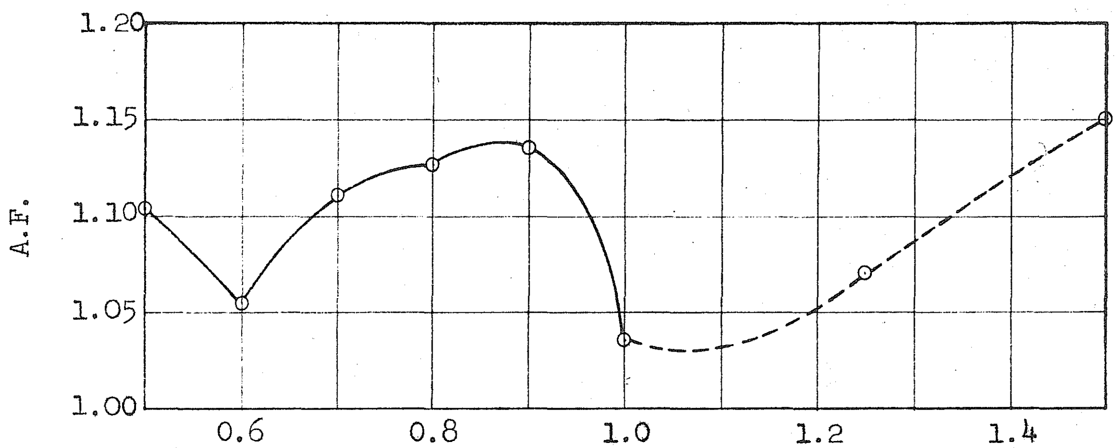

Frequency Ratio, f_v/f_b

(c) Amplification Factor for D_4

FIG. 25 EFFECT OF FREQUENCY RATIO ON AMPLIFICATION FACTORS -- SINGLE-AXLE LOADING

$a = 0.8$, $c/c_{cr} = 0$, $W/W_b = 0.175$, $\alpha = 0.18$

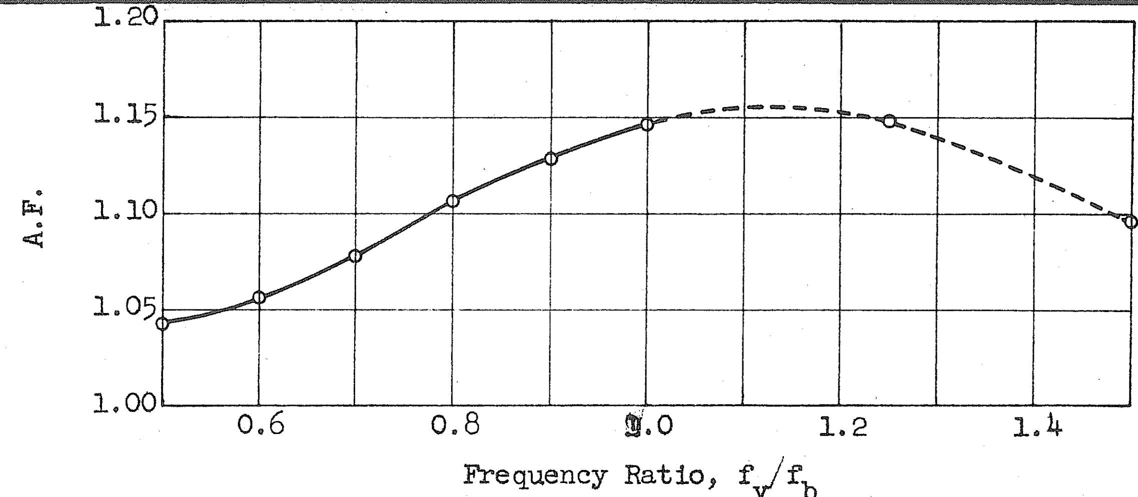

(d) Amplification Factor for M_1

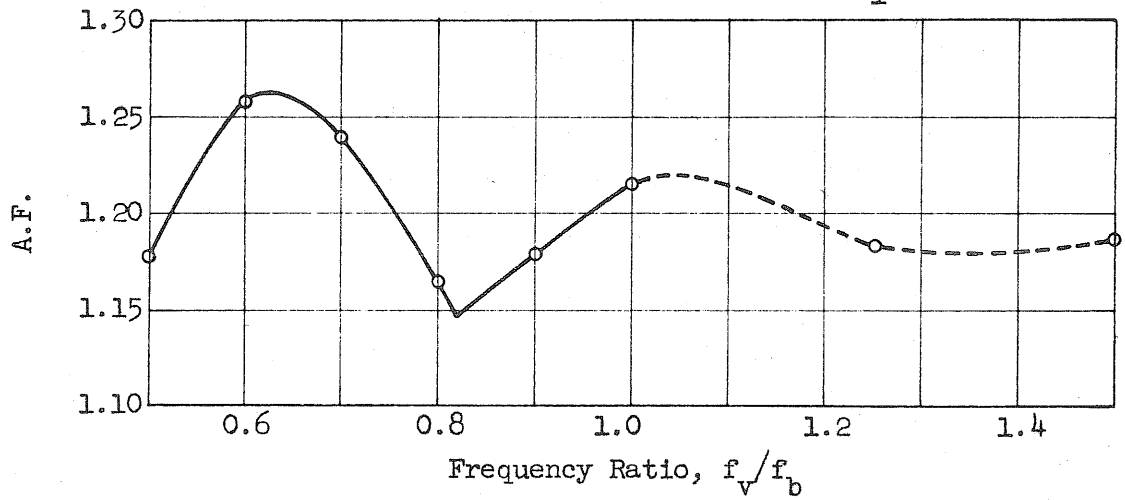

(e) Amplification Factor for M_2

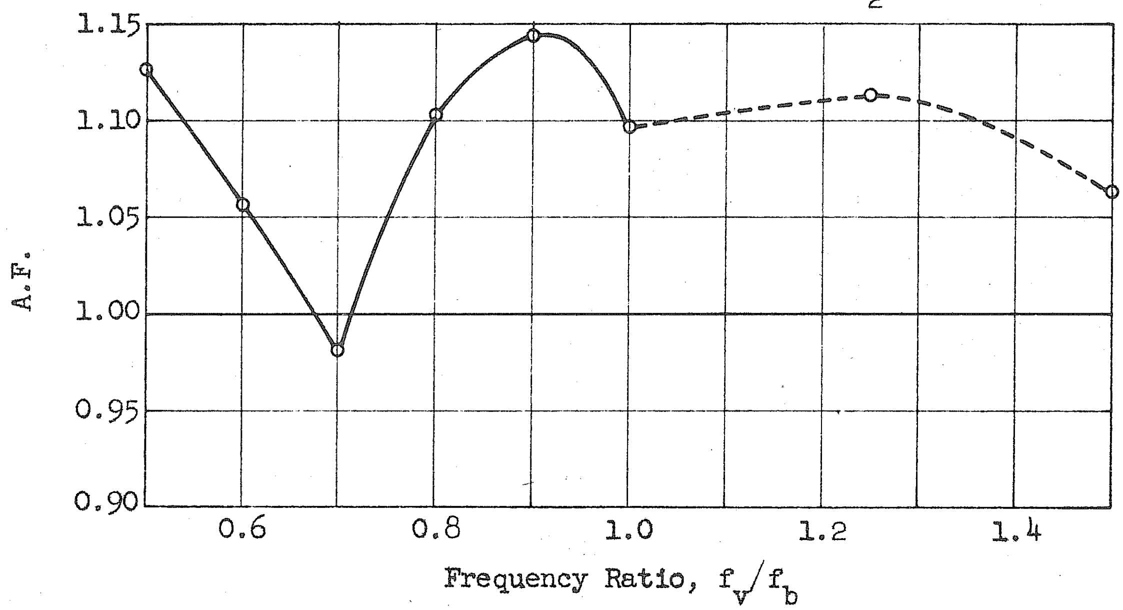

(f) Amplification Factor for M_c

FIG. 25 (Cont'd) EFFECT OF FREQUENCY RATIO ON AMPLIFICATION FACTORS -- SINGLE-AXLE LOADING

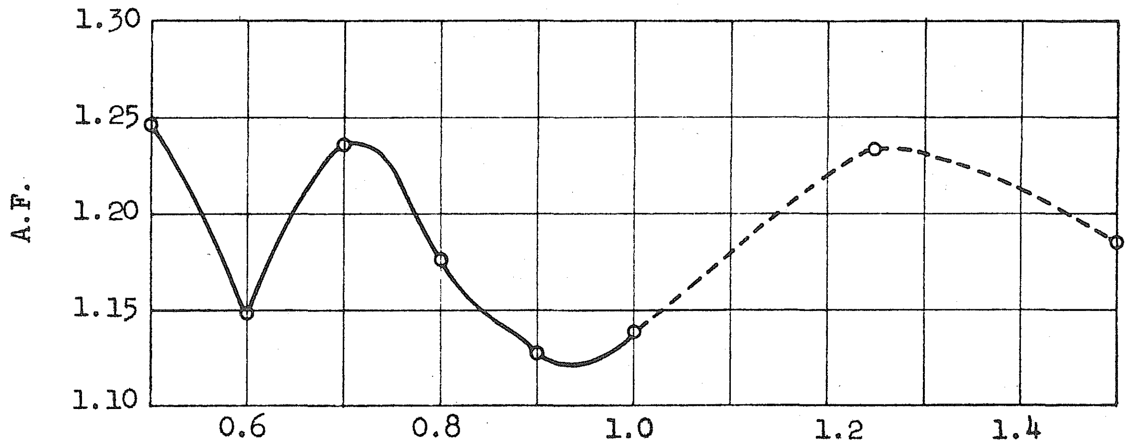

Frequency Ratio, f_v/f_b

(g) Amplification Factor for M_3

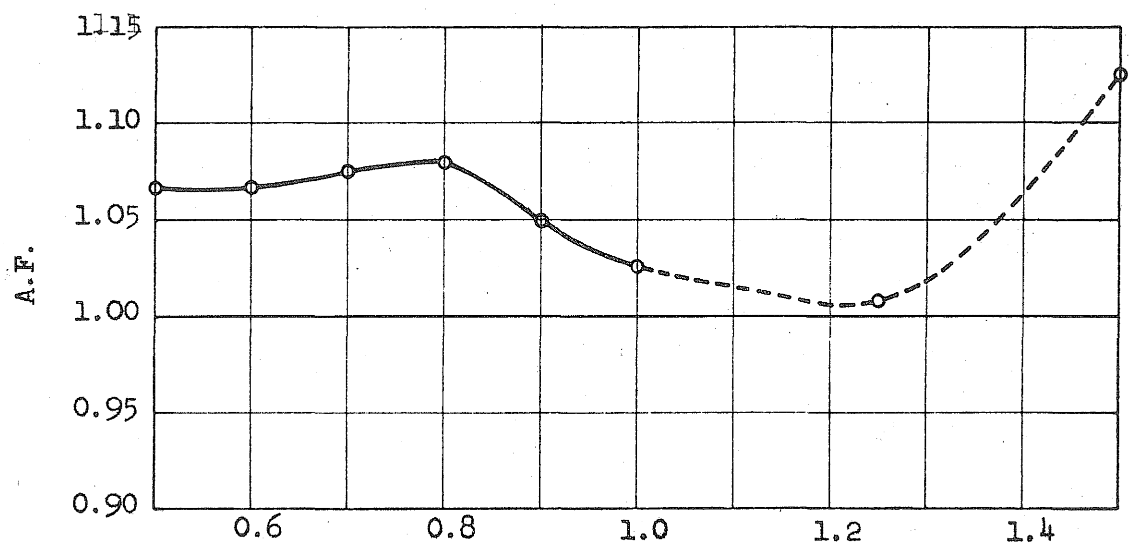

Frequency Ratio, f_v/f_b

(h) Amplification Factor for M_4

FIG. 25 (Cont'd) EFFECT OF FREQUENCY RATIO ON AMPLIFICATION FACTORS -- SINGLE-AXLE LOADING

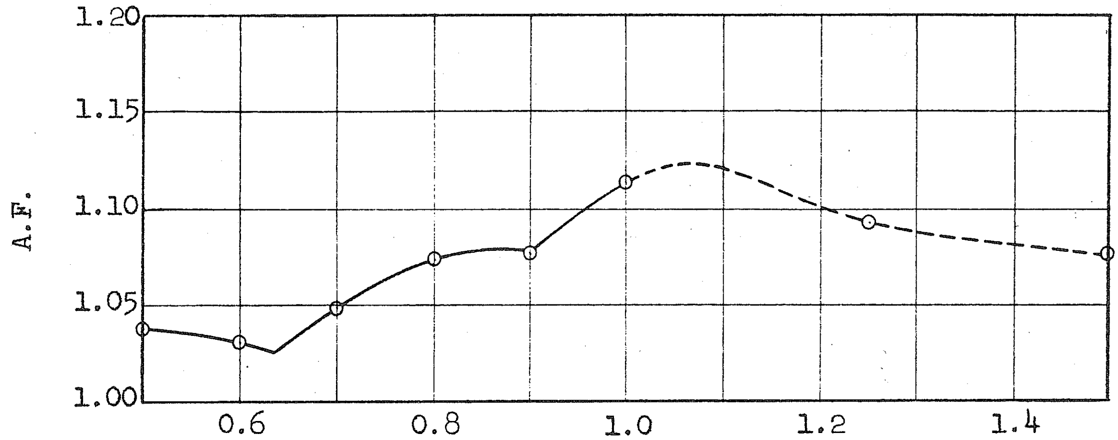

Frequency Ratio, f_v/f_b

(i) Amplification Factor for R_2

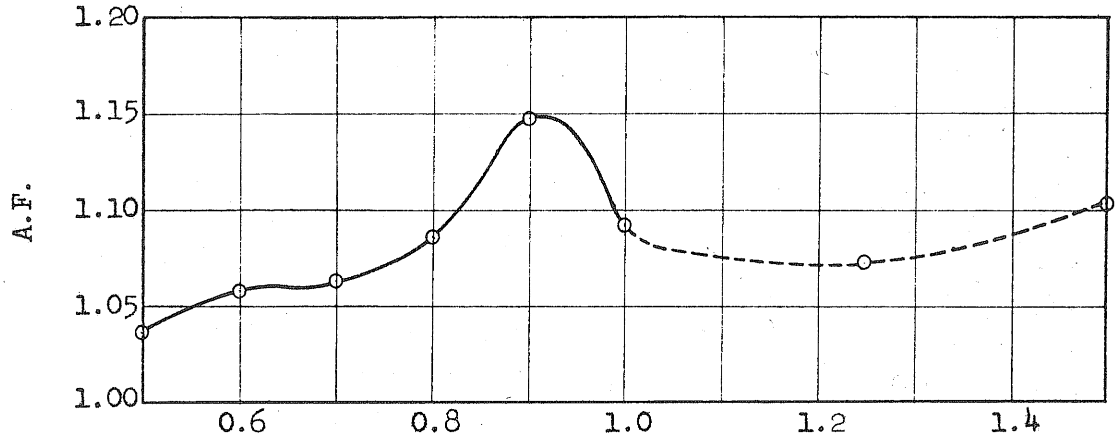

Frequency Ratio, f_v/f_b

(j) Amplification Factor for R_3

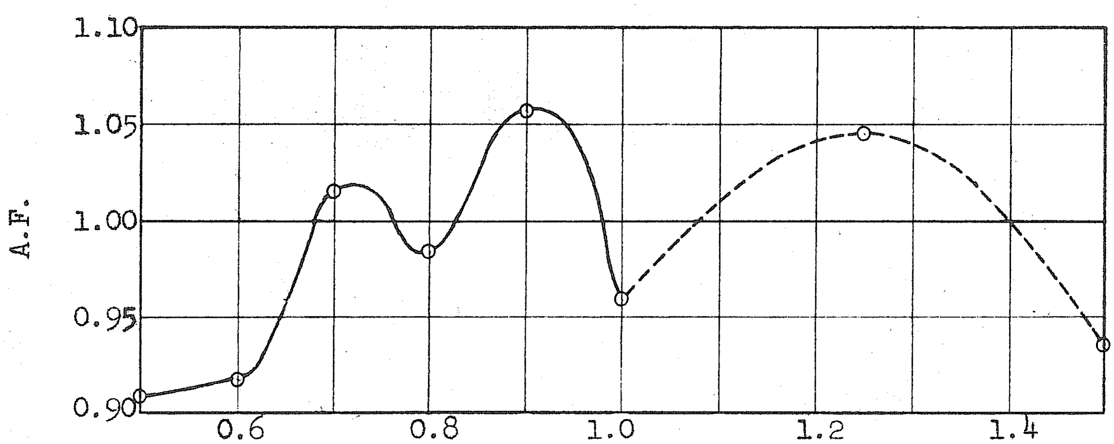

Frequency Ratio, f_v/f_b

(k) Amplification Factor for R_4

FIG. 25 (Cont'd) EFFECT OF FREQUENCY RATIO ON AMPLIFICATION FACTORS -- SINGLE-AXLE LOADING

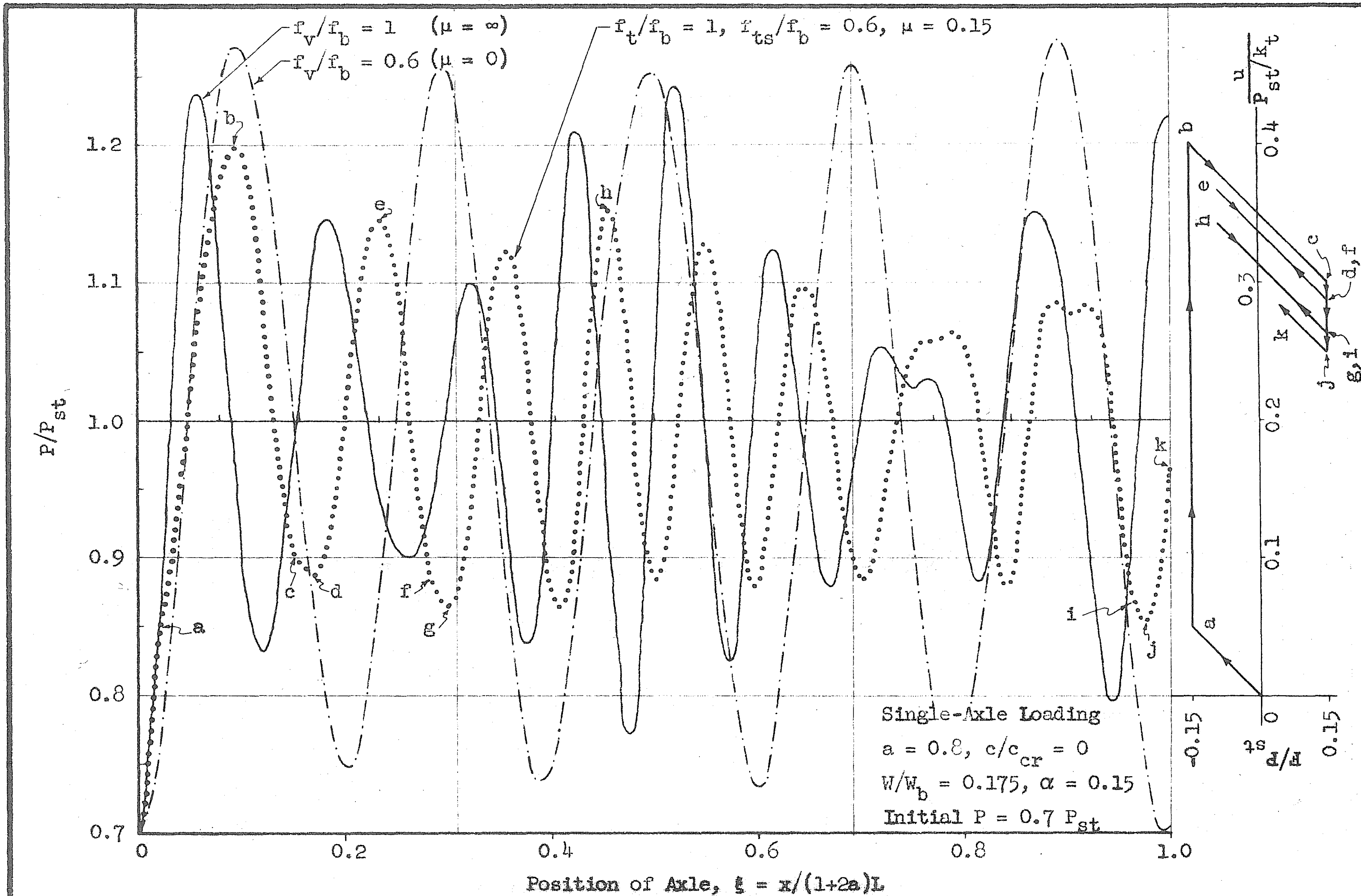

FIG. 26 EFFECT OF INTERLEAF FRICTION ON INTERACTING FORCE, P, AND FRICTIONAL FORCE, F -- INITIALLY OSCILLATING VEHICLE

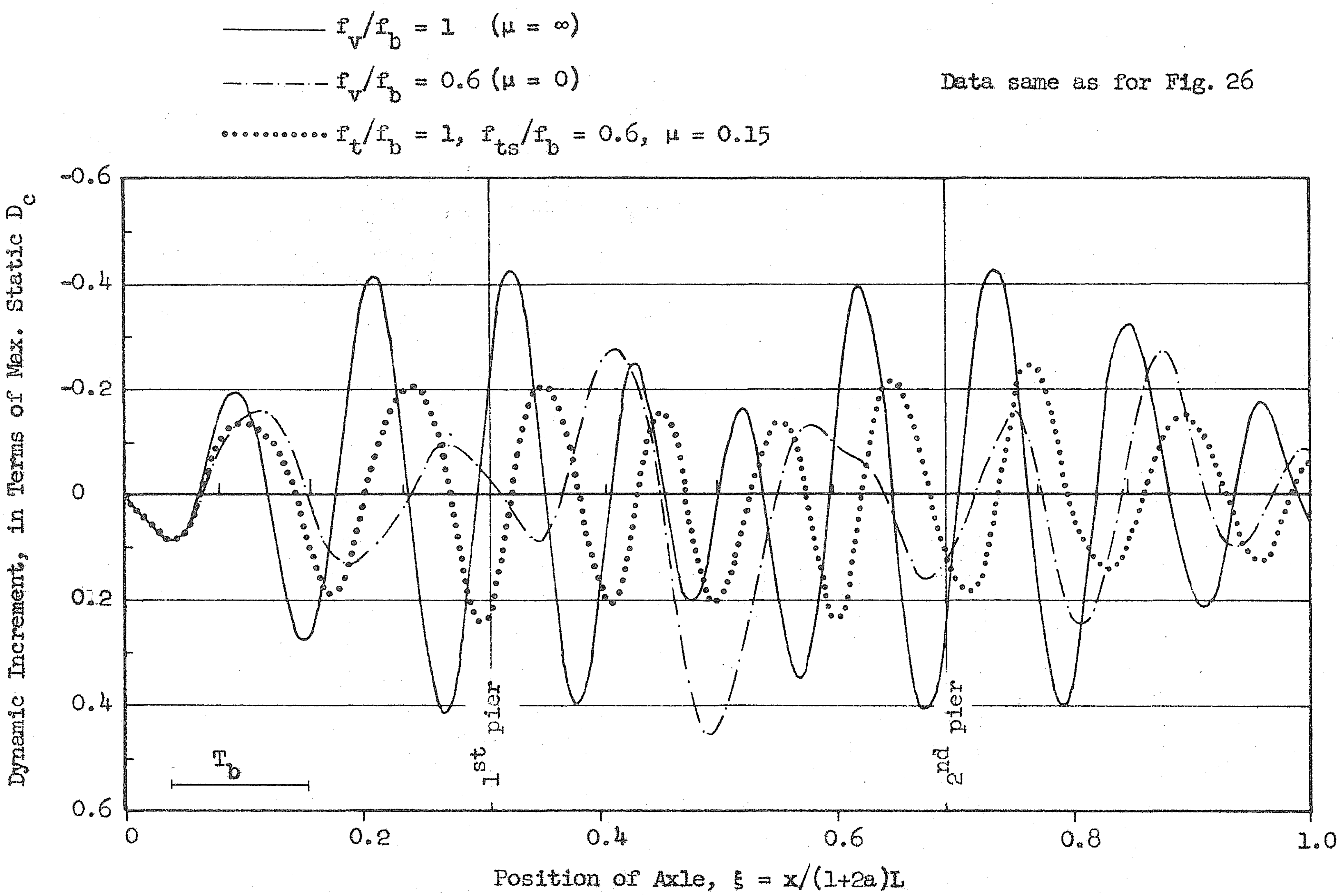

FIG. 27 EFFECT OF INTERLEAF FRICTION ON DYNAMIC INCREMENT FOR D_c -- INITIALLY OSCILLATING VEHICLE

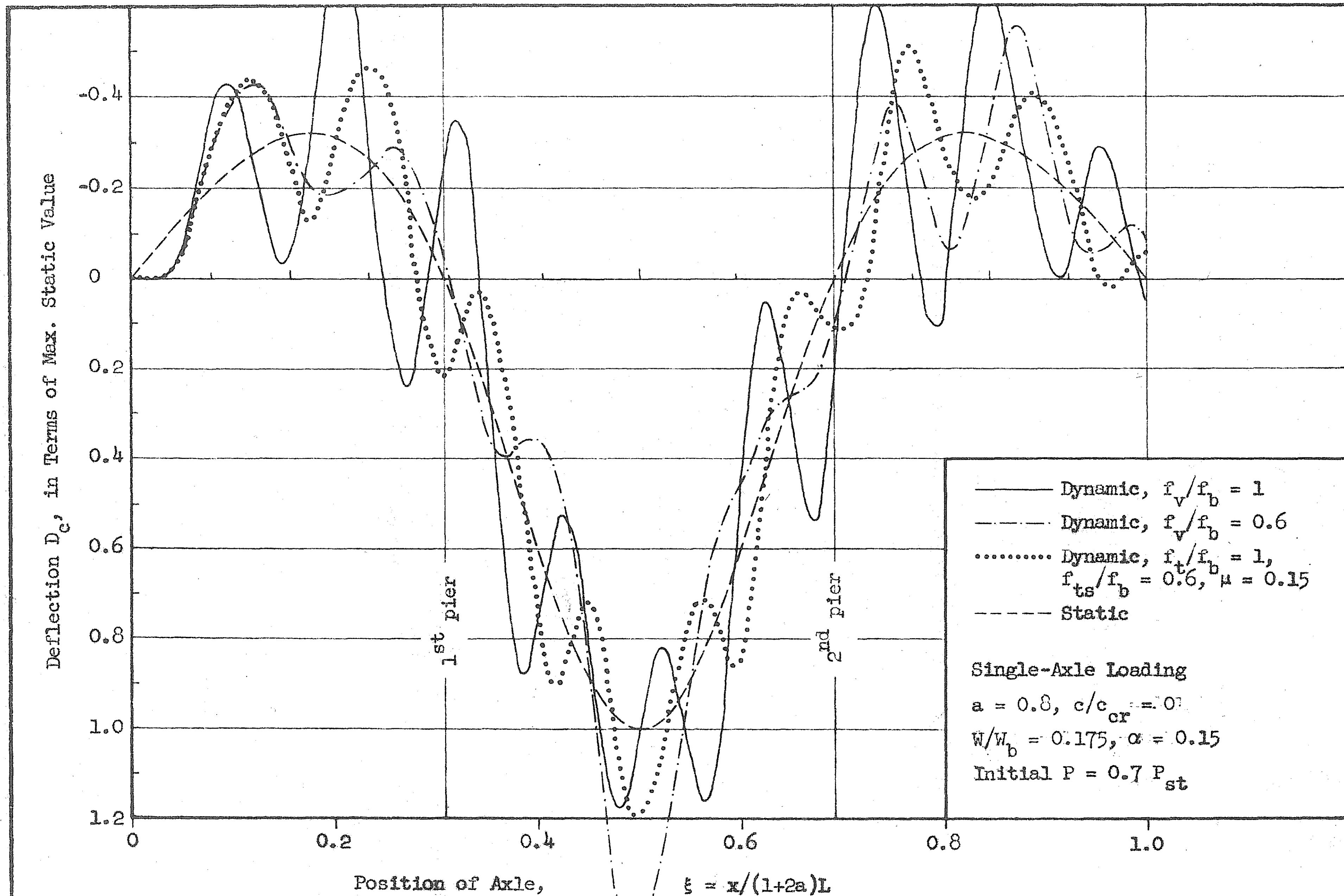

FIG. 28a EFFECT OF INTERLEAF FRICTION ON DEFLECTION D_c -- INITIALLY OSCILLATING VEHICLE

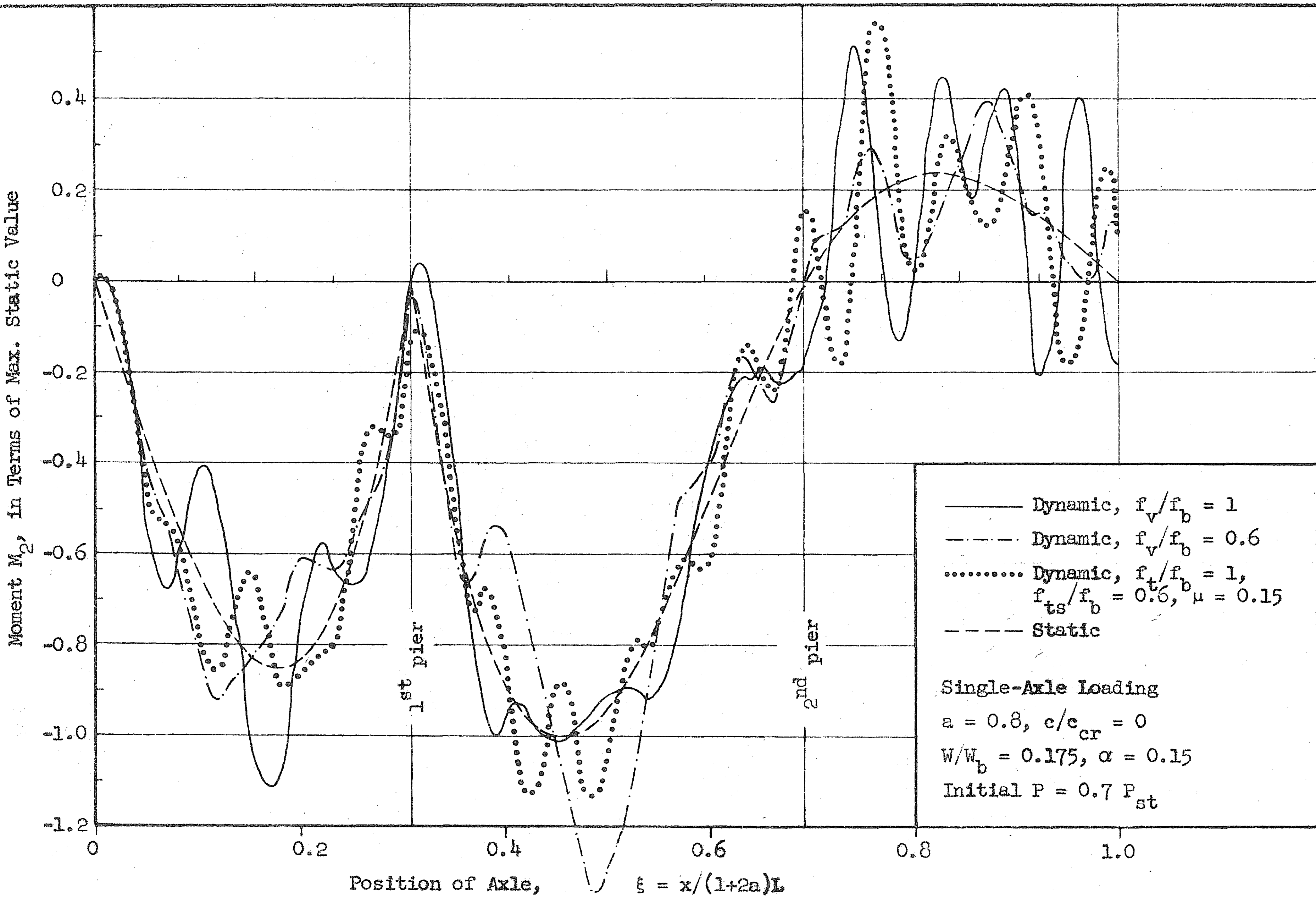

FIG. 28b EFFECT OF INTERLEAF FRICTION ON MOMENT M_2 -- INITIALLY OSCILLATING VEHICLE

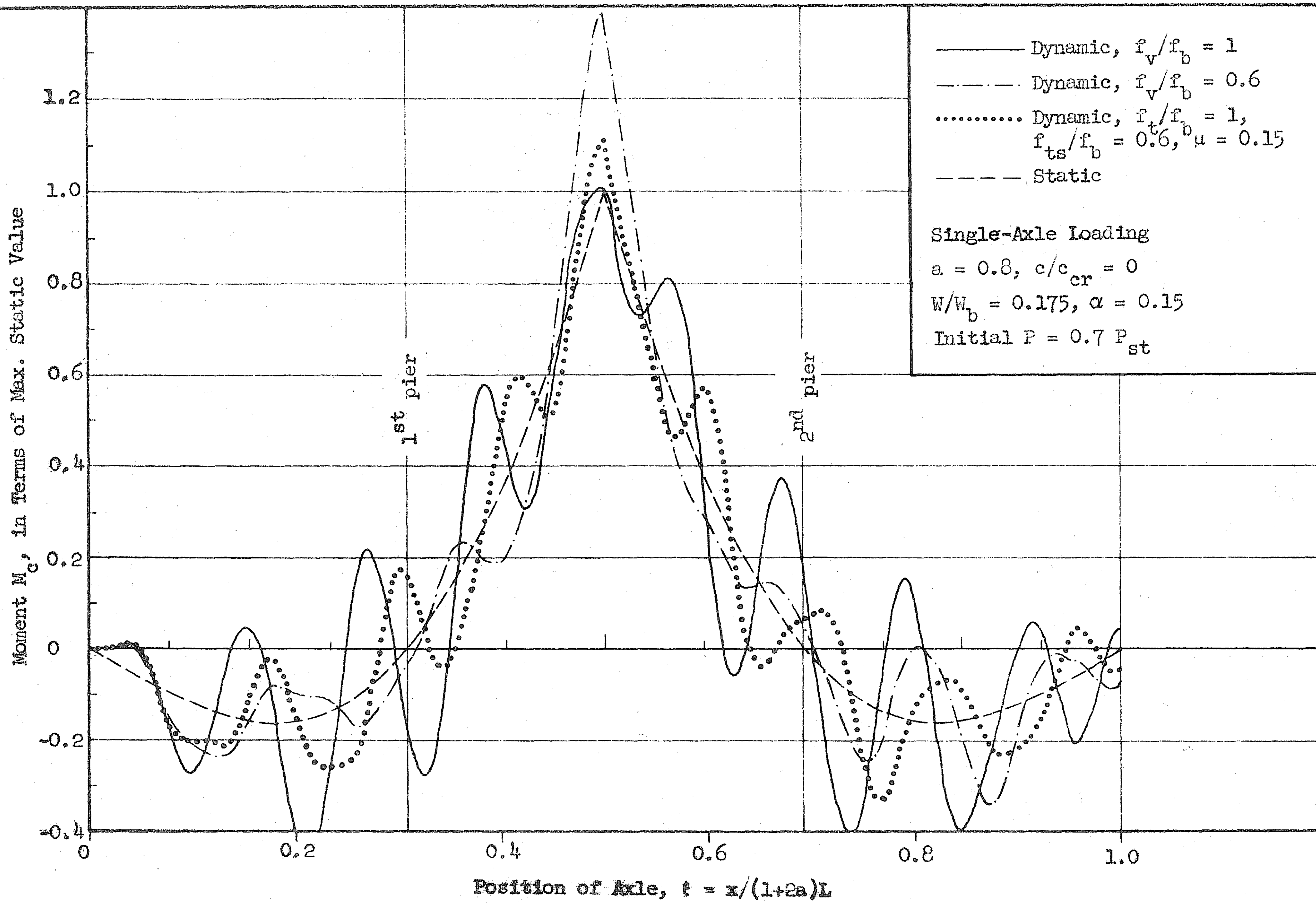

FIG. 28c EFFECT OF INTERLEAF FRICTION ON MOMENT M_c -- INITIALLY OSCILLATING VEHICLE

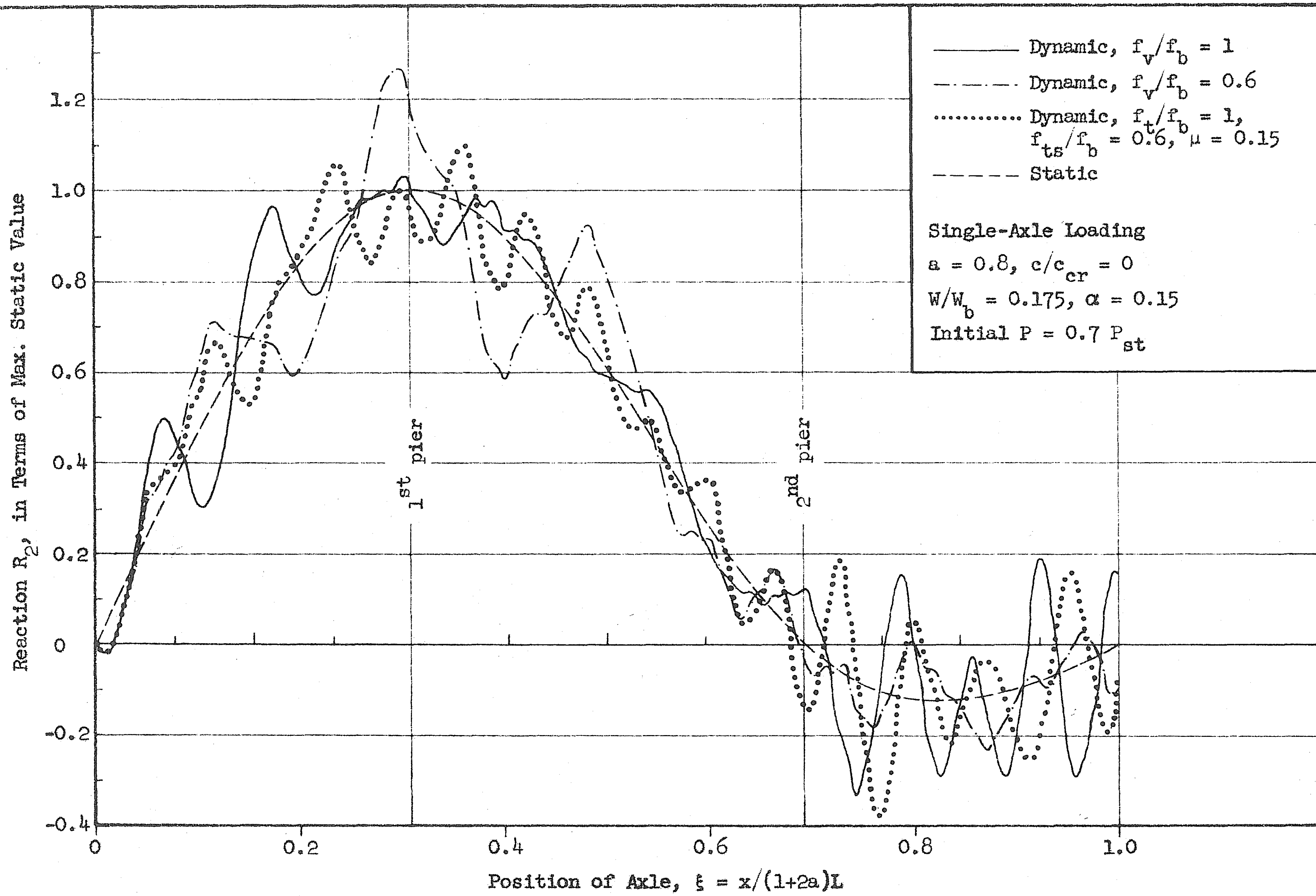

FIG. 28d EFFECT OF INTERLEAF FRICTION ON REACTION R_2 -- INITIALLY OSCILLATING VEHICLE

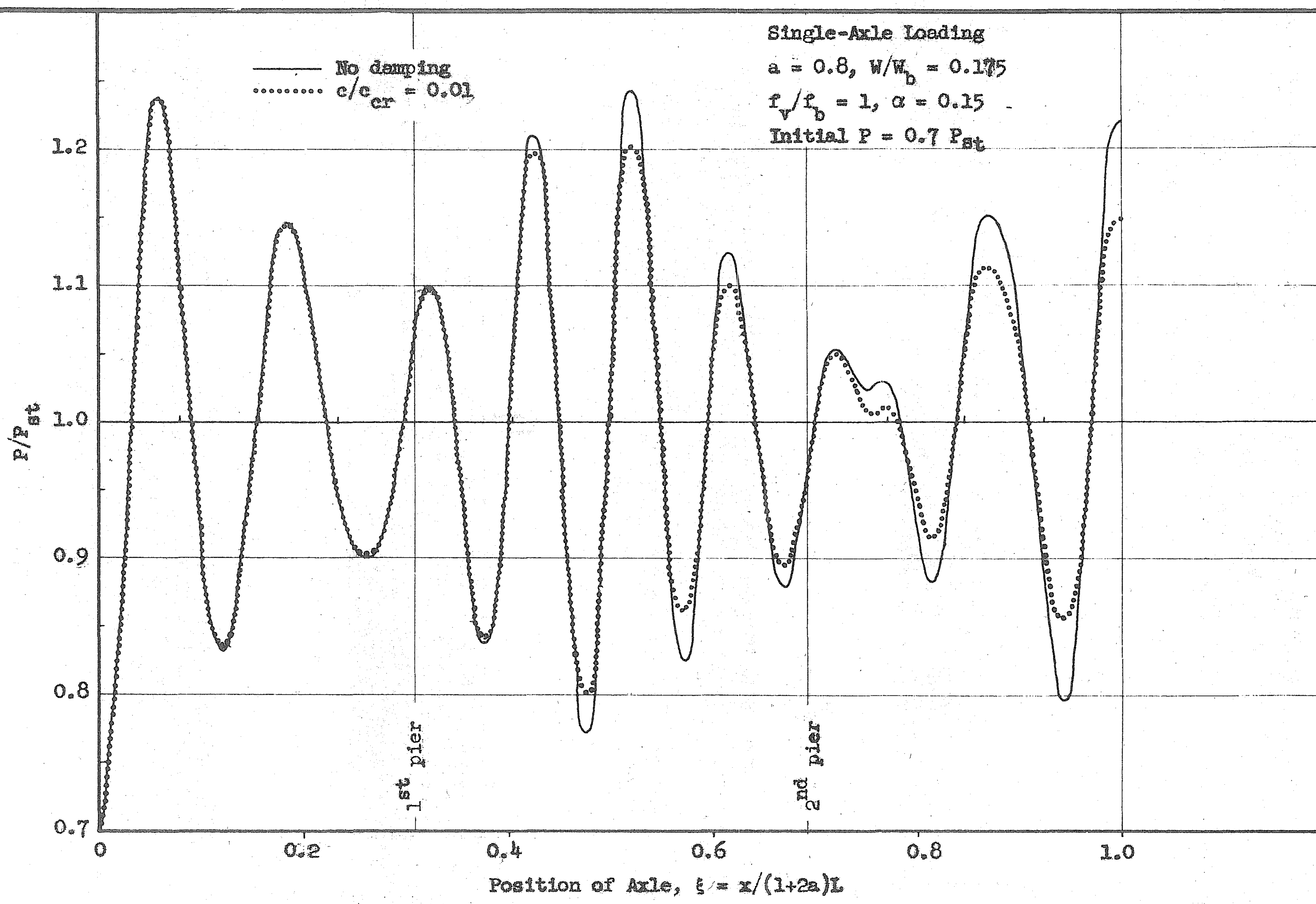

FIG. 29 EFFECT OF BRIDGE DAMPING ON INTERACTING FORCE, P -- INITIALLY OSCILLATING VEHICLE

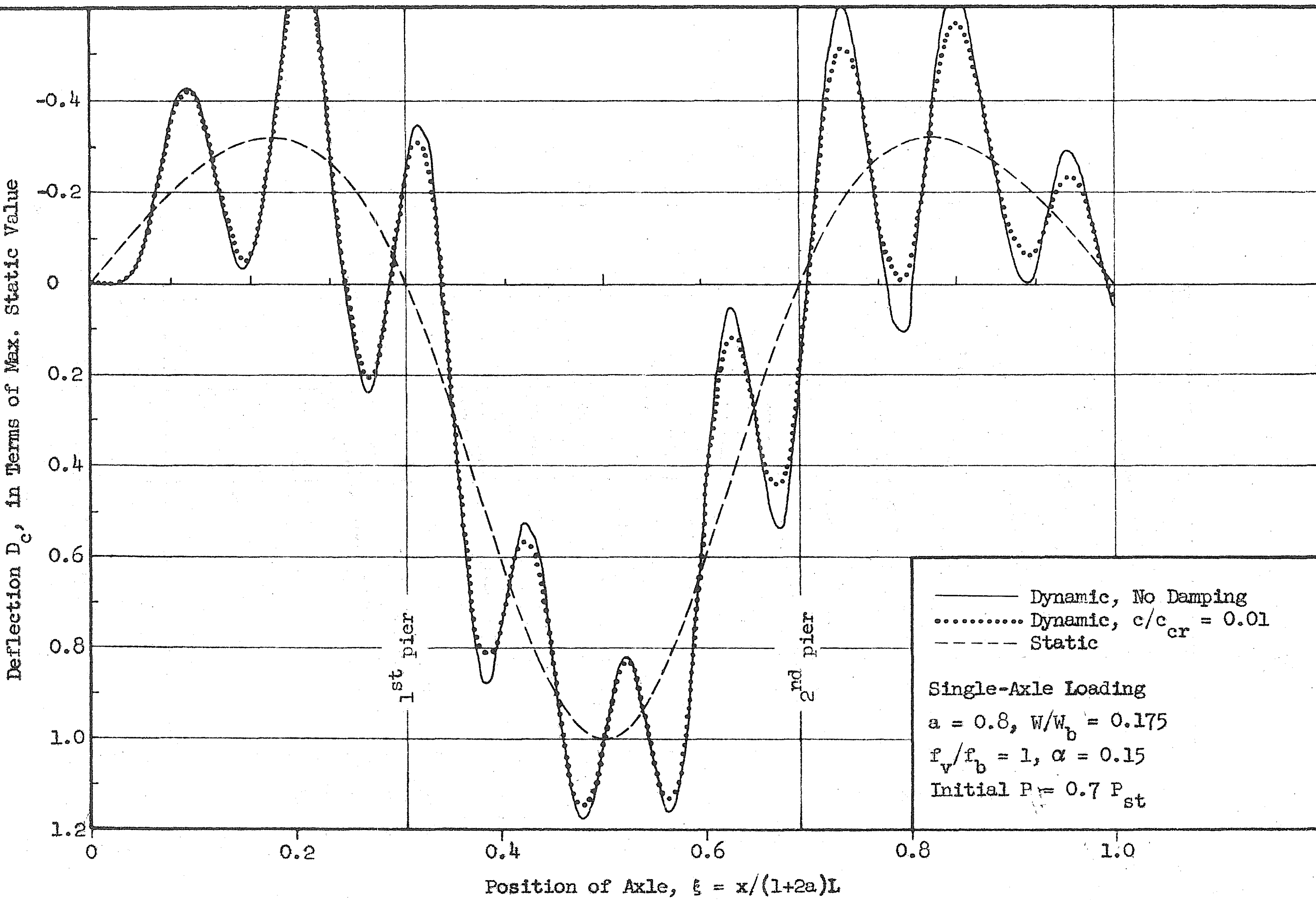

FIG. 30 EFFECT OF BRIDGE DAMPING ON DEFLECTION D_c -- INITIALLY OSCILLATING VEHICLE

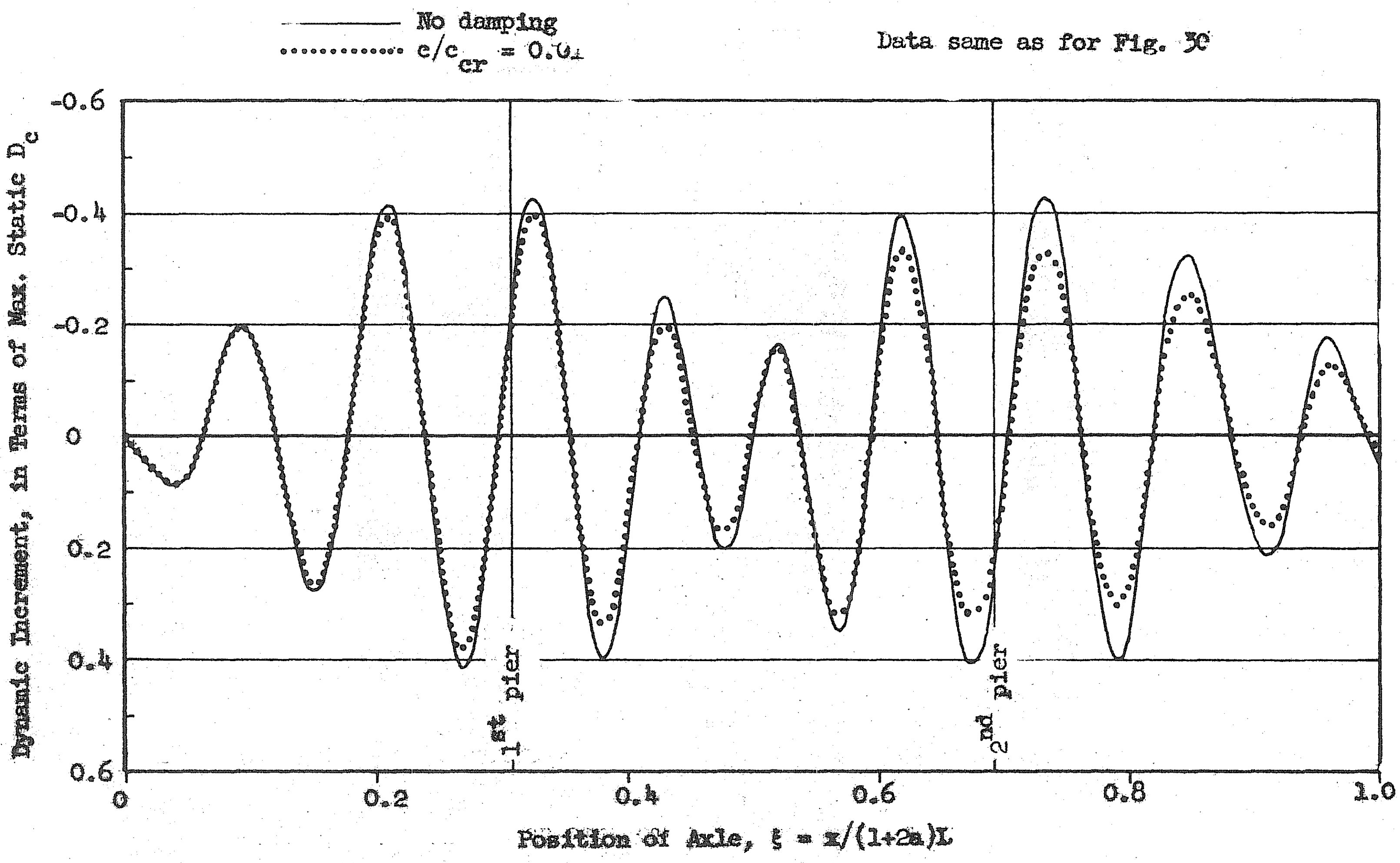

FIG. 31 EFFECT OF BRIDGE DAMPING ON DYNAMIC INCREMENT FOR D_c -- INITIALLY OSCILLATING VEHICLE

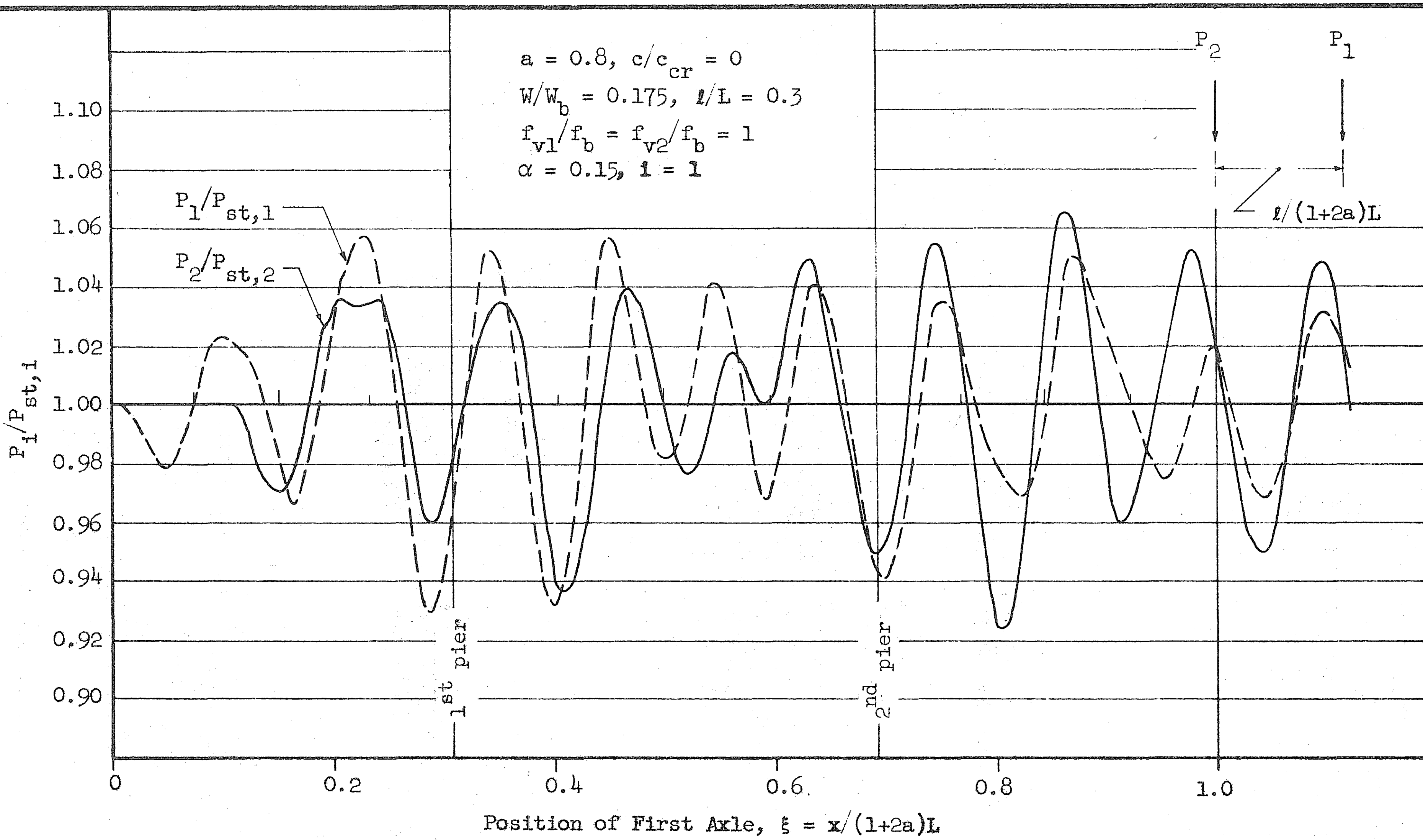

FIG. 32a HISTORY CURVES FOR INTERACTING FORCES, P_i -- "TYPICAL" TWO-AXLE TRAILER

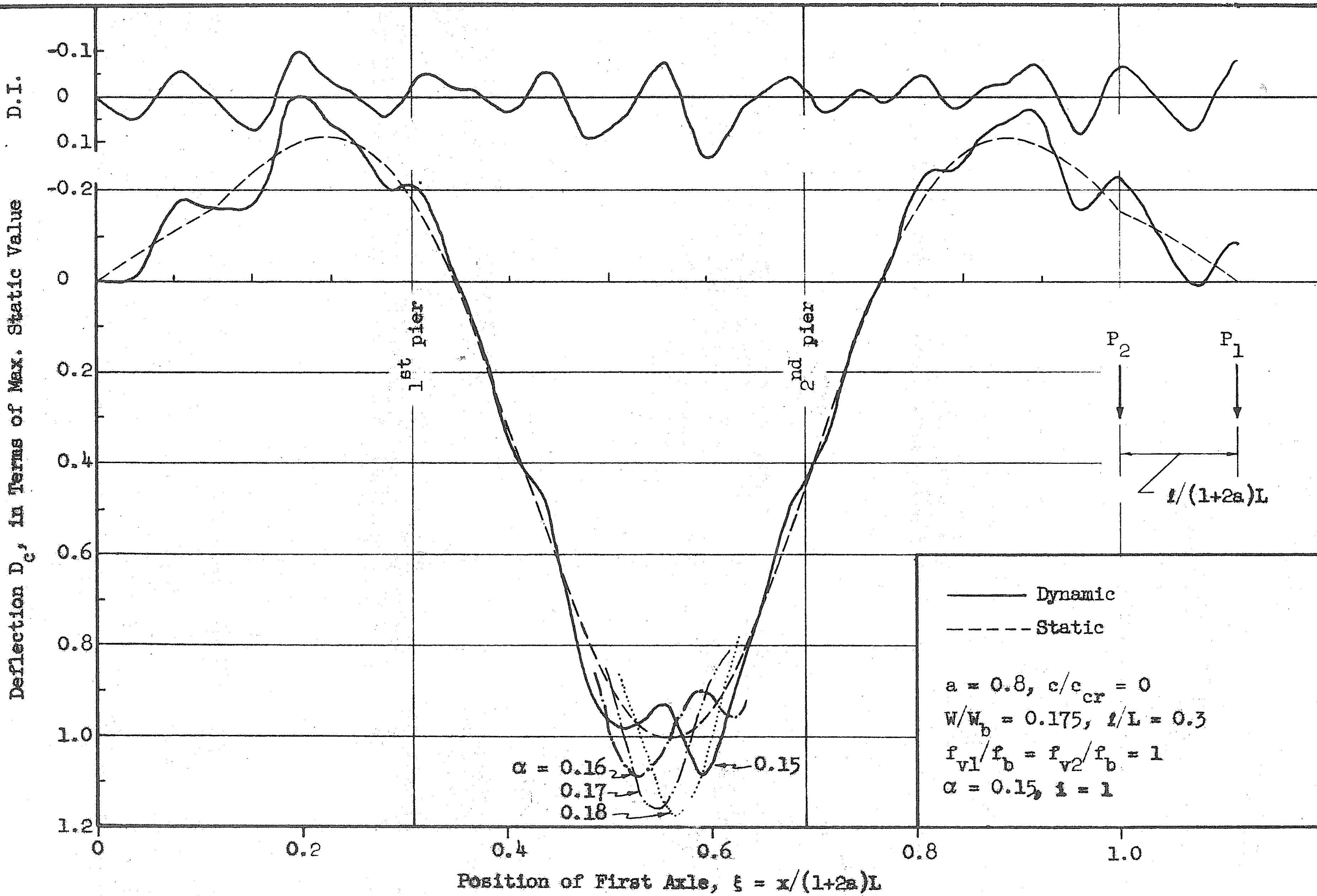

FIG. 32b HISTORY CURVES FOR D_c AND CORRESPONDING DYNAMIC INCREMENT -- "TYPICAL" TWO-AXLE TRAILER

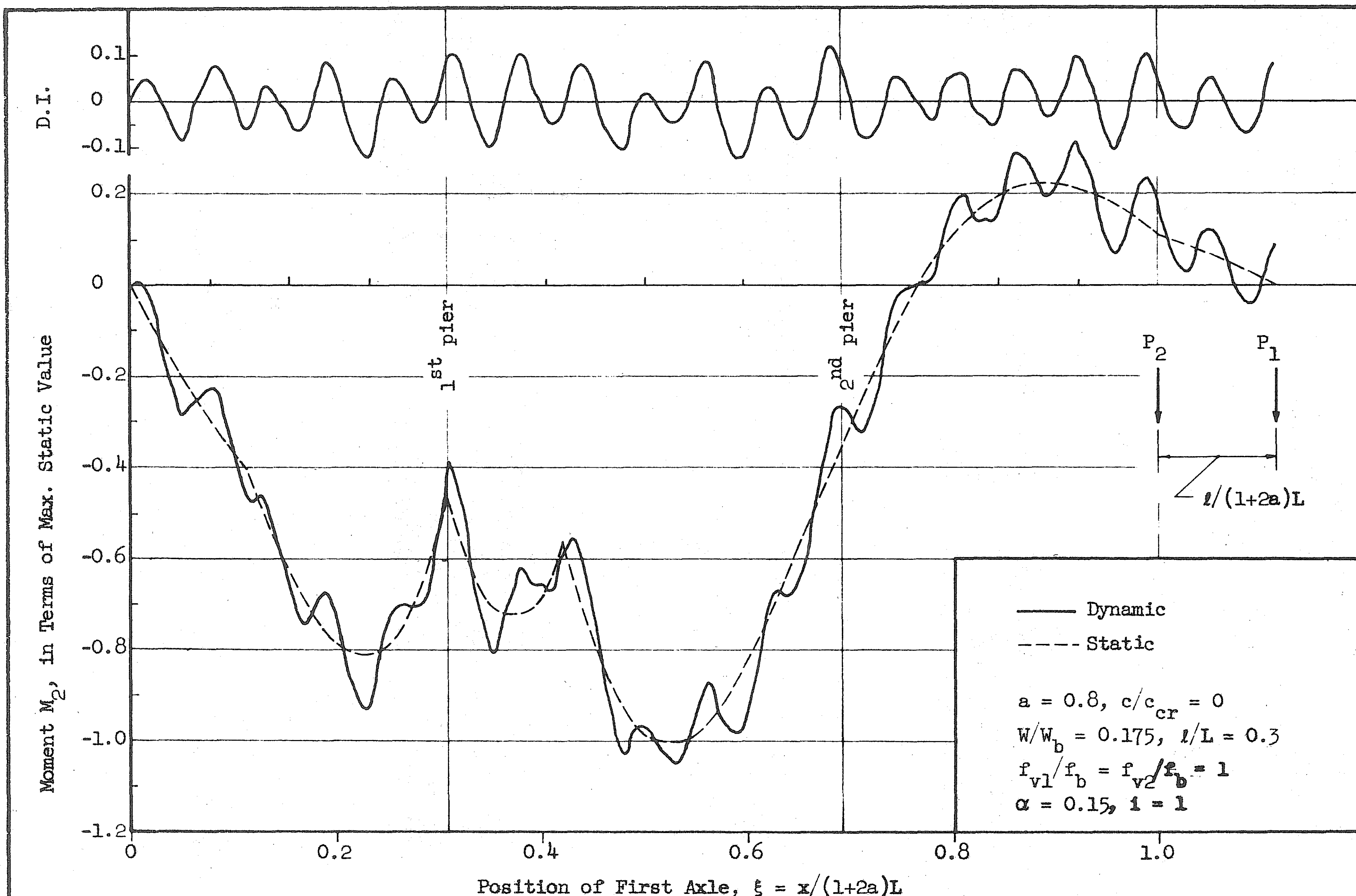

FIG. 32c HISTORY CURVES FOR M_2 AND CORRESPONDING DYNAMIC INCREMENT -- "TYPICAL" TWO-AXLE TRAILER

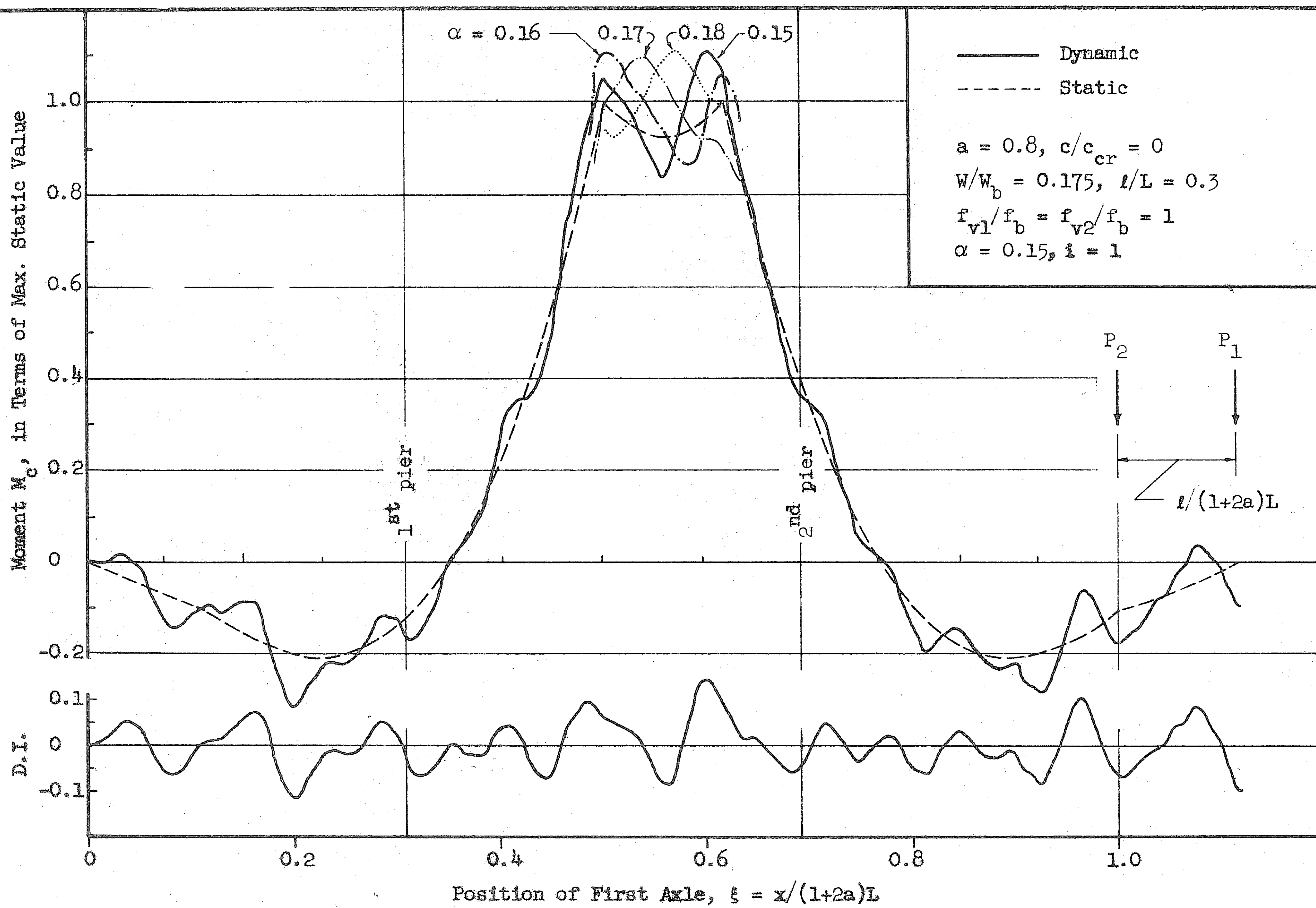

FIG. 32d HISTORY CURVES FOR M_c AND CORRESPONDING DYNAMIC INCREMENT -- "TYPICAL" TWO-AXLE TRAILER

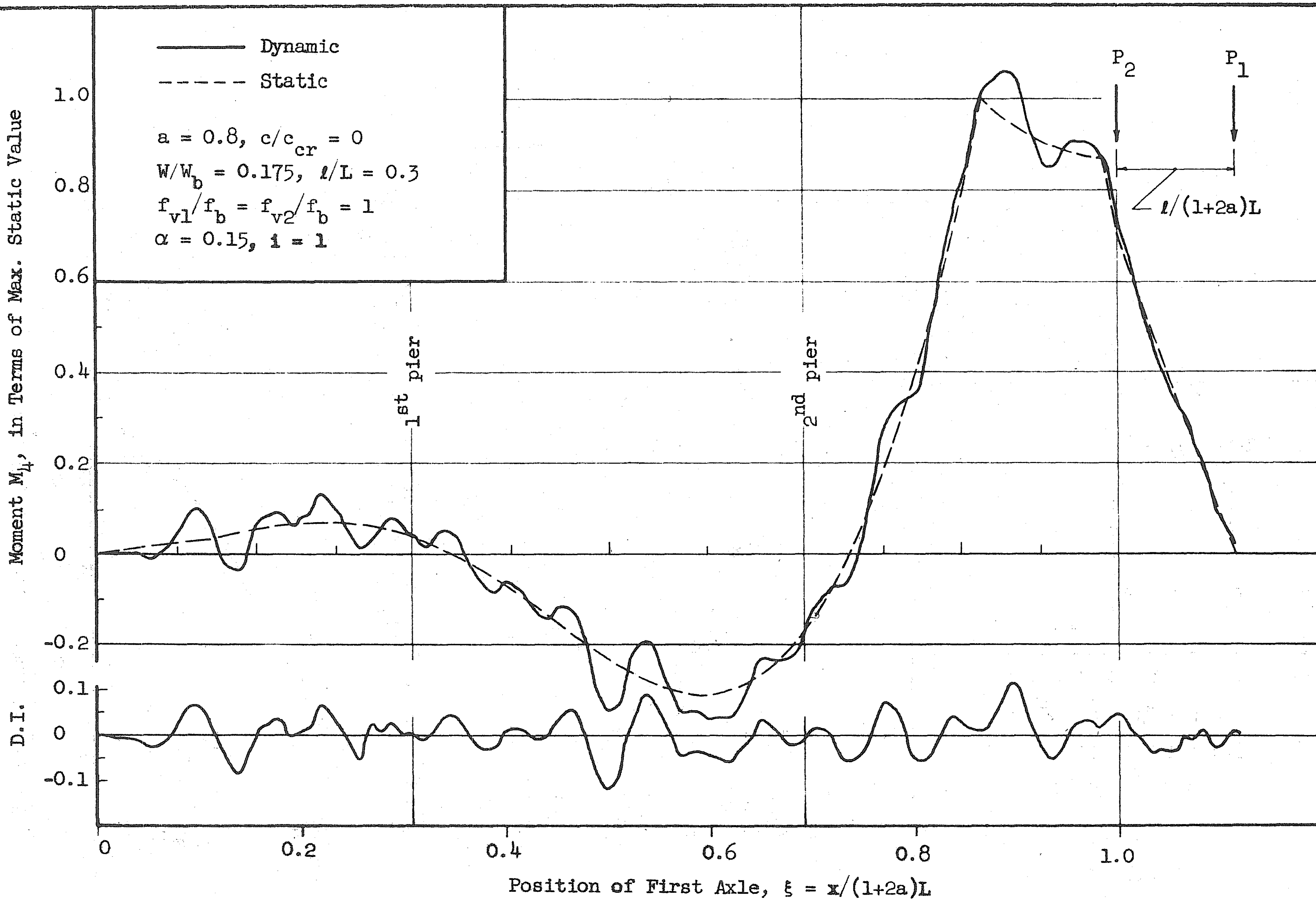

FIG. 32e HISTORY CURVES FOR M_4 AND CORRESPONDING DYNAMIC INCREMENT -- "TYPICAL" TWO-AXLE TRAILER

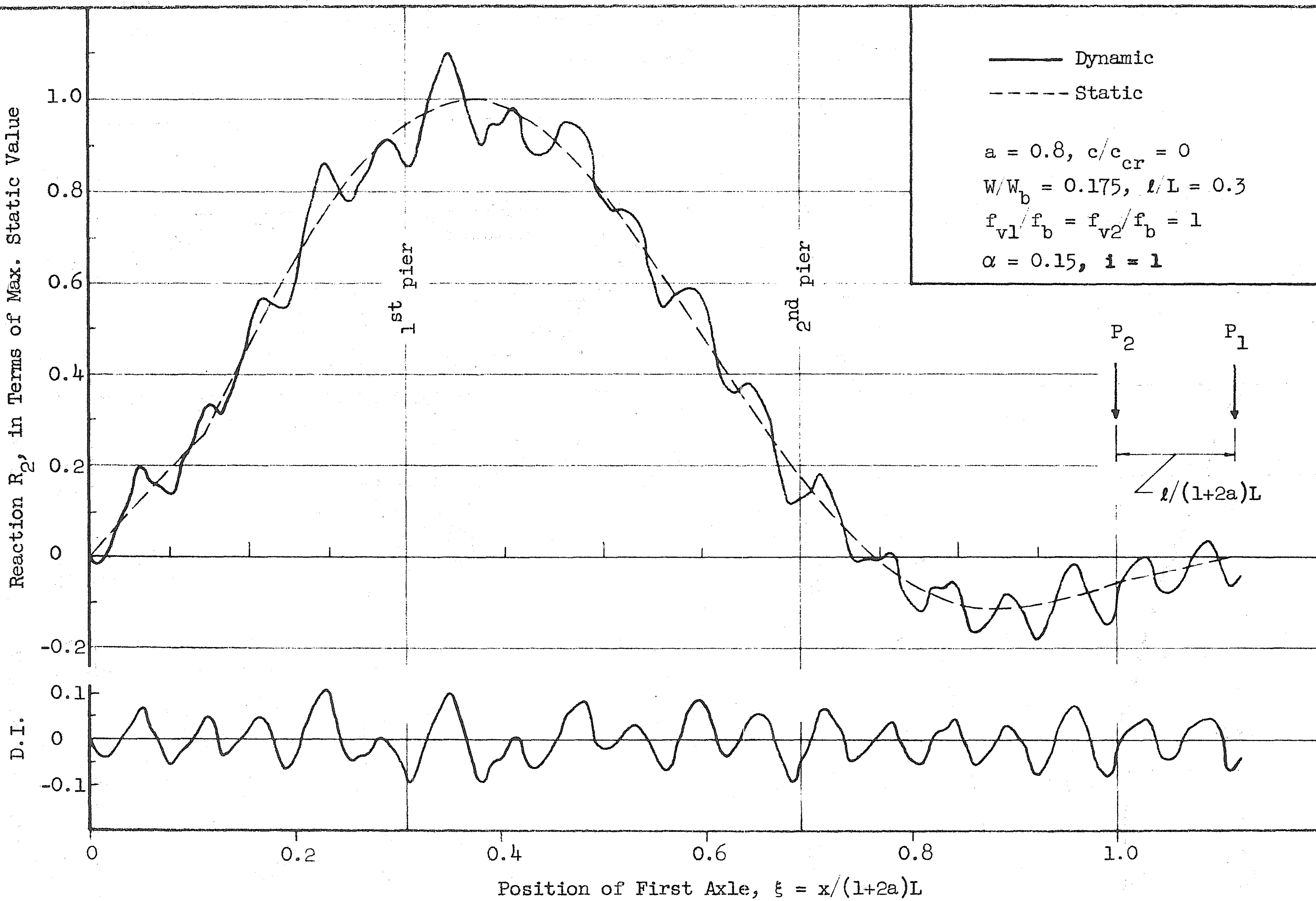

FIG. 32f HISTORY CURVES FOR R_2 AND CORRESPONDING DYNAMIC INCREMENT -- "TYPICAL" TWO-AXLE TRAILER

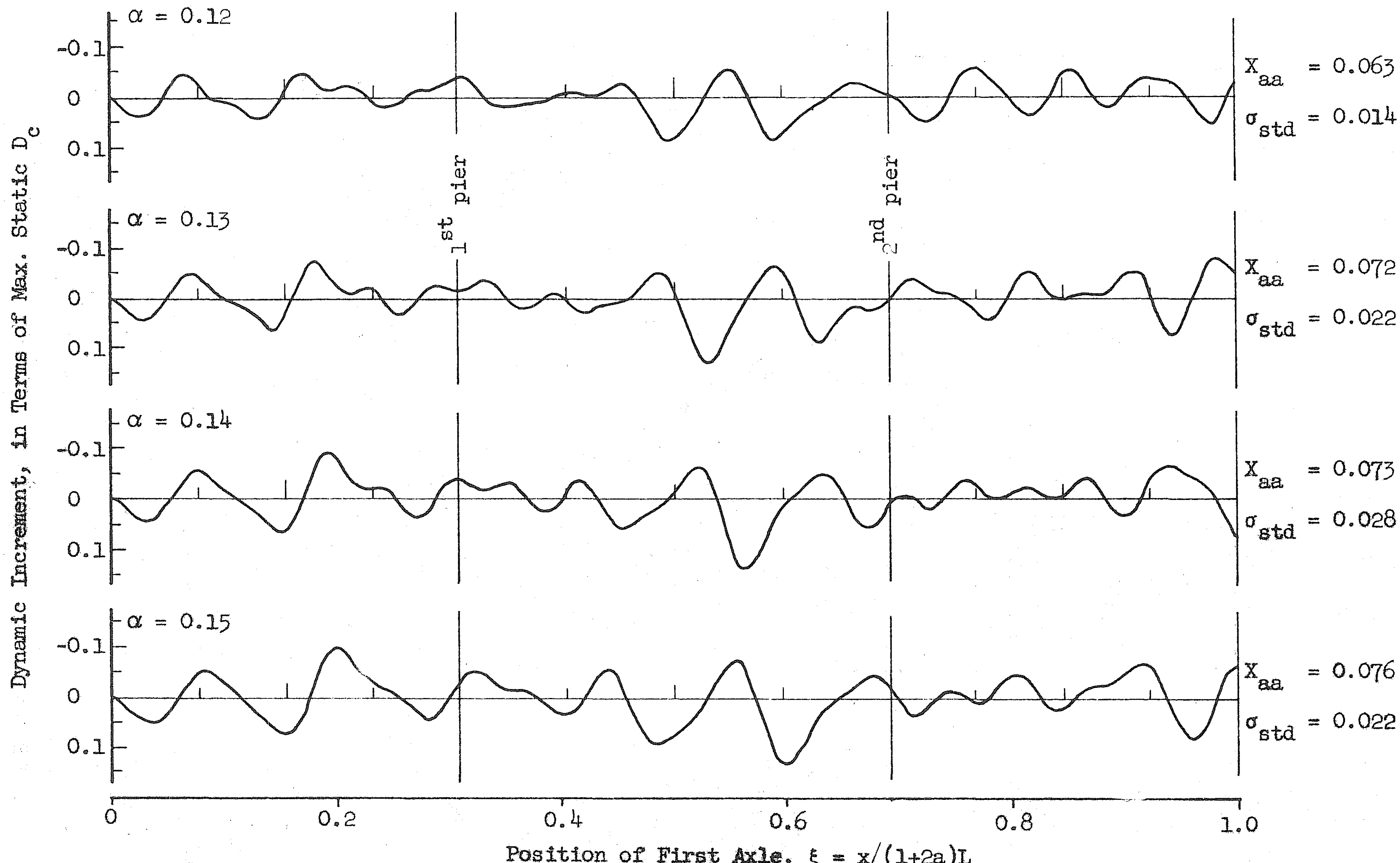

FIG. 33a EFFECT OF SPEED ON DYNAMIC INCREMENT FOR D_c -- "TYPICAL" TWO-AXLE TRAILER

$a = 0.8$, $c/c_{cr} = 0$, $W/W_b = 0.175$, $\ell/L = 0.3$, $f_{v1}/f_b = f_{v2}/f_b = 1$, $i = 1$

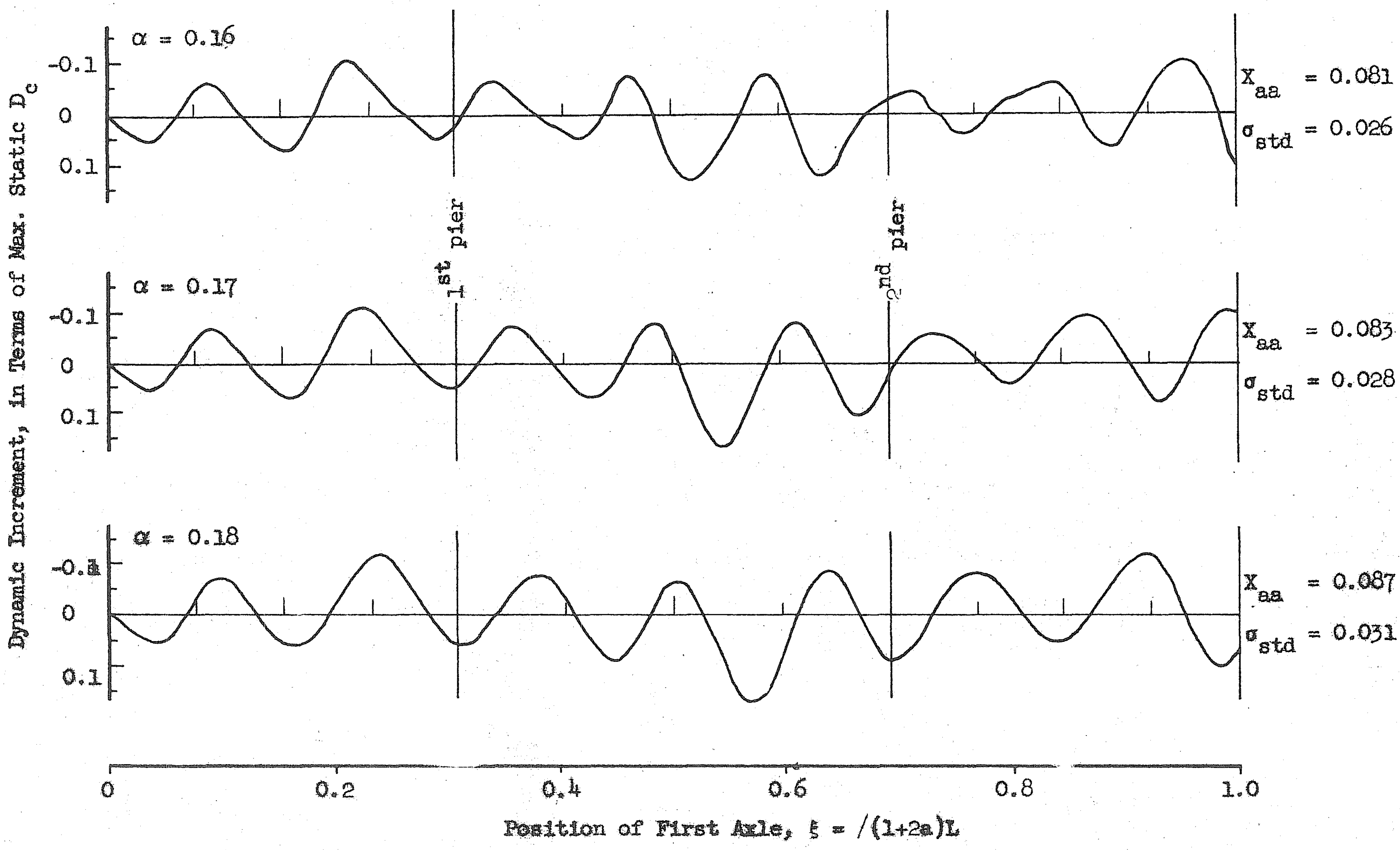

FIG. 33b EFFECT OF SPEED ON DYNAMIC INCREMENT FOR D_c -- "TYPICAL" TWO-AXLE TRAILER

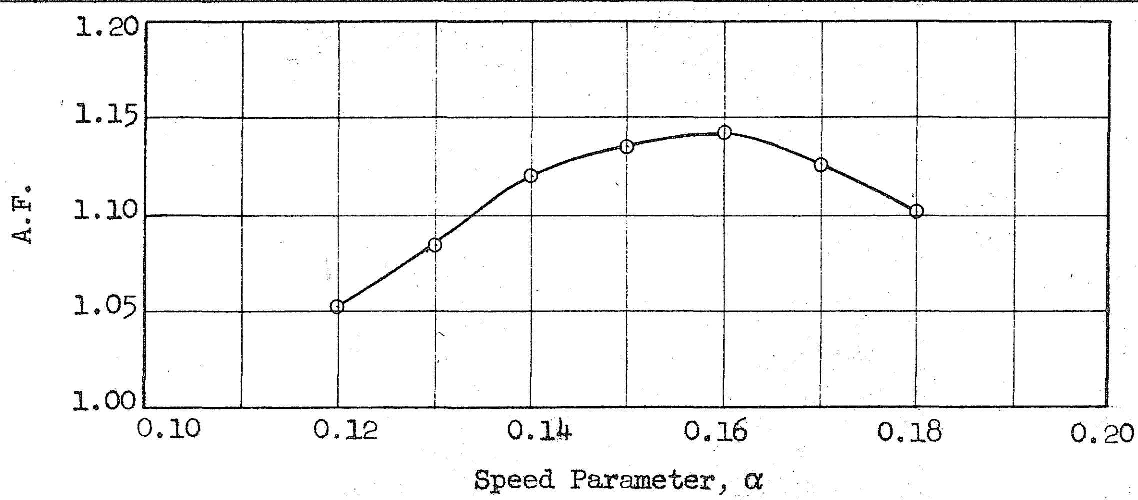

(a) Amplification Factor for D_1

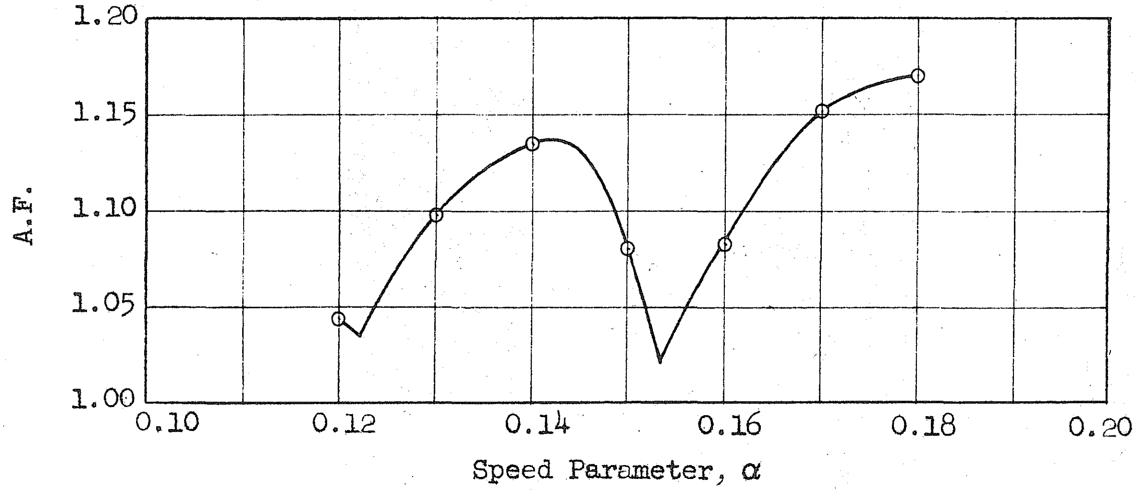

(b) Amplification Factor for D_c

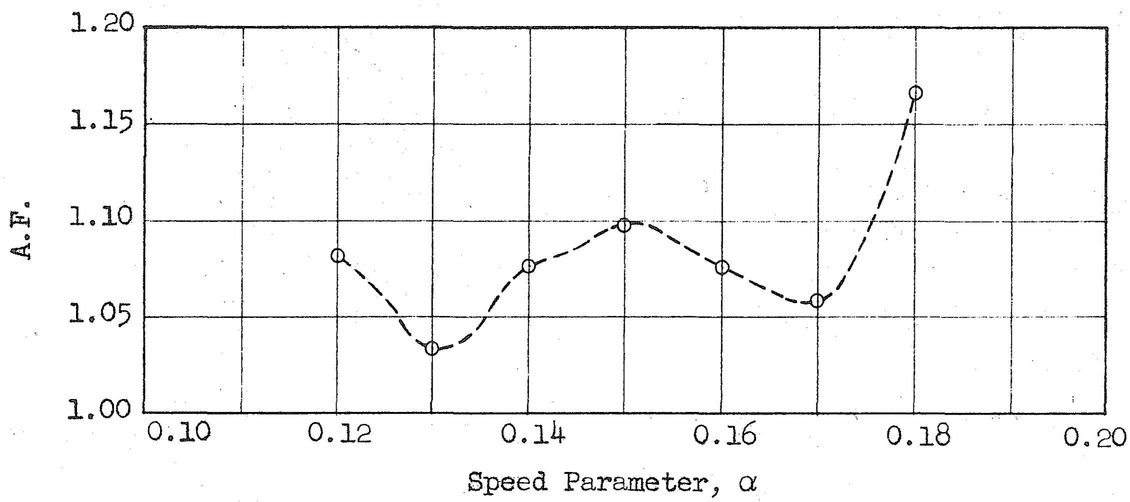

(c) Amplification Factor for D_4

FIG. 34 EFFECT OF SPEED ON AMPLIFICATION FACTORS -- "TYPICAL" TWO-AXLE TRAILER
$a = 0.8$, $c/c_{cr} = 0$, $W/W_b = 0.175$, $\ell/L = 0.3$, $f_{v1}/f_b = f_{v2}/f_b = 1$, $i = 1$

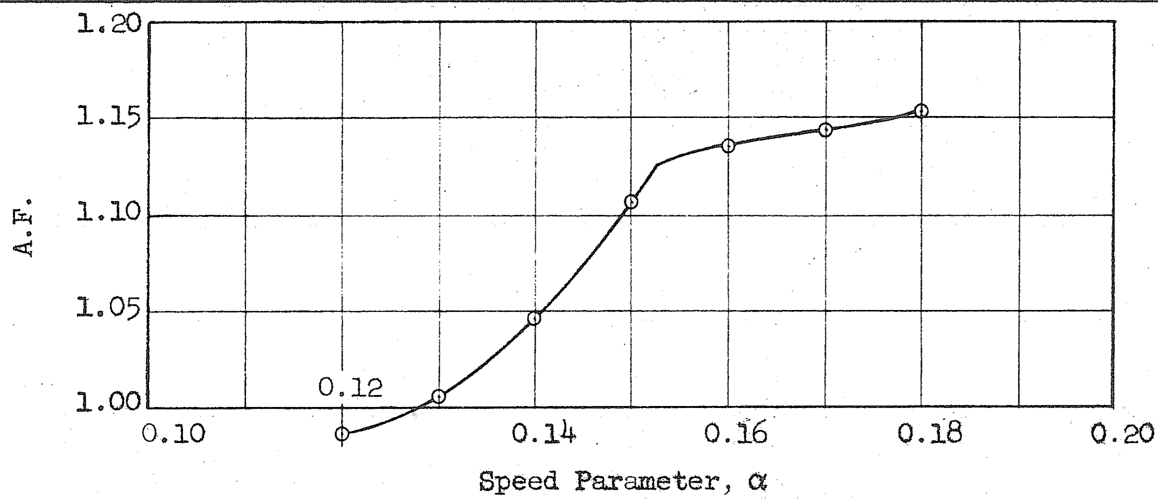

(d) Amplification Factor for M_1

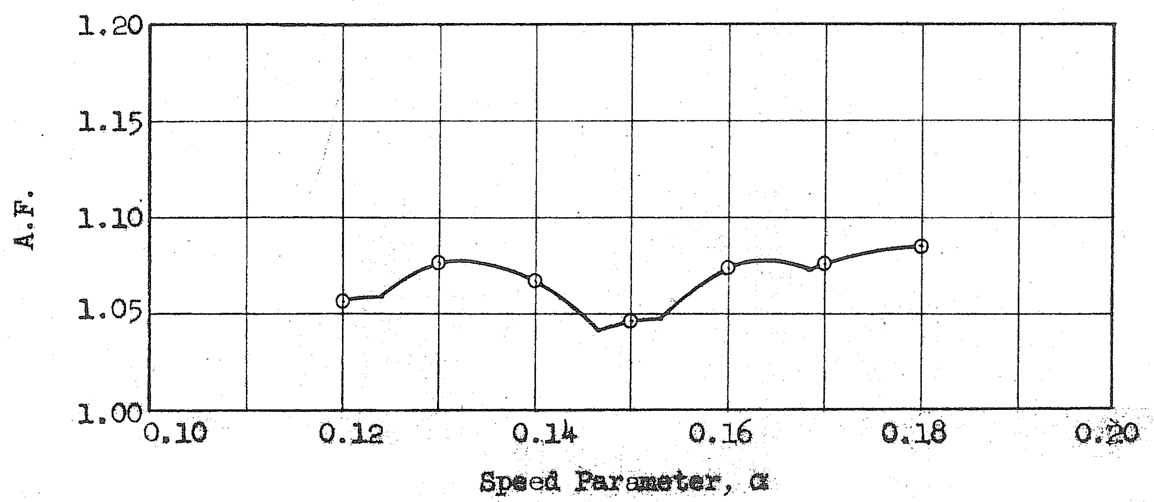

(e) Amplification Factor for M_2

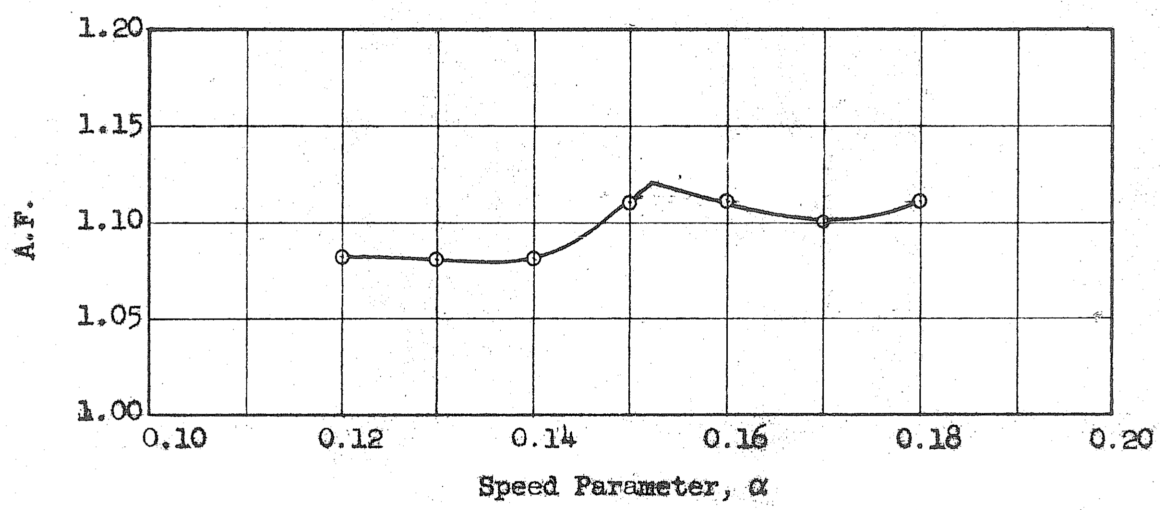

(f) Amplification Factor for M_c

FIG. 34 (Cont'd) EFFECT OF SPEED ON AMPLIFICATION FACTORS -- "TYPICAL" TWO-AXLE TRAILER

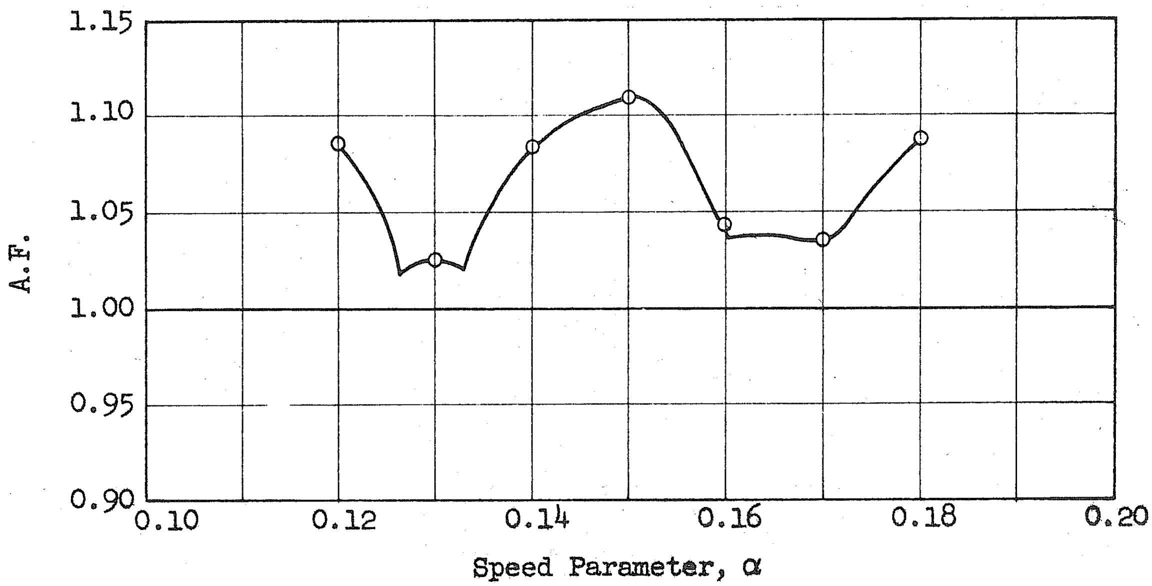

(g) Amplification Factor for M_3

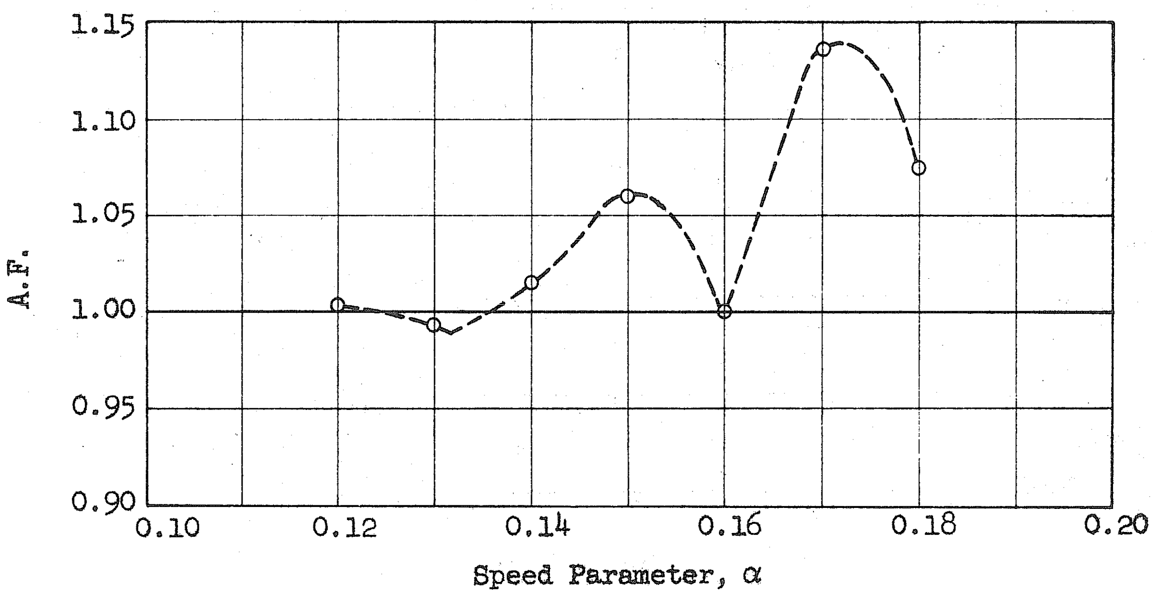

(h) Amplification Factor for M_4

FIG. 34 (Cont'd) EFFECT OF SPEED ON AMPLIFICATION FACTORS -- "TYPICAL" TWO-AXLE TRAILER

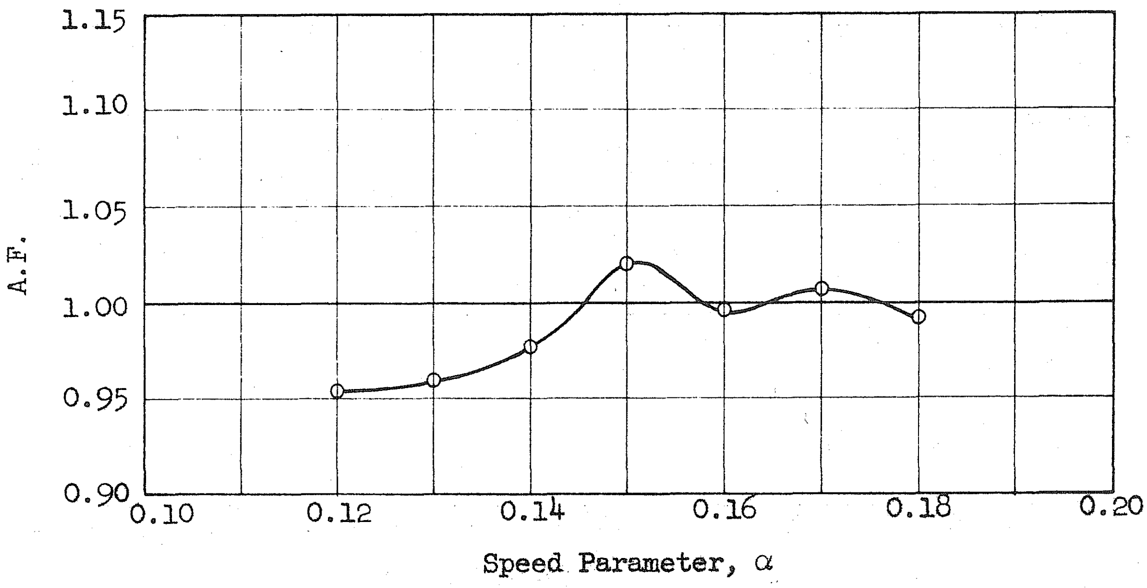

(i) Amplification Factor for R_1

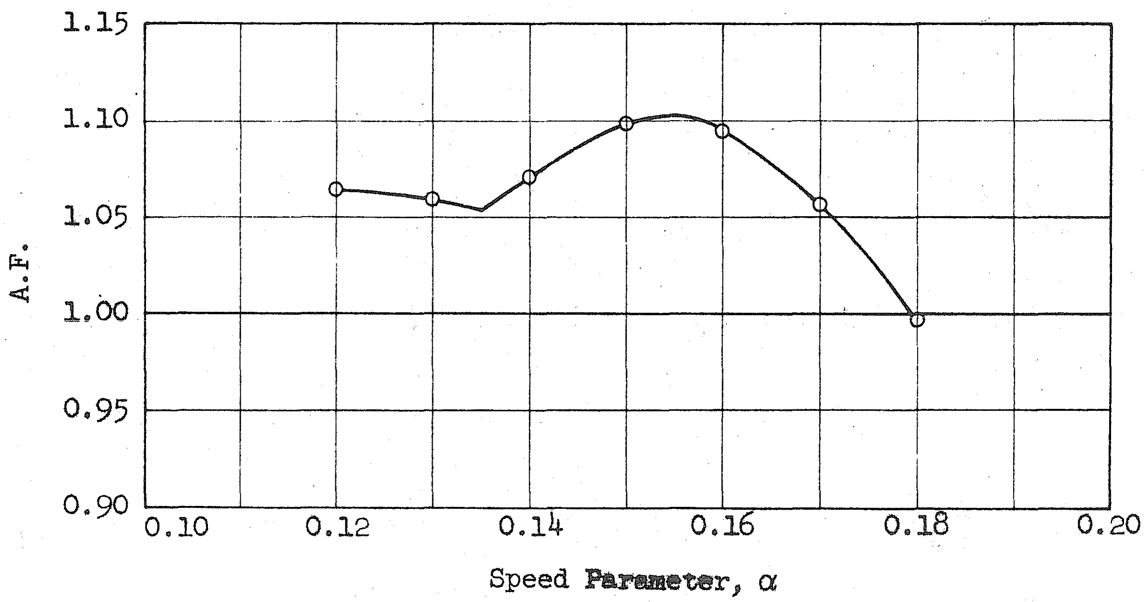

(j) Amplification Factor for R_2

FIG. 34 (Cont'd) EFFECT OF SPEED ON AMPLIFICATION FACTORS -- "TYPICAL" TWO-AXLE TRAILER

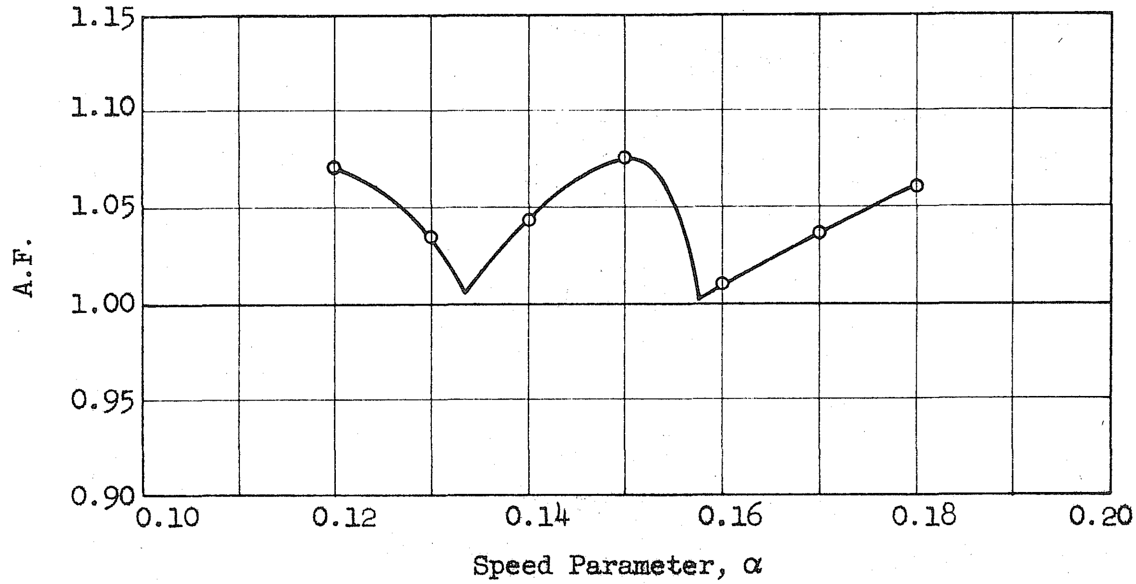

(k) Amplification Factor for R_3

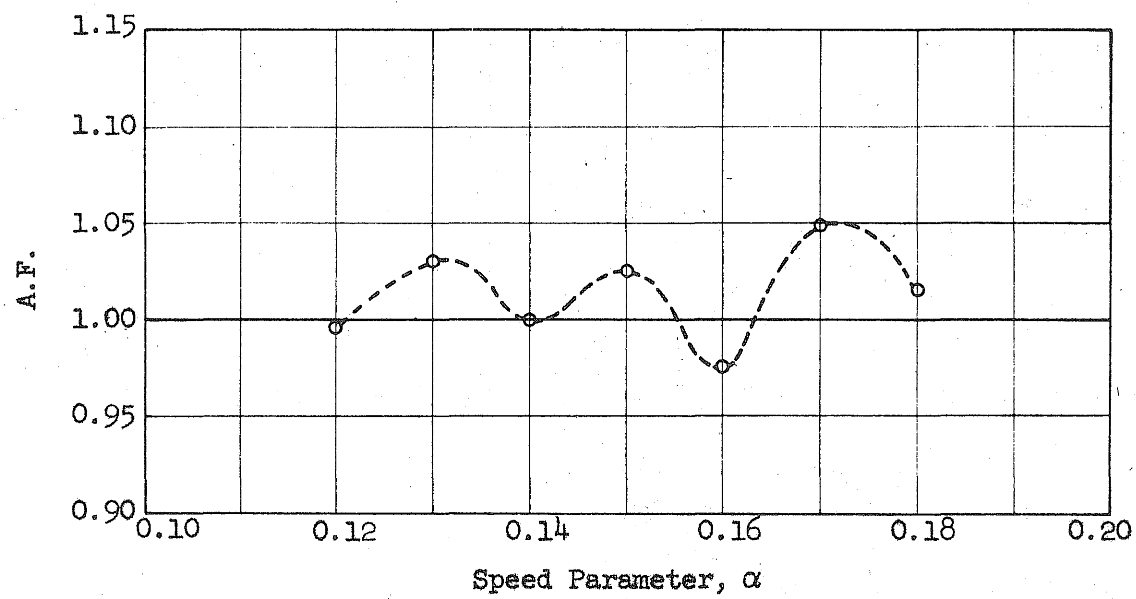

(ℓ) Amplification Factor for R_4

FIG. 34 (Cont'd) EFFECT OF SPEED ON AMPLIFICATION FACTORS -- "TYPICAL" TWO-AXLE TRAILER

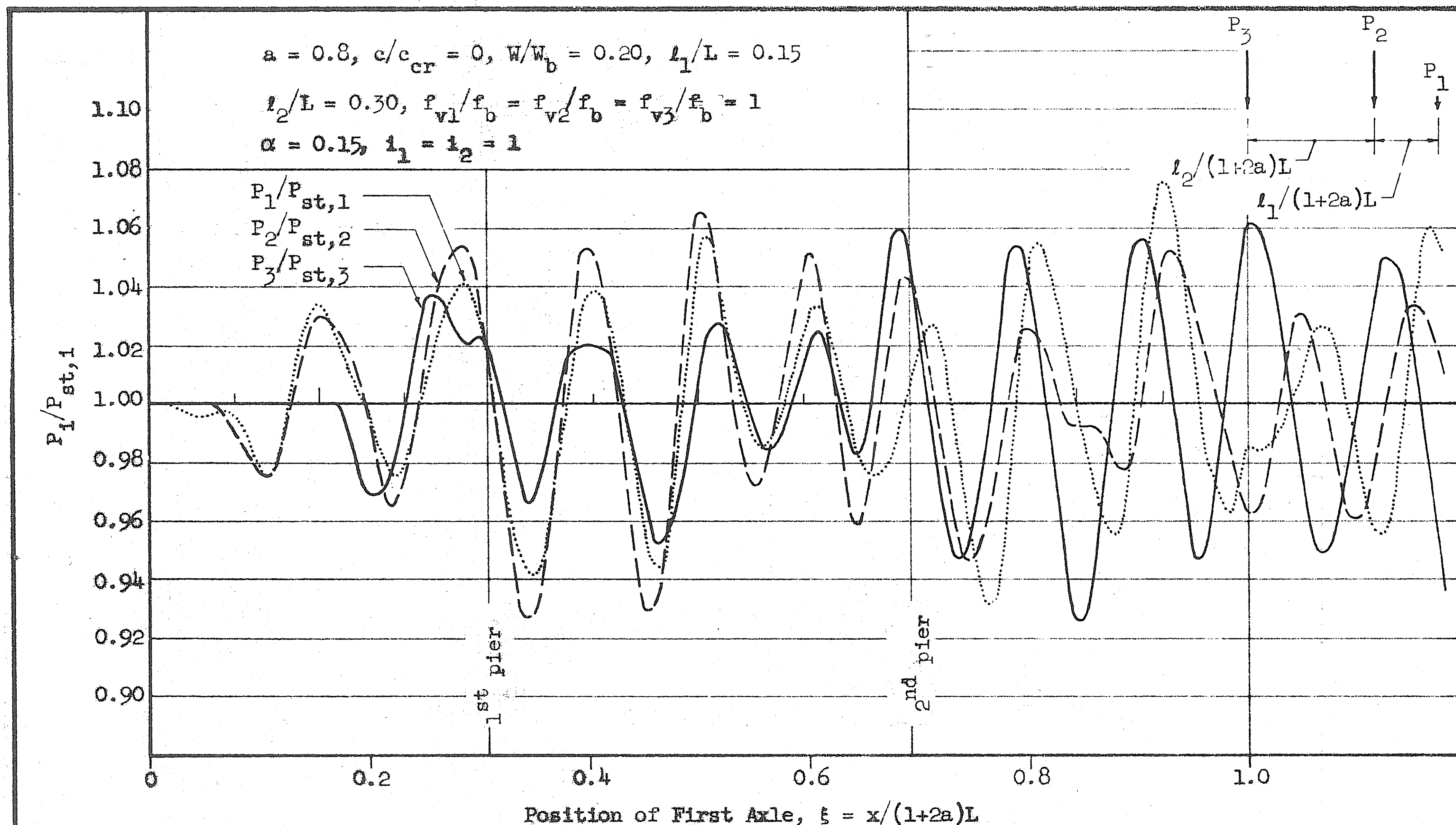

FIG. 35a HISTORY CURVES FOR INTERACTING FORCES, P_i -- "TYPICAL" THREE-AXLE VEHICLE

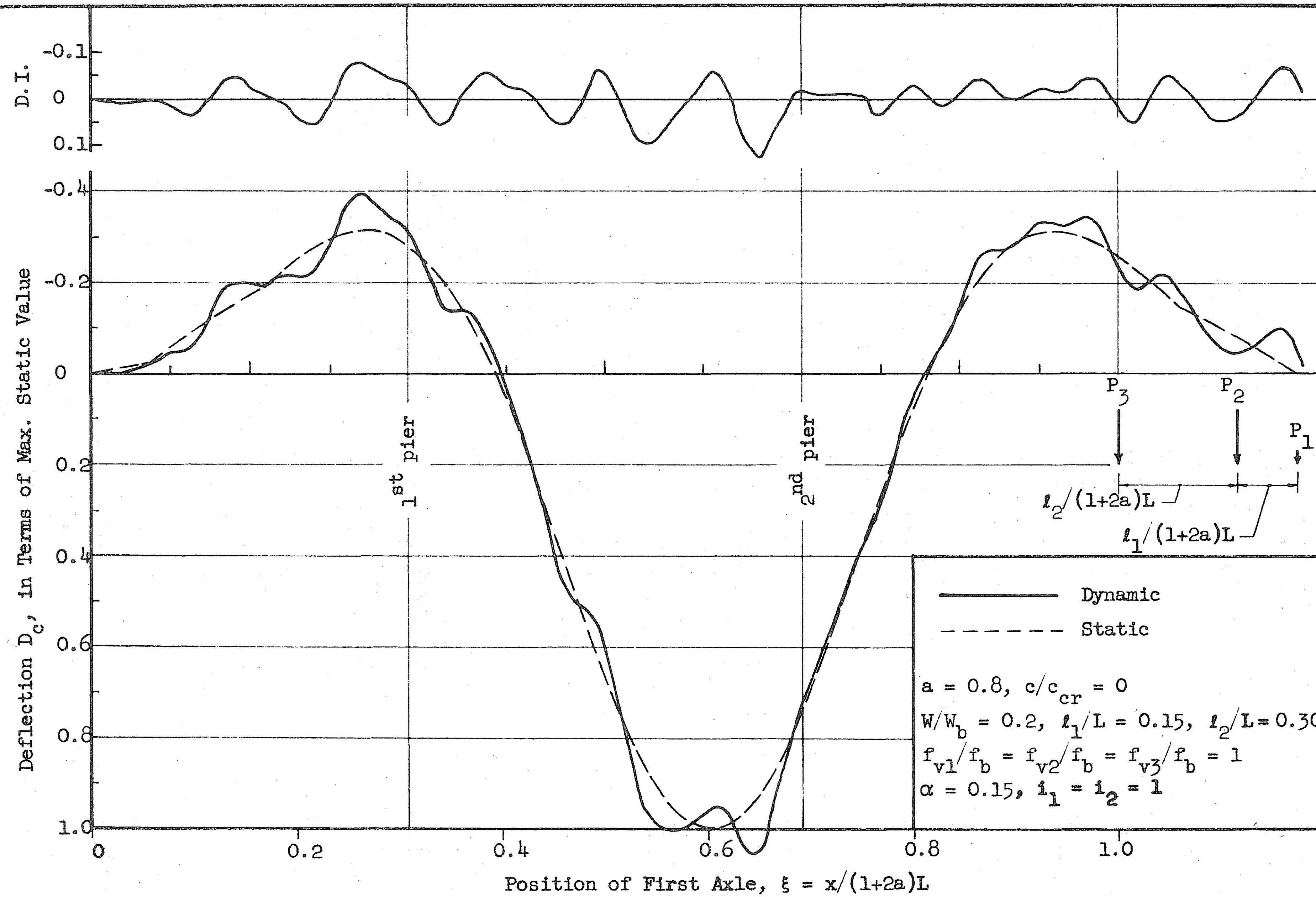

FIG. 35b HISTORY CURVES FOR D_c AND CORRESPONDING DYNAMIC INCREMENT -- "TYPICAL" THREE-AXLE VEHICLE

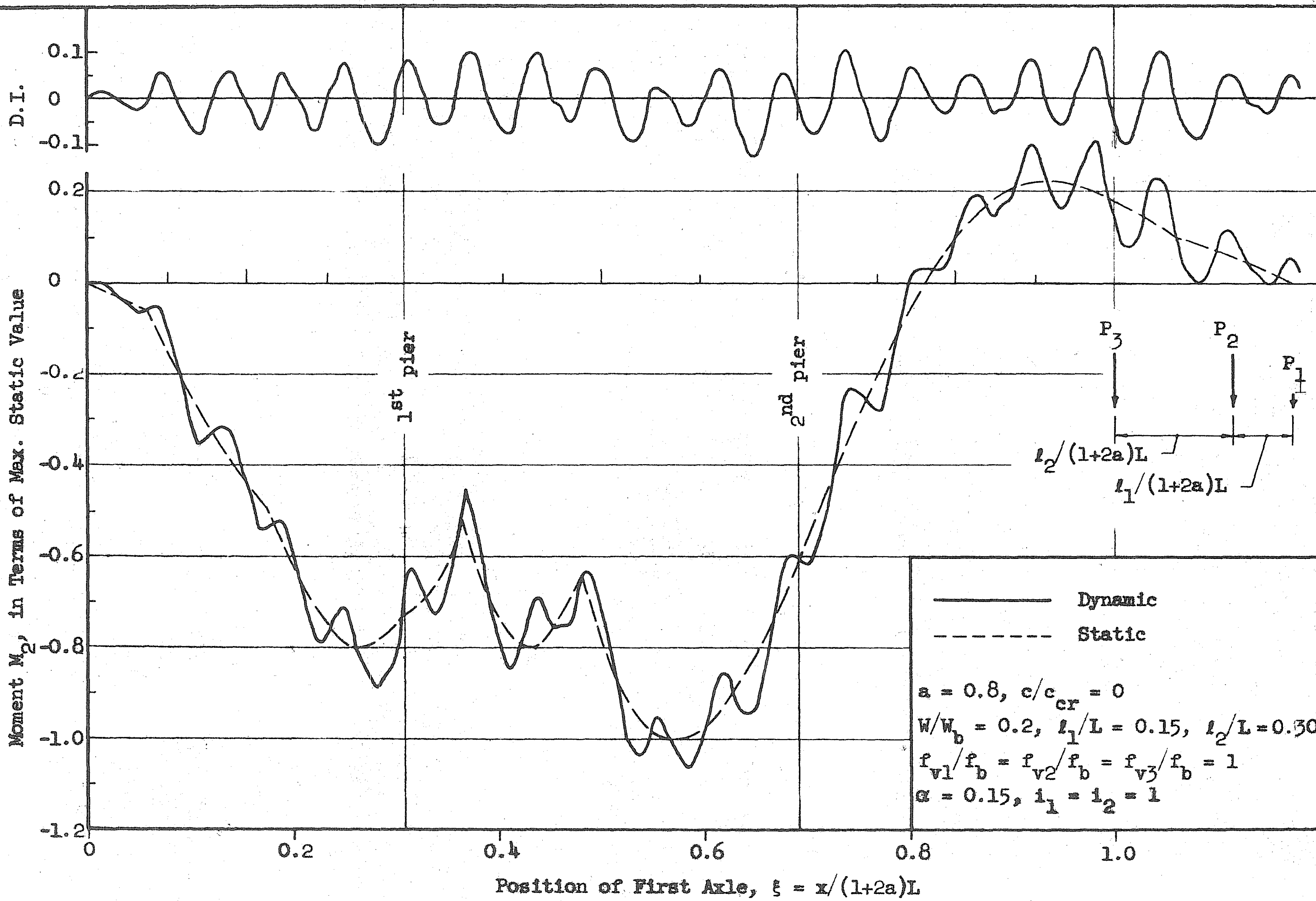

FIG. 35e HISTORY CURVES FOR M_2 AND CORRESPONDING DYNAMIC INCREMENT -- "TYPICAL" THREE-AXLE VEHICLE

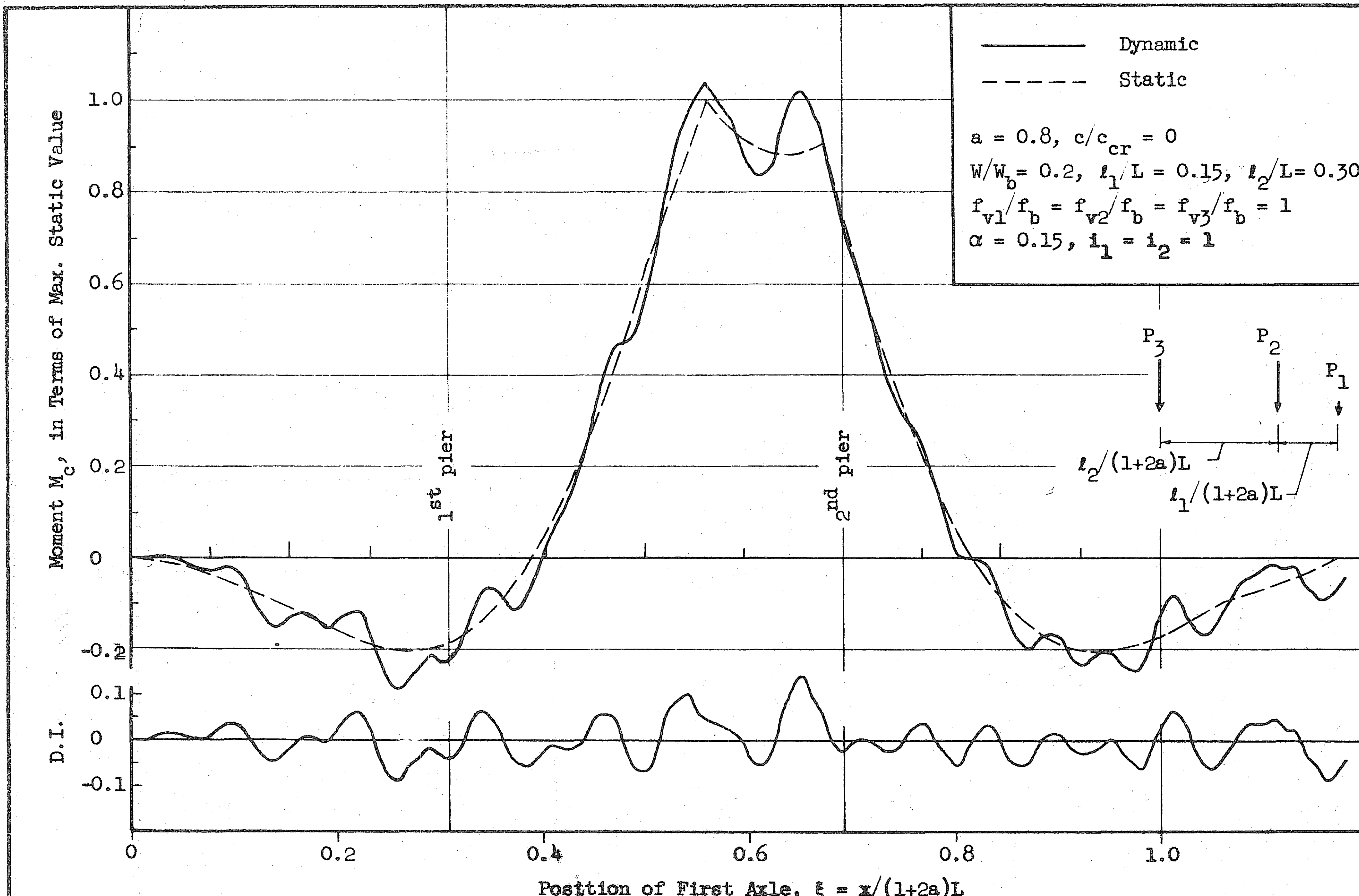

FIG. 35d HISTORY CURVES FOR M_c AND CORRESPONDING DYNAMIC INCREMENT -- "TYPICAL" THREE-AXLE VEHICLE

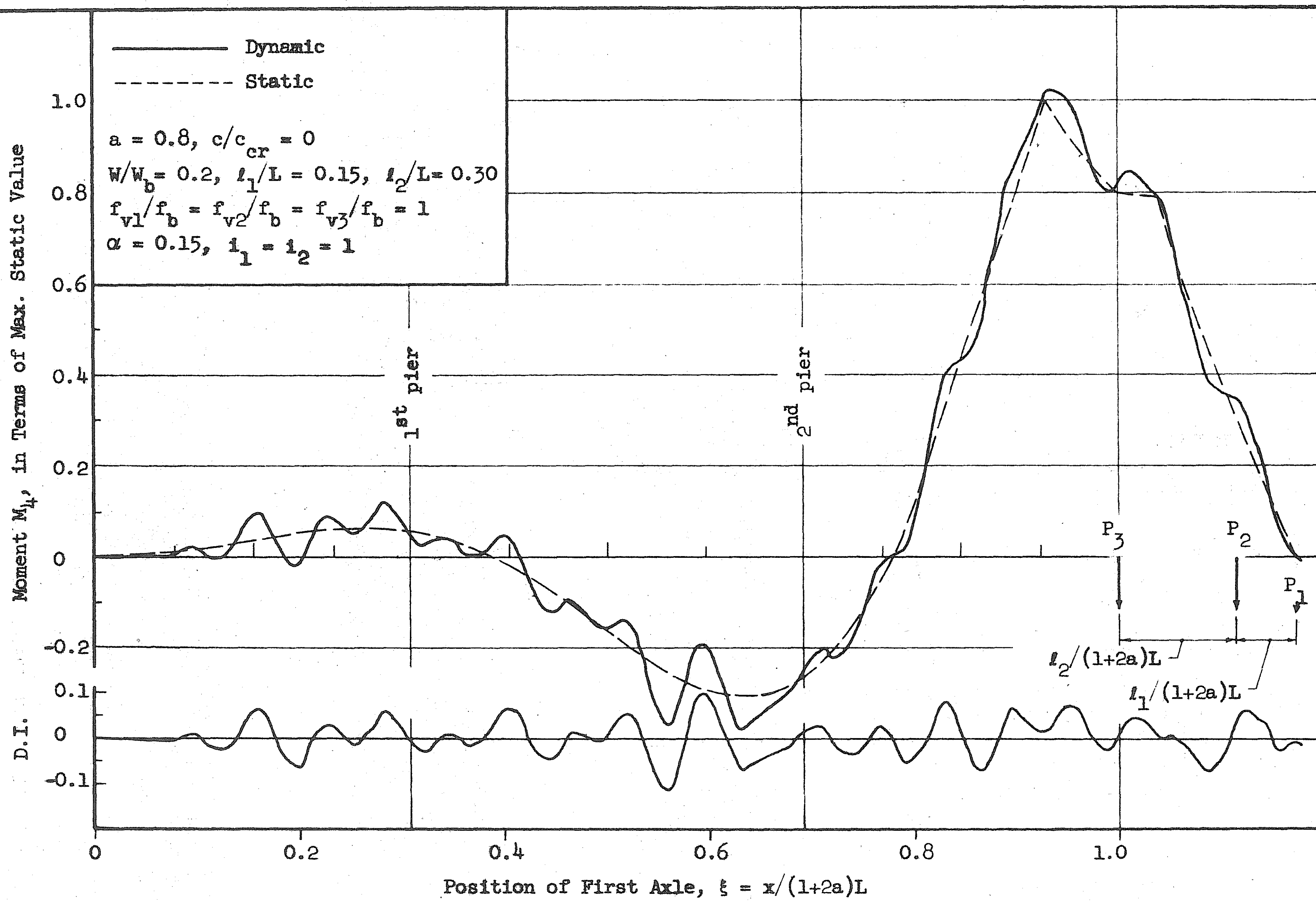

FIG. 35e HISTORY CURVES FOR M_4 AND CORRESPONDING DYNAMIC INCREMENT -- "TYPICAL" THREE-AXLE VEHICLE

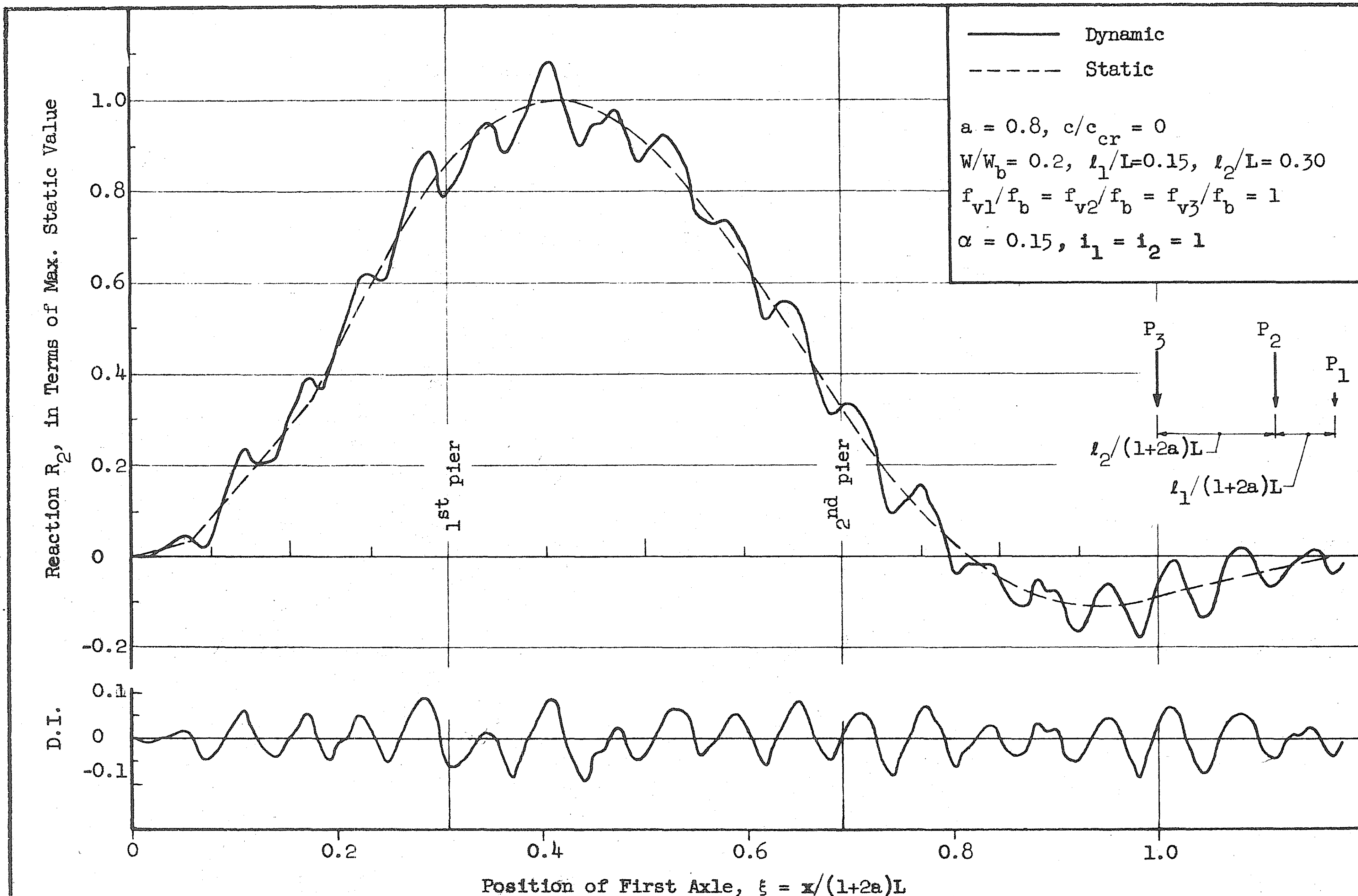

FIG. 35f HISTORY CURVES FOR R_2 AND CORRESPONDING DYNAMIC INCREMENT -- "TYPICAL" THREE-AXLE VEHICLE

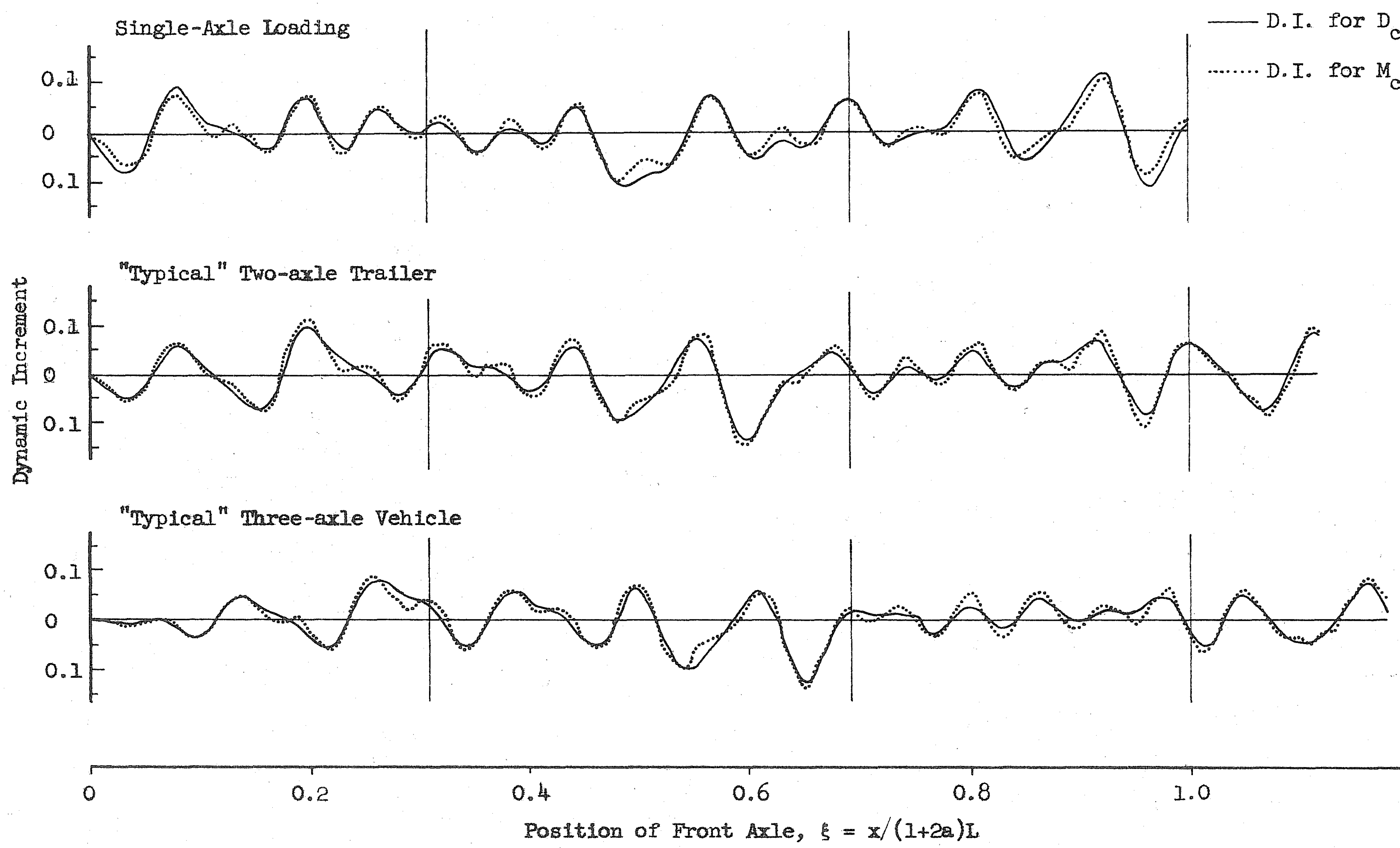

FIG. 36 COMPARISON OF DYNAMIC INCREMENT CURVES FOR D_c AND M_c

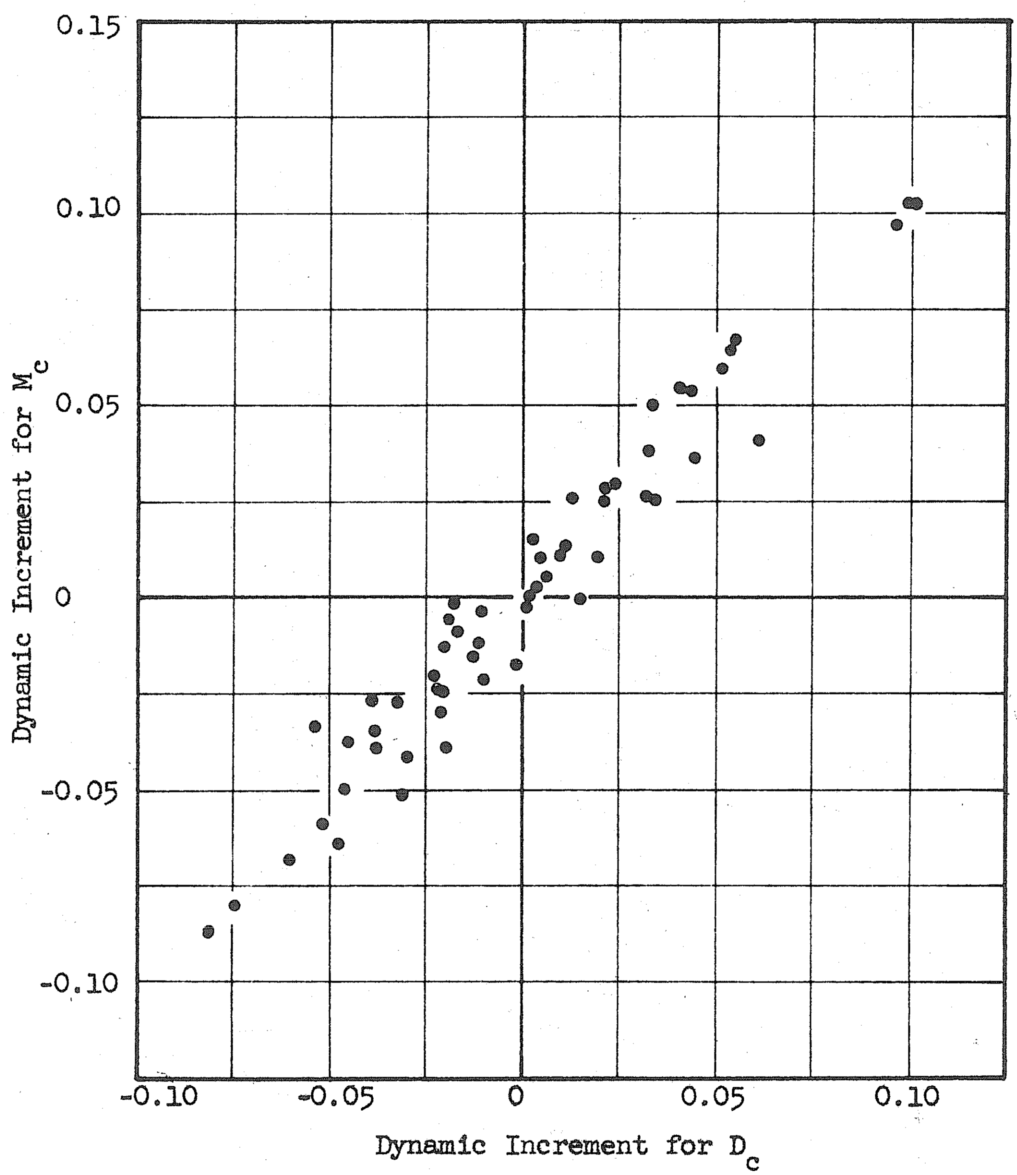

FIG. 37 SCATTER DIAGRAM OF D.I. FOR M_c VERSUS D.I. FOR D_c AT SAME INSTANT

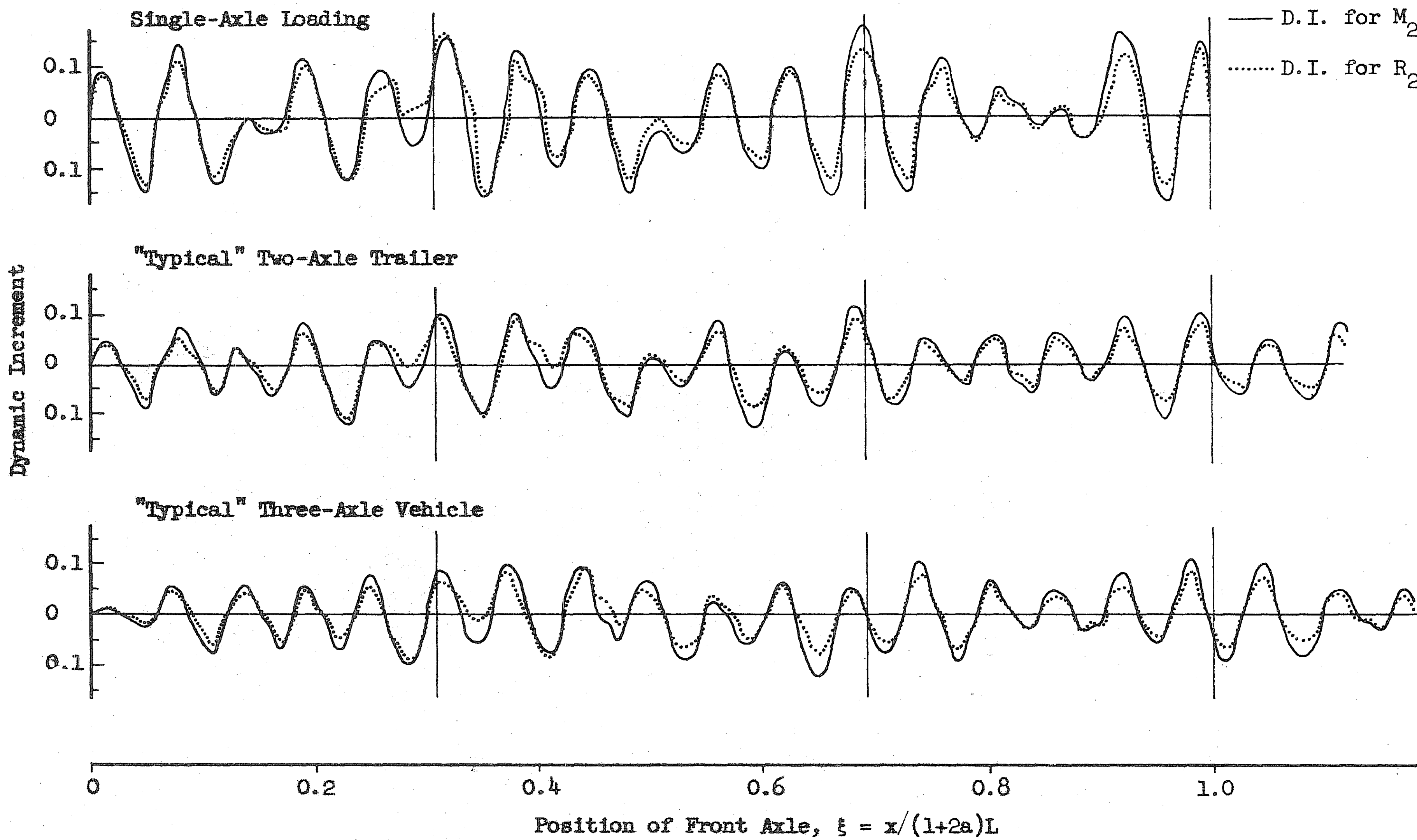

FIG. 38 COMPARISON OF DYNAMIC INCREMENT CURVES FOR M_2 AND R_2

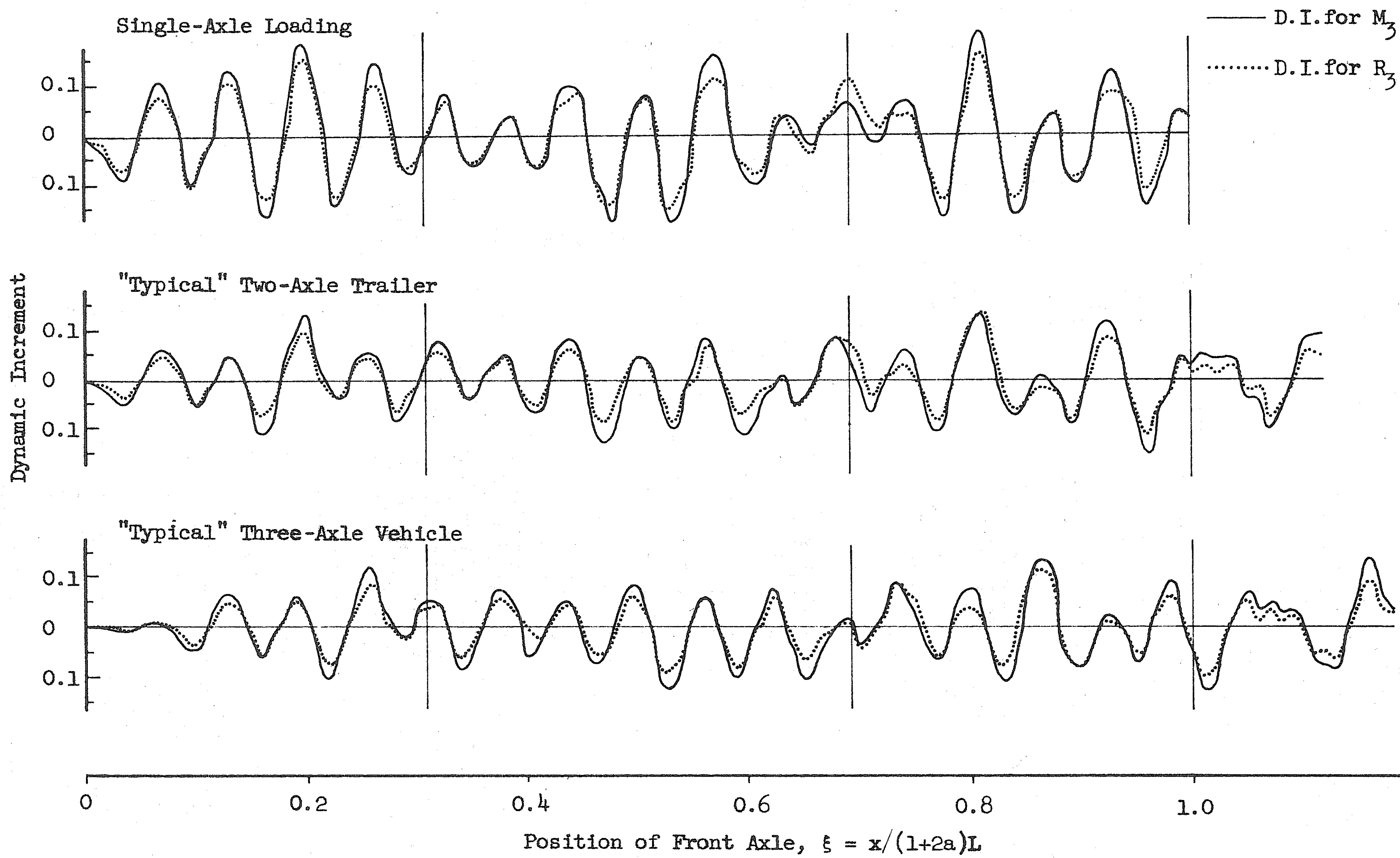

FIG. 39 COMPARISON OF DYNAMIC INCREMENT CURVES FOR M_3 AND R_3

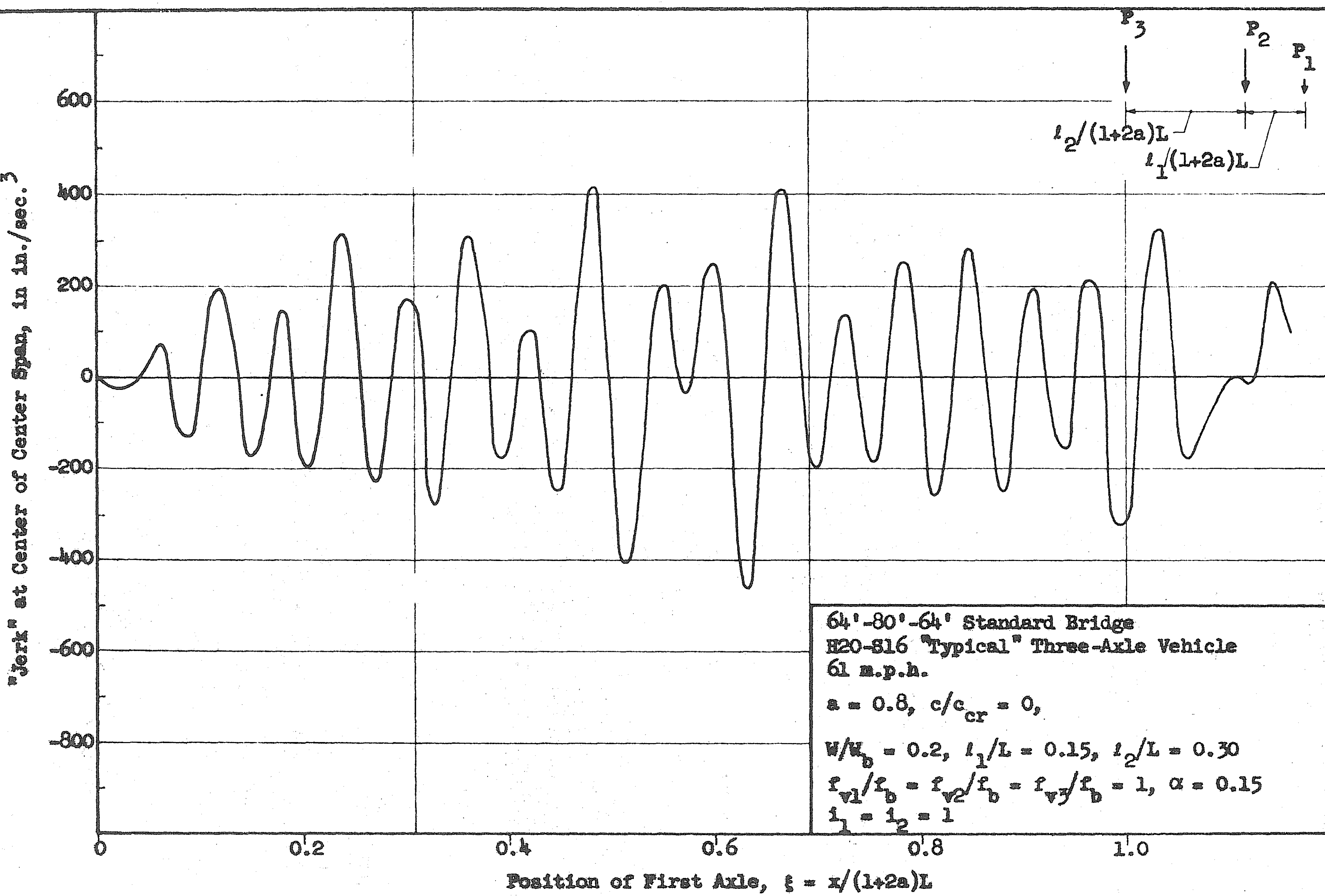

FIG. 40 HISTORY CURVE FOR "JERK" AT CENTER OF CENTER SPAN

APPENDIX A

DERIVATION OF EQUATION OF MOTION FOR VEHICLE

A1. Notation:

In addition to the symbols used in the text, the following notation is introduced:

F_{ta1}, F_{ta2} = vertical inertia forces of W_1 and W_2, respectively

f_{ta1}, f_{ta2}, f_{ta3} = vertical inertia forces of w_1, w_2 and w_3, respectively

T_{ta1}, T_{ta2} = inertia torques of W_1 and W_2, respectively

R_v = the difference between the dynamic and static components of the vertical interacting forces at the "fifth wheel pivot".

I_1, I_2 = rotary moments of inertia of W_1 and W_2, respectively. These quantities are given by the equations

$$\frac{I_1}{\ell_1^2} = a_1 a_2 i_1 \frac{W_1}{g} , \quad \frac{I_2}{\ell_3^2} = a_3 a_4 i_2 \frac{W_2}{g}$$

A2. Derivation of Equations:

Consider first the trailer as a free body, as shown in Fig. A1.

Then,

Elevation of the "fifth wheel pivot"

$$= a_5 z_1 + (1-a_5) z_2 + \text{a constant}$$

Elevation of the C.G. of W_2

$$= a_4 z_3 + a_3 \text{ (elev. of "fifth wheel pivot") + a constant}$$
$$= a_3 a_5 z_1 + a_3(1-a_5) z_2 + a_4 z_3 + \text{a constant}$$

Angular rotation of W_2

$$= \frac{1}{\ell_3} \text{ (elev. of "fifth wheel pivot" } - z_3) + \text{a constant}$$

$$= \frac{1}{\ell_3} [\, a_5 z_1 + (1-a_5) z_2 - z_3] + \text{a constant}$$

$$F_{ta2} = \frac{W_2}{g} [a_3 a_5 \ddot{z}_1 + a_3(1-a_5)\ddot{z}_2 + a_4 \ddot{z}_3] \tag{A1}$$

$$f_{ta3} = \frac{w_3}{g} [\ddot{z}_3] \tag{A2}$$

$$T_{ta2} = \frac{I_2}{\ell_3} [a_5 \ddot{z}_1 + (1-a\ )\ddot{z}_2 - \ddot{z}_3] \tag{A3}$$

Taking moments about the "fifth wheel pivot", we have,

$$a_4 F_{ta2} + f_{ta3} - \frac{T_{ta2}}{\ell_3} + (P_3 - P_{st,3}) = 0,$$

and substituting the above expressions for F_{ta2}, f_{ta3}, and T_{ta2} into the latter equation, we obtain

$$a_3 a_4 a_5 (1-i_2) \frac{W_2}{g} \ddot{z}_1 + a_3 a_4 (1-a_5)(1-i_2) \frac{W_2}{g} \ddot{z}_2$$

$$+ [(a_4^2 + a_3 a_4 i_2) \frac{W_2}{g} + \frac{w_3}{g}] \ddot{z}_3 + (P_3 - P_{st,3}) = 0,$$

or

$$[a_3 a_4 a_5 (1-i_2) \frac{W_2}{W}] \ddot{z}_1 + [a_3 a_4 (1-a_5)(1-i_2) \frac{W_2}{W}] \ddot{z}_2$$

$$+ [(a_4^2 + a_3 a_4 i_2) \frac{W_2}{W} + \frac{w_3}{W}] \ddot{z}_3 + \frac{g}{W} (P_3 - P_{st,3}) = 0. \tag{A4}$$

Taking moments about point a, we obtain the equation

$$R_v + a_3 F_{ta2} + \frac{T_{ta2}}{\ell_3} = 0 ,$$

which, by use of Eqs. A1 and A2, becomes

$$R_v = -a_5(a_3^2 + a_3 a_4 i_2) \frac{W_2}{g} \ddot{z}_1 - (1-a_5)(a_3^2 + a_3 a_4 i_2) \frac{W_2}{g} \ddot{z}_2$$

$$- a_3 a_4 (1-i_2) \frac{W_2}{g} \ddot{z}_3 \tag{A5}$$

Next, consider the tractor as a free body (see Fig. A2). Then,

Elev. of C.G. of W_1 $= a_1 z_1 + a_2 z_2$ + a constant

Angular rotation of $W_1 = \frac{1}{\ell_1} (z_1 - z_2)$ + a constant

$$F_{ta1} = \frac{W_1}{g} (a_1\ddot{z}_1 + a_2\ddot{z}_2) \tag{A6}$$

$$f_{ta1} = \frac{w_1}{g} \ddot{z}_1 \tag{A7}$$

$$f_{ta2} = \frac{w_2}{g} \ddot{z}_2 \tag{A8}$$

$$T_{ta1} = \frac{I_1}{\ell_1} (\ddot{z}_1 - \ddot{z}_2) \tag{A9}$$

Taking moments about point c, we have

$$a_2F_{ta1} - (1-a_5)R_v - \frac{T_{ta1}}{\ell_1} + f_{ta2} + (P_2 - P_{st,2}) = 0.$$

and substituting Eqs. A5 through A9 into the above identity, we obtain

$$\begin{aligned} &[a_1a_2(1-i_1) \frac{W_1}{W} + a_5(1-a_5)(a_3^2 + a_3a_4i_2) \frac{W_2}{W}] \ddot{z}_1 \\ &+ [(a_2^2 + a_1a_2i_1) \frac{W_1}{W} + (a_3^2 + a_3a_4i_2)(1-a_5)^2 \frac{W_2}{W} + \frac{w_2}{W}] \ddot{z}_2 \\ &+ [a_3a_4(1-a_5)(1-i_2) \frac{W_2}{W}] \ddot{z}_3 + \frac{g}{W} (P_2 - P_{st,2}) = 0. \end{aligned} \tag{A10}$$

Taking moments about point b, we have

$$a_1F_{ta1} - a_5R_v + \frac{T_{ta1}}{\ell_1} + f_{ta1} + (P_1 - P_{st,1}) = 0,$$

and making use of Eqs. A5, A6, A7 and A9, we obtain

$$\begin{aligned} &[(a_1^2 + a_1a_2i_1) \frac{W_1}{W} + a_5^2 (a_3^2 + a_3a_4i_2) \frac{W_2}{W} + \frac{w_1}{W}] \ddot{z}_1 \\ &+ [a_1a_2(1-i_1) \frac{W_1}{W} + a_5(1-a_5)(a_3^2 + a_3a_4i_2) \frac{W_2}{W}] \ddot{z}_2 \\ &+ a_3a_4a_5(1-i_2) \frac{W_2}{W} \ddot{z}_3 + \frac{g}{W} (P_1 - P_{st,1}) = 0 . \end{aligned} \tag{A11}$$

Equations A4, A10 and A11 correspond to Eq. 2 given in the text in matrix form.

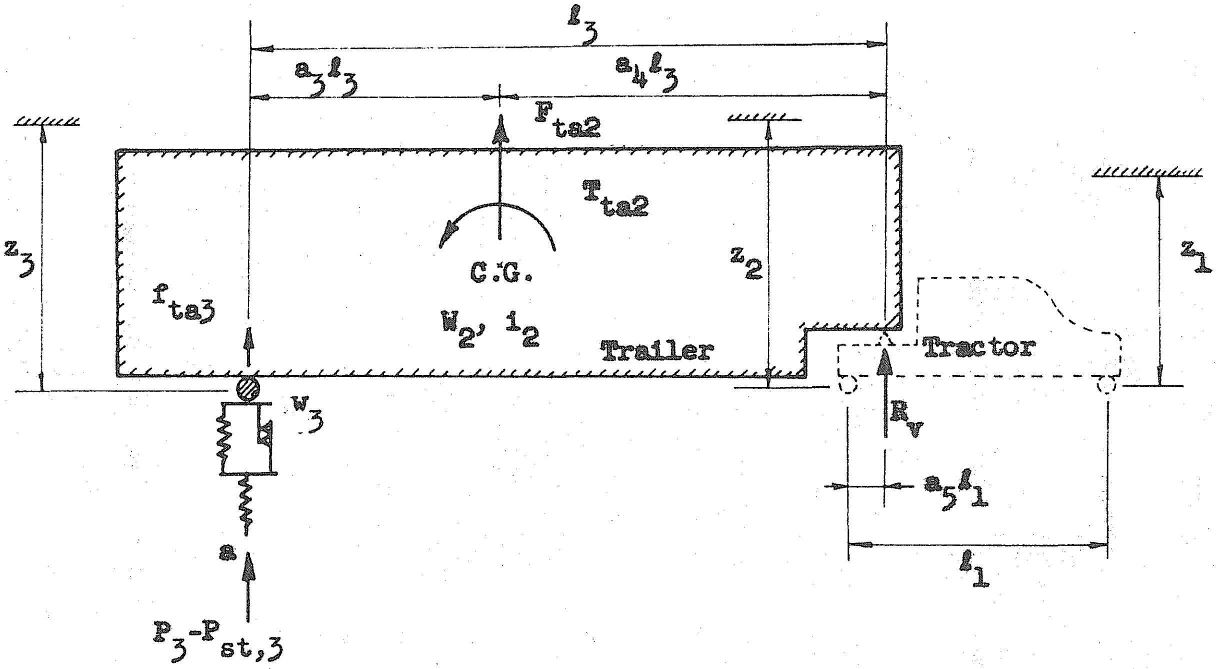

FIG. A1 FREE BODY DIAGRAM OF TRAILER

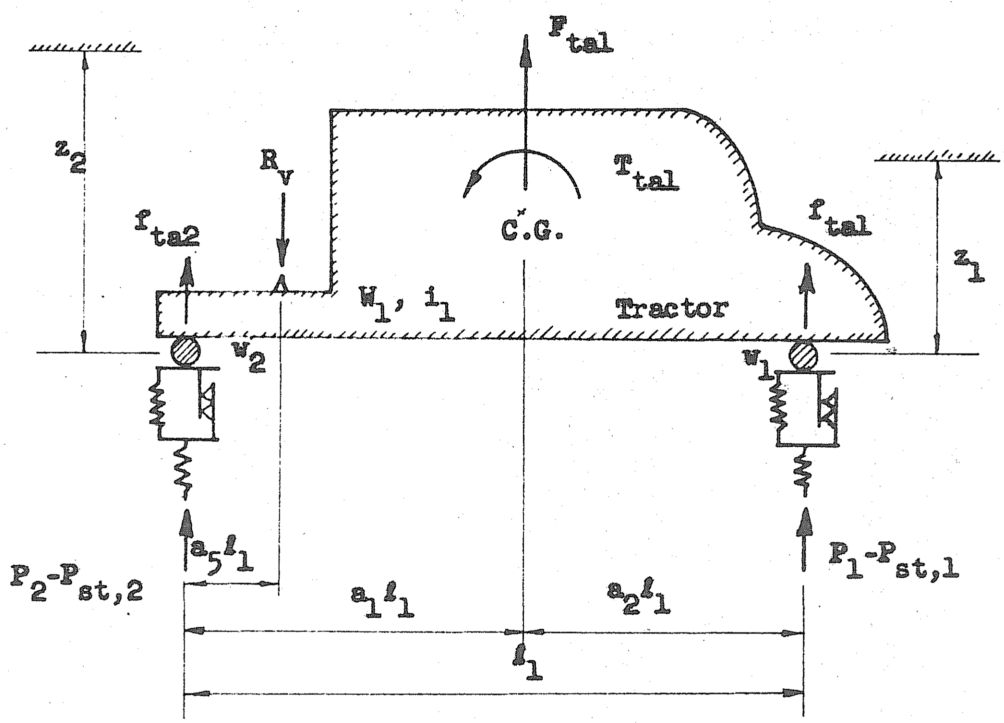

FIG. A2 FREE BODY DIAGRAM OF TRACTOR

APPENDIX B

ILLUSTRATION OF NUMERICAL INTEGRATION PROCEDURE

Table B1 summarizes the details of the numerical integration procedure for the 30^{th} time interval of integration for the problem presented in Art. 22 when the frequency ratio $f_v/f_b = 1$. The values of the response at the end of the 29^{th} time interval are those evaluated on ILLIAC. The integration is accomplished by use of Eqs. 1, 4, 16 and 17, which for ease in computation are transformed into the following forms:

$$(\Delta t)^2\, \ddot{y}_r = \left(-cm_r \dot{y}_r + \sum_j R_r^j\, y_j + \sum_i Q_r^i\, P_i\right) \frac{(\Delta t)^2}{m_r} \tag{B1}$$

$$(\Delta t)^2\, \ddot{z}_i = \sum_j \left[(\Delta t)^2 \cdot \frac{g}{W} \cdot b_{ij}\right] (P_j - P_{st,j}) \tag{B2}$$

$$(\Delta t)\dot{y}_{r,30} = (\Delta t)\dot{y}_{r,29} + \frac{1}{2}\left[(\Delta t)^2\, \ddot{y}_{r,29} + (\Delta t)^2\, \ddot{y}_{r,30}\right] \tag{B3a}$$

$$(\Delta t)\dot{z}_{i,30} = (\Delta t)\dot{z}_{i,29} + \frac{1}{2}\left[(\Delta t)^2\, \ddot{z}_{i,29} + (\Delta t)^2\, \ddot{z}_{i,30}\right] \tag{B3b}$$

$$y_{r,30} = y_{r,29} + (\Delta t)\dot{y}_{r,29} + \frac{1}{3}(\Delta t)^2\, \ddot{y}_{r,39} + \frac{1}{6}(\Delta t)^2\, \ddot{y}_{r,30} \tag{B4a}$$

$$z_{i,30} = z_{i,39} + (\Delta t)\dot{z}_{i,29} + \frac{1}{3}(\Delta t)^2\, \ddot{z}_{i,29} + \frac{1}{6}(\Delta t)^2\, \ddot{z}_{i,30} \tag{B4b}$$

For the particular problem considered,

$$(\Delta t)^2 \cdot \frac{g}{W} \cdot b_{11} = -\, 0.00060334\, \frac{L^3}{2EI}$$

The sequence of operation is shown in the last column of the table. The numbers one through ten designate the ten coordinates involved. The letters following the numbers designate the order of computation for the coordinate considered. The complete sequence of operation is from 1a to 10i. Steps 9a through 10i refer to the second and third axles of a three-axle vehicle. For a single-axle loading, which is the case considered in this illustration, these steps are inapplicable.

TABLE B1

EXAMPLE OF NUMERICAL INTEGRATION PROCEDURE

Quantity	Equation Used	Value of Quantity at t_{29} (Known)	Value of Quantity at t_{30} for Iteration Cycle Shown: Starting Cycle	First Cycle	Second Cycle	Third Cycle	Operation Sequence for Cycles 1, 2 and 3
$C^*(\Delta t)^2\ddot{y}_1$		-0.00525		-0.00969	-0.00661	-0.00667	1a
$C(\Delta t)^2\ddot{y}_2$		-0.01035		-0.01174	-0.01233	-0.01232	2a
$C(\Delta t)^2\ddot{y}_4$		-0.01161		-0.01203	-0.01205	-0.01205	3a
$C(\Delta t)^2\ddot{y}_5$	Eq. B1	-0.01840	Same as for t_{29}	-0.01761	-0.01760	-0.01760	4a
$C(\Delta t)^2\ddot{y}_6$		-0.01001		-0.00879	-0.00882	-0.00882	5a
$C(\Delta t)^2\ddot{y}_8$		+0.00540		+0.00435	+0.00443	+0.00443	6a
$C(\Delta t)^2\ddot{y}_9$		+0.00270		+0.00560	+0.00555	+0.00555	7a
$C(\Delta t)^2\ddot{z}_1$		-0.00744		-0.01390	-0.01390	-0.01390	8g
$C(\Delta t)^2\ddot{z}_2$	Eq. B2	-		-	-	-	9g
$C(\Delta t)^2\ddot{z}_3$		-		-	-	-	10g
$C(\Delta t)\dot{y}_1$		+0.43080	+0.42554	+0.42333	+0.42487	+0.42484	1b
$C(\Delta t)\dot{y}_2$		+0.34420	+0.33385	+0.33315	+0.33286	+0.33286	2b
$C(\Delta t)\dot{y}_4$		-0.18052	+0.19213	-0.19234	-0.19235	-0.19235	3b
$C(\Delta t)\dot{y}_5$	Eq. B3a	-0.20236	-0.22076	-0.22036	-0.22036	-0.22036	4b
$C(\Delta t)\dot{y}_6$		-0.11362	-0.12362	-0.12301	-0.12303	-0.12303	5b
$C(\Delta t)\dot{y}_8$		+0.01866	+0.02046	+0.02354	+0.02357	+0.02357	6b
$C(\Delta t)\dot{y}_9$		-0.01814	-0.01544	-0.01400	-0.01402	-0.01402	7b

*$C = EI/500WL^3$

TABLE B1 (Cont'd)

$C(\Delta t)\dot{z}_1$	Eq. B3b	+2.57842	+2.57099	+2.56775	+2.56775	+2.56775	8h
$C(\Delta t)\dot{z}_2$		-	-	-	-	-	9h
$C(\Delta t)\dot{z}_3$		-	-	-	-	-	10h
Cy_1	Eq. B4a	+7.70922	+8.13719	+8.13665	+8.13717	+8.13715	1c
Cy_2		+5.32299	+5.66201	+5.66178	+5.66168	+5.66168	2c
Cy_4		-1.71463	-1.90095	-1.90102	-1.90103	-1.90103	3c
Cy_5		-1.19933	-1.41089	-1.41075	-1.41075	-1.41075	4c
Cy_6		-0.37802	-0.49664	-0.49644	-0.49644	-0.49644	5c
Cy_8		-0.03213	-0.01077	-0.01094	-0.01093	-0.01093	6c
Cy_9		-0.07743	-0.09422	-0.09374	-0.09375	-0.09375	7c
Cz_1	Eq. B4b	+51.45245	+54.02715	+54.02607	+54.02607	+54.02607	8i
Cz_2		-	-	-	-	-	9i
Cz_3		-	-	-	-	-	10i
Cy_{P1}	Refer to Art. 9.2	+5.08435		+5.47726	+5.47859	+5.47858	8a
Cy_{P2}		-		-	-	-	9a
Cy_{P3}		-		-	-	-	10a
Cu_1	Eq. 6 in text	+46.36810		+48.54881	+48.54748	+48.54749	8b
Cu_2		-		-	-	-	9b
Cu_3		-		-	-	-	10b
$C\Delta u_1$				+2.18071	+2.17938	+2.17939	8c
$C\Delta u_2$				-	-	-	9c
$C\Delta u_3$				-	-	-	10c

TABLE B1 (Concluded)

$k_1^{**}(\Delta u_1)/W$			+0.01072	+0.01071	+0.01071	8d
$k_2\ (\Delta u_2)/W$			-	-	-	9d
$k_3\ (\Delta u_3)/W$			-	-	-	10d
P_1/W		1.01233	1.02305	1.02304	1.02304	8e
P_2/W		-	-	-	-	9e
P_3/W		-	-	-	-	10e
$(P_1-P_{st,1})/W$			+0.02305	+0.02304	+0.02304	8f
$(P_2-P_{st,2})/W$			-	-	-	9f
$(P_3-P_{st,3})/W$			-	-	-	10f
Cu_1^u		-24.39430			-26.57359	
Cu_2^u		-			-	
Cu_3^u		-			-	
Cu_1^ℓ	Refer to Art. 9.2	-46.36810			-48.54749	
Cu_2^ℓ		-			-	
Cu_3^ℓ		-			-	

$$^{**}\ k_1 = P_{st,1}\ \lambda^4 \frac{W}{W_B} \left(\frac{f_v}{f_b}\right)^2 \frac{EI}{WL^3} = 4.914945\ \frac{2EI}{L^3}$$